Evaluating the efficacy of curcumin derivatives on adipocyte dysfunction and adipocyte differentiation

M.T. Moetlediwa



orcid.org 0000-0001-9062-5650

Dissertation accepted in fulfilment of the requirements for the degree *Master of Sciences in Biochemistry* at the North-West University

Supervisor: Prof. S.E. Mazibuko-Mbeje

Graduation: 3 October 2024

DECLARATION

I **Marakiya Tiriwangani Moetlediwa** hereby truthfully declare that this thesis titled **"Evaluating the efficacy of curcumin derivatives on adipocyte dysfunction and adipocyte differentiation"** is fully my work submitted to the North-West University in the fulfilment of my Master of Science degree in Biochemistry under the supervision of Prof. Sithandiwe Mazibuko-Mbeje, Dr. Babalwa Jack, and Prof. Salam Titinchi. I declare that all views and ideas expressed in this thesis are mine and all references included are acknowledged accordingly, and none of the results reported are fabricated.

Author: Mr Marakiya Tiriwangani Moetlediwa

Signature: ..... **Date:** 19 March 2024

ACKNOWLEDGMENTS

As a Christian, I would first like to thank God for giving me life, strength, and good health throughout this project.

I would like to acknowledge the following individuals and institutions for their handful contributions throughout this research project:

- Professor S.E. Mazibuko-Mbeje from North-West University (NWU) for her wonderful supervision, guidance, motivation, patience, support, training, mentoring, and encouragement, and for helping me to establish myself in this research field. She held me by hand throughout this project and ensured its completion.

- Doctor B.U. Jack and Professor C. Pheiffer from the Biomedical Research and Innovation Platform (BRIP), South African Medical Research Council (SAMRC) for their utmost and best supervision in my research training, inspiration, support, and guidance that made the completion of this project possible. Not only did they supervise, but they also became mentors for the duration of the research project.

- Professor S.J.J. Titinchi from the Catalysis Laboratory, Chemistry Department, University of the Western Cape (UWC) for his help with the synthesis and characterization of the three synthetic curcumin derivatives (1A6, 1A8, and 1B8). He also provided guidance during the write-up of this thesis and published manuscripts.

- Doctor P. Ramharack and Doctor E. Salifu from BRIP, SAMRC for their kindness in facilitating the *insilico* training and helping with computational data analysis, reporting, and discussion, as well as preparation of the published *in silico* analysis chapter of this thesis.

- Associate Professor Phiwayinkosi V. Dludla and Doctor Sihle E. Mabhida for their mentorship and skill development in establishing myself as a young upcoming scientist.

- Family and friends who stood by my side in times of hardship and joy, they played a big role in maintaining my focus throughout my academic years.

- The SAMRC for providing funding for this project and hosting this project in their laboratories at BRIP which made this project a success. A special thanks to Mrs. Nnini Obonye, Dr. Stephanie Dias, Dr. Jyoti Sharma, and the BRIP staff, I am grateful for your assistance and guidance throughout this project.

- The National Research Foundation (NRF) Thuthuka grant (Grant Number: 129508) for funding contributions of this project and the NRF scholarship bursary.

- The NWU for its financial and academic support in the registration and affiliation of my Master of Science in Biochemistry at the Biochemistry department.

ABSTRACT

The prevalence of obesity has increased worldwide, necessitating the need to explore novel therapeutic interventions as the existing treatment options may not always be safe and effective over the long term. As such, natural compounds such as curcumin, a natural polyphenol derived from the turmeric plant, have shown promise in combating obesity through its diverse pharmacological properties, including anti-adipogenic, anti-lipolytic, and anti-inflammatory effects. However, the therapeutic efficacy of curcumin is limited due to its poor pharmacokinetic profile. This has prompted the development of synthetic curcumin derivatives to overcome these limitations and enhance the anti-obesity potential of curcumin. Thus, this study aimed to evaluate the effects of

curcumin and the three synthetic curcumin derivatives on adipocyte dysfunction and adipogenesis using *in silico* and *in vitro* experimental approaches.

The three synthetic curcumin derivatives, namely two chloro curcumin derivatives (1A6 and 1A8) and an asymmetric curcumin derivative (1B8), were synthesized via a chemical reaction of 3-chloroacetylacetone (1A6 and 1A8) or acetylacetone (1B8) with boric oxide. Three spectroscopic techniques, including high resolution - mass spectrometry - electrospray ionization (HR-MS-ESI), fourier transform - infrared (FT-IR) spectroscopy, and proton nuclear magnetic resonance (^{1}H-NMR) spectroscopy were used for the characterization of the synthesized curcumin derivatives. Thereafter, *in silico* computational tools such as Protox II and SwissADME were used to predict the toxicity and pharmacokinetic properties of curcumin and the three synthetic curcumin derivatives. Additionally, SwissTargetPrediction and similarity ensemble approach (SEA) online tools were used to identify potential biological targets of curcumin and three synthetic derivatives. Molecular docking and molecular dynamic simulation were also used to predict the binding affinities and molecular interactions of curcumin, 1A6, 1A8, and 1B8 with the selected target proteins involved in adipogenesis, lipid metabolism, and inflammation. In addition, the bioactivity of curcumin, 1A6, 1A8, and 1B8 was assessed *in vitro* in 3T3-L1 adipocytes induced with tumor necrosis factor alpha (TNFα), lipopolysaccharide (LPS), and palmitic acid (PA) combination treatment. Metabolic activity, lipolysis, and lipid accumulation were assessed using the adenosine triphosphate (ATP), glycerol release, and Oil Red O staining assays, respectively. Adiponectin (ADIPOQ) and interleukin 6 (IL-6) secreted levels were quantified using enzyme-linked immunosorbent assays and the expression of genes involved in lipid metabolism and inflammation was measured using quantitative real-time polymerase chain reaction (qRT–PCR).

The three curcumin derivatives (1A6, 1A8, and 1B8) were synthesized with high purity and thermal stability, and their chemical structures were elucidated by HR-MS-ESI, FT-IR, and ^{1}H-NMR spectroscopic techniques. *In silico* predictive screening showed that curcumin and the three synthetic curcumin derivatives (1A6, 1A8, and 1B8) similarly exhibit low toxicity, improved drug-like attributes, and favorable pharmacokinetic profiles. Molecular docking and molecular dynamic simulations showed that curcumin, 1A6, 1A8, and 1B8 similarly exhibit favorable binding scores to the predicted biological target proteins, with the most stable binding for peroxisome proliferatoractivated receptor gamma (PPARγ), cyclooxygenase 2 (COX2), and fatty acid synthase (FAS), which are key proteins involved in adipogenesis, inflammation, and lipid metabolism. TNFα, LPS, and PA combination treatment induced metabolic dysfunction in 3T3-L1 adipocytes by reducing metabolic activity, increasing

lipolysis, decreasing lipid accumulation, reducing anti-inflammatory, and increasing pro-inflammatory markers. ATP assay showed that treatment with curcumin, 1A6, and 1A8 at 40 μM reduced metabolic activity, while lower concentrations of these compounds (1.25 – 20 μM) and 1B8 did not affect metabolic activity in 3T3-L1 adipocytes induced with TNFα, LPS, and PA combination.

Similarly, lipolysis was attenuated by treatment with curcumin (5 – 20 μM), 1A6 (2.5 – 20 μM), and 1A8 (2.5 and 10 μM), while 1B8 had no effect. In contrast, treatment with curcumin and 1B8 (10 and 20 μM) increased lipid accumulation, while no effects were observed in cells treated with the chloro curcumin derivatives (1A6 and 1A8). The mRNA expression of the lipolytic gene, patatin-like phospholipase domain containing 3 (*Pnpla3*) was upregulated by treatment with 1B8 (20 μM). In contrast, acetyl-CoA carboxylase alpha (*Acaca*) mRNA expression was reduced by 1A6 (20 μM), while fatty acid synthase (*Fasn*) mRNA expression was also decreased by curcumin (10 μM), 1A6 (10 and 20 μM), and 1A8 (10 and 20 μM). Curcumin (10 and 20 μM), 1A6 (10 and 20 μM), 1A8 (20 μM), and 1B8 (10 and 20 μM) reduced cyclooxygenase 2 (*Cox2*) mRNA expression levels. Surprisingly, the results showed increased monocyte chemoattractant protein 1 (*Mcp1*) mRNA expression in cells treated with curcumin and 1A8 at 10 μM. In addition, treatment with curcumin (10 and 20 μM), 1A6 (10 and 20 μM), 1A8 (20 μM), and 1B8 (10 and 20 μM) decreased IL-6 secretion levels. This study suggests that curcumin and the three synthetic curcumin derivatives (1A6, 1A8, and 1B8) ameliorate adipocyte dysfunction by modulating lipid metabolism and inflammation and regulate adipogenesis by targeting key adipogenic and lipid metabolism proteins, thus exerting potential anti-obesity effects. Further experimental work is warranted to explore the anti-obesity potential and mechanism of action of the synthetic curcumin derivatives.

TABLE OF CONTENTS

DECLARATION I

ACKNOWLEDGMENTS II

..... ii

CHAPTER 1 1

INTRODUCTION 2

PROBLEM STATEMENT 4

RATIONALE 5

RESEARCH HYPOTHESIS 5

STUDY AIM 5

OBJECTIVES 6

REFERENCES 7

CHAPTER 2 10

ABSTRACT 12
INTRODUCTION 13
PHYSIOCHEMICAL, STRUCTURAL, AND BIOLOGICAL PROPERTIES OF CURCUMIN 14
THE PHARMACOKINETIC PROFILE OF CURCUMIN 16
EFFICACY OF CURCUMIN DERIVATIVES AGAINST OBESITY AND ASSOCIATED METABOLIC COMPLICATIONS 20
In vitro studies reporting on the therapeutic effects of curcumin derivatives against obesity and associated 20
metabolic complications 20
In vivo studies reporting on the therapeutic effects of curcumin derivatives on obesity-associated metabolic complications 27
SUMMARY AND CONCLUSIONS 36
REFERENCES 38
CHAPTER 3 46
INTRODUCTION 47
METHODS 47
Synthesis of the symmetric chloro curcumin derivatives 47
Synthesis of an asymmetric curcumin derivative 49
Characterization of the three synthetic curcumin derivatives 49
RESULTS AND DISCUSSION 51
Synthesis of three curcumin derivatives 51
Characterisation of synthetic curcumin derivatives 52
CONCLUSION 58
CHAPTER 4 62
ABSTRACT 64
INTRODUCTION 65
RESULTS 66
Prediction of toxicity for curcumin and synthetic curcumin derivatives 66
Prediction of the pharmacokinetic and physicochemical properties, druglikeness, and synthetic scores of 67
curcumin and synthetic curcumin derivatives 67
Prediction of the potential biological targets of curcumin and synthetic curcumin derivatives 69
Assessment of protein-ligand binding score by molecular docking and post-docking analysis 70
Assessment of protein-ligand complex stability and conformational flexibility by MD simulations 75
Calculation of the binding free energy using the MM/GBSA approach 80
Analyzing molecular interactions in MD simulation systems using LigPlot 81
DISCUSSION 84
MATERIALS AND METHODS 91
Prediction of toxicological properties of curcumin and synthetic curcumin derivatives 91
Predicting the pharmacokinetic, physicochemical, and druglikeness properties of curcumin and synthetic 91
curcumin derivatives 91
Identification of the potential biological targets of curcumin and synthetic curcumin derivatives 92

Molecular docking of curcumin and synthetic curcumin derivatives to the target 92
Molecular dynamic simulations of curcumin and synthetic curcumin derivatives 94
Post-molecular dynamic simulations analysis 95
Binding free energy calculations 95
Data analysis 96
CONCLUSIONS 96
REFERENCES 98
CHAPTER 5 106
INTRODUCTION 107
MATERIALS AND METHODS 108
Cell culture and differentiation 108
Treatment 108
Metabolic activity 109
Lipolysis 109
Lipid accumulation 110
Messenger RNA (mRNA) gene expression 110
Adipokine secretion 111
Data and statistical analysis 112
RESULTS 112
The effects of curcumin and the three synthetic curcumin derivatives on metabolic activity 112
The effects of curcumin, 1A6, 1A8, and 1B8 on lipolysis 114
The effects of curcumin and the three synthetic curcumin derivatives on lipid accumulation 116
The effects of curcumin, 1A6, 1A8, and 1B8 on mRNA gene expression levels 119
The effects of curcumin and the three synthetic curcumin derivatives (1A6, 1A8, and 1B8) on ADIPOQ 125
and IL-6 secreted levels 125
DISCUSSION 126
CONCLUSION 131
CHAPTER 6 138
SUMMARY 139
STRENGTH AND LIMITATIONS 141
CONCLUSION 142
FUTURE WORK 142
REFERENCES 142
ABSTRACT III
RESEARCH OUTPUTS VIII
LIST OF TABLES X
LIST OF FIGURES XI
ABBREVIATIONS AND ACRONYMS XIII

APPENDIX A SUPPLEMENTARY INFORMATION I

ETHICS APPROVAL FOR THIS STUDY I

LIST OF REAGENTS AND CHEMICALS USED IN THIS STUDY III

LIST OF EQUIPMENT AND MATERIALS USED IN THIS STUDY IV

EFFECTS OF DMSO ON CELL VIABILITY V

CELL DENSITY (CRYSTAL VIOLET) V

PCR STANDARD CURVE AND OPTIMIZATION VI

RESEARCH OUTPUTS

Conferences and Symposia:

- **Marakiya T. Moetlediwa**, Pritika Ramharack, Carmen Pheiffer, Salam J.J. Titinchi, Sithandiwe E. Mazibuko-Mbeje, and Babalwa Jack. "Evaluating the efficacy of curcumin derivatives on lipid metabolism and inflammation in 3T3-L1 adipocytes". *13th Annual Biomedical Research and Innovation Platform (BRIP) Research Symposium 2023*. 17 October 2023, Cape Town, South Africa.

- **Marakiya T. Moetlediwa**, Babalwa Jack, Sithandiwe E. Mazibuko-Mbeje, Carmen Pheiffer, Salam J.J. Titinchi, Elliasu Salifu, and Pritika Ramharack. "Therapeutic effects of Curcumin and its Synthetic Derivatives: A computational perspective for anti-obesity treatments". *CHPC National Conference 2023. Machine learning, Cloud and Quantum computing: The changing landscapes of HPC*. 4 – 7 December 2023, Mpumalanga, South Africa.

Workshop presentation:

- Virtual Winter School: 26-28 July 2023 (trainer), "INTRODUCTION TO CHEMINFORMATICS IN DRUG DISCOVERY". Biomedical Research and Innovation Platform (BRIP), Cape Town, South Africa.

Journal Publications resulting from my research project:

- **Marakiya T. Moetlediwa**, Babalwa U. Jack, Sithandiwe E. Mazibuko-Mbeje, Carmen Pheiffer, Salam J. J. Titinchi, Elliasu Y. Salifu, and Pritika Ramharack. "Evaluating the Therapeutic Potential of Curcumin and Synthetic Derivatives: A Computational Approach to Anti-Obesity Treatments". Molecular Sciences, p. 2603. (2024).

- **Marakiya T. Moetlediwa**, Rudzani Ramashia, Carmen Pheiffer, Salam J. J. Titinchi, Sithandiwe E. Mazibuko-Mbeje, and Babalwa U. Jack. "Therapeutic Effects of Curcumin Derivatives against Obesity and Associated Metabolic Complications: A Review of *in vitro* and *in vivo* Studies". Molecular Sciences, p. 14366. (2023).

Using the skills and training obtained during my studies, I contributed to the following publications during my MSc.

Journal Publications:

- Sidney Hanser, Joel Choshi1, Haskly Mokoena, Sihle Mabhida, Zandile Mchiza, **Marakiya T. Moetlediwa**, Ndivhuwo Muvhulawa, Bongani Nkambule, Duduzile Ndwandwe, Unati Nqebelele, Andre Pascal Kengne, Phiwayinkosi V. Dludla. "A Systematic Review Assessing the Potential Use of Cystatin

C as a Biomarker for Kidney Disease in People Living with HIV on Highly Active Antiretroviral Therapy". Frontiers in Medicine, p. 3389. (2024)

- Khanyisani Ziqubu, Phiwayinkosi V. Dludla, **Marakiya T. Moetlediwa**, Thembeka A. Nyawo, Carmen Pheiffer, Babalwa U. Jack, Bongani Nkambule, Sithandiwe E. Mazibuko-Mbeje. "Disease progression promotes changes in adipose tissue signatures in type 2 diabetic (db/db) mice: The potential pathophysiological role of batokines". Life Sciences, p. 121273. (2023).

- Phiwayinkosi V. Dludla, Ilenia Cirilli, Fabio Marcheggiani, Sonia Silvestri, Patrick Orlando, Ndivhuwo Muvhulawa, **Marakiya T. Moetlediwa**, Bongani B. Nkambule, Sithandiwe E. Mazibuko-Mbeje, Nokulunga Hlengwa, Sidney Hanser, Duduzile Ndwandwe, Jeanine L. Marnewick, Albertus K. Basson, and Luca Tiano. "Potential Benefits of Coffee Consumption on Improving Biomarkers of Oxidative Stress and Inflammation in Healthy Individuals and Those at Increased Risk of Cardiovascular Disease". Molecules, p. 6440. (2023).

- Phiwayinkosi V. Dludla, Ilenia Cirilli, Fabio Marcheggiani, Sonia Silvestri, Patrick Orlando, Ndivhuwo Muvhulawa, **Marakiya T. Moetlediwa**, Bongani B. Nkambule, Sithandiwe E. Mazibuko-Mbeje, Nokulunga Hlengwa, Sidney Hanser, Duduzile Ndwandwe, Jeanine L. Marnewick, Albertus K. Basson and Luca Tiano. "Bioactive Properties, Bioavailability Profiles, and Clinical Evidence of the Potential Benefits of Black Pepper (*Piper nigrum*) and Red Pepper (*Capsicum annum*) against Diverse Metabolic Complications". Molecules, p. 6569. (2023).

- Sinenhlanhla X.H. Mthembu, Sithandiwe E. Mazibuko-Mbeje, **Marakiya T. Moetlediwa**, Ndivhuwo Muvhulawa, Sonia Silvestri, Patrick Orlando, Bongani B. Nkambule, Christo J.F. Muller, Duduzile Ndwandwe, Albertus K. Basson g, Luca Tiano, and Phiwayinkosi V. Dludla. "Sulforaphane: A nutraceutical against diabetes-related complications". Pharmacological Research, p. 1043-6618. (2023).

- Ndivhuwo Muvhulawa, Sithandiwe E. Mazibuko-Mbeje, Duduzile Ndwandwe, Sonia Silvestri, Khanyisani Ziqubu, **Marakiya T. Moetlediwa**, Sinenhlanhla X.H. Mthembu, Jeanine L. Marnewick, Francois H. Van der Westhuizen, Bongani B. Nkambule, Albertus K. Basson, Luca Tiano, Phiwayinkosi V. Dludla. "Sarcopenia in a type 2 diabetic state: Reviewing literature on the pathological consequences of oxidative stress and inflammation beyond the neutralizing effect of intracellular antioxidants". Life Sciences, p.122125. (2023).

Book chapter:

- Yonela Ntamo, Duduzile Ndwandwe, Bongani B. Nkambule, **Marakiya T. Moetlediwa**, Asanda Mayeye, Nomahlubi Luphondo, Ndivhuwo Muvhulawa, Musawenkosi Ndlovu, Sihle E.Mabhida, Sithandiwe E.Mazibuko-Mbeje, Nokulunga Hlengwa, Sidney Hanser, Jeanine Marnewick, Patrick Orlando, Luca Tiano, and Phiwayinkosi V. Dludla "Potential benefits of tea consumption against risk factors associated with the development of coronary artery disease". Elsevier books, Chapter 30, (2024)

LIST OF TABLES

Table 2.1: Summary of *in vitro* studies reporting on the therapeutic effects of curcumin derivatives on obesity and associated metabolic complications 26
Table 2.2: Summary of *in vivo* studies reporting on the therapeutic effect of curcumin derivatives on obesity and associated metabolic complications 34
Table 3.1: The yield, purity, and melting points of the three synthetic curcumin derivatives 52
Table 3.2: Major FT-IR spectrum bands (cm^{-1}) of the three synthetic curcumin derivatives 55
Table 4.1: Predicted toxicity profiles of curcumin, 1A6, 1A8, and 1B8 66
Table 4.2: Predicted pharmacokinetic profiles of curcumin and 1A6, 1A8, and 1B8 6 67
Table 4.3: The predicted chemical parameters of curcumin, 1A6, 1A8, and 1B8 68
Table 4.4: The analysis of the MM/BGSA-based binding free energy contributed by residues of the active site of protein–ligand complex 78
Table 4.5: The LigPlot analysis for the molecular interactions of curcumin, 1A6, 1A8, 1B8, and their corresponding reference standards bound to PPARγ, COX2, and FAS..... 80
Table 4.6: The predicted target proteins of curcumin and the three synthetic curcumin derivatives 89
Table 4.7: Grid box co-ordinates of molecular docking for the predicted protein targets 90
Table 5.1: Taqman gene expression assays used in this study 108

LIST OF FIGURES

Figure 2.1: The turmeric (Curcuma longa) plant and rhizome 16
Figure 2.2: An illustration of curcumin tautomerization and metabolic pathways .....
Figure 2.3: Applications of various strategies (including formulations, adjuvant therapies, and synthetic derivatives) to overcome low bioavailability of curcumin 20
Figure 2.4: Schematic summary of the potential therapeutic effects of curcumin derivatives on obesity and its associated metabolic complications 36
Figure 3.1: The synthetic route for the two chloro curcumin derivatives, 1A6 and 1A8..... 48
Figure 3.2: The synthetic route for the asymmetric curcumin derivative, 1B8 49
Figure 3.3: The chemical structures of curcumin and the three synthetic curcumin derivatives 51
Figure 3.4: Representative mass spectrum data of the three synthetic curcumin derivatives 53
Figure 3.5: Representative ^{1}H-NMR spectral data for the three synthetic curcumin derivatives 58
Figure 4.1: *In silico* binding affinity scores and superimposed docked complexes of curcumin and its synthetic curcumin derivatives bound to human target proteins involved in adipogenesis, including PPARγ, MAPK14, and STAT3 69
Figure 4.2: *In silico* binding affinity scores and superimposed docked complexes of curcumin and synthetic curcumin derivatives bound to human target proteins of inflammation such as COX2, IL–6, and Adiponectin . 70
Figure 4.3: *In silico* binding affinity scores and superimposed docked complexes of curcumin and synthetic curcumin derivatives bound to human target proteins involved in lipid metabolism such as ACC, FAS, and GSK3β 71
Figure 4.4: Analysis of the MD simulations of PPARγ in complex with GW9662, curcumin, 1A6, 1A8, and 1B8 73
Figure 4.5: Analysis of the MD simulations of COX2 in complex with Naproxen, curcumin, 1A6, 1A8, and 1B8 75
Figure 4.6: Analysis of the MD simulations of FAS in complex with Orlistat, curcumin, 1A6, 1A8, and 1B8 .. 77
Figure 4.7: The schematic diagram of the study design 87
Figure 5.1: The effects of curcumin and the three curcumin derivatives on the metabolic activity of 3T3–L1 adipocytes co-treated with TNFα, LPS, and PA combination 111
Figure 5.2: The effects of curcumin and the three curcumin derivatives on lipolysis in 3T3–L1 adipocytes induced with TNFα, LPS, and PA combination 112
Figure 5.3: The effects of curcumin and the three curcumin derivatives on lipid accumulation in 3T3–L1 adipocytes induced with TNFα, LPS, and PA combination 114
Figure 5.4: The effects of curcumin and the three curcumin derivatives on the mRNA expression of Lipe (A) and Pnpla3 (B) in 3T3–L1 adipocytes induced with TNFα, LPS, and PA combination 115
Figure 5.5: The effects of curcumin and the three curcumin derivatives on the mRNA expression of *Pparγ* (A), *Srebf1* (B), *Acaca* (C), *Fasn* (D), *Lpl* (E), and *Gsk3a* (F) in 3T3–L1 adipocytes induced with TNFα, LPS, and PA combination 118
Figure 5.6: The effects of curcumin and the three curcumin derivatives on the mRNA expression of AdipoQ (A), Il-6 (B), Mcp1 (C), Cox2 (D), Mapk14 (E), and Stat3 (F) in 3T3–L1 adipocytes induced with TNFα, LPS, and PA combination 120
Figure 5.7: The effects of curcumin and the three curcumin derivatives on ADIPOQ (A) and IL-6 (B) secretion in 3T3–L1 adipocytes induced with TNFα, LPS, and PA combination 121

ABBREVIATIONS AND ACRONYMS

^{1}H-NMR – Proton–nuclear magnetic resonance

3-NT – 3-nitrotyrosine

Acaca – Acetyl-CoA carboxylase alpha

ACC – Acetyl-CoA carboxylase

AdipoQ –Adiponectin

ADME – Administration, distribution, metabolism, and excretion

AKT – Protein kinase B

AKT/mTOR – Protein kinase B/mammalian target of rapamycin

ALT – Alanine transaminase

AMPK – Adenosine-monophosphate-activated protein kinase

AMR – ATP monitoring reagent ANOVA

– One-way analysis of variance aP2 –

Adipocyte Protein 2 AST – Aspartate

aminotransferase

ATG5 – Autophagy related 5

ATP – Adenosine triphosphate

B2m – Beta 2 microglubulin

BAT – Brown adipose tissue

BCL-2/BAX – B-cell lymphoma 2/Bcl-2 associated X protein

BDMC – Bisdemethoxycurcumin

BMI – Body mass index

B_2O_3 – Boric oxide

C/EBPα – CCAAT/enhancer-binding protein alpha

CASTp – Computed atlas of surface topography of proteins

Ccl2/Mcp1 – Chemokine (C-C motif) ligand 2

CD68 – Cluster of differentiation 68 cDNA –

complimentary DNA

CDPP – Curcumin-3,4-Dichloro Phenyl Pyrazole

CO_2 – Carbon dioxide

COX2 ¬ Cyclooxygenase 2

CREB – cAMP response element-binding protein

CUR5-8 – curcumin5-8

CVDs – Cardiovascular diseases

Dex – Dexamethasone

DHC – Dihydrocurcumin

DHZ – Dehydrozingerone

DMA – Dimethylacetamide

DMC – Demethoxycurcumin

DMEM – Dulbecco's modified eagle's medium

DMSO – Dimethyl sulfoxide

eIF2α – Eukaryotic initiation factor 2 alpha

ELISA – Enzyme-linked immunoscobent assay

ESOL – water solubility

FAS – Fatty acid synthase

FAS – Fatty acid synthase

FBS – Fetal bovine serum

FDA – Food and drug administration

FFAs – Free fatty acids

FTIR – Fourier-transform infrared spectroscopy

G6Pase – Glucose-6-phosphatase

GAFF – General amber force field

GLUT4 – Glucose transporter type 4

GRP78 – Glucose-regulated protein 78

GSA - Non-polar solvation energy

GSK3β – Glycogen synthase kinase 3 beta

HDL-c – High-density lipoprotein cholesterol

HFD – High fat diet

HHC ¬ Hexahydrocurcumin hMSC –

Human mesenchymal stem cells Ho-1 –

Heme oxygenase-1 HOMA-IR –

Homeostasis model assessmentestimated

insulin resistance

HRMS-ESI – High-resolution mass spectrometry electrospray ionization

IBMX3 – Isobutyl-1-methylxanthine

Icam-1 – Intercellular adhesion molecule-1

IL–6, 1β, 17A, 22, and 23 – Interleukin 6, 1β, 17A, 22, and 23

iLOGP – Lipophilic

score INS – Insulin

IR – Insulin receptor

IRS-1 – insulin receptor substrate-1

IκB – Inhibitor of nuclear factor kappa B LC3-

ATG7 – Microtubule-associated protein light–

chain 3-autophagy related 7

LD50 –50% lethal dose
LDL-c – Low-density lipoprotein cholesterol
LFD – Low-fat diet
Lipe – Lipase E
LogP – octanol-water partition coefficient
Lpl – Lipoprotein lipase
LPS – Lipopolysaccharide
LRo5 – Lipinski's rules of five
Lxrα – Liver X receptor alpha
MD simulations – Molecular dynamic simulations MM/GBSA – Molecular mechanics with generalised Born and surface area solvation
MMFF94s – Ghemical and Merck molecular force fields 94
mRNA – Messenger ribonucleic acid
MS – Mass Spectrometry
NADPH – Nicotinamide adenine dinucleotide phosphate
NAFLD – Non-alcoholic fatty liver disease
NF-κB/JNK – Nuclear factor kappa B/c-Jun N-terminal kinase
NPT – Isobaric–isothermal ensemble
Nqo-1 – NADPH quinone dehydrogenase 1
NRF2 – Nuclear factor erythroid 2–related factor 2
OHC Octahydrocurcumin ORO – Oil Red O p38 MAPK – p38 mitogen activated protein kinases p62 – Sequestosome 1 PA – Palmitic acid
PDB – Protein data bank
PEG – Polyethylene glycol
Pepck – Phosphoenolpyruvate carboxykinase PGC1α – Peroxisome-proliferator-activated receptor gamma coactivator 1 alpha ORO – Oil Red O
p38 MAPK – p38 mitogen activated protein kinases
p62 – Sequestosome 1 PA – Palmitic acid
PDB – Protein data bank
PEG – Polyethylene glycol
Pepck – Phosphoenolpyruvate carboxykinase
PGC1α – Peroxisome-proliferator-activated receptor gamma coactivator 1 alpha
P-gp – P-glycoprotein
Pnpla3 – Patatin-like phospholipase domain-containing protein 3
Pparα – Peroxisome-proliferator-activated receptor alpha
PPARγ – Peroxisome-proliferator-activated receptor gamma
PTP1B – Protein tyrosine phosphatase 1B
PUFAs – Polyunsaturated fatty acids qRT-PCR – quantitative reverse transcriptionpolymerase chain reaction
RESP – Restrained electrostatic potential
RMSD – Root mean square of deviation
RMSF – Root mean square of fluctuation
ROS ¬ Reactive oxygen species
Rpl13a – Ribosomal protein L13a
SASA ¬ Solvent accessible surface area
SEA – Similarity ensemble approach
SEM – Standard error of mean SREBP1 – Sterol regulatory element binding transcription factor 1
STAT3 – Signal transducer and activator of transcription 3
T2D – Type 2 diabetes
TGF-β1 – Transforming growth factor-β
THC – Tetrahydrocurcumin
TNFα – Tumor necrosis factor alpha
$(MeO)B_3$ – Trimethyl borate
UCP1 – Uncoupling protein 1
VCAM-1 – Vascular cell adhesion molecule-1
WAT – White adipose tissue
WHO – World Health Organization

CHAPTER 1

Chapter outline:

This chapter provides an overview of the background, problem statement, rationale, hypothesis, and the aim and objectives of this research study.

Introduction

Obesity is a multifactorial disease characterized by excessive fat accumulation to the extent that it negatively affects health and decreases life expectancy [1,2]. Over the past decades, the global prevalence of overweight and obesity has significantly increased, with approximately 39% of the world's adults currently being overweight (body mass index [BMI] ≥ 25 kg/m^2), as reported by the World Health Organization (WHO) [3]. Recent estimates show that over 650 million (13%) adults worldwide are obese (BMI ≥ 30 kg/m^2), with obesity rates projected to reach 20% by 2025 if the current trends continue to increase without effective interventions [4,3]. Although historically linked to developed countries, obesity rates are sharply rising in low- and middle-income nations, which is attributed to various factors including urbanization, sedentary lifestyles, and unhealthy diets. [5]. Obesity is associated with an increased risk of developing chronic conditions such as type two diabetes (T2D) [6], cardiovascular diseases (CVDs) [7], and several types of cancers [8]. In recent years, accumulative evidence has demonstrated an urgent need to explore innovative therapeutic strategies that specifically target adipose tissue function to curb the escalating global prevalence of obesity and associated complications.

Adipose tissue is a connective tissue mostly composed of adipocytes, which are cells specialized for storing excess energy as fat (triglycerides). Two major types of AT exist, white adipose tissue (WAT), involved in maintaining energy balance by storing excess energy as triglycerides and releasing it as free fatty acids (FFAs) when required, and brown adipose tissue (BAT), which regulates thermogenesis thereby increasing energy expenditure [9]. During obesity, the excessive expansion of adipose tissue occurs by either hyperplasia (increase of adipocyte numbers) or hypertrophy (increased size of existing adipocytes) to accommodate excess triglyceride storage [10]. Adipocyte hyperplasia occurs via adipogenesis, which is a complex biological process through which precursor cells, known as preadipocytes, undergo differentiation and maturation into adipocytes [11,12]. Studies have shown that adipocyte hyperplasia is higher in obese insulin-resistant individuals compared to healthy individuals and that it is associated with metabolic dysfunction [13]. However, it has also been proposed that impaired adipogenesis, or restricted hyperplasia, may lead to ectopic fat deposition, contributing to the pathogenesis of obesity-related disorders [13–15]. In addition, the abnormal expansion of adipose tissue by hypertrophy induces adipocyte dysfunction, which is characterized by excessive lipolysis and altered secretion of adipokines [16]. This subsequently leads to dysregulated lipid metabolism, low-grade chronic inflammation, insulin resistance in adipocytes, and ectopic lipid deposition in peripheral tissues, which are key pathophysiological mechanisms that

underlie the development of obesity-associated chronic disease [17–19]. As such, targeting adipose tissue offers a promising approach to treat obesity and mitigate its adverse effects.

Current anti-obesity strategies, such as lifestyle modifications (calorie restriction and increased physical activity) and pharmacotherapeutic drugs, face challenges with adherence and adverse effects [20,21], while bariatric surgery is limited to morbidly obese individuals (BMI $\geq$ 40 kg/m^2) [22]. Thus, there is an urgent need for safe, effective, and long-term anti-obesity therapeutics to address the global prevalence of obesity. Natural compounds such as curcumin are gaining attention due to their safety, non-toxic effects, and various health benefits [23]. Curcumin, or diferuloylmethane ([1E,6E]-1,7-bis[4-hydroxy-3-methoxyphenyl]-1,6- heptadiene-3,5-dione), is a polyphenolic compound naturally isolated from the rhizome of turmeric (*Curcuma longa L.*) and is commonly utilized as a traditional medicine in Asian countries [24]. Curcumin is the most bioactive and abundant component in turmeric, with two other curcuminoids, demethoxycurcumin (DMC) and bisdemethoxycurcumin (BDMC), present in lower quantities [25]. Curcumin exerts diverse biological activities, including anti-inflammatory, antimicrobial, anti-oxidant, anti-cancer, anti-diabetic, and anti-obesity effects, as well as cardioprotective and neuroprotective benefits [18,26,27,28,29,30].

The anti-obesity effect of curcumin is supported by both pre-clinical and clinical studies. *In vitro* findings indicate that curcumin and its derivatives, demethoxy curcuminoids (DMC and BDMC), inhibit adipogenesis in 3T3-L1 preadipocytes by reducing lipid accumulation and suppressing the expression of adipogenic and lipogenic genes [25,31]. In addition, curcumin has been shown to alleviate adipocyte inflammation by reducing pro-inflammatory adipokines, increasing anti-inflammatory adipokines, and targeting key genes involved in inflammatory signaling pathways [32,33]. In addition, curcumin suppresses lipolysis by reducing FFAs and glycerol secretion [34], improves insulin sensitivity, and enhances glucose uptake [35–37]. Despite curcumin demonstrating various health benefits [25,31], its practical use as a therapeutic drug for obesity prevention and treatment is restricted due to challenges such as low solubility, instability in aqueous conditions, poor bioavailability, and limited absorption and permeability following oral administration [38,39]. To address the limitations associated with the natural form of curcumin and enhance its biological effectiveness, several studies have explored various approaches to modify the structure of curcumin, thus developing synthetic curcumin derivatives [40].

Synthetic curcumin derivatives are chemically modified analogs of curcumin that are synthesized to increase the pharmacokinetic profile and medicinal efficacy of curcumin. Previously, 19 novel curcumin derivatives were synthesized and investigated for their anti-cancer potential by assessing their cytotoxic effects and P-glycoprotein

(P-gp) inhibitory activity towards drug-sensitive acute lymphoblastic CCRF–CEM leukemia cells and their multidrug-resistant P-gp-overexpressing subline CEM/ADR5000 [41]. In both the sensitive and resistant cell lines, the 19 synthetic curcumin derivatives displayed potent cytotoxic activity. Particularly, the two chloro curcumin derivatives, (1E,6E)-4-chloro-1,7-bis(3,4-dimethoxyphenyl)hepta-1,6-diene-3,5-dione (1A6) and (1E,6E)-4-chloro-1,7-bis(3-hydroxyphenyl)hepta-1,6-diene-3,5-dione (1A8), and an asymmetric curcumin derivative, (1E,6E,8E)-1-(3,4-dimethoxyphenyl)-9-phenyldeca-1,6,8-triene-3,5-dione (1B8), showed potent cytotoxic efficacy in CEM/ADR5000 cells and remarkably increased doxorubicin uptake rates in CEM/ADR5000 cells when compared to curcumin [41].

Problem statement

Over the past few decades, the prevalence of obesity has rapidly increased, posing a significant threat to public health [1]. Obesity is a major source of morbidity and premature mortality worldwide, increasing the risk of developing chronic diseases such as T2D, CVDs, and several types of cancers [1]. Therefore, the development of effective drug therapies is a public health priority to curb the increasing prevalence of obesity and its associated co-morbidities. Lifestyle modifications, including calorie restriction and increased physical activity, are currently the primary intervention strategies for obesity prevention and treatment [20]. Poor adherence to these lifestyle modifications has led to an increased reliance on pharmacological drugs, which are faced with several side effects and pose limited efficacy [21]. Thus, there is an urgent need to develop novel, effective, and safer alternative therapeutics to combat obesity and obesity-related metabolic diseases. Currently, the investigation of natural compounds such as curcumin as potential anti-obesity agents is of high interest. Curcumin, the main bioactive polyphenolic compound of the turmeric spice, has gained scientific attention due to its medicinal benefits [42]. Amongst the many pharmacological benefits of curcumin, several pre-clinical and clinical studies have reported the potential anti-obesity properties of this compound, with adipose tissue as a potential therapeutic target [30].

Despite its widely reported anti-obesity potential, the application of curcumin as an anti-obesity drug is currently limited due to its low solubility in aqueous solvents; instability in aqueous conditions; poor bioavailability; and poor absorption and cellular uptake [43]. As such, structural modification of curcumin via the synthesis of novel curcumin-based derivatives is a potential approach to overcome these limitations and improve its biological efficacy. Hence, this study will investigate the anti-obesity efficacy of three synthetic curcumin derivatives, with previously reported anti-cancer properties, by comparing them with curcumin in an *in vitro* adipocyte cell culture model.

Rationale

Several *in vitro* and *in vivo* studies have provided evidence for the anti-obesity properties of curcumin [37,44,45,46]. Although curcumin has attracted considerable attention in treating obesity, its clinical application as a potential anti-obesity drug is hindered by its poor bioavailability [47]. Subsequently, researchers have tried different approaches to enhance its bioavailability including the modification of the curcumin structure using synthetic chemistry. To date, many derivatives of curcumin, both natural and synthetic, have been discovered and assessed for their improved efficacy compared to curcumin. In a recent literature review, we demonstrated that curcumin derivatives have improved potency in mitigating obesity and related metabolic complications [48]. In a previous study by Ooko et al., [41], 19 novel curcumin derivatives were synthesized and shown to exhibit potential anti-cancer effects. From these 19 novel synthetic derivatives of curcumin, three of them including 1A6, 1A8, and 1B8 were assessed for their anti-obesity properties in this study.

The use of curcumin derivatives with demonstrated anti-cancer properties in this study is rooted in the relationship between cancer and obesity. Research has increasingly recognized obesity as a risk factor for various types of cancers [8]. However, the mechanisms underlying this association are multifaceted and may involve chronic inflammation, altered hormone levels, insulin resistance, and changes in the adipose tissue microenvironment, all of which contribute to the progression of tumors [49–52]. Moreover, obesity is characterized by dysregulated metabolic pathways, including insulin signaling, adipokine secretion, and lipid metabolism, which create an environment conducive to tumorigenesis [53,54]. Therefore, the metabolic relationship between obesity and cancer provides a solid foundation for exploring the anti-obesity properties of the three synthetic curcumin derivatives with previously reported anti-cancer properties.

Research hypothesis

In this study, we hypothesized that curcumin and the three synthetic curcumin derivatives, (1A6, 1A8, and 1B8), previously reported to exhibit potent anti-cancer effects [41], will display anti-obesity effects by attenuating adipocyte dysfunction and inhibiting adipogenesis.

Study aim

This study aimed to evaluate the effects of curcumin and the three synthetic curcumin derivatives on adipocyte dysfunction and adipogenesis using *in silico* and *in vitro* experimental approaches.

Objectives

I. To synthesize and characterize three synthetic curcumin derivatives (1A6, 1A8, 1B8).

II. To predict the toxicity, pharmacokinetic profiles, biological targets, and molecular interactions of curcumin and the three synthetic curcumin derivatives with predicted biological targets using the *in silico* computational approach.

III. To assess the effects of curcumin and the three synthetic curcumin derivatives on cell viability, lipolysis, lipid accumulation, and inflammatory adipokine secretion in 3T3-L1 adipocytes induced with a combination of tumor necrosis factor alpha (TNFα), lipopolysaccharide (LPS) and palmitic acid (PA).

IV. To investigate the effects of curcumin and the three synthetic curcumin derivatives on the expression of genes involved in lipid metabolism and inflammation in 3T3-L1 adipocytes induced with a combination of TNFα, LPS, and PA.

References

[1] A. Hruby and F. B. Hu, "The Epidemiology of Obesity: A Big Picture," Pharmacoeconomics, vol. 33, no. 7, pp. 673–689, 2015, doi: 10.1007/s40273-014-0243-x.

[2] C. Pozza and A. M. Isidori, "What's Behind the Obesity Epidemic," in Imaging in Bariatric Surgery, Springer International Publishing, 2018, pp. 1–8. doi: 10.1007/978-3-319-49299-5_1.

[3] WHO, "Obesity and overweight," World Health Organization, 2020.

[4] M. Di Cesare et al., "Trends in adult body-mass index in 200 countries from 1975 to 2014: a pooled analysis of 1698 population-based measurement studies with 19·2 million participants," Lancet, vol. 387, no. 10026, pp. 1377–1396, Apr. 2016, doi: 10.1016/S0140-6736(16)30054-X.

[5] N. D. Ford, S. A. Patel, and K. M. V. Narayan, "Obesity in Low- and Middle-Income Countries: Burden, Drivers, and Emerging Challenges," Annu. Rev. Public Health, vol. 38, pp. 145–164, 2017, doi: 10.1146/annurev-publhealth-031816-044604.

[6] D. R. Leitner et al., "Obesity and Type 2 Diabetes: Two Diseases with a Need for Combined Treatment Strategies - EASO Can Lead the Way," Obes. Facts, vol. 10, no. 5, pp. 483–492, Nov. 2017, doi: 10.1159/000480525.

[7] T. M. Powell-Wiley et al., Obesity and Cardiovascular Disease A Scientific Statement from the American Heart Association, vol. 143, no. 21. Circulation, 2021, pp. E984–E1010. doi: 10.1161/CIR.0000000000000973.

[8] S. H. Davoodi, T. Malek-Shahabi, A. Malekshahi-Moghadam, R. Shahbazi, and S. Esmaeili, "Obesity as an important risk factor for certain types of cancer.," Iran. J. cancer Prev., vol. 6, no. 4, pp. 186–94, 2013, Accessed: May 17, 2023. [Online]. Available: http://www.ncbi.nlm.nih.gov/pubmed/25250133

[9] A. J. Richard, U. White, C. M. Elks, and J. M. Stephens, Adipose Tissue: Physiology to Metabolic Dysfunction. MDText.com, Inc., 2020. Accessed: Apr. 01, 2021. [Online]. Available: http://www.ncbi.nlm.nih.gov/pubmed/32255578

[10] J. Jo et al., "Hypertrophy and/or hyperplasia: Dynamics of adipose tissue growth," PLoS Comput. Biol., vol. 5, no. 3, 2009, doi: 10.1371/journal.pcbi.1000324.

[11] A. Armani et al., "Cellular models for understanding adipogenesis, adipose dysfunction, and obesity," J. Cell. Biochem, vol. 110, no. 3, pp. 564–572, 2010, doi: 10.1002/jcb.22598.

[12] Y. Ando et al., "Placental extract suppresses differentiation of 3T3-L1 preadipocytes to mature adipocytes via accelerated activation of p38 MAPK during the early phase of adipogenesis," Nutr. Metab, vol. 16, no. 1, pp. 1–13, 2019, doi: 10.1186/s12986-019-0361-8.

[13] U. White and E. Ravussin, "Dynamics of adipose tissue turnover in human metabolic health and disease," Diabetologia, vol. 62, no. 1, pp. 17–23, Jan. 2019, doi: 10.1007/S00125-018-4732X/TABLES/1.

[14] E. Danforth, "Failure of adipocyte differentiation causes type II diabetes mellitus?" vol. 26, no. september, p. 2000, 2000.

[15] P. Isakson, A. Hammarstedt, B. Gustafson, and U. Smith, "Impaired preadipocyte differentiation in human abdominal obesity: Role of Wnt, tumor necrosis factor-α, and inflammation," Diabetes, vol. 58, no. 7, pp. 1550–1557, 2009, doi: 10.2337/db08-1770.

[16] L. A. Muir et al., “Adipose tissue fibrosis, hypertrophy, and hyperplasia: correlations with diabetes in human obesity,” Obesity, vol. 24, no. 3, pp. 597–605, 2016, doi: 10.1002/oby.21377.

[17] F. Zatterale et al., “Chronic Adipose Tissue Inflammation Linking Obesity to Insulin Resistance and Type 2 Diabetes,” Front. Physiol., vol. 10, p. 1607, Jan. 2020, doi: 10.3389/fphys.2019.01607.

[18] F. Baldini et al., “Adipocyte hypertrophy parallels alterations of mitochondrial status in a cell model for adipose tissue dysfunction in obesity,” Life Sci., vol. 265, p. 118812, 2021, doi: 10.1016/j.lfs.2020.118812.

[19] T. Kawai, M. V. Autieri, and R. Scalia, “Adipose tissue inflammation and metabolic dysfunction in obesity,” Am. J. Physiol. - Cell Physiol., vol. 320, no. 3, pp. C375–C391, Mar. 2021, doi: 10.1152/AJPCELL.00379.2020/ASSET/IMAGES/LARGE/AJ-ACEL210014F002.JPEG.

[20] Y. T. Lagerros and S. Rössner, “Obesity management: What brings success?” Therap. Adv. Gastroenterol., vol. 6, no. 1, pp. 77–88, 2013, doi: 10.1177/1756283X12459413.

[21] D. K. Patel and F. C. Stanford, “Safety and tolerability of new-generation anti-obesity medications: a narrative review” Postgrad. Med., vol. 130, no. 2, pp. 173–182, Mar. 2018, doi: 10.1080/00325481.2018.1435129.

[22] R. Kassir et al., “Complications of bariatric surgery: Presentation and emergency management,” Int. J. Surg., vol. 27, pp. 77–81, Mar. 2016, doi: 10.1016/J.IJSU.2016.01.067.

[23] S. M. Barbalho et al., “The Effects of Curcumin on Diabetes Mellitus : A Systematic Review,” Front. Endocrinol. (Lausanne), vol. 12, no. May, p. 443, May 2021, doi: 10.3389/fendo.2021.669448.

[24] V. Soleimani, A. Sahebkar, and H. Hosseinzadeh, “Turmeric (Curcuma longa) and its major constituent (curcumin) as nontoxic and safe substances: Review,” Phyther. Res., vol. 32, no. 6, pp. 985–995, Jun. 2018, doi: 10.1002/ptr.6054.

[25] D. J. Den Hartogh et al., “Antidiabetic Properties of Curcumin I: Evidence from *In vitro* Studies,” Nutrients, vol. 12, no. 1, pp. 1–32, Jan. 2020, doi: 10.3390/nu12010118.

[26] A. Amalraj, A. Pius, S. Gopi, and S. Gopi, “Biological activities of curcuminoids, other biomolecules from turmeric and their derivatives – A review,” J. Tradit. Complement. Med., vol. 7, no. 2, pp. 205– 233, Apr. 2017, doi: 10.1016/J.JTCME.2016.05.005.

[27] S. J. S. S. J. Hewlings, D. S. Kalman, D. K.- Foods, undefined 2017, and D. S. Kalman, “Curcumin: A review of its effects on human health,” Foods, vol. 6, no. 10, p. 92, Oct. 2017, doi: 10.3390/FOODS6100092.

[28] S. Rivera-Mancía, J. Trujillo, and J. P. Chaverri, “Utility of curcumin for the treatment of diabetes mellitus: Evidence from preclinical and clinical studies,” J. Nutr. Intermed. Metab, vol. 14, pp. 29–41, 2018, doi: 10.1016/j.jnim.2018.05.001.

[29] F. J. Alsharif and Y. A. Almuhtadi, “The effect of curcumin supplementation on anthropometric measures among overweight or obese adults,” Nutrients, vol. 13, no. 2, pp. 1–14, 2021, doi: 10.3390/nu13020680.

[30] K. Kasprzak-Drozd, T. Oniszczuk, M. Gancarz, A. Kondracka, R. Rusinek, and A. Oniszczuk, “Curcumin and Weight Loss: Does It Work?,” Int. J. Mol. Sci., vol. 23, no. 2, p. 639, Jan. 2022, doi:

10.3390/ijms23020639.

[31] A. Alalaiwe, J.-Y. J. Y. Fang, H.-J. H. J. Lee, C. H. C.-H. Chiu, and C. Y. C.-Y. Hsu, "The demethoxy derivatives of curcumin exhibit greater differentiation suppression in 3T3-L1 adipocytes than curcumin: A mechanistic study of adipogenesis and molecular docking," Biomolecules, vol. 11, no. 7, pp. 1–18, Jul. 2021, doi: 10.3390/biom11071025.

[32] R. Varì, B. Scazzocchio, A. Silenzi, C. Giovannini, and R. Masella, "Obesity-associated inflammation: Does curcumin exert a beneficial role?" Nutrients, vol. 13, no. 3, pp. 1–13, 2021, doi: 10.3390/nu13031021.

[33] T. Islam et al., "Curcumin Reduces Adipose Tissue Inflammation and Alters Gut Microbiota in Diet-Induced Obese Male Mice" Mol. Nutr. Food Res., vol. 65, no. 22, p. e2100274, Nov. 2021, doi: 10.1002/mnfr.202100274.

[34] L. Wang, B. Zhang, F. Huang, B. Liu, and Y. Xie, "Curcumin inhibits lipolysis via suppression of ER stress in adipose tissue and prevents hepatic insulin resistance," J. Lipid Res., vol. 57, no. 7, pp. 1243–1255, Jul. 2016, doi: 10.1194/JLR.M067397.

[35] S. L. Wang et al., "Curcumin, a potential inhibitor of Up-regulation of TNF-alpha and IL6 induced by palmitate in 3T3-L1 adipocytes through NF-kappaB and JNK pathway," Biomed. Environ. Sci., vol. 22, no. 1, pp. 32–39, Feb. 2009, doi: 10.1016/S0895-3988(09)60019-2.

[36] J. C. Schell et al., "Control of intestinal stem cell function and proliferation by mitochondrial pyruvate metabolism," Nat. Cell Biol., vol. 19, no. 9, pp. 1027–1036, Sep. 2017, doi: 10.1038/ncb3593.

[37] Y. Pan et al., "Curcumin improves glycolipid metabolism through regulating peroxisome proliferator activated receptor γ signalling pathway in high-fat diet-induced obese mice and 3T3-L1 adipocytes," R. Soc. Open Sci., vol. 4, no. 11, p. 170917, Nov. 2017, doi: 10.1098/rsos.170917.

[38] M. Zintle, V. Khwaza, and A. A. Blessing, "Curcumin and Its Derivative agents in Prostate, Colon and Breast Cancers," 2019.

[39] S. Oliveira, T. Monteiro-Alfredo, S. Silva, and P. Matafome, "Curcumin derivatives for Type 2 Diabetes management and prevention of complications," Arch. Pharm. Res., vol. 43, no. 6, pp. 567–581, Jun. 2020, doi: 10.1007/s12272-020-01240-3.

[40] F. Olotu, C. Agoni, O. Soremekun, and M. E. S. Soliman, "An Update on the Pharmacological Usage of Curcumin: Has it Failed in the Drug Discovery Pipeline?" Cell Biochem. Biophys. vol. 78, no. 3, pp. 267–289, Jun. 2020, doi: 10.1007/s12013-020-00922-5.

[41] E. Ooko et al., "Modulation of P-glycoprotein activity by novel synthetic curcumin derivatives in sensitive and multidrug-resistant T-cell acute lymphoblastic leukemia cell lines," Toxicol. Appl. Pharmacol., vol. 305, pp. 216–233, Aug. 2016, doi: 10.1016/j.taap.2016.06.002.

[42] L. T. Marton et al., "The Effects of Curcumin on Diabetes Mellitus: A Systematic Review," Front. Endocrinol. (Lausanne). vol. 12, no. May, May 2021, doi: 10.3389/fendo.2021.669448.

[43] N. Ghalandarlaki, A. M. Alizadeh, and S. Ashkani-esfahani, "Nanotechnology-Applied Curcumin for Different Diseases Therapy," vol. 2014, 2014, doi: 10.1155/2014/394264.

[44] J. Lone, J. H. Choi, S. W. Kim, and J. W. Yun, "Curcumin induces brown fat-like phenotype in 3T3-L1 and primary white adipocytes," J. Nutr. Biochem, vol. 27, pp. 193–202, Jan. 2016, doi: 10.1016/j.jnutbio.2015.09.006.

[45] N. Maithilikarpagaselvi, M. G. Sridhar, R. P. Swaminathan, R. Sripradha, and B. Badhe, "Curcumin inhibits hyperlipidemia and hepatic fat accumulation in high-fructose-fed male Wistar rats.," Pharm. Biol., vol. 54, no. 12, pp. 2857–2863, Dec. 2016, doi: 10.1080/13880209.2016.1187179.

[46] C. Y. Kim, T. T. Le, C. Chen, J. X. Cheng, and K. H. Kim, "Curcumin inhibits adipocyte differentiation through modulation of mitotic clonal expansion," J. Nutr. Biochem, vol. 22, no. 10, pp. 910–920, Oct. 2011, doi: 10.1016/j.jnutbio.2010.08.003.

[47] A. L. Lopresti, "The problem of curcumin and its bioavailability: Could its gastrointestinal influence contribute to its overall health-enhancing effects?" Advances in Nutrition, vol. 9, no. 1. Elsevier, pp. 41–50, Jan. 01, 2018. doi: 10.1093/advances/nmx011.

[48] M. T. Moetlediwa, R. Ramashia, C. Pheiffer, S. J. J. Titinchi, S. E. Mazibuko-Mbeje, and B. U. Jack, "Therapeutic Effects of Curcumin Derivatives against Obesity and Associated Metabolic Complications: A Review of *In vitro* and *In vivo* Studies," Int. J. Mol. Sci., vol. 24, no. 18, p. 14366, Sep. 2023, doi: 10.3390/ijms241814366.

[49] A. E. Harvey, L. M. Lashinger, and S. D. Hursting, "The growing challenge of obesity and cancer: an inflammatory issue," Ann. N. Y. Acad. Sci., vol. 1229, no. 1, pp. 45–52, Jul. 2011, doi: 10.1111/j.17496632.2011.06096.x.

[50] O. A. Maguire et al., "Creatine-mediated crosstalk between adipocytes and cancer cells regulates obesity-driven breast cancer," Cell Metab., vol. 33, no. 3, pp. 499-512.e6, Mar. 2021, doi: 10.1016/j.cmet.2021.01.018.

[51] A. R. Saltiel and J. M. Olefsky, "Inflammatory mechanisms linking obesity and metabolic disease," J. Clin. Invest, vol. 127, no. 1, pp. 1–4, 2017, doi: 10.1172/JCI92035.

[52] I. Patimah, M. S. Ellulu, H. Khaza'ai, A. Rahmat, and Y. Abed, "Obesity and inflammation: the linking mechanism and the complications," Arch Med Sci, vol. 13, pp. 851–863, 2017, doi: 10.5114/aoms.2016.58928.

[53] J. Xiao et al., "Obesity promotes lipid accumulation in lymph node metastasis of gastric cancer: a retrospective case–control study," Lipids Health Dis., vol. 21, no. 1, p. 123, Nov. 2022, doi: 10.1186/s12944-022-01734-7.

[54] J. Barbi et al., "Visceral Obesity Promotes Lung Cancer Progression—Toward Resolution of the Obesity Paradox in Lung Cancer," J. Thorac. Oncol, vol. 16, no. 8, pp. 1333–1348, Aug. 2021, doi: 10.1016/j.jtho.2021.04.020.

CHAPTER 2

Chapter outline:

This chapter is presented as a review article that provides a comprehensive review of the literature on *in vitro* and *in vivo* studies evaluating the effects of curcumin and synthetic curcumin derivatives against obesity and

obesityassociated complications. The article is written adhering to the International Journal of Molecular Sciences guidelines and formats.

Status: (Published)

Review article published in the International Journal of Molecular Sciences, 2023, 24, 18:14366, doi: https://doi.org/10.3390/ijms241814366

Therapeutic Effects of Curcumin Derivatives against Obesity and Associated

Metabolic Complications: A Review of *In vitro* and *In vivo* Studies

Marakiya T. Moetlediwa [1,2], Rudzani Ramashia [1,3], Carmen Pheiffer [1,3,4], Salam J. J. Titinchi [5], Sithandiwe E. Mazibuko-Mbeje [2] and Babalwa U. Jack [1,*]

[1] Biomedical Research and Innovation Platform, South African Medical Research Council, Tygerberg 7505, South Africa; marakiya.moetlediwa@mrc.ac.za (M.T.M.); rudzani.ramashia@mrc.ac.za (R.R.); carmen.pheiffer@mrc.ac.za (C.P.)

[2] Department of Biochemistry, North-West University, Mmabatho 2745, South Africa; sithandiwe.mazibukombeje@nwu.ac.za

[3] Centre for Cardio-Metabolic Research in Africa (CARMA), Division of Medical Physiology, Faculty of Medicine and Health Sciences, University of Stellenbosch, Tygerberg 7505, South Africa.

[4] Department of Obstetrics and Gynaecology, Faculty of Health Sciences, University of Pretoria, Pretoria 0001, South Africa.

[5] Department of Chemistry, Faculty of Natural Science, University of the Western Cape, Bellville 7535, South Africa; stitinchi@uwc.ac.za

* Correspondence: babalwa.jack@mrc.ac.za; Tel.: +27-219-380-336

Abstract

Obesity is a major cause of morbidity and mortality globally, increasing the risk for chronic diseases. Thus, the need to identify more effective anti-obesity agents has spurred significant interest in the health-promoting properties of natural compounds. Of these, curcumin, the most abundant and bioactive constituent of turmeric, possesses a variety of health benefits including anti-obesity effects. However, despite its anti-obesity potential, curcumin has demonstrated poor bioavailability, which limits its clinical applicability. Synthesizing curcumin derivatives, which are structurally modified analogs of curcumin, has been postulated to improve bioavailability while maintaining therapeutic efficacy. This review summarizes *in vitro* and *in vivo* studies that assessed the effects of curcumin derivatives against obesity and its associated metabolic complications. We identified eight synthetic curcumin derivatives that were shown to ameliorate obesity and metabolic dysfunction in diet-induced obese animal models, while five of these derivatives also attenuated obesity and associated metabolic complications in cell culture models. These curcumin derivatives modulated adipogenesis, lipid metabolism, insulin resistance, steatosis, lipotoxicity, inflammation, oxidative stress, endoplasmic reticulum stress, apoptosis, autophagy, fibrosis, and dyslipidemia to a greater extent than curcumin. In conclusion, the findings from this

review show that compared to curcumin, synthetic curcumin derivatives present potential candidates for further development as therapeutic agents to modulate obesity and obesity-associated metabolic complications.
Keywords: curcumin; curcumin derivatives; synthetic compounds; curcuminoids; obesity; obesity-associated complications.

Introduction

Obesity is considered a public health crisis, with its prevalence rapidly increasing over the past few decades [1]. Currently, it is estimated that 13% (650 million) of the global adult population is obese (body mass index [BMI] $\geq$ 30 kg/m^2), with the prevalence projected to reach 20% by 2045 if no effective therapeutic interventions are established [2]. Obesity is associated with metabolic disorders including insulin resistance [3], inflammation [4], lipotoxicity [5], dyslipidemia [6], and non-alcoholic fatty liver disease (NAFLD) [7]. As such, obesity is considered the major risk factor for the development of non-communicable diseases such as type 2 diabetes (T2D) [8], cardiovascular disease (CVD) [9], and certain types of cancers [10]. Effective therapeutic agents are needed to decrease the burden of obesity and its associated complications.

Obesity is characterized by the excessive accumulation of fat due to an imbalance between energy intake and energy expenditure [11]. Consequently, lifestyle modifications that include reduced caloric consumption and increased physical activity are the primary anti-obesity treatment strategies [12]. However, adherence to lifestyle modifications is poor, leading to an increased reliance on pharmaceutical agents to treat obesity. The use of antiobesity drugs is plagued with adverse effects such as cardiovascular effects, stroke, cancer, and psychiatric disorders among others [13], and many have been withdrawn from the market [14]. Bariatric surgery, although shown to be an effective anti-obesity strategy, is recommended for morbidly obese individuals only (BMI $\geq$ 40 kg/m^2) and is associated with post-surgical complications [15]. This indicates the need for the development of safer and more effective therapeutic agents to overcome the limitations associated with current anti-obesity intervention strategies.

Accumulating evidence has demonstrated that natural compounds derived from plant sources are effective in treating obesity and its associated metabolic complications. One such natural compound is curcumin, the main bioactive and abundant compound found in the rhizome of the turmeric (*Curcuma longa*) plant, which is used for culinary and medicinal purposes globally [16]. Curcumin has been extensively studied for many years with several

beneficial health effects being demonstrated. Of relevance to this review, studies have reported antioxidant and anti-inflammatory [17], hepatoprotective [18], cardioprotective [19], anti-diabetic [20], and anti-obesity [21] properties, without any toxicity being displayed [16]. Despite curcumin's potential as an anti-obesity therapeutic, its poor bioavailability due to its low absorption, rapid metabolism, and extensive elimination following oral administration limits its clinical applicability [22,23]. To address these challenges, research efforts have focused on the development and evaluation of curcumin derivatives as strategies to improve bioavailability and biological efficacy [24]. Curcumin derivatives, which are structural analogs of curcumin, have been shown to display an improved pharmacokinetic profile, enhanced bioavailability, and improved delivery to target sites when compared to the parent curcumin compound [25–27]. In addition, these derivatives possess anti-cancer [28], anti-diabetic [29], antioxidant [30], and anti-inflammatory [31] efficacy.

Several experimental studies have evaluated the effects of curcumin derivatives to treat obesity and its associated metabolic complications. However, there is no clear indication of the efficacy of these compounds especially when compared to curcumin and their potential clinical application. Hence, in this review, we summarize and critically assess *in vitro* and *in vivo* studies that have evaluated the therapeutic efficacy of curcumin derivatives against obesity and associated metabolic disorders. Moreover, if data were available, we compared the bioactivity of curcumin and its derivatives in these experimental models. The search strategy was developed using three major search databases including PubMed, Web of Science, and SCOPUS. Search terms included "curcumin derivatives", "obesity", and "obesity associated metabolic disease", and relevant synonyms per search term were used. The search of the literature was conducted from inception until May 2023. Only *in vitro* and *in vivo* experimental studies that used synthetic curcumin derivatives with or without pure-form curcumin were selected for further review. Studies assessing curcumin formulations and curcumin metabolites or adjuvants of curcumin and review articles and clinical studies were excluded from this review. Two authors independently conducted the search of the literature and data analysis.

Physiochemical, structural, and biological properties of curcumin

Curcumin, also known as diferuloylmethane, is a natural polyphenolic compound originally derived from the rhizome of turmeric (*Curcuma longa*) (Figure 2.1) and other Curcuma spp. [16]. Curcumin was first discovered in 1815 [32] and isolated in 1842 [33] by Henri Auguste Vogel and Pierre Joseph Pelletier. Its chemical structure was first characterized as a diferuloylmethane or (1E,6E)-1,7-bis[4-hydroxy-3-methoxyphenyl]-1,6-

heptadiene3,5-dione in 1910 [34], whilst it was first synthesized in 1913 [35]. Curcumin is an orange-yellow crystalline powder, with a chemical formula of C21H20O6, a molecular weight of 368.38 g/mol, and a melting temperature of 183 °C [36]. It is a hydrophobic molecule with a partition coefficient or logP value of approximately 3.0 that is not soluble in water, but only in solvents such as dimethyl sulfoxide, ethanol, methanol, chloroform, acetonitrile, and ethyl acetate [36]. The chemical structure of curcumin is a bis-α,β-unsaturated β-diketone that consists of two aromatic rings, each comprising one hydroxy and one methoxy substituent that are connected by a seven-carbon linker chain consisting of an α,β-unsaturated β-diketone moiety [36, 37]. The β-diketone moiety is subject to keto– enol tautomerization with the keto form being predominant under neutral and acidic conditions, while the enol form is predominant in alkaline solutions (Figure 2.2) [38]. Curcumin, which makes up 60–70% of curcuminoid extract, co-exists with other curcuminoids, including demethoxycurcumin or 1-(4-hydroxy-3-methoxyphenyl)-7(4-hydroxyphenyl)-1,6-heptadiene-3,5-dione, constituting 20–27% of curcuminoid extract, and bisdemethoxycurcumin or 1,7-bis(4-hydroxyphenyl)-1,6-heptadiene-3,5-dione, constituting 10–15% of curcuminoid extract (Figure 2.1) [39].

Turmeric has long been used as a traditional medicinal herb to treat various ailments such as wound healing, dermatological diseases, pneumonia, hepatic disorders, coughs, and arthritis [40]. Curcumin itself is known to possess several biological and pharmacological activities including anti-microbial, anti-fungal, anti-viral, antioxidant, anti-cancer, anti-inflammatory, anti-diabetic, and anti-obesity effects, as well as cardioprotective and neuroprotective properties [41]. Many studies have reported that the anti-obesity effects of curcumin are mediated by inhibiting adipogenesis, regulating lipid metabolism, stimulating energy expenditure, and improving gut microbiota as recently reviewed [42]. In addition, curcumin ameliorates obesity-associated metabolic disorders including insulin resistance, inflammation, oxidative stress [43], dyslipidemia, NAFLD [44], CVD [45], T2D [46], and various cancer types [47]. Curcumin has a long-established safety record with a GRAS (generally recognized as safe) status from the Food and Drug Administration [48], and several studies have shown that it is safe to use in animals and humans, even at doses up to 8 g/day [49].

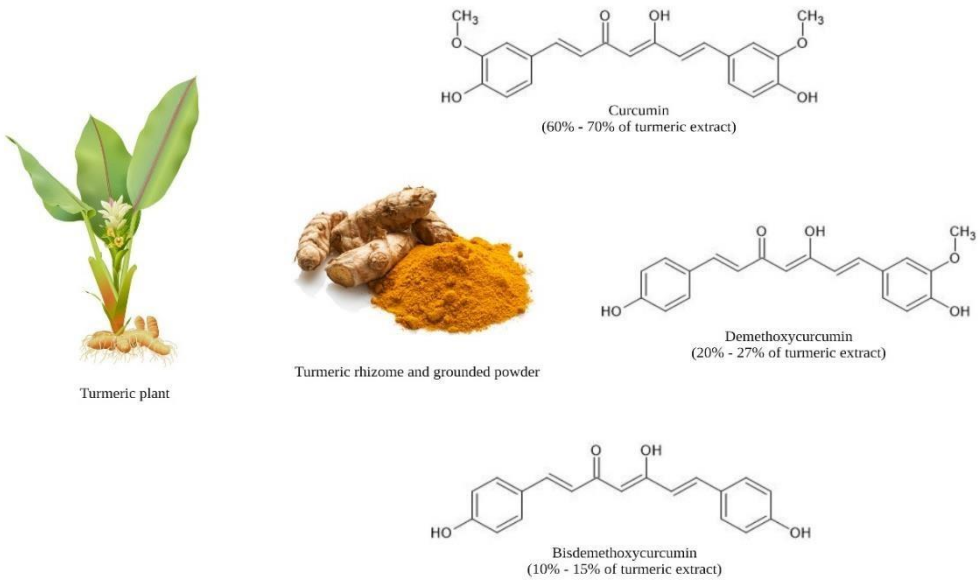


Figure 2.1: The turmeric (*Curcuma longa*) plant and rhizome, and the chemical structures of the curcuminoids including curcumin, demethoxycurcumin, and bisdemethoxycurcumin. Figure adapted and modified from Nelson et al., [39].

The pharmacokinetic profile of curcumin

Despite its efficacy and safety, several preclinical and clinical studies have shown that the pharmacokinetic profile of curcumin is unfavorable, leading to its poor bioavailability and its limited clinical applicability [22,23]. The poor bioavailability of curcumin is attributed to its low aqueous solubility and physiological instability. Curcumin has a very low aqueous solubility especially in acidic or neutral pH conditions, while at pH values above neutral it dissociates to increase its solubility but undergoes rapid degradation [50]. The major factors postulated to contribute to curcumin's low bioavailability include low gastrointestinal absorption, poor distribution, extensive metabolism, and rapid excretion [51]. Following oral administration, the majority of curcumin is excreted unchanged in the feces (≤90%), while only a small proportion is absorbed in the intestine, followed by rapid metabolism in plasma and the liver [51]. Trace amounts of orally ingested curcumin are eliminated as urinary metabolites [52].

The absorption, bioavailability, and distribution of curcumin has been extensively studied in humans and rodents. Preclinical *in vivo* studies that investigated the pharmacokinetics of curcumin in rats showed that 60–500 ng/ml

of curcumin was present in the blood following oral administration of 0.5–1 g curcumin [53], [54], indicating that only ~1% of curcumin is bioavailable [54]. Furthermore, a study conducted in healthy human subjects could not detect curcumin in serum following a single oral dose of curcumin standardized powder extract with doses ranging from 0.5 to 12 g [55]. Another study only detected the major conjugate metabolites of curcumin, including curcumin glucuronide and sulfate conjugates but not curcumin in the plasma of healthy human subjects administered either a 10 g or 12 g single dose of curcumin [56]. These studies suggest that curcumin is rapidly metabolized following oral administration and may be detected as metabolites in plasma.

The absorbed curcumin primarily undergoes rapid phase I and phase II metabolism in the hepatic and intestinal tissues [57]. Phase I metabolism occurs due to reduction reactions and leads to the reduction of curcumin to dihydrocurcumin (DHC), tetrahydrocurcumin (THC), hexahydrocurcumin (HHC), and octahydrocurcumin (OHC) by reductases, while phase II metabolism occurs due to conjugation, resulting in curcumin sulfate and curcumin glucuronide (Figure 2.2) [58]. Phase I reduced metabolites are also transformed into their corresponding glucuronide-conjugates via phase II metabolism [59]. Alternatively, curcumin metabolism also occurs in the intestinal microbiota via a nicotinamide adenine dinucleotide phosphate (NADPH) dependent reductase pathway of *Escherichia coli* to form DHC and THC [60]. Several studies have reported that curcumin metabolites possess various biological activities including antioxidant, anti-inflammatory, anti-cancer, anti-diabetic, cardioprotective, and neuroprotective effects [61]. As such, it has been suggested that the therapeutic efficacy of curcumin is facilitated by its metabolites [58]. Other than the circulation, the levels of curcumin and its metabolites, DHC and THC, were also detected in the livers and kidneys of mice following intravenous administration of curcumin, while only curcumin was found in the brain of these mice [62]. This suggests that curcumin but not its metabolites can cross the blood-brain barrier.

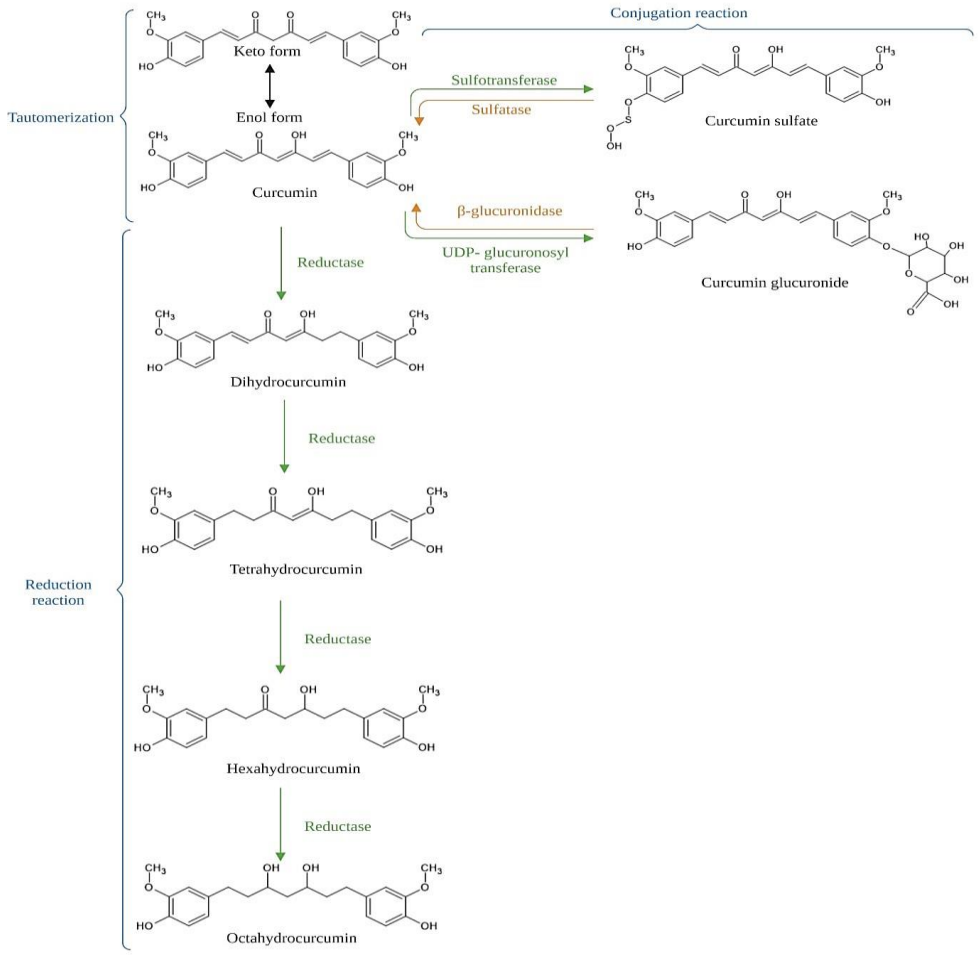


Figure 2.2. An illustration of curcumin tautomerization and metabolic pathways including the conjugation and reduction reactions. Figure adapted and modified from Pandey et al., [58].

While there is ongoing research on various pharmaceutical strategies to overcome the poor bioavailability of curcumin and subsequently improve its biological efficacy, research efforts to develop curcumin formulations to increase its solubility, improve intestinal stability and absorption route, and inhibit degradation have garnered great interest [51,63]. These formulations include various small particles such as liposomes, micelles, cyclodextrin, microgels, solid lipid nanoparticles, nanostructured lipid carriers, biopolymer nanoparticles, phospholipid complexes, microemulsions, and nano-emulsions that have been complexed with curcumin or used to encapsulate curcumin by means of either chemical or physical assembly (Figure 2.3) [64]. Although several of these curcumin formulations have been established, only a few have been tested in clinical settings using doses that are clinically relevant when compared with standard turmeric extract containing 95% curcuminoids. For instance, Fança-Berthon and colleagues compared the pharmacokinetics of curcuminoids in five different formulations including a turmeric dried colloidal suspension, a standardized turmeric extract, a liquid micellar preparation, a piperine–curcuminoid combination, and a phytosome formulation and demonstrated that low dose

(300 mg) dried colloidal suspension led to high absorption of curcuminoids (both unconjugated and conjugated) compared to a high dose (1500 mg) of standard extract [65].

Furthermore, adjunct formulations, also known as combination therapy, produced by complexing curcumin to piperine have been shown to inhibit its rapid metabolism and increase its absorption, thus improving curcumin levels in serum and enhancing its bioavailability (Figure 2.3) [66]. Other adjuvant formulations such as silibinin, quercetin, and doxorubicin have been explored and shown to improve the biological activity of curcumin (Figure 2.3) [67,68]. In addition, several studies have intensively explored the use of medicinal chemistry strategies to modify the structure of curcumin by synthesizing curcumin derivatives or analogs, thereby enhancing curcumin's bioavailability and improving its therapeutic efficacy (Figure 2.3) [69–71]. The pharmacological efficacy of curcumin derivatives is attributed to key elements in its structure [72].

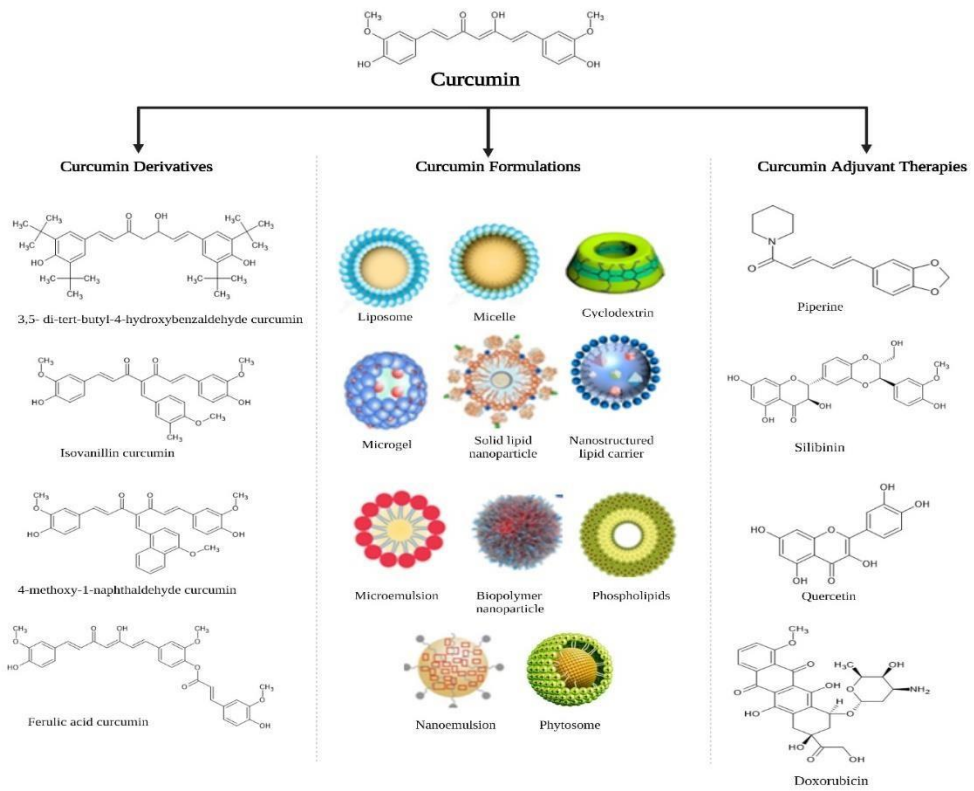


Figure 2.3: Applications of various strategies (including formulations, adjuvant therapies, and synthetic derivatives) to overcome low bioavailability of curcumin and improve its therapeutic efficacy. Images of the various formulations were obtained from Wong et al. [64] and Pastorelli et al. [73], the structures of adjuvant therapies were taken from Zhang et al. [67] and Moorthi et al. [68], and the structures of curcumin derivatives were obtained from Law et al. [74].

Efficacy of curcumin derivatives against obesity and associated metabolic complications

In the current review, we identified eight synthetic curcumin derivatives that were shown to ameliorate obesity and associated metabolic complications. All these compounds were reported using *in vivo* animal models of obesity and associated metabolic complications, while five of these derivatives were also demonstrated in the *in vitro* cell culture models of obesity and associated metabolic complications. Five of the eight curcumin derivatives reported here were shown to be more effective at ameliorating obesity and its associated metabolic complications when compared to curcumin, while the other three curcumin derivatives were not compared to curcumin.

***In vitro* studies reporting on the therapeutic effects of curcumin derivatives against obesity and associated metabolic complications**

Panzhinskiy et al. [75] evaluated a pyrazole derivative of curcumin, CNB-001 or [4-((1E)-2-(5-(4-hydroxy-3methoxystyryl-)-1-phenyl-1H-pyrazoyl-3-yl)vinyl)-2-methoxy-phenol)] previously synthesized and characterized by Liu and colleagues [76]. It was shown that CNB-001 reversed palmitic acid (PA)-induced insulin resistance by increasing the expression of the phosphorylated form of the insulin receptor (IR), insulin receptor substrate-1 (IRS-1), and protein kinase B (AKT), thereby stimulating insulin-stimulated glucose uptake in C2C12 myotubes (Table 2.1) [75]. This study did not include curcumin treatment; therefore, it was not possible to assess whether CNB-001 has improved efficacy on insulin resistance compared to curcumin.

Another pyrazole curcumin derivative, Curcumin-3,4-Dichloro Phenyl Pyrazole (CDPP), previously synthesized and shown to exhibit antioxidant, cyclooxygenase inhibitory, and anti-inflammatory effects when using non-cellbased assays [77], was evaluated for its effects on adipogenesis and lipogenesis *in vitro* in differentiating 3T3-L1 preadipocytes, C3H10T1/2 multipotential mesenchymal stem cells, human mesenchymal stem cells (hMSC), and mature 3T3-L1 adipocytes (Table 2.1) [78]. CDPP inhibited adipocyte differentiation of these cells by decreasing lipid content, particularly early-phase adipogenesis [78]. CDPP also reduced both messenger ribonucleic acid (mRNA) and protein expression of adipogenesis and lipogenesis-related genes including CCAAT/enhancerbinding protein alpha (C/EBPα), adipocyte Protein 2 (aP2), sterol regulatory element binding transcription factor 1 (SREBP1), peroxisome-proliferator-activated receptor gamma (PPARγ), and fatty acid

synthase (FAS) [78]. In addition, CDPP was shown to inhibit adipogenesis in 3T3-L1 preadipocytes by suppressing the protein kinase B/mammalian target of rapamycin (AKT/mTOR) pathway and inhibiting mitotic clonal expansion via cell cycle arrest (Table 2.1) [78]. In mature 3T3-L1 adipocytes, CDPP had no effects on lipolysis but increased oxygen consumption rate and the expression of uncoupling protein 1 (UCP1) and peroxisome-proliferator-activated receptor gamma coactivator 1 alpha (PGC1α), suggesting that CDPP increases energy utilization in these cells (Table 2.1) [78]. Interestingly, when compared to curcumin at 20 μM, this study found that CDPP at 10 and 20 μM is a potent inhibitor of adipogenesis in 3T3-L1 preadipocytes and C3H10T1/2 cells [78].

The therapeutic effect of the curcumin analog, curcumin5-8 (CUR5-8) previously synthesized by Woo et al. [79] was compared with that of curcumin *in vitro* in PA-induced murine AML12 hepatocyte cells (Table 2.1) [80]. Lee et al. [80] reported that CUR5-8 ameliorates NAFLD by reducing lipid droplet formation, decreasing SREBP1 expression, and increasing adenosine-monophosphate-activated protein kinase (AMPK) phosphorylation. CUR58 also induced autophagy by increasing microtubule-associated protein light chain 3-autophagy related 7 (LC3ATG7) expression and inhibited apoptosis by increasing B-cell lymphoma 2/Bcl-2 associated X protein (BCL-

2/BAX) ratio expression in these cells even more effectively than curcumin treatment (Table 2.1) [80].

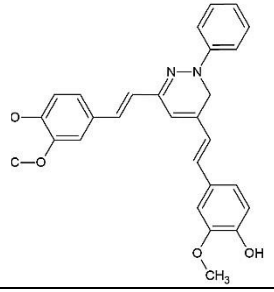
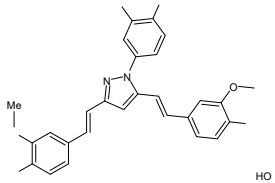
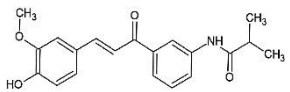
Dehydrozingerone (DHZ), (E)-4-(4-hydroxy-3-methoxyphenyl)-but-3-en-2-one, also known as the feruloylmethane half analog of curcumin, is naturally isolated from ginger (*Zingiber officinale*) and also derived through laboratory-based synthesis procedures [81]. Studies have demonstrated the protective effects of DHZ against various metabolic dysfunctions including obesity-associated skeletal muscle insulin resistance [82] and renal lipotoxicity-induced inflammation and reactive oxygen species (ROS) formation [83]. DHZ inhibited inflammatory signals and ROS production by increasing the expression of phosphorylated AMPK and reducing phosphorylated p38 mitogen activated protein kinases (p38 MAPK) expression in high glucose (HG)-induced mouse mesangial (MES-13) cells [83]. Furthermore, the treatment of PA-induced MES-13 cells with DHZ reduced lipid accumulation, decreased phosphorylated p38 MAPK, phosphorylated cAMP response element-binding protein (CREB), and cyclooxygenase 2 (COX2) expression levels (Table 2.1) [83]. Similarly, in PA exposed mouse podocytes, Lee et al. [83] showed that treatment with DHZ reduced ROS formation and exerted protective effects against cellular toxicity by regulating oxidative stress and lipid metabolism (Table 2.1). In

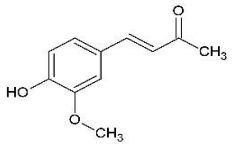
C2C12 myoblasts, DHZ activated AMPK phosphorylation and the p38 MAPK signaling pathway, upregulated glucose transporter type 4 (GLUT4) mRNA and protein expression, and increased IRS-1 and AKT phosphorylation, while in L6 myotubes DHZ improved insulin resistance by stimulating basal and insulin-stimulated glucose uptake [82].

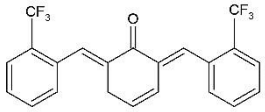
Furthermore, these *in vitro* experiments confirmed that DHZ exhibited stronger effects for AMPK phosphorylation than curcumin [82, 83].

Over the years, several monocarbonyl analogs of curcumin, including (2E,6E)-2,6-bis[2-(trifluoromethyl)benzylidene]cyclohexanone (the so-called C66 curcumin analog), have been widely synthesized and studied for their biological activities [84–87], including their potential to modulate obesity-associated metabolic complications such as obesity-induced renal injury [88] and myocardial dysfunction [89]. In cultured mouse glomerular mesangial cells (SV40-MES-13), C66 was able to attenuate the profibrotic mechanisms, apoptosis, inflammatory responses, and the nuclear factor kappa B/c-Jun N-terminal kinase (NF-κB/JNK) activated signaling pathway induced by treatment with PA (Table 2.1) [88]. Similarly, in PA-challenged H9c2 cardiomyocytes, C66 provided cardio-protection by preventing myocardial injury and apoptosis, which was accompanied by inhibition of the NF-κB/JNK activation pathway and reduced inflammation (Table 2.1) [89]. Although these studies investigated the ameliorative effects of C66 in obesity-induced renal and myocardial injuries, none of them compared the efficacy of C66 with curcumin.

Table 2.1: Summary of *in vitro* studies reporting on the therapeutic effects of curcumin derivatives on obesity and associated metabolic complications.

Curcumin Derivative	Chemical Structure	Aim, Experimental Model, Treatment Dose, and Treatment Period	Outcomes	Reference
CNB-001 [4-((1E)-2-(5-(4-hydroxy-3methoxystyryl-)-1-phenyl-1H-pyrazoyl-3-yl) vinyl)-2-methoxy-phenol]		The effect of CNB-001 on insulin resistance was examined. Mouse C2C12 myotubes were treated with 400 µM palmitic acid (PA) and co-treated with 0.1, 1, or 5 µM CNB-001 for 12 h under basal glucose and insulin-stimulated conditions (50 nM insulin, 30 min).	CNB-001 restored PA-induced insulin resistance and impaired insulin signaling by improving insulin-stimulated glucose uptake and increasing insulin-stimulated p-IR, IRS-1, and p-AKT expression levels.	[75]
Curcumin-4,4′-diyl) bis(ethene-2,1-diyl) bis(2-methoxyphenol)		3,4-Dichloro Phenyl Pyrazole (CDPP) preadipocytes, mouse C3H10T1/2 mesenchymal stem cells, and human mesenchymal stem cells (hMSC) were treated with 5, 10, and 20 µM (1E,1′E)-2,2′-(1-(3,4-dichlorophenyl)-1H-pyrazole-3,5-diyl) bis(ethene-2,1-diyl) bis(2-methoxyphenol) (7 days). Mature 3T3-L1 adipocytes were treated with 20 µM CDPP for 24 h.	CDPP inhibited adipogenesis by dose-dependently decreasing lipid accumulation, reducing C/EBPα, aP2, SREBP1c, PPARγ, and FAS mRNA and protein expression, and downregulating the AKT/mTOR pathway. In 3T3-L1 preadipocytes, CDPP inhibited mitotic clonal expansion by arresting cells at G1-phase and S-phase, decreasing Cyclin D1, Cyclin D3, CDK2, CDK4, CDK6, and p-ERK1/2 expression, and increasing p-p27 expression. CDPP increased oxygen consumption rate and UCP1 and PGC1α expression in 3T3-L1 adipocytes. Compared to curcumin, adipogenesis was significantly inhibited by CDPP.	[78]
Curcumin5-8 (CUR5-8)		The effect of CUR5-8 on hepatic steatosis was investigated. Mouse AML12 hepatocyte cells	CUR5-8 decreased PA-induced lipid droplet formation by reducing SREBP1 expression and increasing p-AMPK. CUR5-8 induced autophagy via increased expression of LC3-ATG7, and inhibited apoptosis via increased BCL-	[80]

		were treated with 250 μM PA with or without 10 μM CUR5-8 or curcumin for 24 h.	2/BAX ratio. The efficacy of CUR5-8 on increased AMPK phosphorylation and autophagy formation and reduced apoptosis was significant compared to curcumin.	
Dehydrozingerone (DHZ)	The efficacy of DHZ was evaluated on renal lipotoxicity. Differentiated mouse podocytes were	NOX-4, NRF2, HO-1, BAX, and SREBP1, and	DHZ inhibited ROS formation, reduced protein expression of	Feruloylmethane
1, 7-bis (4-hydroxy-3-methoxyphenyl)-1, 6-heptadiene-3, 5-dione	treated with 400 μM PA in the presence or absence of 20 μM DHZ for 24 h.	downregulated mRNA expression of *Tgf-β* and *Icam*. DHZ increased BCL-2 and podocin protein expression.		[83]
6-heptadiene-3, 5-dione 	The efficacy of DHZ was evaluated on renal lipotoxicity. Mouse glomerular mesangial MES-13 cells were treated with either 30 mM of high glucose (HG) or 250 μM PA in the presence or absence of 20 μM DHZ for 24 h. MES-13 cells were treated with 20 μM DHZ or 20 μM curcumin for 24 h.		DHZ reduced HG-induced ROS production and inflammatory signals by increasing p-AMPK and reducing pp38 MAPK expression. DHZ decreased PA-induced lipid accumulation, decreased p-p38 MAPK, p-CREB, and COX2 expression, and increased p-AMPK activation. The p-AMPK expression was significantly higher in DHZ-treated cells compared with curcumin.	
	The effect of DHZ on the metabolic profile of skeletal muscle was evaluated. Mouse C2C12 myoblasts were treated with 1, 3, 10, 30, or 100 μM DHZ for either 0.1, 0.5, 1, 3, 6, 12, or 24 h. Rat L6 skeletal muscle myotubes were treated with 1, 3, 10, or 30 μM DHZ for 1 h in the presence or absence of 100 nM insulin.		DHZ increased the activation of p-AMPK and p-p38 MAPK signal pathways in C2C12 cells. DHZ upregulated GLUT4, p-IRS-1, and p-AKT expression in C2C12 cells. DHZ induced basal and insulin-stimulated glucose uptake in L6 myotubes. Compared with curcumin, p-AMPK expression was significantly higher in DHZ treated C2C12 cells.	[82]

C66 (2E,6E)-2,6-bis (2-(tri-fluoromethyl)benzylidene) cyclohexanone		C66 attenuated PA-induced fibrosis by reducing mRNA and protein expression of TGF-β, Col-IV, and MMP-9. C66 The protective effect of C66 on renal ameliorated PA-induced apoptosis by reducing apoptotic lipotoxicity and injury was investigated. Mouse positive cells, decreasing BAX and cleaved caspase-3 glomerular mesangial SV40-MES-13 cells expression, and increasing BCL-2 expression. C66 protected were pre-treated with 2.5, 5, and 10 μM C66 against PA-induced inflammation by reducing NF-κB/JNK for 2 h followed by treatment with 200 μM PA activation via increased IκBα accumulation, reduced p65 for 2, 12, or 24 h. phosphorylation and translocation to the nucleus, and reduced JNK phosphorylation. C66 reduced TNFα, IL-6, and IL-1β secretion levels and mRNA expression.	[88]
		C66 prevented PA-induced hypertrophy and fibrosis by reducing MyHC, ANP, BNP, TGF-β, Col-I, and MMP-9 mRNA and protein expression. C66 reduced PA-induced The protective effect of C66 on cardiomyocyte apoptosis by decreasing positive apoptotic cells, reducing dysfunction was tested. Rat embryonic heart- expression of cleaved caspase-3 and BAX, and increasing derived H9c2 cells were pre-treated with 2.5, 5, BCL-2 expression. C66 ameliorated PA-induced and 10 μM C66 for 2 h, then treated with 200 μM inflammation by reducing NF-κB activation via reduced p65 PA for 24 h. phosphorylation and translocation to the nucleus and increased IκBα accumulation. C66 also reduced JNK activation and decreased *Tnfα, Il-6, Il-1β, Vcam-1, and Icam1* mRNA expression.	[89]

Abbreviations: ANP: A-type natriuretic peptide; aP2: adipocyte Protein 2; ATG7: autophagy related 7; BAX: Bcl-2 associated X protein; BCL-2: B-cell lymphoma 2; BNP: B-type natriuretic peptide; C/EBPα: CCAAT/enhancer-binding protein alpha; CDK2/4/6: cyclin-dependent kinase 2/4/6; CDPP: Curcumin-3:4-Dichloro Phenyl Pyrazole; Col-I: collagen type-I; Col-IV: collagen type-IV; COX2: cyclooxygenase 2; CUR5-8: Curcumin5-8; DHZ: Dehydrozingerone; FAS: fatty acid synthase; GLUT4: glucose transporter type 4; HG: high glucose; hMSC: human mesenchymal stem cell; HO-1: heme oxygenase-1; ICAM-1: intercellular adhesion molecule-1; IL-1β: interleukin 1 beta; IL–6: interleukin 6; IκBα: inhibitor of nuclear factor kappa B; JNK: c-Jun N-terminal kinase; LC3: light chain 3; MMP-9: matrix Metallopeptidase 9; mRNA: messenger ribonucleic acid; mTOR: mammalian target of rapamycin; MyHC: myosin heavy chain; NF-κB: nuclear factor kappa B; NOX-4: NADPH oxidase-4; NRF2: nuclear factor erythroid 2–related factor 2; p38 MAPK: p38 mitogen-activated protein kinases; p65: nuclear factor kappa B subunit; PA: palmitic acid; p-AKT: phosphorylated protein kinase B; p-AMPK: phosphorylated adenosine monophosphate-activated protein kinase; p-CREB: phosphorylated cAMP response element-binding protein; p-ERK1/2: phosphorylated extracellular signal-regulated protein kinases 1 and 2; PGC1α: peroxisome proliferator-activated receptor gamma coactivator 1 alpha; p-IR: phosphorylated insulin

receptor; p-IRS-1: phosphorylated insulin receptor substrate-1; PPARγ: peroxisome proliferator-activated receptor gamma; ROS: reactive oxygen species; SREBP1: sterol regulatory element binding transcription factor 1; TGF-β: transforming growth factor beta; TNFα: tumor necrosis factor alpha; UCP1: uncoupling protein 1; VCAM-1: vascular cell adhesion molecule-1.

In vivo studies reporting on the therapeutic effects of curcumin derivatives on obesity-associated metabolic complications

An ortho-hydroxyl group-substituted analog of curcumin (known as salicylcurcumin), previously synthesized [90] and reported to be effective in treating skin tumors compared to other curcuminoids such as curcumin [91], was evaluated for its efficacy to ameliorate alcohol and polyunsaturated fatty acids (PUFAs)-induced hyperlipidemia when compared to curcumin [92]. It was shown that salicylcurcumin reduced cholesterol, triglycerides (TGs), FFAs, and phospholipids (PLs) plasma levels (Table 2.2) [92]. Furthermore, salicylcurcumin treatment was demonstrated to be more effective in attenuating the circulating lipid profiles than curcumin in this study [93].

In high fat diet (HFD)-fed mice, CNB-001 treatment reversed obesity-associated metabolic complications by reducing body weight gain, decreasing overall adiposity, and increasing energy expenditure (Table 2.2) [75]. In addition, CNB001 ameliorated hepatic steatosis while decreasing serum triglyceride and interleukin 6 (IL-6) levels. Furthermore,
CNB-001 improved glucose tolerance and insulin resistance and increased *ex vivo* gastrocnemius muscle glucose uptake (Table 2.2) [75]. At the molecular level, CNB-001 restored insulin signaling by inducing the phosphorylation of AKT and IR, attenuated endoplasmic reticulum (ER) stress by decreasing eukaryotic initiation factor 2 alpha (eIF2α) phosphorylation and glucose-regulated protein 78 (GRP78) expression, and reduced protein tyrosine phosphatase 1B (PTP1B) expression in the gastrocnemius muscles of HFD-fed mice (Table 2.2) [75]. While CNB-001 treatment had no significant effect in the low-fat diet (LFD)-fed mice, this study did not assess whether CNB-001 has improved efficacy compared to curcumin [75].

Another novel monocarbonyl curcumin analog, (2E,6E)-2-(2-bromobenzylidene)-6-(2-(trifluoromethyl) benzylidene) cyclohexanone (Y20), was designed and synthesized by Qian and colleagues via structural modification of the C66 curcumin analog by substituting one of the trifluoromethyls with a bromine [94]. Y20 was hypothesized to possess dual anti-inflammatory and antioxidant properties, hence being investigated for its cardioprotective effects in obese rats induced by HFD [94]. It was reported that Y20 attenuated HFD-induced myocardial inflammation by reducing the expression of cardiac pro-inflammatory markers including tumor necrosis factor alpha (TNFα), cluster of differentiation 68 (CD68), *Il-6*, interleukin 1 beta (*Il-1β*), and cyclooxygenase-2 (*Cox-2*) (Table 2.2) [94]. Y20 also ameliorated HFD-induced myocardial inflammation by

reducing the expression of cell adhesion molecules including vascular cell adhesion molecule-1 (VCAM-1) and intercellular adhesion molecule-1 (*Icam-1*) while reversing the degradation of inhibitor of nuclear factor kappa B (IκB) (Table 2.2) [94].

The administration of Y20 reversed HFD-induced cardiac oxidative stress by reducing superoxide anion production and 3-nitrotyrosine (3-NT) accumulation and increasing the expression of nuclear factor erythroid 2–related factor 2 (NRF2) and its downstream antioxidant genes, including heme oxygenase-1 (*Ho-1*), and NADPH quinone dehydrogenase 1 (*Nqo-1*) (Table 2.2) [94]. Moreover, these authors suggested that the attenuation of myocardial inflammation and oxidative stress by Y20 treatment subsequently improved cardiac remodeling by reducing hypertrophy, fibrosis, and apoptosis, although decreased body weight gain and serum TGs levels may also partially contribute to the cardioprotective effects of Y20 (Table 2.2) [94]. Interestingly, data from this study demonstrated that Y20 exhibited more anti-inflammatory, antioxidant, anti-fibrosis, and anti-apoptotic effects than curcumin, even at a lower dose (20 mg/kg for Y20 vs. 50 mg/kg for curcumin) [94].

Similarly to the *in vitro* data, Gupta and et al. also demonstrated the ameliorative effects of the curcumin derivative CDPP on obesity and dyslipidemia in an HFD-fed Syrian golden hamster model [78]. This was mediated by significant reductions in body weight gain and reduced serum TGs, total cholesterol (TC), and low-density lipoprotein cholesterol (LDL-c) levels, as well as decreased TGs/high-density lipoprotein cholesterol (HDL-c) ratio (Table 2.2) [78]. The serum aspartate aminotransferase (AST) and alanine transaminase (ALT) levels were also significantly reduced, suggesting the hepatoprotective effects of CDPP (Table 2.2) [78]. CDPP also reduced liver and epididymal white adipose tissue (eWAT) weights, decreased hepatic lipid accumulation and adipocyte hypertrophy, and lowered expression of FAS, C/EBPα, aP2, and PPARγ as well as their translated proteins in eWAT, while upregulating hepatic mRNA levels of peroxisome proliferator-activated receptor alpha (*Pparα*) and liver X receptor alpha (*Lxrα*) (Table 2.2) [78]. These authors also reported that CDPP attenuated dyslipidemia by activating the reverse cholesterol transport from adipose tissue to liver via related gene expression (Table 2.2). Cumulatively, the results from this study show that CDPP was more effective in ameliorating obesity-induced dyslipidemia than curcumin [78].

The structural modification of natural compounds such as curcumin with polyethylene glycol (PEG) has been shown to improve solubility and physicochemical properties of curcumin [95]. As such, a water-soluble curcumin derivative was synthesized by conjugating two low-molecular-weight PEGs (mPEG454) via β-thioester bonds to curcumin (Curc-mPEG454) and was shown to improve water solubility (>50 mg/ml) and produce approximately 50–500 times higher serum curcumin levels and greater curcumin distribution in the liver tissue compared to curcumin [96]. Moreover, Curc-mPEG454 previously displayed potent anti-inflammatory [30], anti-fibrotic [97], antioxidant [30], anti-steatosis [95] effects. Of interest in the current review is the hepatic-lipid-lowering effect of Curc-mPEG454 in NAFLD-induced obese mice as previously reported [98]. These authors showed that treatment with Curc-mPEG454 reduced body weight, serum and liver TGs levels, and hepatic lipid accumulation in HFDinduced NAFLD mice (Table 2.2) [98]. Moreover, Curc-mPEG454 reversed HFD-induced hepatic steatosis and hypertriglyceridemia by modulating the hepatic CREB/PPARγ/cluster of differentiation 36 (CD36) pathway through the activation of CREB phosphorylation and inhibition of PPARγ and CD36 expression (Table 2.2) [98]. However, these authors did not assess whether Curc-mPEG454 has improved efficacy compared to curcumin.

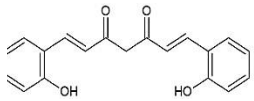
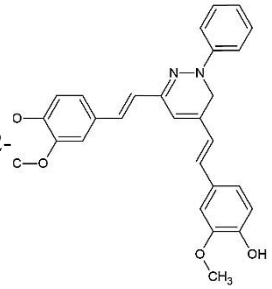
Like the *in vitro* data, Lee et al. [80] also reported ameliorative effects of CUR5-8 against NAFLD and insulin resistance in HFD-induced obese mice. In this study, treatment with CUR5-8 was shown to decrease bodyweight gain. CUR5-8 improved insulin resistance by restoring insulin sensitivity, reducing insulin levels, and lowering homeostasis model assessment-estimated insulin resistance (HOMA-IR) values (Table 2.2) [80]. In addition, CUR5-8 blocked hepatic lipogenesis and TGs accumulation by regulating the expression of lipogenic genes such as decreased FAS, SREBP1, Adipophilin, and PPARγ expression and increased phosphorylation of AMPK (Table 2.2) [80]. CUR5-8 also inhibited apoptosis by regulating autophagy-related genes such as decreased autophagy related 5 (ATG5) and increased sequestosome 1 (p62) expression (Table 2.2) [80]. CUR5-8 was shown to reduce body weight gain, enhance insulin sensitivity, and decrease fatty liver to a greater extent than curcumin in this study [80].

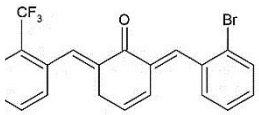
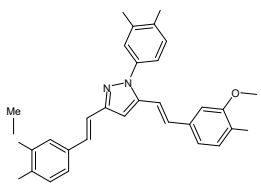
The efficacy of DHZ to ameliorate insulin resistance and renal lipotoxicity *in vivo* in animal models of obesity was also investigated [82], [83]. In HFD-fed mice, DHZ suppressed body weight gain and visceral fat accumulation while also reversing hyperglycemia by lowering plasma glucose, insulin, and leptin levels and improving glucose tolerance (Table 2.2) [82]. Treatment with DHZ also reduced liver weight and fatty liver

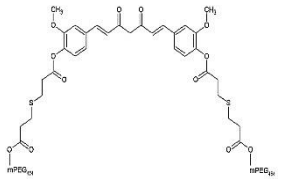
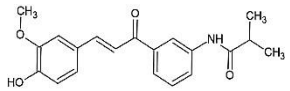
accumulation, and this was mediated by a reduction in the hepatic expression of gluconeogenic genes, including phosphoenolpyruvate carboxykinase (*Pepck*) and glucose-6-phosphatase (*G6Pase*), and the insulin resistance marker, *Fetuin* (Table 2.2) [82]. A follow-up study by Lee et al. [83] reported that DHZ decreased body weight gain and reversed HFD-induced renal damage by suppressing inflammation (Table 2.2). DHZ also ameliorated renal lipid metabolism dysregulated by HFD (Table 2.2) [83]. These studies did not compare the efficacy of DHZ to curcumin in their *in vivo* models.

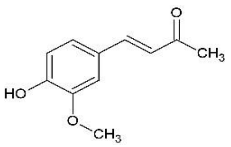
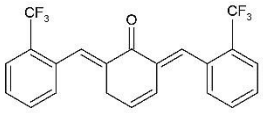
In addition to the *in vitro* studies, the protective effect of C66 on renal dysfunction [88] and myocardial injury [89] was demonstrated *in vivo* in HFD-induced obese mice. Along with reducing body weight gain, decreasing serum TGs, LDL-c, and cholesterol levels, and increasing serum HDL-c levels, treatment with C66 attenuated renal dysfunction and adverse kidney remodeling by improving renal function and suppressing kidney fibrosis (Table 2.2) [88]. In addition, C66 treatment ameliorated HFD-induced renal apoptosis and chronic inflammation via inhibiting NF-κB/JNK activation (Table 2.2) [88]. Likewise, treatment of HFD-induced obese mice with C66 decreased body weight, reduced serum levels of TGs, LDL-c, and cholesterol and increased serum HDL-c levels, while exhibiting protective effects against myocardial dysfunction and hypertrophy (Table 2.2) [89]. These authors similarly reported that C66 treatment ameliorated HFD-induced cardiac fibrosis, apoptosis, and inflammation via the inhibition of the NF-κB/JNK activation pathway (Table 2.2) [89]. The efficacy of C66 was not compared to curcumin in these studies.

Table 2.2: Summary of *in vivo* studies reporting on the therapeutic effect of curcumin derivatives on obesity and associated metabolic complications.

Curcumin Derivative	Chemical Structure	Aim, Experimental Model, Treatment Dose, and Treatment Period	Outcomes	Reference
Salicylcurcumin *O*-hydroxy-substituted analog of curcumin		The antihyperlipidemic effect of salicylcurcumin was investigated. Male albino Wistar rats were either	Salicylcurcumin reduced TC, TGs, FFAs, and PLs plasma orally administered 20% EtOH (alcohol-induced) or levels. The reduction in TC, TGs, FFAs, and PLs plasma fed 15% sunflower oil in a HFD (ΔPUFA-induced) or levels was more significant in the salicylcurcumin-treated fed a combination of both in the presence or absence groups compared to the curcumin-treated groups. of 80 mg/kg salicylcurcumin or curcumin for 45 days.	[93]
CNB-001 [4-((1E)-2-(5-(4-hydroxy-3methoxystyryl-)-1-phenyl-1H-pyrazoyl-3-yl) vinyl)-2-methoxy-phenol]		The effect of CNB-001 on obesity-induced insulin resistance was examined. Male C57BL6 mice were fed a HFD and intraperitoneally injected with CNB001 (40 mg/kg/day, except weekends) for 22 weeks.	CNB-001 reduced BW gain, adiposity, heart weight, liver weight, serum TGs, and IL-6 levels. CNB-001 increased energy expenditure, reduced fasting glucose concentrations, improved glucose tolerance and insulin sensitivity, and increased *ex vivo* gastrocnemius muscle glucose uptake. CNB-001 attenuated hepatic steatosis by decreasing lipid accumulation and hepatic TG content. CNB-001 restored insulin signaling via upregulation of p-AKT and p-IR expression, reduced ER stress via decreased p-eIF2α and GRP78 expression, and decreased PTP1B expression in gastrocnemius muscles.	[75]

Y20 (2E,6E)-2-(2bromobenzylidene)-6-(2(trifluoromethyl) benzylidene) cyclohexanone		The protective effects and underlying mechanisms of Y20 on obesity-induced cardiac injury was investigated. HFD-fed male Wistar rats were orally gavaged with 20 mg/kg Y20 or 50 mg/kg curcumin daily for 4 weeks during HFD feeding.	Y20 reduced BW gain and serum TGs levels. Y20 attenuated myocardial inflammation by decreasing the protein and mRNA expression of TNFα, CD68, IL-6, IL-1β, COX2, VCAM-1, and ICAM-1, and reversing IκB degradation. Y20 reversed cardiac oxidative stress by reducing superoxide anion production and 3-NT accumulation and increasing the protein and mRNA expression of NRF2 and its downstream antioxidant genes, *Ho-1* and *Nqo-1*. Y20 attenuated cardiac hypertrophy by decreasing cardiomyocyte size and the protein and mRNA expression of cardiac hypertrophic markers, ANP and BNP. Y20 ameliorated cardiac fibrosis by reducing Col-I synthesis and deposition and decreasing the protein and mRNA expression of Col-1, TGF-β, MMP-2, and MMP-9. Y20 reversed myocardial apoptosis by reducing the percentage of apoptotic cardiac cells, increasing BCL-2 expression, and decreasing BAX and cleaved PARP expression levels. Y20 exhibited more anti-inflammatory, antioxidant, anti-fibrosis, and anti-apoptotic efficacy than curcumin.	[94]
Curcumin-3,4-Dichloro Phenyl Pyrazole (CDPP) 4,4′-(1E,1′E)-2,2′-(1-(3,4-dichlorophenyl)-1H-pyrazole-3,5-diyl)bis(ethene-2,1-diyl)bis(2-methoxyphenol)		The role of CDPP was evaluated on obesity-induced dyslipidemia. Male Syrian golden hamsters were fed a HFD for 4 days then orally administered either 100 mg/kg CDPP or curcumin daily for 7 days during	CDPP reduced BW gain and serum levels of TGs, TC, LDL-c, ALT, AST, and the TGs/HDL-c ratio. CDPP decreased serum AST and ALT levels. CDPP reduced liver weight, decreased hepatic lipid accumulation, and upregulated hepatic *Pparα* and *Lxrα* mRNA expression. CDPP decreased eWAT weight, adipocyte hypertrophy, and reduced the expression of FAS, C/EBPα, aP2, and PPARγ in eWAT. CDPP activated reverse cholesterol transport	[78]

diyl) bis(ethene-2,1-diyl) bis(2-methoxyphenol)	°HFD feeding.	machinery from adipose tissue to liver by increasing *Abca1* expression in	HO and *Srb1* and decreasing *Abcg1* mRNA eWAT, and increasing hepatic *Abcg8*, *Lcat*, *Cyp7a1*, and *Srb1* mRNA expression. The efficacy of CDPP in ameliorating dyslipidemia was more significant compared to curcumin.	
Curc-mPEG454 PEGylated curcumin derivative		The effects of Curc-mPEG454 on obesity-associated hepatic steatosis was evaluated. HFD-fed male C57BL/6J mice were intraperitoneally injected every day with 50 and 100 mg/kg Curc-mPEG454 for 16 weeks during HFD feeding.	Curc-mPEG45 lowered BW gain and serum TGs levels. Curc-mPEG454 reduced hepatic steatosis by decreasing TGs content, decreasing lipid accumulation, and attenuating macrovesicular and microvesicular steatosis. Curcother mPEG454 reduced hepatic PPARγ and CD36 protein and mRNA expression. Curc-mPEG454 activated hepatic pCREB.	[98]
Curcumin5-8 (CUR5-8)		The effect of CUR5-8 on obesity-associated hepatic steatosis and insulin resistance was investigated. Male C57BL/6 mice were fed a HFD chow mixed with either CUR5-8 or curcumin (100 mg/kg/day) for 13 weeks.	CUR5-8 reduced BW gain without suppressing appetite. CUR5-8 reversed insulin resistance by improving insulin sensitivity, lowering serum insulin levels, and reducing the HOMA-IR index. CUR5-8 protected the liver by decreasing liver weight, reducing fatty liver and TG accumulation, and reducing serum levels of ALT. CUR5-8 regulated hepatic lipid metabolism by decreasing FAS, SREBP1, adipophilin, and PPARγ mRNA and protein expression and increasing p-AMPK expression. CUR5-8 regulated autophagy in the liver by decreasing ATG5 and increasing p62 expression. CUR5-8 reduced apoptosis in the liver by decreasing cleaved caspase-3 staining. Compared to curcumin, the efficacy of CUR5-8 in ameliorating hepatic steatosis and insulin resistance was more significant.	[80]

Dehydrozingerone (DHZ) Feruloylmethane 1, 7-bis (4-hydroxy-3methoxyphenyl)-1, 6-heptadiene-3, 5-dione		The efficacy of DHZ on obesity-induced renal lipotoxicity, skeletal muscle metabolism, and the underlying mechanisms was investigated. Male C57BL/6 mice were fed a HFD with or without 100 mg/kg DHZ for 12 weeks.	DHZ reduced BW gain and restored HFD-induced renal damage by decreasing kidney weight, urinary albumin, and urinary ACR. DHZ increased *Podocin* and decreased *Il-1β* mRNA expression. DHZ increased nephrin expression and reduced CD68 and ARGINASE 2 expression. DHZ regulated renal lipid metabolism by reducing renal glycerol, FFAs and cholesteryl ester levels, decreasing mRNA and protein expression of SREBP1, SREBP2, FAS, and ACC, and increasing mRNA and protein expression of PPARα, CPT1, and p-AMPK.	[83]
			DHZ suppressed HFD-induced BW gain, decreased perirenal fat, epididymal fat, and liver weight, and reduced adipocyte size and lipid accumulation in the liver and epididymal fat. DHZ decreased plasma glucose, insulin, and leptin levels, and improved glucose tolerance. DHZ decreased hepatic mRNA expression of *G6Pase*, *Pepck*, and *Fetuin*.	[82]
C66 (2E,6E)-2,6-bis (2-(tri-fluoromethyl)benzylidene) cyclohexanone		The protective effect of C66 on obesity-induced renal dysfunction was evaluated. HFD-fed SPF C57BL/6 mice were orally administered 5, 10, and 20 mg/kg of C66 every 2 days for 11 weeks during HFD feeding.	C66 reduced BW gain, decreased serum TGs and LDL-c levels, and increased serum HDL-c levels. C66 decreased kidney weight, serum BUN and CRE levels, and urine CRE and albumin levels. C66 reduced fibrosis by reducing collagen and ECM deposition and decreasing the mRNA and protein expression of Col-IV, TGF-β, and MMP-9. C66 reversed apoptosis by reducing TUNEL positive stained cells, decreasing cleaved caspase-3 and BAX expression, and increasing BCL-2 expression. C66 attenuated chronic inflammation by reducing macrophage infiltration, decreasing *Tnfα*, *Il-6*, and *Il-1β* mRNA expression levels, and inhibiting NF-κB/JNK activation via increased IκBα accumulation, and reduced expression of p-p65 and p-JNK.	[88]
			C66 reduced BW gain and decreased serum TGs, LDL-c, and cholesterol levels, and increased HDL-c serum levels. C66 restored cardiac function by improving EF% and FS%. C66 decreased myocardial hypertrophy by reducing heart weight to tibia length ratio, cardiomyocyte	

		longitudinal and transverse section area, and the circulating and mRNA	
	The protective effect of C66 on obesity-induced cardiomyopathy through inhibition of JNK-mediated inflammation was investigated. Male C57BL/6 mice were fed HFD for 11 weeks followed by oral administration with 5, 10, and 20 mg/kg of C66 every 2 days for a further 7 weeks during HFD feeding.	expression levels of CK-MB, ANP, and BNP. C66 attenuated cardiac fibrosis by decreasing collagen deposition and reducing MyHc, TGF-β, and Col-I protein and mRNA expression levels. C66 suppressed myocardial apoptosis by reducing TUNEL positive stained cells, decreasing cleaved caspase-3 and BAX expression, and increasing BCL-2 expression. C66 ameliorated cardiac inflammation by decreasing macrophage infiltration, reducing *Tnfα*, *Il-6*, and *Il-1β* mRNA expression levels, and reversing NF-κB/JNK activation via increased IκBα accumulation, and reduced expression of p-p65 and p-JNK.	[89]

Abbreviations: 3-NT: 3-nitrotyrosine; ABCG1: ATP binding cassette subfamily G member 1; ABCG8: ATP binding cassette subfamily G member 8; ABCA1: ATP binding cassette subfamily A member 1; ACC: acetyl-CoA carboxylase; ALT: alanine transaminase; ANP: A-type natriuretic peptide; aP2: adipocyte Protein 2; AST: aspartate aminotransferase; ATG5: autophagy related 5; BAX: Bcl-2 associated X protein; BCL-2: B-cell lymphoma 2 protein; BNP: B-type natriuretic peptide; BUN: blood urea nitrogen; BW: body weight; C/EBPα: CCAAT/enhancer-binding protein alpha; CD36: cluster of differentiation 36; CD68: cluster of differentiation 68; CDPP: Curcumin-3:4-Dichloro Phenyl Pyrazole; CK-MB: creatine kinase MB; Col-I: collagen type-I; Col-IV: collagen type-IV; COX2: cyclooxygenase-2; CPT1: carnitine palmitoyltransferase 1; CRE: creatinine; CUR5-8: Curcumin5-8; Curc-mPEG454: PEGylated curcumin derivative; CYP7A1: cholesterol 7 alpha-hydroxylase; DHZ: Dehydrozingerone; ECM: extracellular matrix; EF%: percentage of ejection fraction; ER: endoplasmic reticulum; EtOH: ethanol; eWAT: epididymal white adipose tissue; FAS: fatty acid synthase; FFAs: free fatty acids; FS%: percentage of fractional shortening; G6Pase: glucose-6-phosphatase; GRP78: glucose-regulated protein 78; HDL-c: highdensity lipoprotein cholesterol; HFD: high-fat diet; HO-1: heme oxygenase-1; HOMA-IR: homeostatic model assessment for insulin resistance; ICAM-1: intercellular adhesion molecule-1; IL1β: interleukin 1 beta; IL–6: interleukin 6; IκBα: inhibitor of nuclear factor kappa B; JNK: c-Jun N-terminal kinase; LCAT: lecithin-cholesterol acyltransferase; LDL-c: low-density lipoprotein cholesterol; LXRα: liver X receptor alpha; MMP-2: matrix metallopeptidase 2; MMP-9: matrix metallopeptidase 9; mRNA: messenger ribonucleic acid; MyHC: myosin heavy chain; NQO-1: NADPH quinone dehydrogenase 1; NRF2: nuclear factor erythroid 2–related factor 2; p62: sequestosome 1; p65: nuclear factor kappa B subunit; p-AKT: phosphorylated protein kinase B; pAMPK: phosphorylated adenosine monophosphate-activated protein kinase; PARP: poly (ADP-ribose) polymerase 1; p-CREB: phosphorylated cAMP response element-binding protein; p-eIF2α: eukaryotic initiation factor 2 alpha; PEPCK: phosphoenolpyruvate carboxykinase; p-IR: phosphorylated insulin receptor; PLs: phospholipids; PPARα: peroxisome proliferator-activated receptor alpha; PPARγ: peroxisome proliferator-activated receptor gamma; PTP1B: protein tyrosine phosphatase 1B; SRB1: scavenger receptor class B type 1; SREBP1: sterol regulatory element binding transcription factor 1; SREBP2: sterol regulatory element binding transcription factor 2; TC: total cholesterol; TGF-β: transforming growth factor beta; TGs: triglycerides; TNFα: tumor necrosis factor alpha; TUNEL: terminal deoxynucleotidyl transferase (TdT) dUTP nick-end labeling; VCAM-1: vascular cell adhesion molecule-1; ΔPUFA: thermally oxidized sunflower oil.

Summary and conclusions

In the present review, we systematically compiled preclinical findings from *in vitro* and *in vivo* studies that explored the efficacy of curcumin derivatives to attenuate obesity and its associated metabolic complications. Furthermore, we also report the efficacy of these curcumin derivatives compared to curcumin. We identified eight synthetic curcumin derivatives (CNB-001, CDPP, CUR5-8, DHZ, C66, Salicylcurcumin, Y20, and CurcmPEG454) that were shown to ameliorate obesity and metabolic dysregulation in animal models (Figure 2.4). Five of these (CNB-001, CDPP, CUR5-8, DHZ, and C66) were also reported to exhibit efficacy on obesity complications in cell culture models (Figure 2.4). In addition, five of the eight curcumin derivatives (CDPP, CUR5-8, Salicylcurcumin, DHZ, and Y20) reported here were shown to exhibit improved efficacy when compared to curcumin, even at lower doses (CDPP and Y20), while the other three curcumin derivatives were not effective compared to curcumin (CNB-001, C66, and Curc-mPEG454) (Figure 2.4). Our search of the literature demonstrated that these derivatives ameliorate obesity-induced metabolic diseases by modulating adipogenesis, lipid metabolism, insulin resistance, hepatic steatosis, lipotoxicity, inflammation, oxidative stress, endoplasmic reticulum stress, apoptosis, autophagy, fibrosis, and dyslipidemia to a greater extent than curcumin (Figure 2.4). These derivatives facilitate their efficacy using various mechanisms of action such as insulin signaling, AMPK and mTOR signaling, NF-κB/JNK and p38 MAPK signaling, and target various transcription factors including C/EBPα, CREB, PGC1α, PPARα, PPARγ, and SREBP1. Moreover, these curcumin derivatives mediate their effects by targeting circulating markers and tissues involved in obesity and metabolic dysfunction including adipose tissue, liver, kidney, skeletal muscle, and the heart (Figure 2.4).

Taken together, these studies demonstrate the efficacy of curcumin derivatives to ameliorate obesity and associated metabolic disorders. However, additional preclinical studies that compare the efficacy of these compounds to conventional anti-obesity drugs are required to substantiate the potential of these derivative compounds to serve as alternative therapeutics for obesity and related metabolic disorders. Furthermore, studies to elucidate the pharmacokinetic and safety profiles prior to clinical development as lead therapeutics are needed. It is worthy to note that curcumin derivatives such as CDPP and DHZ have been experimentally shown to exhibit better pharmacokinetic profiles than curcumin [78, 99]. Similarly, various studies have been conducted to evaluate the safety of these curcumin derivatives. Like curcumin, CNB-001, for example, has been shown to exert neuroprotective effects by penetrating the blood–brain barrier while maintaining therapeutic safety [76,100].

Further studies are also required to establish standardized formulations of these lead synthetic curcumin derivatives and evaluate their safety and efficacy in clinical studies.

In conclusion, this review demonstrates the efficacy of synthetic curcumin derivatives to ameliorate obesity and obesity-related metabolic complications even more effectively compared to curcumin. These studies highlight the significance of synthetic curcumin derivatives as potential therapeutic agents to modulate obesity and associated metabolic dysfunction. Thus, we recommend more research studies to assess the bioavailability of curcumin derivatives using pharmacokinetic and pharmacodynamic approaches. In addition, randomized clinical trials are required to assess the clinical efficacy and safety of these derivatives to ameliorate obesity and its associated metabolic complications.

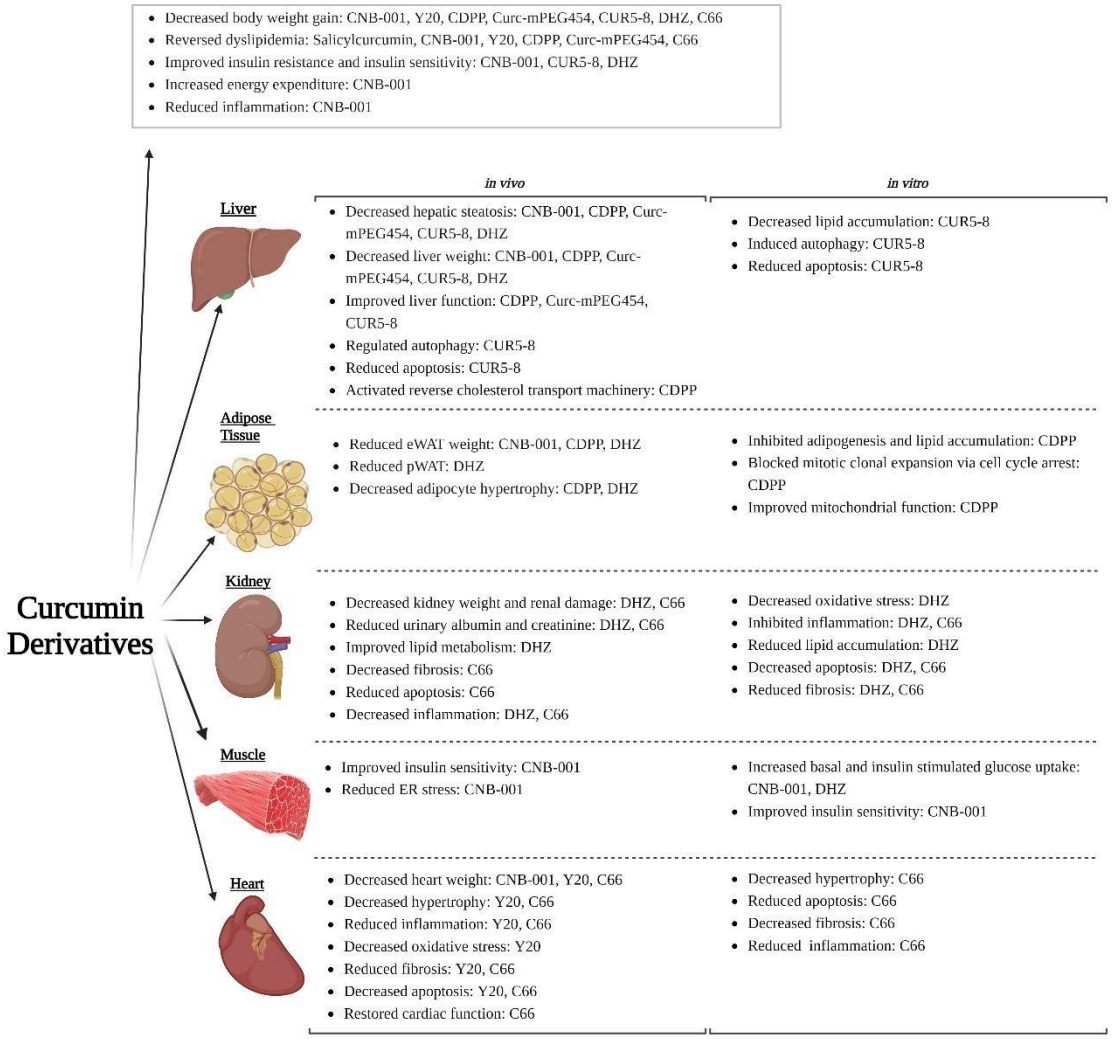


Figure 2.4: Schematic summary of the potential therapeutic effects of curcumin derivatives on obesity and its associated metabolic complications. The *in vitro* and *in vivo* studies summarized in the current review show that the curcumin derivatives exhibit their anti-obesity effects by modulating adipogenesis, lipid metabolism, insulin resistance, hepatic

steatosis, lipotoxicity, inflammation, oxidative stress, endoplasmic reticulum stress, apoptosis, autophagy, fibrosis, and dyslipidemia. These effects are mediated by targeting circulating markers and tissues involved in obesity and metabolic dysfunction including the liver, white adipose tissue, kidney, skeletal muscle, and the heart. (Image created with BioRender.com.)

Author Contributions: Conceptualization, M.T.M. and B.U.J.; investigation, M.T.M. and R.R.; validation, B.U.J.; writing—original draft preparation, M.T.M., B.U.J., and C.P.; writing—review and editing, M.T.M., R.R., C.P., S.J.J.T., S.E.M.-M., and B.U.J.; visualization, M.T.M. and B.U.J.; supervision, B.U.J., C.P., S.J.J.T., and S.E.M.-M. All authors have read and agreed to the published version of the manuscript.

Funding: This research was funded by the South African Medical Research Council (SAMRC) and the NRF Thuthuka Programme (Grant number: 129508).

Institutional Review Board Statement: Not applicable.

Informed Consent Statement: Not applicable.

Data Availability Statement: No new data were created or analyzed in this study. Data sharing is not applicable to this article.

Acknowledgments: Marakiya T. Moetlediwa and Rudzani Ramashia are funded by the National Research Foundation (NRF) of South Africa.

Conflicts of Interest: The authors declare no conflicts of interest.

References

[1] Ng, M.; Fleming, T.; Robinson, M.; Thomson, B.; Graetz, N.; Margono, C.; Mullany, E.C.; Biryukov, S.; Abbafati, C.; Abera, S.F.; et al. Global, Regional, and National Prevalence of Overweight and Obesity in Children and Adults during 1980–2013: A Systematic Analysis for the Global Burden of Disease Study 2013. *Lancet* 2014, *384*, 766–781. https://doi.org/10.1016/S0140-6736(14)60460-8

[2] Di Cesare, M.; Bentham, J.; Stevens, G.A.; Zhou, B.; Danaei, G.; Lu, Y.; Bixby, H.; Cowan, M.J.; Riley, L.M.; Hajifathalian, K.; et al. Trends in Adult Body-Mass Index in 200 Countries from 1975 to 2014: A Pooled Analysis of 1698 Population-Based Measurement Studies with 19.2 Million Participants. *Lancet* 2016, *387*, 1377–1396. https://doi.org/10.1016/S0140-6736(16)30054-X

[3] Al-Sulaiti, H.; Diboun, I.; Agha, M.V.; Mohamed, F.F.S.; Atkin, S.; Dömling, A.S.; Elrayess, M.A.; Mazloum, N.A. Metabolic Signature of Obesity-Associated Insulin Resistance and Type 2 Diabetes. *J. Transl. Med.* 2019, *17*, 348. https://doi.org/10.1186/s12967-019-2096-8

[4] Wu, H.; Ballantyne, C.M. Metabolic Inflammation and Insulin Resistance in Obesity. *Circ. Res.* 2020, *126*,

1549–1564. https://doi.org/10.1161/CIRCRESAHA.119.315896

[5] Yazıcı, D.; Sezer, H. Insulin Resistance, Obesity and Lipotoxicity. *Adv. Exp. Med. Biol.* 2017, *960*, 277– 304. https://doi.org/10.1007/978-3-319-48382-5_12.

[6] Vekic, J.; Zeljkovic, A.; Stefanovic, A.; Jelic-Ivanovic, Z.; Spasojevic-Kalimanovska, V. Obesity and Dyslipidemia. *Metabolism* 2019, *92*, 71–81. https://doi.org/10.1016/j.metabol.2018.11.005

[7] Polyzos, S.A.; Kountouras, J.; Mantzoros, C.S. Obesity and Nonalcoholic Fatty Liver Disease: From Pathophysiology to Therapeutics. *Metabolism* 2019, *92*, 82–97. https://doi.org/10.1016/j.metabol.2018.11.014

[8] Leitner, D.R.; Frühbeck, G.; Yumuk, V.; Schindler, K.; Micic, D.; Woodward, E.; Toplak, H. Obesity and Type 2 Diabetes: Two Diseases with a Need for Combined Treatment Strategies—EASO Can Lead the Way. *Obes. Facts* 2017, *10*, 483–492. https://doi.org/10.1159/000480525

[9] Powell-Wiley, T.M.; Poirier, P.; Burke, L.E.; Després, J.-P.; Gordon-Larsen, P.; Lavie, C.J.; Lear, S.A.; Ndumele, C.E.; Neeland, I.J.; Sanders, P.; et al. Obesity and Cardiovascular Disease: A Scientific Statement from the American Heart Association. *Circulation* 2021, *143*, e984–e1010. https://doi.org/10.1161/CIR.0000000000000973

[10] Davoodi, S.H.; Malek-Shahabi, T.; Malekshahi-Moghadam, A.; Shahbazi, R.; Esmaeili, S. Obesity as an Important Risk Factor for Certain Types of Cancer. *Iran. J. Cancer Prev.* 2013, *6*, 186–194.

[11] Löffler, M.C.; Betz, M.J.; Blondin, D.P.; Augustin, R.; Sharma, A.K.; Tseng, Y.-H.; Scheele, C.; Zimdahl, H.; Mark, M.; Hennige, A.M.; et al. Challenges in Tackling Energy Expenditure as Obesity Therapy: From Preclinical Models to Clinical Application. *Mol. Metab.* 2021, *51*, 101237. https://doi.org/10.1016/j.molmet.2021.101237

[12] Lagerros, Y.T.; Rössner, S. Obesity Management: What Brings Success? *Therap. Adv. Gastroenterol.* 2013, *6*, 77–88. https://doi.org/10.1177/1756283X12459413

[13] Tak, Y.J.; Lee, S.Y. Long-Term Efficacy and Safety of Anti-Obesity Treatment: Where Do We Stand? *Curr. Obes. Rep.* 2021, *10*, 14–30. https://doi.org/10.1007/s13679-020-00422-w

[14] Müller, T.D.; Blüher, M.; Tschöp, M.H.; DiMarchi, R.D. Anti-Obesity Drug Discovery: Advances and Challenges. *Nat. Rev. Drug Discov.* 2022, *21*, 201–223. https://doi.org/10.1038/s41573-021-00337-8

[15] Lim, R.; Beekley, A.; Johnson, D.C.; Davis, K.A. Early and Late Complications of Bariatric Operation. *Trauma Surg. Acute Care Open* 2018, *3*, e000219. https://doi.org/10.1136/tsaco-2018-000219 [16] Soleimani, V.; Sahebkar, A.; Hosseinzadeh, H. Turmeric (Curcuma Longa) and Its Major Constituent (Curcumin) as Nontoxic and Safe Substances: Review. *Phytother. Res.* 2018, *32*, 985–995. https://doi.org/10.1002/ptr.6054

[17] Menon, V.P.; Sudheer, A.R. Antioxidant and Anti-Inflammatory Properties of Curcumin. *Adv. Exp. Med. Biol.* 2007, *595*, 105–125. https://doi.org/10.1007/978-0-387-46401-5_3

[18] Khan, H.; Ullah, H.; Nabavi, S.M. Mechanistic Insights of Hepatoprotective Effects of Curcumin: Therapeutic Updates and Future Prospects. *Food Chem. Toxicol.* 2019, *124*, 182–191. https://doi.org/10.1016/j.fct.2018.12.002

[19] Zhang, Q.; Wu, L. *In vitro* and *In vivo* Cardioprotective Effects of Curcumin against Doxorubicin-Induced Cardiotoxicity: A Systematic Review. *J. Oncol.* 2022, *2022*, 7277562. https://doi.org/10.1155/2022/7277562

[20] Xia, Z.-H.; Zhang, S.-Y.; Chen, Y.-S.; Li, K.; Chen, W.-B.; Liu, Y.-Q. Curcumin Anti-Diabetic Effect Mainly Correlates with Its Anti-Apoptotic Actions and PI3K/Akt Signal Pathway Regulation in the Liver. *Food Chem. Toxicol.* 2020, *146*, 111803. https://doi.org/10.1016/j.fct.2020.111803

[21] Chen, Y.; Wu, R.; Chen, W.; Liu, Y.; Liao, X.; Zeng, B.; Guo, G.; Lou, F.; Xiang, Y.; Wang, Y.; et al. Curcumin Prevents Obesity by Targeting TRAF4-induced Ubiquitylation in m 6 A-dependent Manner. *EMBO Rep.* 2021, *22*, e52146. https://doi.org/10.15252/embr.202052146

[22] Lopresti, A.L. The Problem of Curcumin and Its Bioavailability: Could Its Gastrointestinal Influence Contribute to Its Overall Health-Enhancing Effects? *Adv. Nutr.* 2018, *9*, 41–50. https://doi.org/10.1093/advances/nmx011

[23] Dei Cas, M.; Ghidoni, R. Dietary Curcumin: Correlation between Bioavailability and Health Potential. *Nutrients* 2019, *11*, 2147. https://doi.org/10.3390/nu11092147

[24] Racz, L.Z.; Racz, C.P.; Pop, L.-C.; Tomoaia, G.; Mocanu, A.; Barbu, I.; Sárközi, M.; Roman, I.; Avram, A.; Tomoaia-Cotisel, M.; et al. Strategies for Improving Bioavailability, Bioactivity, and Physical-Chemical Behavior of Curcumin. *Molecules* 2022, *27*, 6854. https://doi.org/10.3390/molecules27206854

[25] Dayton, A.; Selvendiran, K.; Kuppusamy, M.L.; Rivera, B.K.; Meduru, S.; Kálai, T.; Hideg, K.; Kuppusamy, P. Cellular Uptake, Retention and Bioabsorption of HO-3867, a Fluorinated Curcumin Analog with Potential Antitumor Properties. *Cancer Biol. Ther.* 2010, *10*, 1027–1032. https://doi.org/10.4161/cbt.10.10.13250

[26] Zeng, Z.; Shen, Z.L.; Zhai, S.; Xu, J.L.; Liang, H.; Shen, Q.; Li, Q.Y. Transport of Curcumin Derivatives in Caco-2 Cell Monolayers. *Eur. J. Pharm. Biopharm.* 2017, *117*, 123–131. https://doi.org/10.1016/j.ejpb.2017.04.004

[27] Noureddin, S.A.; El-Shishtawy, R.M.; Al-Footy, K.O. Curcumin Analogues and Their Hybrid Molecules as Multifunctional Drugs. *Eur. J. Med. Chem.* 2019, *182*, 111631. https://doi.org/10.1016/j.ejmech.2019.111631

[28] Ooko, E.; Alsalim, T.; Saeed, B.; Saeed, M.E.M.; Kadioglu, O.; Abbo, H.S.; Titinchi, S.J.J.; Efferth, T. Modulation of P-Glycoprotein Activity by Novel Synthetic Curcumin Derivatives in Sensitive and Multidrug-Resistant T-Cell Acute Lymphoblastic Leukemia Cell Lines. *Toxicol. Appl. Pharmacol.* 2016, *305*, 216–233. https://doi.org/10.1016/j.taap.2016.06.002

[29] Abdel Aziz, M.T.; El-Asmar, M.F.; El-Ibrashy, I.N.; Rezq, A.M.; Al-Malki, A.L.; Wassef, M.A.; Fouad, H.H.; Ahmed, H.H.; Taha, F.M.; Hassouna, A.A.; et al. Effect of Novel Water Soluble Curcumin Derivative on Experimental Type-1 Diabetes Mellitus (Short Term Study). *Diabetol. Metab. Syndr.* 2012, *4*, 30. https://doi.org/10.1186/1758-5996-4-30

[30] Cheng, F.; Chen, Y.; Zhan, Z.; Liu, Y.; Hu, P.; Ren, H.; Tang, H.; Peng, M. Curc-MPEG454, a PEGylated Curcumin Derivative, Improves Anti-Inflammatory and Antioxidant Activities: A Comparative Study. *Inflammation* 2018, *41*, 579–594. https://doi.org/10.1007/s10753-017-0714-2

[31] Wang, Z.S.; Chen, L.Z.; Liu, X.H.; Chen, F.H. Diarylpentadienone Derivatives (Curcumin Analogues): Synthesis and Anti-Inflammatory Activity. *Bioorganic. Med. Chem. Lett.* 2017, *27*, 1803–1807. https://doi.org/10.1016/j.bmcl.2017.02.056

[31] Vogel, A.; Pelletier, J. Examen Chimique de La Racine de Curcuma. *J. Pharm.* 1815, *1*, 289–300.

[32] Vogel, E. Die Bibliothek Der Benediktinerabtei Sponheim. *Serapeum* 1842, *3*, 312–328.

[33] Lampe, V.; Milobedzka, J.; Kostanecki, S.V. Zur Kenntnis Des Curcumins. *Berichte Dtsch. Chem. Ges.* 1910, *43*, 2163–2170.

[34] Lampe, V.; Milobedzka, J. Studien Über Curcumin. *Berichte Dtsch. Chem. Ges.* 1913, *46*, 2235–2240. https://doi.org/10.1002/cber.191304602149

[35] Priyadarsini, K.I. The Chemistry of Curcumin: From Extraction to Therapeutic Agent. *Molecules* 2014, *19*, 20091–20112.

[36] Kawano, S.I.; Inohana, Y.; Hashi, Y.; Lin, J.M. Analysis of Keto-Enol Tautomers of Curcumin by Liquid Chromatography/Mass Spectrometry. *Chin. Chem. Lett.* 2013, *24*, 685–687. https://doi.org/10.1016/j.cclet.2013.05.006

[37] Kazakova, O.; Lipkovska, N.; Barvinchenko, V. Keto-Enol Tautomerism of Curcumin in the Preparation of Nanobiocomposites with Fumed Silica. *Spectrochim. Acta—Part A Mol. Biomol. Spectrosc.* 2022, *277*, 121287. https://doi.org/10.1016/j.saa.2022.121287

[38] Nelson, K.M.; Dahlin, J.L.; Bisson, J.; Graham, J.; Pauli, G.F.; Walters, M.A. The Essential Medicinal Chemistry of Curcumin. *J. Med. Chem.* 2017, *60*, 1620–1637. https://doi.org/10.1021/acs.jmedchem.6b00975

[39] Eigner, D.; Scholz, D. Ferula Asa-Foetida and Curcuma Longa in Traditional Medical Treatment and Diet in Nepal. *J. Ethnopharmacol.* 1999, *67*, 1–6. https://doi.org/10.1016/S0378-8741(98)00234-7

[40] EL-Kenawy, A.E.-M.; Hassan, S.M.A.; Mohamed, A.M.M.; Mohammed, H.M.A. Tumeric or Curcuma Longa Linn. In *Nonvitamin and Nonmineral Nutritional Supplements*; Nabavi, S.M., Silva, A.S., Eds.; Academic Press: Cambridge, MA, USA, 2019; pp. 447–453; ISBN 978-0-12-812491-8

[41] Kasprzak-Drozd, K.; Oniszczuk, T.; Gancarz, M.; Kondracka, A.; Rusinek, R.; Oniszczuk, A. Curcumin and Weight Loss: Does It Work? *Int. J. Mol. Sci.* 2022, *23*, 639. https://doi.org/10.3390/ijms23020639.

[42] Maithilikarpagaselvi, N.; Sridhar, M.G.; Swaminathan, R.P.; Sripradha, R. Preventive Effect of Curcumin on Inflammation, Oxidative Stress and Insulin Resistance in High-Fat Fed Obese Rats. *J. Complement. Integr. Med.* 2016, *13*, 137–143. https://doi.org/10.1515/jcim-2015-0070

[43] Mokgalaboni, K.; Ntamo, Y.; Ziqubu, K.; Nyambuya, T.M.; Nkambule, B.B.; Mazibuko-Mbeje, S.E.; Gabuza, K.B.; Chellan, N.; Tiano, L.; Dludla, P.V. Curcumin Supplementation Improves Biomarkers of Oxidative Stress and Inflammation in Conditions of Obesity, Type 2 Diabetes and NAFLD: Updating the Status of Clinical Evidence. *Food Funct.* 2021, *12*, 12235–12249. https://doi.org/10.1039/d1fo02696h

[44] Campbell, M.S.; Ouyang, A.; Krishnakumar, I.M.; Charnigo, R.J.; Westgate, P.M.; Fleenor, B.S. Influence of Enhanced Bioavailable Curcumin on Obesity-Associated Cardiovascular Disease Risk Factors and Arterial Function:

A Double-Blinded, Randomized, Controlled Trial. *Nutrition* 2019, *62*, 135–139. https://doi.org/10.1016/j.nut.2019.01.002

[45] Abdulmalek, S.; Eldala, A.; Awad, D.; Balbaa, M. Ameliorative Effect of Curcumin and Zinc Oxide Nanoparticles on Multiple Mechanisms in Obese Rats with Induced Type 2 Diabetes. *Sci. Rep.* 2021, *11*, 20677. https://doi.org/10.1038/s41598-021-00108-w

[46] Shehzad, A.; Khan, S.; Sup Lee, Y. Curcumin Molecular Targets in Obesity and Obesity-Related Cancers. *Futur. Oncol.* 2012, *8*, 179–190. https://doi.org/10.2217/fon.11.145

[47] Hewlings, S.J.; Kalman, D.S. Curcumin: A Review of Its Effects on Human Health. *Foods* 2017, *6*, 92. https://doi.org/10.3390/foods6100092

[48] Sharifi-Rad, J.; Rayess, Y.E.; Rizk, A.A.; Sadaka, C.; Zgheib, R.; Zam, W.; Sestito, S.; Rapposelli, S.; Neffe-Skocińska, K.; Zielińska, D.; et al. Turmeric and Its Major Compound Curcumin on Health: Bioactive Effects and Safety Profiles for Food, Pharmaceutical, Biotechnological and Medicinal Applications. *Front. Pharmacol.* 2020, *11*, 01021. https://doi.org/10.3389/fphar.2020.01021

[49] Tønnesen, H.H.; Másson, M.; Loftsson, T. Studies of Curcumin and Curcuminoids. XXVII. Cyclodextrin Complexation: Solubility, Chemical and Photochemical Stability. *Int. J. Pharm.* 2002, *244*, 127–135. https://doi.org/10.1016/S0378-5173(02)00323-X

[50] Ma, Z.; Wang, N.; He, H.; Tang, X. Pharmaceutical Strategies of Improving Oral Systemic Bioavailability of Curcumin for Clinical Application. *J. Control. Release* 2019, *316*, 359–380. https://doi.org/10.1016/j.jconrel.2019.10.053

[51] Parsamanesh, N.; Moossavi, M.; Bahrami, A.; Butler, A.E.; Sahebkar, A. Therapeutic Potential of Curcumin in Diabetic Complications. *Pharmacol. Res.* 2018, *136*, 181–193.

[52] Maiti, K.; Mukherjee, K.; Gantait, A.; Saha, B.P.; Mukherjee, P.K. Curcumin-Phospholipid Complex: Preparation, Therapeutic Evaluation and Pharmacokinetic Study in Rats. *Int. J. Pharm.* 2007, *330*, 155–163. https://doi.org/10.1016/j.ijpharm.2006.09.025

[53] Yang, K.Y.; Lin, L.C.; Tseng, T.Y.; Wang, S.C.; Tsai, T.H. Oral Bioavailability of Curcumin in Rat and the Herbal Analysis from Curcuma Longa by LC-MS/MS. *J. Chromatogr. B Anal. Technol. Biomed. Life Sci.* 2007, *853*, 183–189. https://doi.org/10.1016/j.jchromb.2007.03.010

[54] Lao, C.D.; Ruffin, M.T., IV; Normolle, D.; Heath, D.D.; Murray, S.I.; Bailey, J.M.; Boggs, M.E.; Crowell, J.; Rock, C.L.; Brenner, D.E. Dose Escalation of a Curcuminoid Formulation. *BMC Complement. Altern. Med.* 2006, *6*, 10. https://doi.org/10.1186/1472-6882-6-10

[55] Vareed, S.K.; Kakarala, M.; Ruffin, M.T.; Crowell, J.A.; Normolle, D.P.; Djuric, Z.; Brenner, D.E. Pharmacokinetics of Curcumin Conjugate Metabolites in Healthy Human Subjects. *Cancer Epidemiol. Biomark. Prev.* 2008, *17*, 1411–1417. https://doi.org/10.1158/1055-9965.EPI-07-2693

[56] Ireson, C.R.; Jones, D.J.L.; Boocock, D.J.; Farmer, P.B.; Gescher, A.J.; Orr, S.; Coughtrie, M.W.H.; Williams, M.L.; Steward, W.P. Metabolism of the Cancer Chemopreventive Agent Curcumin in Human and Rat Intestine. *Cancer Epidemiol. Biomark. Prev.* 2002, *11*, 105–111.

[57] Pandey, A.; Chaturvedi, M.; Mishra, S.; Kumar, P.; Somvanshi, P.; Chaturvedi, R. Reductive Metabolites of Curcumin and Their Therapeutic Effects. *Heliyon* 2020, *6*, e05469.

https://doi.org/10.1016/j.heliyon.2020.e05469

[58] Pan, M.H.; Huang, T.M.; Lin, J.K. Biotransformation of Curcumin through Reduction and Glucuronidation in Mice. *Drug Metab. Dispos.* 1999, *27*, 486–494.

[59] Hassaninasab, A.; Hashimoto, Y.; Tomita-Yokotani, K.; Kobayashi, M. Discovery of the Curcumin Metabolic Pathway Involving a Unique Enzyme in an Intestinal Microorganism. *Proc. Natl. Acad. Sci. USA* 2011, *108*, 6615–6620. https://doi.org/10.1073/pnas.1016217108

[60] Luca, S.V.; Macovei, I.; Bujor, A.; Miron, A.; Skalicka-Woźniak, K.; Aprotosoaie, A.C.; Trifan, A. Bioactivity of Dietary Polyphenols: The Role of Metabolites. *Crit. Rev. Food Sci. Nutr.* 2020, *60*, 626–659. https://doi.org/10.1080/10408398.2018.1546669

[61] Wang, J.; Yu, X.; Zhang, L.; Wang, L.; Peng, Z.; Chen, Y. The Pharmacokinetics and Tissue Distribution of Curcumin and Its Metabolites in Mice. *Biomed. Chromatogr.* 2018, *32*, e4267. https://doi.org/10.1002/bmc.4267.

[62] Stohs, S.J.; Chen, O.; Ray, S.D.; Ji, J.; Bucci, L.R.; Preuss, H.G. Highly Bioavailable Forms of Curcumin and Promising Avenues for Curcumin-Based Research and Application: A Review. *Molecules* 2020, *25*, 1397. https://doi.org/10.3390/molecules25061397

[63] Wong, K.E.; Ngai, S.C.; Chan, K.G.; Lee, L.H.; Goh, B.H.; Chuah, L.H. Curcumin Nanoformulations for Colorectal Cancer: A Review. *Front. Pharmacol.* 2019, *10*, 152. https://doi.org/10.3389/fphar.2019.00152

[64] Fança-Berthon, P.; Tenon, M.; Bouter-Banon, S.L.; Manfré, A.; Maudet, C.; Dion, A.; Chevallier, H.; Laval, J.; Van Breemen, R.B. Pharmacokinetics of a Single Dose of Turmeric Curcuminoids Depends on Formulation: Results of a Human Crossover Study. *J. Nutr.* 2021, *151*, 1802–1816. https://doi.org/10.1093/jn/nxab087

[64] Shoba, G.; Joy, D.; Joseph, T.; Majeed, M.; Rajendran, R.; Srinivas, P.S.S.R. Influence of Piperine on the Pharmacokinetics of Curcumin in Animals and Human Volunteers. *Planta Med.* 1998, *64*, 353–356. https://doi.org/10.1055/s-2006-957450

[65] Zhang, Y.; Yang, C.; Wang, W.; Liu, J.; Liu, Q.; Huang, F.; Chu, L.; Gao, H.; Li, C.; Kong, D.; et al. CoDelivery of Doxorubicin and Curcumin by PH-Sensitive Prodrug Nanoparticle for Combination Therapy of Cancer. *Sci. Rep.* 2016, *6*, 21225. https://doi.org/10.1038/srep21225

[66] Moorthi, C.; Kathiresan, K. Curcumin–Piperine/Curcumin–Quercetin/Curcumin–Silibinin Dual DrugLoaded Nanoparticulate Combination Therapy: A Novel Approach to Target and Treat Multidrug-Resistant Cancers. *J. Med. Hypotheses Ideas* 2013, *7*, 15–20. https://doi.org/10.1016/j.jmhi.2012.10.005

[67] Rivera-Mancía, S.; Lozada-García, M.C.; Pedraza-Chaverri, J. Experimental Evidence for Curcumin and Its Analogs for Management of Diabetes Mellitus and Its Associated Complications. *Eur. J. Pharmacol.* 2015, *756*, 30–37. https://doi.org/10.1016/j.ejphar.2015.02.045

[68] Oliveira, S.; Monteiro-Alfredo, T.; Silva, S.; Matafome, P. Curcumin Derivatives for Type 2 Diabetes Management and Prevention of Complications. *Arch. Pharm. Res.* 2020, *43*, 567–581. https://doi.org/10.1007/s12272-020-01240-3

[69] Idoudi, S.; Bedhiafi, T.; Hijji, Y.M.; Billa, N. Curcumin and Derivatives in Nanoformulations with Therapeutic Potential on Colorectal Cancer. *AAPS PharmSciTech* 2022, *23*, 115. https://doi.org/10.1208/s12249-022-02268-y

[70] Aggarwal, B.B.; Deb, L.; Prasad, S. Curcumin Differs from Tetrahydrocurcumin for Molecular Targets, Signaling Pathways and Cellular Responses. *Molecules* 2014, *20*, 185–205. https://doi.org/10.3390/molecules20010185

[71] Pastorelli, D.; Fabricio, A.S.C.; Giovanis, P.; D'Ippolito, S.; Fiduccia, P.; Soldà, C.; Buda, A.; Sperti, C.; Bardini, R.; Da Dalt, G.; et al. Phytosome Complex of Curcumin as Complementary Therapy of Advanced Pancreatic Cancer Improves Safety and Efficacy of Gemcitabine: Results of a Prospective Phase II Trial. *Pharmacol. Res.* 2018, *132*, 72–79. https://doi.org/10.1016/j.phrs.2018.03.013

[78] Law, S.K.; Lo, C.; Han, J.; Yang, F.; Leung, A.; Chuanshan, X. Design, Synthesis and Characterization of Novel Curcumin Derivatives. *Nat. Prod. Chem. Res.* 2020, *8*, 367. https://doi.org/10.35248/23296836.20.8.367.

[79] Panzhinskiy, E.; Hua, Y.; Lapchak, P.A.; Topchiy, E.; Lehmann, T.E.; Ren, J.; Nair, S. Novel Curcumin Derivative CNB-001 Mitigates Obesity-Associated Insulin Resistance. *J. Pharmacol. Exp. Ther.* 2014, *349*, 248–257. https://doi.org/10.1124/jpet.113.208728

[80] Liu, Y.; Dargusch, R.; Maher, P.; Schubert, D. A Broadly Neuroprotective Derivative of Curcumin. *J. Neurochem.* 2008, *105*, 1336–1345. https://doi.org/10.1111/j.1471-4159.2008.05236.x

[81] Selvam, C.; Jachak, S.M.; Thilagavathi, R.; Chakraborti, A.K. Design, Synthesis, Biological Evaluation and Molecular Docking of Curcumin Analogues as Antioxidant, Cyclooxygenase Inhibitory and AntiInflammatory Agents. *Bioorg. Med. Chem. Lett.* 2005, *15*, 1793–1797. https://doi.org/10.1016/j.bmcl.2005.02.039

[82] Gupta, A.; Singh, V.K.; Kumar, D.; Yadav, P.; Kumar, S.; Beg, M.; Shankar, K.; Varshney, S.; Rajan, S.; Srivastava, A.; et al. Curcumin-3,4-Dichloro Phenyl Pyrazole (CDPP) Overcomes Curcumin's Low Bioavailability, Inhibits Adipogenesis and Ameliorates Dyslipidemia by Activating Reverse Cholesterol Transport. *Metabolism* 2017, *73*, 109–124. https://doi.org/10.1016/j.metabol.2017.05.005

[83] Woo, H.B.; Shin, W.-S.; Lee, S.; Ahn, C.M. Synthesis of Novel Curcumin Mimics with Asymmetrical Units and Their Anti-Angiogenic Activity. *Bioorg. Med. Chem. Lett.* 2005, *15*, 3782–3786. https://doi.org/10.1016/j.bmcl.2005.05.064

[84] Lee, E.S.; Kwon, M.H.; Kim, H.M.; Woo, H.B.; Ahn, C.M.; Chung, C.H. Curcumin Analog CUR5–8 Ameliorates Nonalcoholic Fatty Liver Disease in Mice with High-Fat Diet-Induced Obesity. *Metabolism* 2020, *103*, 154015. https://doi.org/10.1016/j.metabol.2019.154015

[85] Kubra, I.R.; Bettadaiah, B.K.; Murthy, P.S.; Rao, L.J.M. Structure-Function Activity of Dehydrozingerone and Its Derivatives as Antioxidant and Antimicrobial Compounds. *J. Food Sci. Technol.* 2014, *51*, 245–255. https://doi.org/10.1007/s13197-011-0488-8

[86] Kim, S.J.; Kim, H.M.; Lee, E.S.; Kim, N.; Lee, J.O.; Lee, H.J.; Park, N.Y.; Jo, J.Y.; Ham, B.Y.; Han, S.H.; et al. Dehydrozingerone Exerts Beneficial Metabolic Effects in High-Fat Diet-Induced Obese Mice via AMPK Activation in Skeletal Muscle. *J. Cell. Mol. Med.* 2015, *19*, 620–629. https://doi.org/10.1111/jcmm.12455

[87] Lee, E.S.; Kang, J.S.; Kim, H.M.; Kim, S.J.; Kim, N.; Lee, J.O.; Kim, H.S.; Lee, E.Y.; Chung, C.H. Dehydrozingerone Inhibits Renal Lipotoxicity in High-Fat Diet–Induced Obese Mice. *J. Cell. Mol. Med.* 2021, *25*, 8725–8733. https://doi.org/10.1111/jcmm.16828

[88] Pan, Y.; Wang, Y.; Cai, L.; Cai, Y.; Hu, J.; Yu, C.; Li, J.; Feng, Z.; Yang, S.; Li, X.; et al. Inhibition of High Glucose-Induced Inflammatory Response and Macrophage Infiltration by a Novel Curcumin Derivative Prevents Renal Injury in Diabetic Rats. *Br. J. Pharmacol.* 2012, *166*, 1169–1182. https://doi.org/10.1111/j.1476-5381.2012.01854.x

[89] Pan, Y.; Zhang, X.; Wang, Y.; Cai, L.; Ren, L.; Tang, L.; Wang, J.; Zhao, Y.; Wang, Y.; Liu, Q.; et al. Targeting JNK by a New Curcumin Analog to Inhibit NF-KB-Mediated Expression of Cell Adhesion Molecules Attenuates Renal Macrophage Infiltration and Injury in Diabetic Mice. *PLoS ONE* 2013, *8*, e79084. https://doi.org/10.1371/journal.pone.0079084

[90] Pan, Y.; Huang, Y.; Wang, Z.; Fang, Q.; Sun, Y.; Tong, C.; Peng, K.; Wang, Y.; Miao, L.; Cai, L.; et al. Inhibition of MAPK-Mediated ACE Expression by Compound C66 Prevents STZ-Induced Diabetic Nephropathy. *J. Cell. Mol. Med.* 2014, *18*, 231–241. https://doi.org/10.1111/jcmm.12175

[91] Sun, X.; Liu, Y.; Li, C.; Wang, X.; Zhu, R.; Liu, C.; Liu, H.; Wang, L.; Ma, R.; Fu, M.; et al. Recent Advances of Curcumin in the Prevention and Treatment of Renal Fibrosis. *Biomed Res. Int.* 2017, *2017*, 2418671. https://doi.org/10.1155/2017/2418671

[92] Ye, L.; Hu, X.; Hu, X.; Yin, S.; Chen, J.; He, H.; Hong, S.; Yang, B.; Singh, K.K.K.; Feng, J.; et al. Curcumin Analogue C66 Attenuates Obesity-Induced Renal Injury by Inhibiting Chronic Inflammation. *Biomed. Pharmacother.* 2021, *137*, 111418. https://doi.org/10.1016/j.biopha.2021.111418

[93] Ye, L.; Chen, X.; Wang, M.; Jin, L.; Zhuang, Z.; Yang, D.; Guan, X.; Samorodov, A.V.; Pavlov, V.N.; Chattipakorn, N.; et al. Curcumin Analogue C66 Attenuates Obesity-Induced Myocardial Injury by Inhibiting JNK-Mediated Inflammation. *Biomed. Pharmacother.* 2021, *143*, 112121. https://doi.org/10.1016/j.biopha.2021.112121

[94] Babu, K.V.; Rajasekharan, K.N. Simplified Condition for Synthesis of Curcumin I and Other Curcuminoids. *Org. Prep. Proced. Int.* 1994, *26*, 674–677. https://doi.org/10.1080/00304949409458165.

[95] Anto, R.J.; George, J.; Dinesh Babu, K.V.; Rajasekharan, K.N.; Kuttan, R. Antimutagenic and Anticarcinogenic Activity of Natural and Synthetic Curcuminoids. *Mutat. Res.—Genet. Toxicol.* 1996, *370*, 127–131. https://doi.org/10.1016/0165-1218(96)00074-2

[96] Rukkumani, R.; Aruna, K.; Suresh Varma, P.; Viswanathan, P.; Rajasekaran, K.N.N.; Menon, V.P. Protective Role of a Novel Curcuminoid on Alcohol and PUFA-Induced Hyperlipidemia. *Toxicol. Mech. Methods* 2005, *15*, 227–234. https://doi.org/10.1080/15376520590945658

[97] Rukkumani, R.; Aruna, K.; Varma, P.S.; Rajasekaran, K.N.; Menon, V.P. Comparative Effects of Curcumin and Its Analog on Alcohol- and Polyunsaturated Fatty Acid-Induced Alterations in Circulatory Lipid Profiles. *J. Med. Food* 2005, *8*, 256–260. https://doi.org/10.1089/jmf.2005.8.256

[98] Qian, Y.; Zhong, P.; Liang, D.; Xu, Z.; Skibba, M.; Zeng, C.; Li, X.; Wei, T.; Wu, L.; Liang, G. A Newly Designed Curcumin Analog Y20 Mitigates Cardiac Injury via Anti-Inflammatory and Anti-Oxidant Actions in Obese Rats. *PLoS ONE* 2015, *10*, e0120215. https://doi.org/10.1371/journal.pone.0120215

[99] Ishihara, H. Current Status and Prospects of Polyethyleneglycol-Modified Medicines. *Biol. Pharm. Bull.* 2013, *36*, 883–888. https://doi.org/10.1248/bpb.b13-00087

[98] Tang, H.; Murphy, C.J.; Zhang, B.; Shen, Y.; Sui, M.; Van Kirk, E.A.; Feng, X.; Murdoch, W.J. Amphiphilic Curcumin Conjugate-Forming Nanoparticles as Anticancer Prodrug and Drug Carriers: *In vitro* and *In vivo* Effects. *Nanomedicine* 2010, *5*, 855–865. https://doi.org/10.2217/nnm.10.67

[99] Xiao, S.; Deng, Y.; Shen, N.; Sun, Y.; Tang, H.; Hu, P.; Ren, H.; Peng, M. Curc-MPEG454, a PEGylated Curcumin Derivative, as a Multi-Target Anti-Fibrotic Prodrug. *Int. Immunopharmacol.* 2021, *101*, 108166. https://doi.org/10.1016/j.intimp.2021.108166

[100] Liu, Y.; Cheng, F.; Luo, Y.; Zhan, Z.; Hu, P.; Ren, H.; Tang, H.; Peng, M. PEGylated Curcumin Derivative Attenuates Hepatic Steatosis via CREB/PPAR-γ/CD36 Pathway. *Biomed Res. Int.* 2017, *2017*, 8234507. https://doi.org/10.1155/2017/8234507

[101] Mapoung, S.; Suzuki, S.; Fuji, S.; Naiki-Ito, A.; Kato, H.; Yodkeeree, S.; Sakorn, N.; Ovatlarnporn, C.; Takahashi, S.; Limtrakul Dejkriengkraikul, P. Dehydrozingerone, a Curcumin Analog, as a Potential AntiProstate Cancer Inhibitor *In vitro* and *In vivo*. *Molecules* 2020, *25*, 2737. https://doi.org/10.3390/molecules25122737

[102] Lapchak, P.A.; McKim, J.M. CeeTox™ Analysis of CNB-001 a Novel Curcumin-Based Neurotrophic/Neuroprotective Lead Compound to Treat Stroke: Comparison with NXY-059 and Radicut. *Transl. Stroke Res.* 2011, *2*, 51–59. https://doi.org/10.1007/s12975-010-0034-4

Disclaimer/Publisher's Note: The statements, opinions and data contained in all publications are solely those of the individual author(s) and contributor(s) and not of MDPI and/or the editor(s). MDPI and/or the editor(s) disclaim responsibility for any injury to people or property resulting from any ideas, methods, instructions or products referred to in the content.

CHAPTER 3

Chapter outline:

This chapter provides background, methodology, results, and discussion for the synthesis and characterization of the three curcumin derivatives, namely 1A6, 1A8, and 1B8. This chapter covers the first objective of this thesis which is to synthesize and characterize three curcumin derivatives (1A6, 1A8, and 1B8).

Introduction

Curcumin, also referred to as diferuloylmethane, is a polyphenolic compound that is abundant in the rhizome of the *Curcuma Longa* (turmeric) plant species within the *Zingiberaceae* family [1]. The history of curcumin dates back to the 18th century [2]. It was first isolated in 1842 [3] and synthesized in 1913 [4]. Curcumin is an orangeyellow colored powder with the chemical formula of $C_{21}H_{20}O_6$, a molecular weight of 368.38 g/mol and a melting temperature of 183 °C [5]. The chemical structure of curcumin is a pair of aromatic rings connected by a sevencarbon chain, featuring hydroxy and methoxy substituents, and this unique structure is known as a bis-α,βunsaturated β-diketone [6,7]. The β-diketone part can switch between its keto and enol forms. In neutral or acidic conditions, the keto form is dominant, whereas in alkaline solutions, the enol form takes precedence [8].

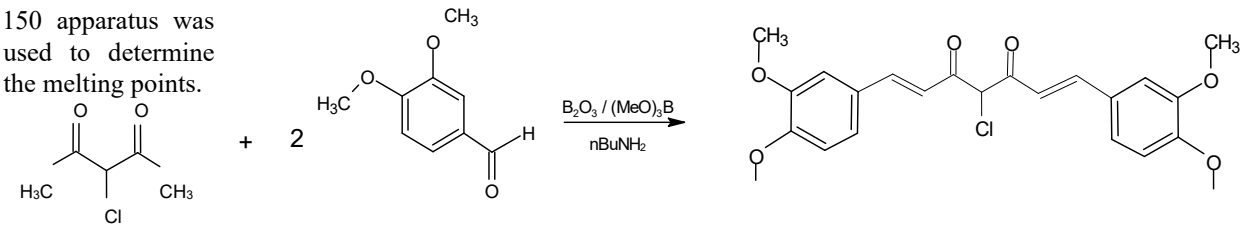
Curcumin has gained significant attention in research due to its therapeutic profile including anti-inflammatory [9], anti-cancer [10], and anti-obesity [11] properties. Although curcumin shows promising therapeutic benefits, its clinical application is compromised by its limited bioavailability resulting from low absorption, rapid metabolism, and extensive elimination after oral ingestion [12]. There is ongoing research on various pharmaceutical alternatives to improve the efficacy of curcumin, including the use of nano formulations, combination therapy, and structural modifications [13,14]. As such, several studies have focused on the use of synthetic chemistry to modify the structure of curcumin by synthesizing curcumin derivatives or analogs, to enhance the bioavailability of curcumin and its therapeutic efficacy [15–17]. The pharmacological efficacy of curcumin derivatives is mainly attributed to key functional groups such as methoxy, hydroxyl, α,β-unsaturated carbonyl moiety, and diketone [18]. Previously, 19 novel curcumin derivatives were designed and assessed for their potential anti-cancer properties [19]. Of these, three synthetic derivatives of curcumin namely 1A6, 1A8, and 1B8 were demonstrated to have improved anti-cancer efficacy by targeting the sensitive and multidrugresistant T-cell acute lymphoblastic leukemia cells. Hence, these three synthetic curcumin derivatives were selected for further analysis of their anti-obesity potential due to the association between cancer and obesity. In this chapter, the synthesis and characterization of the three synthetic curcumin derivatives (1A6, 1A8, and 1B8) are discussed.

Methods

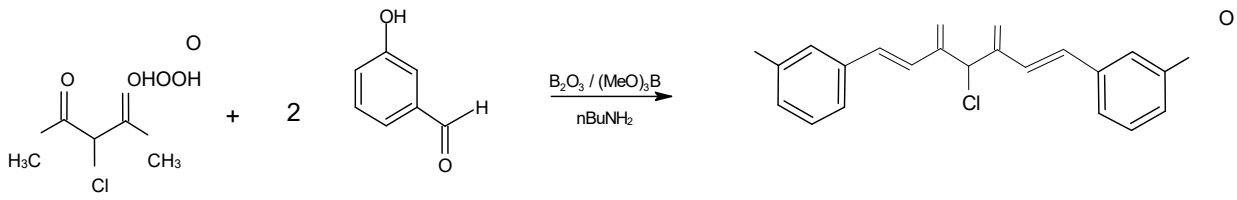
Synthesis of the symmetric chloro curcumin derivatives

The two chloro curcumin derivatives, (1E,6E)-4-chloro-1,7-bis(3,4-dimethoxyphenyl)hepta-1,6-diene-3,5-dione (1A6) and (1E,6E)-4-chloro-1,7-bis(3-hydroxyphenyl)hepta-1,6-diene-3,5-dione (1A8) were synthesized as

previously described [19], using the general synthetic procedure outlined in Figure 3.1. Briefly, 2 g (0.0155 mol) of 3-chloroacetylacetone was mixed with 1.03 g (0.0146 mol) of boric oxide (B_2O_3) by stirring for 1 hour until completely dissolved. Thereafter, two symmetrical appropriate aldehydes (3,4-dimethoxybenzaldehyde for 1A6 and 3-hydroxybenzaldehyde for 1A8) (0.031 mol) dissolved in 50 mL of dry dimethylacetamide (DMA) were added and the reaction mixture was stirred in a water bath at 80 °C. Trimethyl borate ($(MeO)B_3$) (3.23 g, 0.013 mol) was then added and the mixture was stirred for a further 5 minutes, and this was followed by gradually adding a solution of 0.5 g (0.006 mol) *n*-butylamine ($nBuNH_2$) in dry DMA for 1 hour. The reaction mixture was stirred for an additional 3 hours and then stored overnight. The next day, 5% acetic acid (43 mL) was added to the reaction mixture (pre-heated at 80 °C) and stirred for 1 hour, followed by cooling down to precipitate the solid product. The solid product was collected by filtration, washed twice with hot water at 50 °C, dried, and purified using thin-layer chromatography. Thin-layer chromatography was conducted using pre-coated silica gel plates of Keisgel Type 60 GF 245. Spot visualization was achieved utilizing a UV lamp (black-Ray B-100A). The purified product for 1A6 was recrystallized from chloroform/ethanol solvent, leading to the formation of orange crystals, while 1A8 purified product was recrystallized from the methanol solvent, thus forming yellow crystals. The Buchi 150 apparatus was used to determine the melting points.



3-chloroacetylacetone 3,4-dimethoxy denzaldehyde 1A6

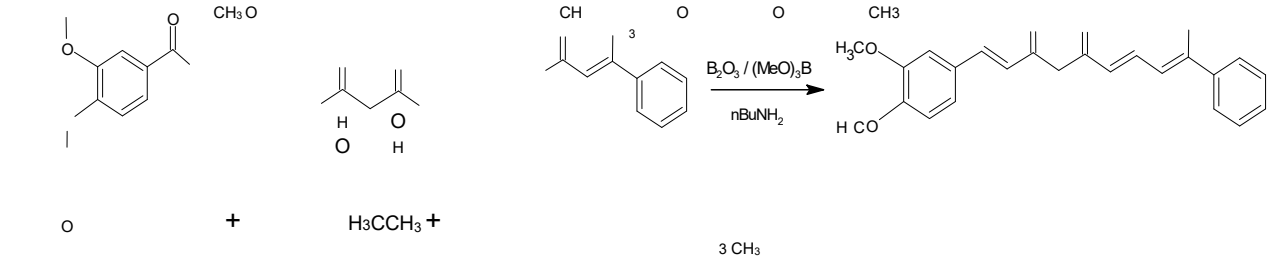


3-chloroacetylacetone 3-hydroxydenzaldehyde 1A8

Figure 3.1: The synthetic route for the two chloro curcumin derivatives, 1A6 and 1A8. Chemical structures constructed using ACD/ChemSketch freeware: www.acdlabs.com (constructed on: 08 March 2024).

Synthesis of an asymmetric curcumin derivative

An asymmetric curcumin derivative, (1E,6E,8E)-1-(3,4-dimethoxyphenyl)-9-phenyldeca-1,6,8-triene-3,5-dione (1B8), was synthesized as previously described [19], using the general synthetic procedure outlined in Figure 3.2. Briefly, 2.5 g (0.0233 mol) of acetylacetone was mixed with 1.2 g (0.017 mol) of B_2O_3 and stirred neat for 1 hour. Thereafter, two different aldehydes (3,4-dimethoxy benzaldehyde and beta-methyl cinnamaldehyde) (0.023 mol) dissolved in 50 mL of dry DMA were added to the reaction mixture, and this was mixed by stirring in a water bath at 80 °C. Afterward, 5 g (0.046 mol) of $MeOB_3$ was added to the mixture and stirred for 5 minutes, and this was followed by adding 0.737 g (0.01 mol) of $nBuNH_2$ in dry DMA for 1 hour, in a drop-wise manner. The mixture was further stirred for 3 hours and then kept overnight. The following day, the reaction mixture was preheated at 80 °C and a solution of 5% (70 mL) acetic acid was then added. The reaction mixture was stirred for 1 hour and then allowed to cool down. The precipitate product was collected by filtration and washed twice with hot water at 50 °C, followed by drying and purification using thin-layer chromatography as previously described. The purified product (1B8) was recrystallized from ethanol solvent, forming orange crystals. The Buchi 150 apparatus was used to determine the melting points.



3,4-dimethoxybenzaldehyde 3-chloroacetylacetone (*2E*)-3-phenylbut-2-enal 1B8

Figure 3.2: The synthetic route for the asymmetric curcumin derivative, 1B8. Chemical structures constructed using ACD/ChemSketch freeware: www.acdlabs.com (constructed on: 08 March 2024).

Characterization of the three synthetic curcumin derivatives

Mass spectroscopy

Mass spectrometry (MS) was used to determine the molecular weight and composition of the synthesized curcumin derivatives. This provides information about the fragmentation pattern of the molecule, which aided in identifying these structures. In this study, the Water Synapt G2 high resolution - mass spectrometry - electrospray ionization (HR-MS-ESI) was used to record mass spectra with the aid of electrospray ionization protocol. Briefly,

the purified synthesized curcumin derivatives were dissolved in methanol to achieve a concentration of 1 mg/mL and filtered through a 0.22 µm membrane prior to analysis to remove particulate matter. Derivatization was not necessarily due to the inherent ionization efficiency of the derivatives. Mass spectra were acquired in positive ionization mode, and instrument parameters were optimized for each derivative to ensure accurate detection of molecular ions and fragmentation patterns.

FT-IR spectroscopy

In this study, the fourier transform - infrared (FT-IR) spectroscopy was used to identify and confirm the functional groups present in the three synthesized curcumin derivatives based on their characteristic absorption frequencies.
This was particularly useful for identifying functional groups like ―OH (alcohol), ―NH2 (amine), and C=O (carbonyl), among others. IR spectra were determined using the Shimadzu FT-IR-84005 and Parkin-Elmer 100 ATR-IR spectrometers. Briefly, each of the three synthetic curcumin derivatives was mixed with potassium bromide (KBr) and ground into a fine powder using a pestle and mortar. Subsequently, the thin and translucent pellets of the powdered mixtures were prepared using a Qwik Handi-Press. These pellets were then analyzed via FT-IR in the 4000 - 350 cm^{-1} region, with background effects adjusted using KBr pellets.

^{1}H-NMR spectroscopy

The proton nuclear magnetic resonance (^{1}H-NMR) spectroscopy was used to determine the connectivity of atoms and identify different functional groups of the three synthetic curcumin derivatives. This provides information about the local environment of various nuclei, such as ^{1}H ions, which helps to elucidate the structures of the synthesized curcumin derivatives. The ^{1}H–NMR spectra were used in this study to record chloroform ($CDCl_3$) or dimethyl sulfoxide-d_6 (DMSO-d_6 or deuterated DMSO) using the Bruker 600 (600 MHz) and Varian 200 (200 MHz) NMR spectrometers. Briefly, the samples were prepared by dissolving 12 mg of each curcumin derivative in a glass vial using either deuterated $CDCl_3$ or DMSO-d_6 solvents. The dissolved samples were then filtered and transferred to an NMR tube. The ^{1}H–NMR analysis was conducted, and the resulting spectra were analyzed using TopSpin 4.0.6 software. Chemical shifts were referenced to tetramethylsilane (TMS) as an internal standard and reported in δ (ppm).

Results and Discussion

Synthesis of three curcumin derivatives

The two chloro curcumin derivatives (1A6 and 1A8) and the asymmetric curcumin derivative (1B8) were successfully synthesized as previously reported [19]. Curcumin has several functional groups that can be modified to alter its properties, including the diketo functionality, the active methylene group, the linker chain, and the aryl side chains [7]. Figure 3.3 illustrates the chemical structures of curcumin, 1A6, 1A8, and 1B8, and demonstrates the functional groups that were structurally modified for the three synthetic curcumin derivatives. The chemical structures of 1A6 and 1A8 depict two symmetrical aldehyde substitutions (3,4-dimethoxy benzaldehyde for 1A6 and 3-hydroxybenzaldehyde for 1A8) in the aryl side chains and an addition of chlorine in the active methylene group (Figure 3.3). Meanwhile, the chemical structure of 1B8 more closely resembles that of curcumin and has two asymmetric aldehydes (3,4-dimethoxy benzaldehyde and beta-methyl cinnamaldehyde) substitutions in the aryl side chains (Figure 3.3). The active methylene group refers to a methylene group (-CH2-) that is positioned between the two carbonyl groups. The active methylene group is typically involved in chemical reactions such as Michael additions, enolization, and condensation reactions [20], and the modification of this group can lead to structural analogs with improved pharmacological properties and enhanced bioavailability [21]. The two aryl side chains of curcumin have various substitutions or functional groups attached to them, and structural modification of these side chains involves the addition of different functional groups such as aldehydes or altering the side chain patterns, thus leading to improved stability, metabolism, and biological activity of a compound [21].

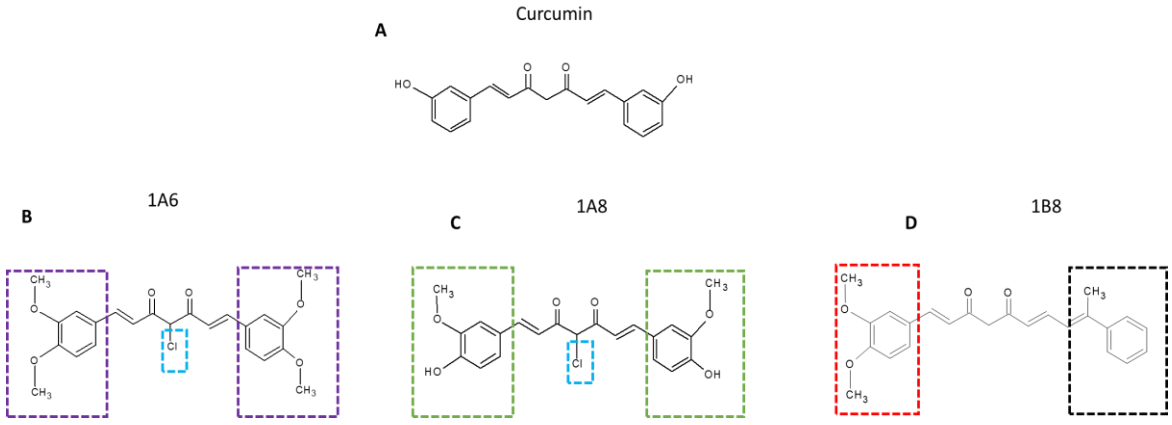


Figure 3.3: The chemical structures of curcumin and the three synthetic curcumin derivatives, 1A6, 1A8, and 1B8. The functional groups that are highlighted in the chemical structures of 1A6, 1A8, and 1B8 demonstrate structural modification in comparison to curcumin. Chemical structures constructed using ACD/ChemSketch freeware: www.acdlabs.com (constructed on: 08 March 2024).

The three synthesized curcumin derivatives attained high purity (>99%) as shown in Table 3.1. Notably, the yield of the three synthesized curcumin derivatives varied, with the percentage yield ranking from 31%, 25%, to 17% for 1A6, 1A8, and 1B8, respectively (Table 3.1). The compound, 1B8, exhibited the lowest yield, and this was attributed to the simultaneous of reaction of acetylacetone and the two distinct aldehydes. Moreover, high melting points of 168°C – 170°C, 218°C – 220°C, and 139°C – 140°C were displayed for 1A6, 1A8, and 1B8, respectively (Table 3.1). Generally, high melting points have been associated with strong intermolecular attractions [22,23], resulting in greater stability. Therefore, the synthesized curcumin derivatives with high melting points are thought to exhibit high thermal stabilities. Also, the presence of aromatic rings with electronic density further stabilize these curcumin derivatives, as previously demonstrated in pharmaceutical compounds [24].

Table 3.1: The yield, purity, and melting points of the three synthetic curcumin derivatives.

Curcumin derivative	Yield	Purity	Melting point
1A6 **(1E,6E)-4-chloro-1,7-bis(3,4-dimethoxyphenyl)hepta-1,6-diene3,5-dione**	31%	>99%	168°C - 170°C
1A8 **(1E,6E)-4-chloro-1,7-bis(3-hydroxyphenyl)hepta-1,6-diene-3,5-dione**	25%	>99%	218°C - 220°C
1B8 **(1E,6E,8E)-1-(3,4-dimethoxyphenyl)-9-phenyldeca-1,6,8-triene-3,5dione**	17%	>99%	139°C - 140°C

Characterisation of synthetic curcumin derivatives

Mass spectroscopy

Mass spectrometry is an analytical technique that measures the mass-to-charge ratio (m/z) of ions and is used to identify and quantify chemical compounds [25]. It provides information about the molecular weight of the compound [26]. The mass spectra of the three synthetic curcumin derivatives demonstrated distinct molecular ion peaks as shown in Figure 3.4. 1A6 displayed a molecular ion peak at m/z 431.1248, matching the calculated molecular mass 430.88 (Figure 3.4A). Similarly, 1A8 exhibited a molecular ion peak at m/z 343.0731, matching the calculated molecular mass 342.77 (Figure 3.4B). Furthermore, the mass spectrum of 1B8 showed a molecular ion peak at m/z 377.1746, which also matched the calculated molecular mass 376.44 (Figure 3.4C). These molecular ion peaks correspond to the intact molecular ions of the respective curcumin derivatives, suggesting that the precise mass values obtained from the mass spectra significantly contribute to the comprehensive characterization of the curcumin derivatives and support their identification. Although the strength of mass spectroscopy relies on its ability to identify molecular mass and confirm molecular formula [24,27], its applicability is constrained as it cannot provide significant insights into the structural formula [28].

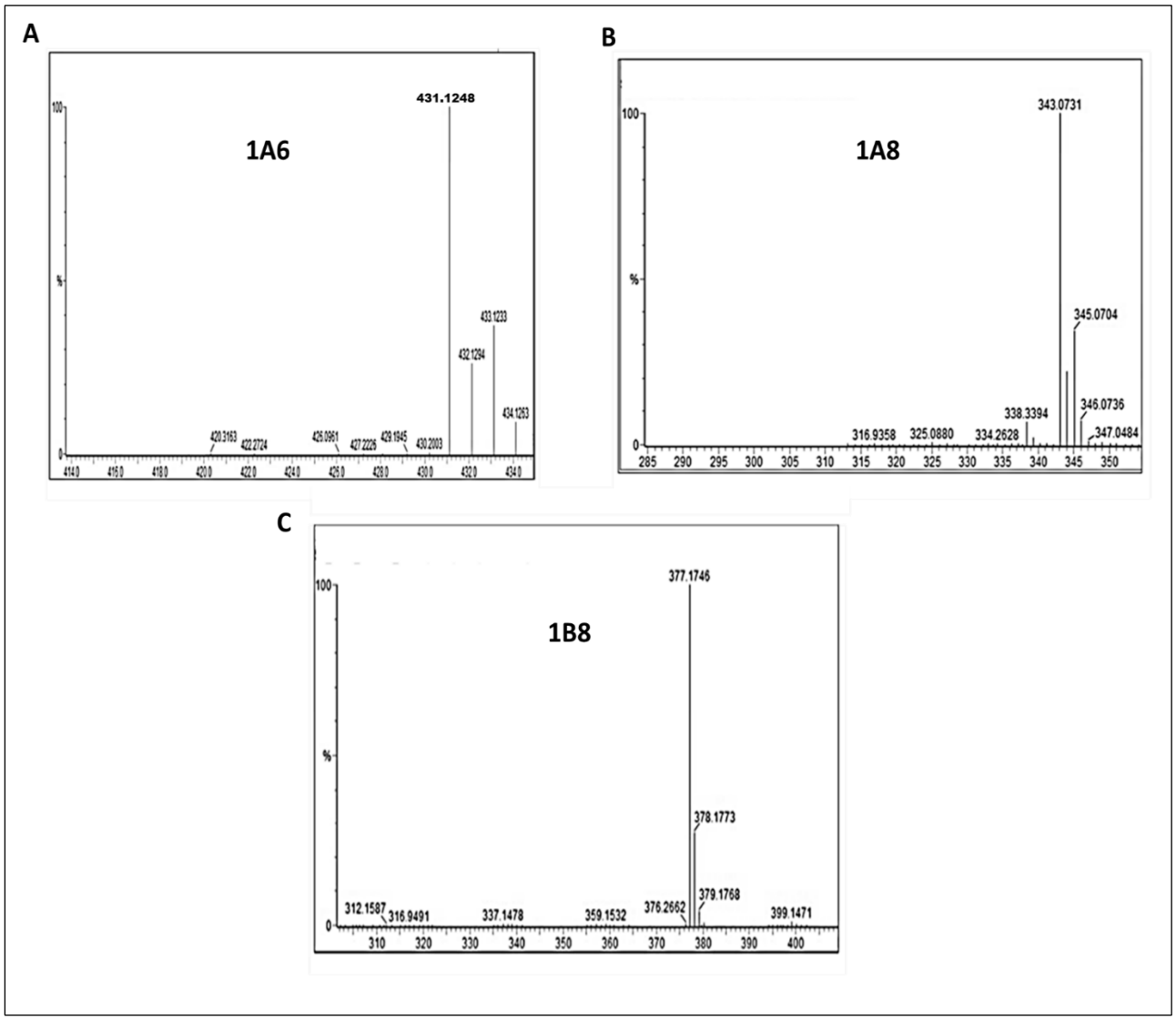


Figure 3.4: Representative mass spectrum data of the three synthetic curcumin derivatives, 1A6 (A), 1A8 (B), and 1B8 (C).

FT-IR spectroscopy

To address the limitations of mass spectrometry in assessing the structural formula, we employed Fouriertransform infrared (FTIR) spectroscopy to identify the functional groups present in the synthesized curcumin derivatives. The major FT-IR spectral peaks of the synthetic curcumin derivatives were recorded (Table 3.2) and the results showed that the three synthetic curcumin derivatives exhibited characteristic peaks at various frequencies, providing valuable insights into their molecular compositions.

Table 3.2: Major FT-IR spectrum bands (cm^{-1}) of the three synthetic curcumin derivatives.

Curcumin Derivatives	υ C-H aromatic	υ C-H aliphatic	υ C=O	υ C=C	υ C-O	others

1A6	3017	2897	1610	1597	1250 and 1022	828 C-H bending
1A8	3002	2897	1619	1589	1257 and 1036	849, 823 C-H bending
1B8	3068		1615	1592	1254 and 1019	

Accordingly, the FT-IR spectra of 1A6 showed the presence of stretching vibrations peak at 3017 cm^{-1}, which indicates the aromatic C-H bonds in the phenyl rings [29]. Additionally, the presence of aliphatic C-H stretching vibrations is evident from the peak at 2897 cm^{-1}, likely originating from the methylene (CH) groups in the molecule [30]. The strong peak at 1660 cm^{-1} indicates the presence of a conjugated carbonyl group (C=O) [31], characteristic of the β-diketone moiety of 1A6. Meanwhile, the peak at 1597 cm^{-1} is attributed to the aromatic C=C stretching vibrations in the phenyl rings [32]. Moreover, the C-O stretching vibrations are evident from the peaks at 1250 cm^{-1}, possibly due to ether linkages or phenolic groups [33]. In addition, the peak at 1022 cm^{-1}, further supports the presence of C-O stretching vibrations (Table 3.2).

The FT-IR spectra for 1A8 showed a peak at 3002 cm^{-1}, which indicates the presence of aromatic C-H stretching vibrations, confirming the existence of phenyl rings in the molecule [29]. Additionally, the peak at 2897 cm^{-1} suggests aliphatic C–H stretching vibrations, pointing to the presence of methylene (CH2) groups [30]. Meanwhile, the peak at 1619 cm^{-1} corresponds to the conjugated carbonyl group (C=O) present in the β-diketone moiety of 1A8 [31], indicating a crucial structural feature. Furthermore, the peak at 1589 cm^{-1} indicates aromatic C=C stretching vibrations, which confirmed the presence of conjugated double bonds in the phenyl rings [32]. The peak at 1257 cm^{-1} represents C–O stretching vibrations, which likely originate from ether linkages or phenolic groups [33] (Table 3.2). The FT-IR spectra for 1B8 showed a peak at 3068 cm^{-1}, which corresponds to the stretching vibration of aromatic C–H bonds, confirming the presence of phenyl rings in the compound [29]. Additionally, the peak at 2989 cm^{-1} indicated the aliphatic C–H stretching vibrations, suggesting the existence of methylene groups [30]. Meanwhile, the peak at 1615 cm^{-1} is indicative of the conjugated carbonyl group (C=O) present in the β-diketone moiety [31], which is a fundamental characteristic of the chemical structure of 1B8 curcumin derivative. Moreover, the peak at 1592 cm^{-1} confirmed the presence of aromatic C=C stretching vibrations, further supporting the presence of conjugated double bonds in the phenyl rings [32]. The peak at 1254 cm^{-1} represented the C–O stretching vibrations, likely originating from ether linkages or phenolic groups [33] (Table 3.2).

The comparison of the FT-IR spectra of the unconjugated ketones with those of the three synthesized curcumin derivatives demonstrated that the stretching frequencies of the carbonyl groups shifted from 1715 cm^{-1} to lower frequencies, specifically in the range of 1620 – 1625 cm^{-1}, due to resonance effects [34]. Additionally, the spectra exhibited medium bands between the frequencies of 1626 – 1620 cm^{-1}, which correspond to the stretching vibrations of the carbonyl groups (Table 3.2). These shifts were attributed to the tautomeric changes in the curcuminoids, indicating the presence of different tautomeric forms in the three synthesized curcumin derivatives [35]. These FT-IR spectrum data align with the proposed chemical structures of the three synthetic curcumin derivatives and collectively contribute to a comprehensive understanding of the functional groups and chemical bonding present in the three synthetic curcumin derivatives.

^{1}H-NMR spectroscopy

Since the synthesized curcumin derivatives, like other organic compounds, are composed of hydrogen atoms distributed across the structure, ^{1}H-NMR spectroscopy was used to assess the arrangement of protons to further deduce the structure of these organic compounds, as previously conducted [19]. The ^{1}H-NMR spectrum results for the three synthetic curcumin derivatives are illustrated in Figure 3.5.

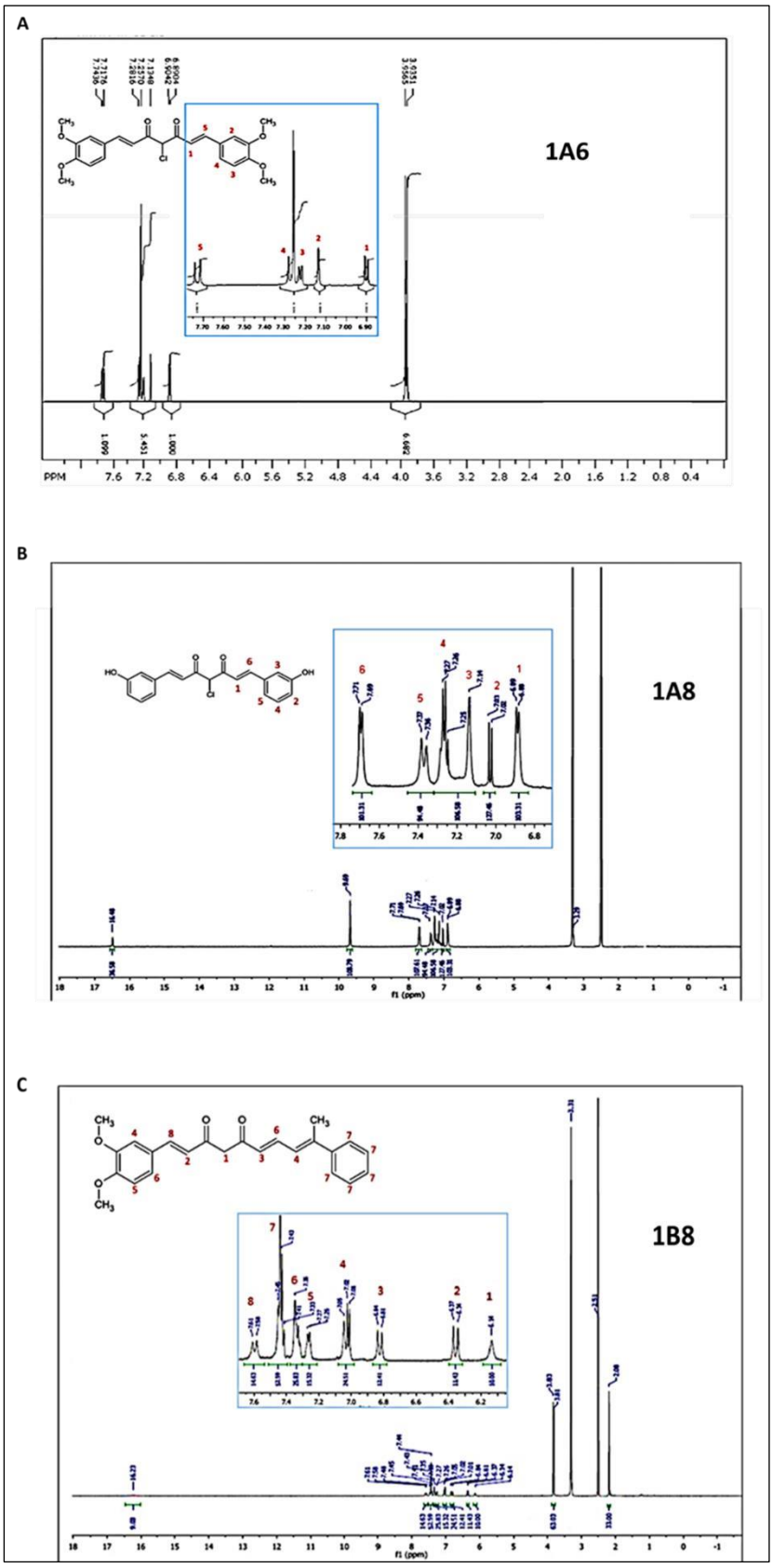


Figure 3.5: Representative ^{1}H-NMR spectral data for the three synthetic curcumin derivatives, 1A6 (A), 1A8 (B), and 1B8 (C).

Briefly, in the ^{1}H-NMR spectrum of 1A6, the presence of two sets of signals at δ = 3.93 ppm (6H, s, p-OCH3) and δ = 3.95 ppm (6H, s, m-OCH3) indicated the occurrence of two distinct methoxy (OCH3) groups [36]. The singlet nature of these peaks suggests that each methoxy group contains six equivalent protons. Notably, the chemical shifts at δ = 6.897 ppm (2H, d, j=12, olefinic protons) and δ = 7.805 ppm (2H, d, j=18, olefinic protons) corresponded to two different olefinic (double bond) systems, each displaying a doublet splitting pattern with coupling constants (J value) of 12 Hz and 18 Hz, respectively [37]. Additionally, the ^{1}H-NMR spectrum of 1A6 displayed signals at δ = 7.134 ppm (2H, s, Ar-H), δ = 7.251 ppm (2H, d, Ar-H, partially overlapping with CDCl3 solvent), and δ = 7.281 ppm (2H, Ar-H, overlapping with CDCl3 solvent), revealing the presence of aromatic protons in the compound (Figure 3.5A) [38].

The ^{1}H-NMR spectrum of 1A8 curcumin derivative displayed the presence of a peak at δ = 6.88 ppm (2H, d, j =6, olefinic proton), which corresponded to two olefinic protons displaying a doublet splitting pattern with a coupling constant of 6 Hz, indicating the presence of a double bond [37]. Another set of olefinic protons appeared at δ = 7.77 ppm (2H, d, j=12, olefinic proton), also exhibiting a doublet splitting pattern but with a larger coupling constant (J = 12 Hz). The presence of these olefinic protons suggests the existence of two different double-bond systems within the compound. Additionally, the ^{1}H-NMR spectrum displayed signals at δ = 7.02 ppm (2H, j=6, Ar-H), δ = 7.14 ppm (2H, s, Ar-H), δ = 7.26 ppm (2H, t, j=6, Ar-H), and δ = 7.36 ppm (2H, d, j=6, Ar-H), each corresponding to two protons attached to aromatic hydrogens [38]. Notably, the peak at δ = 7.14 ppm appeared as a singlet, indicating that both protons are in the same local environment. On the other hand, the signals at δ = 7.02 ppm, δ = 7.26 ppm, and δ = 7.36 ppm exhibited different coupling patterns with a coupling constant of 6 Hz, suggesting diverse local environments for these aromatic protons. Furthermore, a significant peak occurred at δ = 9.69 ppm (2H, s, OH), representing two protons attached to a hydroxyl (OH) group [39]. This signal appeared as a singlet, indicating that both hydroxyl protons are in the same chemical environment (Figure 3.5B). It is worth noting that the confirmed structure occurred in the enantiomer form with the chloro group forming the chiral center of the structure therefore, these findings confirm both parts of the enantiomeric form of chloro series derivatives.

The asymmetric curcumin derivative (1B8) demonstrated peaks at δ = 2.08 ppm (3H, s, CH3), δ = 3.81 ppm (3H, s, OCH3), and δ = 3.83 ppm (3H, s, OCH3) that correspond to three sets of protons attached to methyl groups (CH3) and methoxy groups [36]. The singlet nature of these peaks indicated that each set of protons is in the same chemical environment. Moreover, the spectrum displayed several peaks in the region between δ = 6 ppm to δ = 7.6

ppm, which are characteristic of aromatic and olefinic protons [38]. The peak at δ = 6.14 ppm (1H, s, vinylic proton) represented a single proton known as a vinylic proton [40], indicating the presence of a vinyl group, while the signals at δ = 6.355 ppm (1H, d, j=18, olefinic proton), δ = 6.823 ppm (1H, d, j=18, olefinic proton), δ = 7.035 ppm (1H, d, j=18, olefinic proton), and δ = 7.595 ppm (1H, d, j=18, olefinic proton) corresponded to four different olefinic protons, each displaying a doublet splitting pattern with a coupling constant of 18 Hz, suggesting the presence of four distinct olefinic bonds in the compound [37]. Additionally, the spectrum showed signals at δ = 7.01 ppm (2H, s, phenylic proton) and δ = 7.265 ppm (1H, d, j=6, phenylic proton) representing two phenylic protons (2H and 1H, respectively) (Figure 3.5C) [38].

The δ = 7.01 ppm peak appeared as a singlet, indicating that both phenylic protons are in the same local environment. The peak at δ = 7.265 ppm exhibited a doublet splitting pattern with a coupling constant of 6 Hz, suggesting different local environments for these phenylic protons. The spectrum also showed a signal at δ = 7.35 ppm (1H, dd, j=18, olefinic proton) representing a single olefinic proton with a doublet-doublet splitting pattern and a coupling constant of 18 Hz. Furthermore, a peak at δ = 7.44 ppm (5H, m, j=6, phenylic proton) corresponds to five phenylic protons exhibiting a multiplet (*m*) pattern with a coupling constant of 6 Hz, further supporting the presence of aromatic rings in the compound (Figure 3.5C) [38]. The ^{1}H-NMR data suggested that the three synthetic curcumin derivatives are complex molecules, incorporating aromatic rings, olefinic, vinylic, and phenyl bonds, hydroxyl, methyl, and methoxy groups. The presence of multiple aromatic and olefinic, vinylic, and phenyl protons indicates the intricate nature of their molecular structures.

Conclusion

In this chapter, three synthetic curcumin derivatives including two chloro curcumin derivatives, 1A6 and 1A8, and one asymmetric curcumin derivative, 1B8, were successfully synthesized and characterized as previously reported [19]. These derivatives were strategically synthesized to enhance specific functional groups, including the active methylene group and aryl side chains of curcumin, aiming to improve their biological properties and pharmacokinetic properties [21]. The synthesis process yielded high-purity compounds (>99%) with varying yields and high melting points, indicative of robust thermal stability and potential applicability in biomedical research. The spectroscopic characterization of these derivatives, including Mass spectrometry, FT-IR, and 1HNMR, provided a detailed analysis of their molecular structures and functional groups. Mass spectrometry analysis confirmed the molecular ion peaks for 1A6, 1A8, and 1B8, aligning closely with their calculated molecular masses. FT-IR spectroscopy revealed characteristic peaks corresponding to aromatic and aliphatic C-

H stretching vibrations, carbonyl groups (C=O), and C=C double bonds, further confirming the structural modifications in each derivative. Meanwhile, ^{1}H-NMR spectra exhibited signals indicative of aromatic rings, olefinic and vinylic bonds, and various functional groups such as hydroxyl, methyl, and methoxy groups, providing detailed structural analysis into these complex molecules.

In conclusion, the comprehensive synthesis and spectroscopic characterization of these curcumin derivatives, 1A6, 1A8, and 1B8, have provided a solid foundation for further investigation into their potential therapeutic applications.

References

[1] V. Soleimani, A. Sahebkar, and H. Hosseinzadeh, "Turmeric (Curcuma longa) and its major constituent (curcumin) as nontoxic and safe substances: Review," Phyther. Res., vol. 32, no. 6, pp. 985–995, Jun. 2018, doi: 10.1002/ptr.6054.

[2] J. Vogel, A. and Pelletier, "Examen chimique de la racine de Curcuma," Pharm, 1815. https://scholar.google.com/scholar?hl=en&as_sdt=0%2C5&q=Vogel%2C+A.+and+Pelletier%2C+J.%2C+1815.+Examen+chimique+de+la+racine+de+Curcuma.+J+Pharm%2C+1%2C+pp.289300.+&btnG= (accessed Oct. 27, 2022).

[3] E. Vogel, "Die bibliothek der benediktinerabtei sponheim," Serapeum, vol. 3, pp. 312–328, 1842.

[4] V. Lampe and J. Milobedzka, "Studien über Curcumin," Berichte der Dtsch. Chem. Gesellschaft, vol. 46, no. 2, pp. 2235–2240, Apr. 1913, doi: 10.1002/cber.191304602149.

[5] K. I. Priyadarsini, "The chemistry of curcumin: from extraction to therapeutic agent," Molecules, vol. 19, no. 12, pp. 20091–112, Dec. 2014, doi: 10.3390/molecules191220091.

[6] S. I. Kawano, Y. Inohana, Y. Hashi, and J.-M. M. Lin, "Analysis of keto-enol tautomers of curcumin by liquid chromatography/mass spectrometry," Chinese Chem. Lett., vol. 24, no. 8, pp. 685–687, Aug. 2013, doi: 10.1016/j.cclet.2013.05.006.

[7] S. C. Gupta et al., "Multitargeting by curcumin as revealed by molecular interaction studies," Nat. Prod. Rep., vol. 28, no. 12, p. 1937, 2011, doi: 10.1039/c1np00051a.

[8] O. Kazakova, N. Lipkovska, and V. Barvinchenko, "Keto-enol tautomerism of curcumin in the preparation of nanobiocomposites with fumed silica," Spectrochim. Acta Part A Mol. Biomol. Spectrosc., vol. 277, p. 121287, Sep. 2022, doi: 10.1016/j.saa.2022.121287.

[9] H. Yin et al., "Curcumin Suppresses IL-1β Secretion and Prevents Inflammation through Inhibition of the NLRP3 Inflammasome," J. Immunol., vol. 200, no. 8, pp. 2835–2846, Apr. 2018, doi: 10.4049/jimmunol.1701495.

[10] C. Yang et al., "Curcumin induces apoptosis and protective autophagy in castration-resistant prostate cancer cells through iron chelation," Drug Des. Devel. Ther, vol. Volume11, pp. 431–439, Feb. 2017, doi: 10.2147/DDDT.S126964.

[11] L.-Y. Y. Wu, C.-W. W. Chen, L.-K. K. Chen, H.-Y. Y. Chou, C.-L. L. Chang, and C.-C. C. Juan, "Curcumin Attenuates Adipogenesis by Inducing Preadipocyte Apoptosis and Inhibiting Adipocyte Differentiation.," Nutrients, vol. 11, no. 10, p. 2307, Sep. 2019, doi: 10.3390/nu11102307.

[12] M. Dei Cas and R. Ghidoni, "Dietary Curcumin: Correlation between Bioavailability and Health Potential," Nutrients, vol. 11, no. 9, p. 2147, Sep. 2019, doi: 10.3390/nu11092147.

[13] Z. Ma, N. Wang, H. He, and X. Tang, "Pharmaceutical strategies of improving oral systemic bioavailability of curcumin for clinical application," J. Control. Release, vol. 316, no. October, pp. 359–380, Dec. 2019, doi: 10.1016/j.jconrel.2019.10.053.

[14] S. J. Stohs, O. Chen, S. D. Ray, J. Ji, L. R. Bucci, and H. G. Preuss, "Highly Bioavailable Forms of Curcumin and Promising Avenues for Curcumin-Based Research and Application: A Review," Molecules, vol. 25, no. 6, p. 1397, Mar. 2020, doi: 10.3390/molecules25061397.

[15] S. Rivera-Mancía, M. C. Lozada-García, and J. Pedraza-Chaverri, “Experimental evidence for curcumin and its analogs for management of diabetes mellitus and its associated complications,” European Journal of Pharmacology, vol. 756. Elsevier, pp. 30–37, Jun. 05, 2015. doi: 10.1016/j.ejphar.2015.02.045.

[16] S. Oliveira, T. Monteiro-Alfredo, S. Silva, and P. Matafome, “Curcumin derivatives for Type 2 Diabetes management and prevention of complications,” Arch. Pharm. Res., vol. 43, no. 6, pp. 567– 581, Jun. 2020, doi: 10.1007/s12272-020-01240-3.

[17] S. Idoudi, T. Bedhiafi, Y. M. Hijji, and N. Billa, “Curcumin and Derivatives in Nanoformulations with Therapeutic Potential on Colorectal Cancer,” AAPS PharmSciTech, vol. 23, no. 5. Springer Science and Business Media Deutschland GmbH, p. 115, Jul. 19, 2022. doi: 10.1208/s12249-022-02268-y.

[18] B. Aggarwal, L. Deb, and S. Prasad, “Curcumin Differs from Tetrahydrocurcumin for Molecular Targets, Signaling Pathways and Cellular Responses,” Molecules, vol. 20, no. 1, pp. 185–205, Dec. 2014, doi: 10.3390/molecules20010185.

[19] E. Ooko et al., “Modulation of P-glycoprotein activity by novel synthetic curcumin derivatives in sensitive and multidrug-resistant T-cell acute lymphoblastic leukemia cell lines,” Toxicol. Appl. Pharmacol., vol. 305, pp. 216–233, Aug. 2016, doi: 10.1016/j.taap.2016.06.002.

[20] R. R. Kotha and D. L. Luthria, “Curcumin: Biological, Pharmaceutical, Nutraceutical, and Analytical Aspects,” Molecules, vol. 24, no. 16, p. 2930, Aug. 2019, doi: 10.3390/molecules24162930.

[21] R. Tabanelli, S. Brogi, and V. Calderone, “Improving Curcumin Bioavailability: Current Strategies and Future Perspectives,” Pharmaceutics, vol. 13, no. 10, p. 1715, Oct. 2021, doi: 10.3390/pharmaceutics13101715.

[22] E. J. Walsh, “book & media reviews,” vol. 74, no. 8, pp. 905–906, 1997.

[23] J. C. Dearden, “The QSAR prediction of melting point, a property of environmental relevance,” Sci. Total Environ., vol. 109–110, pp. 59–68, Dec. 1991, doi: 10.1016/0048-9697(91)90170-J.

[24] E. Lizarraga, C. Zabaleta, and J. A. Palop, “Thermal stability and decomposition of pharmaceutical compounds,” J. Therm. Anal. Calorim, vol. 89, no. 3, pp. 783–792, Sep. 2007, doi: 10.1007/s10973006-7746-4.

[25] L. Li and Z. Tian, “Interpreting raw biological mass spectra using isotopic mass-to-charge ratio and envelope fingerprinting,” Rapid Commun. Mass Spectrom., vol. 27, no. 11, pp. 1267–1277, Jun. 2013, doi: 10.1002/rcm.6565.

[26] S. Jarussophon et al., “Automated molecular formula determination by tandem mass spectrometry (MS/MS),” Analyst, vol. 134, no. 4, p. 690, 2009, doi: 10.1039/b818398h.

[27] F. Cuyckens and M. Claeys, “Mass spectrometry in the structural analysis of flavonoids,” J. Mass Spectrom., vol. 39, no. 1, pp. 1–15, Jan. 2004, doi: 10.1002/jms.585.

[28] Y. Ünver, N. Süleymanoğlu, R. Ustabaş, K. İ. Bektaş, E. Bektaş, and H. İ. Güler, “3-(5-(1 H -imidazol-1-yl) pent-1-en-1-yl)-9-ethyl-9 H -carbazole: synthesis, characterization (IR, NMR), DFT, antimicrobial-antioxidant activities and docking study,” J. Biomol. Struct. Dyn, vol. 40, no. 23, pp. 12990–13000, Dec. 2022, doi: 10.1080/07391102.2021.1977708.

[29] J. Coates, “Interpretation of Infrared Spectra, A Practical Approach,” in Encyclopedia of Analytical Chemistry, Wiley, 2000, pp. 10815–10837. doi: 10.1002/9780470027318.a5606.

[30] R. Lu, W. Gan, B. Wu, Z. Zhang, Y. Guo, and H. Wang, “C−H Stretching Vibrations of Methyl, Methylene and Methine Groups at the Vapor/Alcohol (n = 1−8) Interfaces,” J. Phys. Chem. B, vol. 109, no. 29, pp. 14118–14129, Jul. 2005, doi: 10.1021/jp051565q.

[31] L. Aibibula et al., “Analyses and identification of the chemical constituents of the Uighur formulation Baixuan Xiatare using three-stage infrared spectroscopy,” J. Tradit. Chinese Med., vol. 40, no. 5, pp. 875–882, 2020, Accessed: Oct. 11, 2023. [Online]. Available: http://journaltcm.com/EN/abstract/abstract6105.shtml

[32] K. Ueno and A. E. Martell, “Infrared Studies on Synthetic Oxygen Carriers.,” J. Phys. Chem., vol. 60, no. 9, pp. 1270–1275, Sep. 1956, doi: 10.1021/j150543a029.

[33] J. E. Kovacic, “The C□ N stretching frequency in the infrared spectra of Schiff’s base complexes—I. Copper complexes of salicylidene anilines,” Spectrochim. Acta Part A Mol. Spectrosc., vol. 23, no. 1, pp. 183–187, Jan. 1967, doi: 10.1016/0584-8539(67)80219-8.

[34] E. Pretsch, P. Bühlmann, and M. Badertscher, Structure Determination of Organic Compounds. Berlin, Heidelberg: Springer Berlin Heidelberg, 2009. doi: 10.1007/978-3-540-93810-1.

[35] P. H. Bong, “Spectral and photophysical behaviors of curcumin and curcuminoids,” Bull. Korean Chem. Soc., vol. 21, no. 1, pp. 81–86, 2000, Accessed: Oct. 11, 2023. [Online]. Available: https://koreascience.kr/article/JAKO200013464475192.page

[36] K. Karaoglu, T. Baran, K. Serbest, M. Er, and I. Degirmencioglu, “Two novel macroacyclic schiff bases containing bis-N2O2 donor set and their binuclear complexes: synthesis, spectroscopic and magnetic properties,” J. Mol. Struct., vol. 922, no. 1–3, pp. 39–45, Mar. 2009, doi: 10.1016/j.molstruc.2009.01.037.

[37] H. M. Vinusha et al., “Preparation, spectral characterization and biological applications of Schiff base ligand and its transition metal complexes,” Results Chem., vol. 1, 2019, doi: 10.1016/j.rechem.2019.100012.

[38] R. Abdelkader, H. Amine, and B. Mohammed, “H-NMR Spectra of Conductive, Anticorrosive and Soluble Polyaniline 1 Exchanged by an Eco-Catalyst Layered (Maghnite-H),” World J. Chem., vol. 8, no. 1, pp. 20–26, 2013, doi: 10.5829/idosi.wjc.2013.8.1.2902.

[39] E. Liepinsh, G. Otting, and K. Wüthrich, “NMR spectroscopy of hydroxyl protons in aqueous solutions of peptides and proteins,” J. Biomol. NMR, vol. 2, no. 5, pp. 447–465, Sep. 1992, doi: 10.1007/BF02192808.

[40] E. L. Eliel and M. Manoharan, “Conformational analysis. 40. Conformation of 1-methyl-1-phenylcyclohexane and conformational energies of the phenyl and vinyl groups,” J. Org. Chem., vol. 46, no. 9, pp. 1959–1962, Apr. 1981, doi: 10.1021/jo00322a056.

CHAPTER 4

Chapter outline:

This chapter is presented as a research article describing the prediction of toxicity, pharmacokinetic profiles, biological targets, and molecular interactions of curcumin and the three synthetic curcumin derivatives with predicted biological targets. This chapter covers objective 2 of this research study. The article is written as per journal's guidelines and formats.

Status: (Published)

Computational article published in International Journal of Molecular Sciences, 2024, 25, 5: 2603, doi: https://doi.org/10.3390/ijms25052603

Evaluating the Therapeutic Potential of Curcumin and Synthetic Derivatives: A Computational Approach to Anti-Obesity Treatments

Marakiya T. Moetlediwa [1,2], Babalwa U. Jack [1,*], Sithandiwe E. Mazibuko-Mbeje [2], Carmen Pheiffer [1,3], Salam J. J. Titinchi [4], Elliasu Y. Salifu [1] and Pritika Ramharack [1,5]

[1] Biomedical Research and Innovation Platform, South African Medical Research Council, Tygerberg 7505, South Africa; marakiya.moetlediwa@mrc.ac.za (M.T.M.); carmen.pheiffer@mrc.ac.za (C.P.); elliasu.salifu@mrc.ac.za (E.Y.S.); pritika.ramharack@mrc.ac.za (P.R.)

[2] Department of Biochemistry, North-West University, Mmabatho 2745, South Africa; sithandiwe.mazibukombeje@nwu.ac.za

[3] Department of Obstetrics and Gynaecology, Faculty of Health Sciences, University of Pretoria, Pretoria 0001, South Africa

[4] Department of Chemistry, Faculty of Natural Science, University of the Western Cape, Bellville 7535, South Africa; stitinchi@uwc.ac.za (S.J.J.T)

[5] Pharmaceutical Sciences, School of Health Sciences, University of KwaZulu-Natal, Westville, Durban 4001, South Africa

* Correspondence: babalwa.jack@mrc.ac.za (B.U.J)

Abstract

Natural compounds such as curcumin, a polyphenolic compound derived from the rhizome of turmeric, have gathered remarkable scientific interest due to their diverse metabolic benefits including anti-obesity potential. However, curcumin faces challenges stemming from its unfavorable pharmacokinetic profile. To address this issue, synthetic curcumin derivatives aimed at enhancing the biological efficacy of curcumin have previously been developed. *In silico* modelling techniques have gained significant recognition in screening synthetic compounds as drug candidates. Therefore, the primary objective of this study was to assess the pharmacokinetic and pharmacodynamic characteristics of three synthetic derivatives of curcumin. This evaluation was conducted in comparison to curcumin, with a specific emphasis on examining their impact on adipogenesis, inflammation, and lipid metabolism as potential therapeutic targets of obesity mechanisms. In this study, predictive toxicity screening confirmed the safety of curcumin, with the curcumin derivatives demonstrating a safe profile based on their LD50 values. The synthetic curcumin derivative 1A8 exhibited inactivity across all selected toxicity endpoints. Furthermore, these compounds were deemed viable candidate drugs as they adhered to Lipinski's rules and exhibited favorable metabolic profiles. Molecular docking studies revealed that both curcumin and its

synthetic derivatives exhibited favorable binding scores, whilst molecular dynamic simulations showed stable binding with peroxisome proliferator-activated receptor gamma (PPARγ), cyclooxygenase 2 (COX2), and fatty acid synthase (FAS) proteins. The binding free energy calculations indicated that curcumin displayed potential as a strong regulator of PPARγ (−60.2 ± 0.4 kcal/mol) and FAS (−37.9 ± 0.3 kcal/mol), whereas 1A8 demonstrated robust binding affinity with COX2 (−64.9 ± 0.2 kcal/mol). In conclusion, the results from this study suggest that the three synthetic curcumin derivatives have similar molecular interactions to curcumin with selected biological targets. However, *in vitro* and *in vivo* experimental studies are recommended to validate these findings.

Keywords: pharmacokinetics; pharmacodynamics; obesity; curcumin; synthetic curcumin derivatives

Introduction

Obesity has emerged as a public health threat, with drastic increases worldwide. According to the World Health Organization (WHO), about 13% of the global population are obese (body mass index [BMI] ≥ 30 kg/m^2) and the prevalence of obesity is projected to increase to 20% by 2025 [1]. Obesity and overweight contribute to the rise of various metabolic complications such as inflammation [2], lipotoxicity [3], and dyslipidemia [4]. Also, the adverse effects of obesity and overweight contribute to the rise of non-communicable diseases such as diabetes [5], cardiovascular diseases (CVDs) [6], and different types of cancers [7]. Therefore, there is an urgent need for innovative therapeutic strategies to curb the prevalence of obesity and its underlying metabolic complications. In recent years, natural products have gained considerable attention due to their potential health benefits [8,9]. Curcumin, a bioactive compound derived from the rhizome of the turmeric plant, otherwise called *Curcuma longa*, which belongs to the Zingiberaceae family, has shown promising anti-obesity properties through its ability to modulate various cellular pathways involved in lipid metabolism [10,11], adipogenesis [12–14], and inflammation [15,16]. While curcumin holds significant potential as an anti-obesity agent, its poor bioavailability and limited systemic exposure have hindered its clinical applications [17]. To address these challenges, studies have focused on the development of synthetic curcumin derivatives that are designed to improve the pharmacokinetic properties and enhance efficacy of curcumin. It is important to note that the cost of developing synthetic derivatives of curcumin depends on the complexity of the structure. In addition, the extraction of natural compounds is associated with a low yield and purity. As such, we previously reported that curcumin derivatives have the potential to ameliorate obesity and obesity-related metabolic complications even more effectively than curcumin [18].

The use of computational techniques in drug discovery and development has shown to be a useful tool for predicting the pharmacological properties of synthetic compounds, thus providing a cost-effective and timeefficient method of assessing their therapeutic potential [19]. Hence, in this study, we used computational techniques to explore the anti-obesity potential of curcumin and three previously synthesized curcumin derivatives. In a study by Ooko at al. [20], two chloro curcumin derivatives, specifically (1E,6E)-4-chloro-1,7bis(3,4-dimethoxyphenyl)hepta-1,6-diene-3,5-dione (1A6) and (1E,6E)-4-chloro-1,7-bis(3-hydroxyphenyl)hepta1,6-diene-3,5-dione (1A8), along with an asymmetric curcumin derivative, (1E,6E,8E)-1-(3,4-dimethoxyphenyl)-9phenyldeca-1,6,8-triene-3,5-dione (1B8), were synthesized using a chemical reaction involving acetylacetone or 3chloroacetylacetone with boric oxide. Subsequently, the synthetic compounds underwent characterization through various spectroscopic techniques, MS, FT-IR, and ^{1}H-NMR spectroscopy [20]. Moreover, these compounds demonstrated potential anti-cancer properties [20]. These findings lay the foundation to further evaluate the bioactivity of these synthetic curcumin derivatives, particularly for their anti-obesity potential. In this context, the present study aims to assess the pharmacokinetics and pharmacodynamics profiles of curcumin and synthetic curcumin derivatives (1A6, 1A8, and 1B8) using *in silico* approaches to identify and evaluate targeted obesity mechanisms. By leveraging computational models, we will evaluate their physicochemical properties, druglikeness, toxicity, and ADME properties, including absorption through the gastrointestinal tract, distribution to target tissues, and metabolism by hepatic enzymes. Furthermore, we explored the interactions between these compounds and their molecular targets involved in adipogenesis, lipid metabolism, and inflammation to predict their potential efficacy in combating obesity.

Results

Prediction of toxicity for curcumin and synthetic curcumin derivatives

Certain medicinal compounds may pose toxic effects, causing harm to organs and cells. Such compounds have the potential to harm the liver, disrupt the immune system, cause cancer, and even become cytotoxic. Protox II was used to predict the toxicity of curcumin and three synthetic curcumin derivatives (1A6, 1A8, and 1B8), and the findings are summarized in Table 4.1. The results indicated that curcumin belongs to Toxicity Class 4 while the synthetic curcumin derivatives belong to Toxicity Class 5. Table 4.1 shows the lethal dose of 2000 mg/kg for curcumin, while 4000 mg/kg of 1A6 and 1B8 and 4400 mg/kg of 1A8 were predicted as lethal doses. Typically, drugs administered orally undergo a first-pass effect in the liver, which can be a primary factor in causing liver

damage. Therefore, it is critical to assess the hepatotoxic effect of drugs. While curcumin, 1A6, and 1A8 were inactive for hepatoxicity at their lethal doses, 1B8 (4000 mg/kg) showed activity on hepatotoxicity (Table 4.1). The carcinogenic potential of curcumin, 1A6, 1A8, and 1B8 was predicted, revealing that the compounds were inactive for carcinogenicity at their lethal doses (Table 4.1). This suggests a non-promotive effect on tumor development. Immunotoxicity, referring to the potential of drugs to induce an undesirable immune response, was also investigated. Curcumin, 1A6, and 1B8 exhibited activity towards immunotoxicity while 1A8 did not display immunotoxicity at their respective lethal doses. The compound 1B8 at 4000 mg/kg demonstrated cytotoxic effects, whereas curcumin, 1A6, and 1A8 exhibited non-cytotoxic profiles at their respective lethal doses.

Table 4.1: Predicted toxicity profiles of curcumin, 1A6, 1A8, and 1B8.

Toxicity	**Curcumin**	**1A6**	**1A8**	**1B8**
LD_{50} (mg/kg)	2000	4000	4400	4000
Class	4	5	5	5
Hepatotoxicity	Inactive; *p* (0.61)	Inactive; *p* (0.52)	Inactive; *p* (0.63)	Active; *p* (0.53)
Carcinogenicity	Inactive; *p* (0.84)	Inactive; *p* (0.64)	Inactive; *p* (0.60)	Inactive; *p* (0.67)
Immunotoxicity	Active; *p* (0.92)	Active; *p* (0.80)	Inactive; *p* (0.61)	Active; *p* (0.96)
Cytotoxicity	Inactive; *p* (0.88)	Inactive; *p* (0.70)	Inactive; *p* (0.75)	Active; *p* (0.73)

It should be noted that these toxicity assessments are based on lethal dose predictions. *p*-value refers to the probability of activity or inactivity.

Prediction of the pharmacokinetic and physicochemical properties, druglikeness, and synthetic scores of curcumin and synthetic curcumin derivatives

Pharmacokinetic and physicochemical properties are critical factors in determining the efficacy and safety of a drug. Apart from experimental models, determining the druglikeness of a compound remains crucial as it directly

affects its absorption, metabolism, distribution, and elimination within the human system [21]. Lipinski's rules (LRo5) are widely accepted as a guideline for predicting the ability of a compound to be a drug candidate. According to LRo5, a drug should have a molecular weight of 500 daltons or less, no more than 5 hydrogen bond donors, no more than 10 hydrogen bond acceptors, and an octanol–water partition coefficient value of 5 or less. However, it is important to note that LRo5 is not an absolute rule but should be used as a general guide. Other factors, such as the drug's target and intended use, can also influence its druglikeness. Physicochemical properties, such as lipophilicity, water solubility, molecular weight, and polarity, influence the absorption, distribution, metabolism, and elimination of a drug in the body [22]. For instance, lipophilic compounds readily dissolve in lipids. Such drugs are more easily absorbed across cell membranes and are usually metabolized at a slower pace than hydrophilic drugs [23]. As depicted in Table 4.2, the predicted lipophilic score (iLOGP) for curcumin, 1A6, 1A8, and 1B8 was 3.27, 3.88, 1.85, and 3.83, respectively. Among these compounds, 1A6 had the highest iLOGP, which suggests better cell membrane penetration in lipid-rich environments.

Typically, drugs with poor water solubility may be poorly absorbed and therefore have reduced bioavailability, while drugs with high polarity may have difficulty crossing cell membranes and reaching their intended target. Curcumin, 1A6, 1A8, and 1B8 were predicted to have poor solubility in water, based on their water solubility score being less than 0 mg/mL (Table 4.2). To understand the absorption and metabolism of curcumin, 1A6, 1A8, and 1B8, the GI absorption and the liver first-pass metabolism facilitated by the P-gp substrate, as well as cytochrome enzymes, were predicted. Curcumin, 1A6, 1A8, and 1B8 were predicted to have high GI absorbability and no inhibitory activity on the P-gp substrate (Table 4.2). All the compounds were predicted to inhibit the CYP3A4 and CYP2C9 enzymes, while 1A6 was predicted to inhibit CYP2D6, and the CYP1A2 enzyme was inhibited by 1A8 and 1B8 (Table 4.2).

Table 4.2: Predicted pharmacokinetic profiles of curcumin and 1A6, 1A8, and 1B8.

	Curcumin	**1A6**	**1A8**	**1B8**
Lipophilicity (iLOGP)	3.27	3.88	1.85	3.83
Water solubility (ESOL, mg/mL)	−3.94	−5.03	−4.45	−5.16
GI absorption	High	High	High	High
P-gp substrate	No	No	No	No
CYP3A4	Yes	Yes	Yes	Yes
CYP1A2	No	No	Yes	Yes

CYP2D6	No	Yes	No	No
CYP2C9	Yes	Yes	Yes	Yes

Based on the LRo5 estimation, the results presented in Table 4.3 demonstrate that all compounds have a molecular weight below 500 daltons. Furthermore, it is observed that none of the compounds exceed the limit of 5 hydrogen bond donors or 10 hydrogen bond acceptors. Additionally, the octanol–water partition coefficient for all the compounds is less than 5. Therefore, these compounds satisfy the LRo5 criteria without any violations. The synthetic score of a compound typically ranges from 1 (easily synthesized) to 10 (difficult to synthesize). In this case, the compounds had a synthetic score lower than 4, indicating that they are relatively easy to synthesize.

Table 4.3. The predicted chemical parameters of curcumin, 1A6, 1A8, and 1B8.

	Curcumin	**1A6**	**1A8**	**1B8**
Molecular weight	368.38 g/mol	430.88 g/mol	342.77 g/mol	376.44 g/mol
Number of hydrogen bond acceptors	6	6	4	4
Number of hydrogen bond donors	2	0	2	0
Octanol/water partition coefficient (logP)	3.37	4.19	3.57	4.91
Druglikeness (Lipinski)	Yes; 0 violation	Yes; 0 violation	Yes; 0 violation	Yes; 0 violation
Synthetic score	2.97	3.76	3.27	3.46

Prediction of the potential biological targets of curcumin and synthetic curcumin derivatives

We used two predictive webservers, SwissTarget prediction and SEA, and two online databases, PubMed and Google Scholar, to identify biological targets related to curcumin in obesity experimental models. This approach yielded a range of potential biological targets. For this study, we prioritized common biological targets

consistently associated with curcumin across three key metabolic pathways: adipogenesis, lipid metabolism, and inflammation.

We identified three common potential biological targets of curcumin in each pathway and compared them to three synthetic derivatives for molecular docking studies. Specifically, for adipogenesis, we selected peroxisome proliferator-activated receptor gamma (PPARγ), mitogen activated protein kinase 14 (MAPK14), and signal transducer and activator of transcription 3 (STAT3) as potential biological targets. In the context of lipid metabolism, we focused on acetyl-CoA carboxylase (ACC), fatty acid synthase (FAS), and glycogen synthase kinase 3 beta (GSK3β) as the chosen potential targets. Similarly, for inflammation, our selection comprised cyclooxygenase 2 (COX2), interleukin 6 (IL-6), and Adiponectin as potential biological targets.

Assessment of protein-ligand binding score by molecular docking and post-docking analysis

Assessing the binding affinities of curcumin and synthetic curcumin derivatives to target proteins involved in adipogenesis

Figure 4.1 illustrates the results of molecular docking experiments conducted on compounds targeting proteins involved in adipogenesis. The control standards used in these experiments were GW9662, LY2228820, and BB1608, established inhibitors of PPARγ, MAPK14, and STAT3, respectively. In comparison to GW9662 (−7.9 kcal/mol), the binding affinities of curcumin and synthetic curcumin derivatives (1A6, 1A8, and 1B8) to the PPARγ protein were found to be improved. Notably, the best docking pose was achieved by 1B8, which exhibited a docking score of −9.1 kcal/mol (Figure 4.1A). Following that, 1A8 displayed the second-best binding score to PPARγ with a docking score of −8.6 kcal/mol, followed by curcumin with a binding affinity of −8.4 kcal/mol. The compound 1A6 exhibited the lowest binding affinity among the docked compounds, with a docking score of −8.0 kcal/mol, although this was still higher than the control (Figure 4.1A).

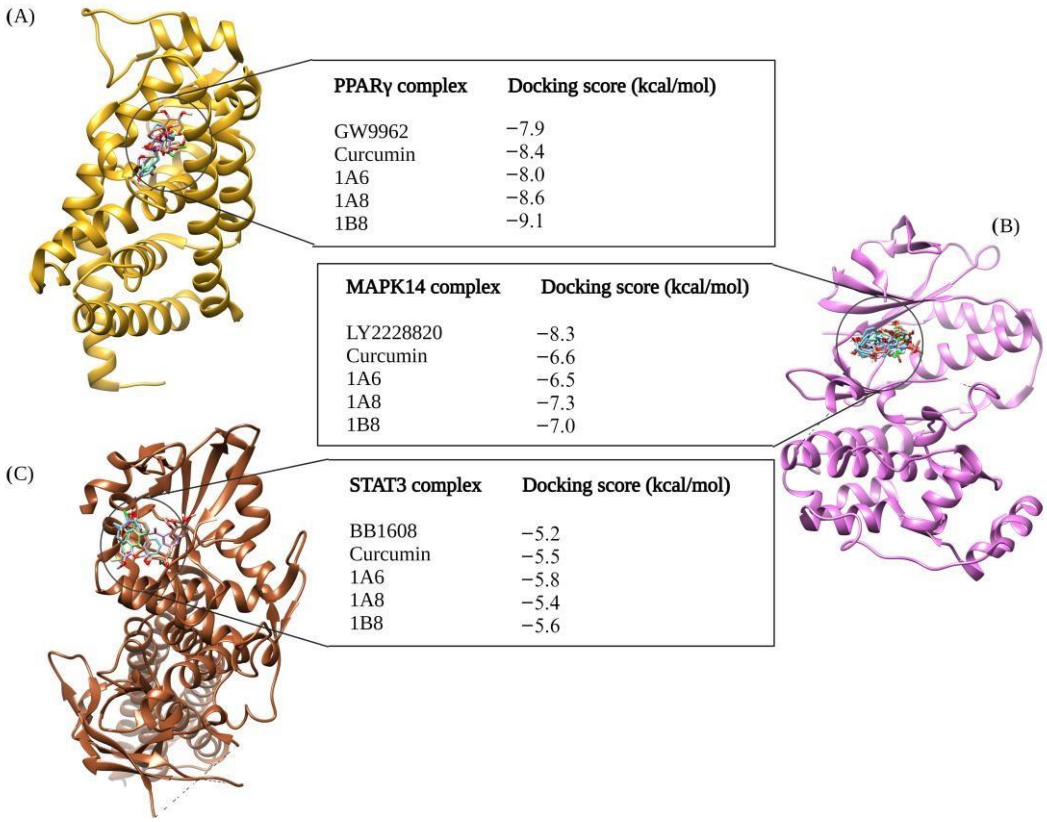


Figure 4.1: *In silico* binding affinity scores and superimposed docked complexes of curcumin and its synthetic curcumin derivatives (1A6, 1A8, and 1B8) bound to human target proteins involved in adipogenesis, including PPARγ (PDB ID: 7WGO), MAPK14 (PDB ID: 5XYX), and STAT3 (PDB ID: 6NUQ). All three target proteins were also docked with experimentally identified inhibiting standards; (A) GW9662 was docked to PPARγ with a binding energy of −7.9 kcal/mol, (B) LY2228820 was docked to MAPK14 with binding energy of −8.3 kcal/mol, and (C) BB1608 was docked to STAT3 with a binding energy of −5.2 kcal/mol. Abbreviations: MAPK14—mitogen-activated protein kinase 14; PPARγ—peroxisome proliferator-activated receptor gamma; STAT3—signal transducer and activator of transcription 3. Created with BioRender.com (accessed on 19 November 2023).

LY2228820 served as the standard control for docking to MAPK14, yielding a docking score of −8.3 kcal/mol, and demonstrated better binding to MAPK14 compared to curcumin and its synthetic curcumin derivatives (Figure 4.1B). Specifically, 1A8 displayed the highest binding score of −7.3 kcal/mol compared to curcumin and its derivatives. Curcumin and 1B8 had docking scores of −6.6 kcal/mol and −7.0 kcal/mol, respectively, while 1A6 exhibited the poorest docking performance with a binding affinity of −6.5 kcal/mol (Figure 4.1B). BB1608 served as the standard control for docking to the STAT3 protein, with a binding score of −5.2 kcal/mol. The molecular docking of 1A6, 1B8, and curcumin outperformed the binding performance of the standard control. Specifically,

1A6 bound to STAT3 protein with a score of −5.8 kcal/mol, 1B8 had a binding affinity of −5.6 kcal/mol, and curcumin exhibited −5.5 kcal/mol. The lowest binding score was demonstrated by 1A8, which was −5.4 kcal/mol. Figure 4.1C depicts the docking scores of the compounds to STAT3 protein.

Assessing the binding affinities of curcumin and synthetic curcumin derivatives to target proteins involved in inflammation

In Figure 4.2, the outcomes of molecular docking predictions are presented for compounds targeting proteins involved in inflammation. The docking predictions were performed using Naproxen, Raloxifene, and Rosiglitazone as reference controls, which are known ligands of COX2, IL-6, and Adiponectin, respectively (Figure 4.2). For the docking of the COX2 protein, 1B8 (−9.0 kcal/mol) showed an improved binding affinity compared to Naproxen. The docking score for curcumin was the same as that of Naproxen at −8.9 kcal/mol. However, 1A6 displayed a lower binding affinity (−8.7 kcal/mol) compared to Naproxen, and 1A8 docked even more poorly to COX2 with a score of −8.5 kcal/mol compared to the other compounds (Figure 4.2A).

In the IL-6 docking complex, 1A8 achieved the highest binding score of −5.9 kcal/mol, surpassing the reference control Raloxifene, which had a docking score of −5.7 kcal/mol (Figure 4.2B). Curcumin and 1B8 had the same binding score of −5.3 kcal/mol, while 1A6 exhibited a lower binding affinity of −5.2 kcal/mol (Figure 4.2B). When docking to Adiponectin, curcumin outperformed other compounds with a docking score of −8.1 kcal/mol. Rosiglitazone and 1B8 had similar binding affinities of −8.0 kcal/mol (Figure 4.2C). On the other hand, 1A6 demonstrated the lowest binding score of 7.4 kcal/mol in this case (Figure 4.2C).

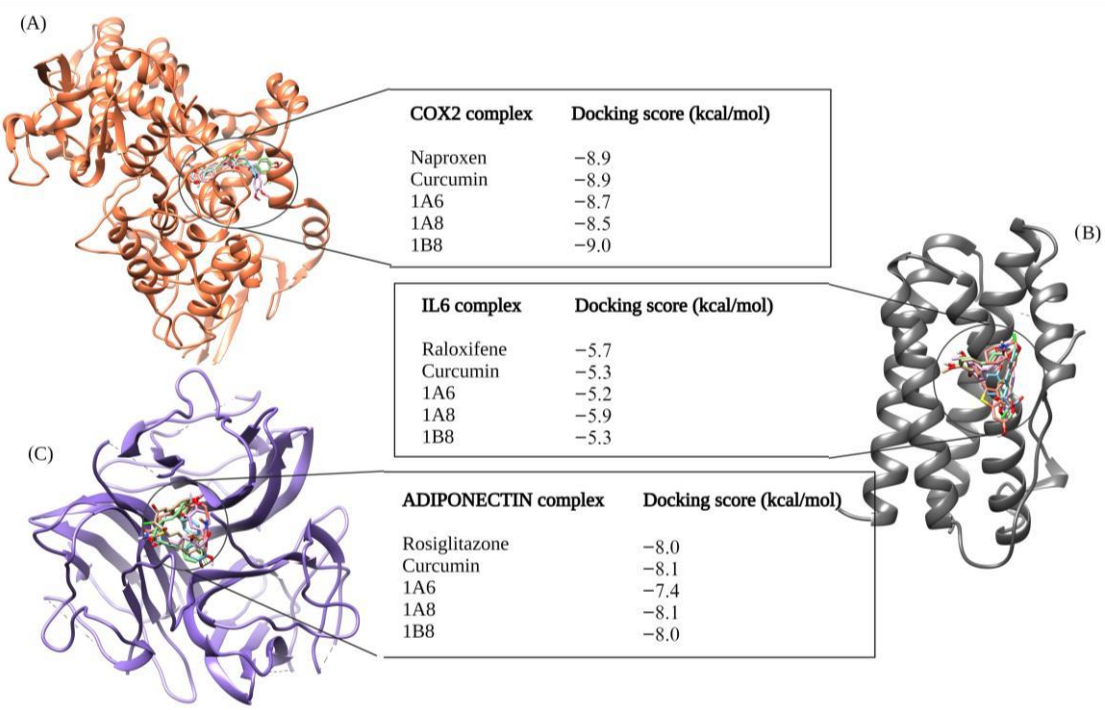


Figure 4.2: *In silico* binding affinity scores and superimposed docked complexes of curcumin and synthetic curcumin derivatives (1A6, 1A8, and 1B8) bound to human target proteins of inflammation such as COX2 (PDB ID: 5F1A), IL–6 (PDB ID: 1ALU), and Adiponectin (PDB ID: 6U66). All three target proteins were docked with experimentally established inhibiting standards; (A) Naproxen was docked to COX2 with a binding energy of −8.9 kcal/mol, (B) Raloxifene was docked to IL-6 with binding energy of −5.7 kcal/mol, and (C) Rosiglitazone was docked to Adiponectin with a binding energy of −8.0 kcal/mol. Abbreviations; COX2—cyclooxygenase 2, IL-6—interleukin 6. Created with BioRender.com (accessed on 19 November 2023).

Assessing the binding affinities of curcumin and synthetic curcumin derivatives to target proteins involved in lipid metabolism

Figure 4.3 depicts the outcomes of molecular docking predictions performed on compounds that target proteins involved in lipid metabolism. The docking predictions utilized PF05221304, Orlistat, and FT30356 as control standards of ACC, FAS, and GSK3β, respectively. When compared to PF05221304 with a −4.3 kcal/mol docking score, both curcumin and 1A8 demonstrated improved binding affinities to the ACC protein. Specifically, 1A8 exhibited the highest docking score of −5.2 kcal/mol, while curcumin achieved the second-highest binding affinity of −4.8 kcal/mol. The compounds 1B8 and 1A6 exhibited weaker binding to ACC compared to PF05221304, with binding affinities of −4.1 kcal/mol and −4.2 kcal/mol, respectively (Figure 4.3A).

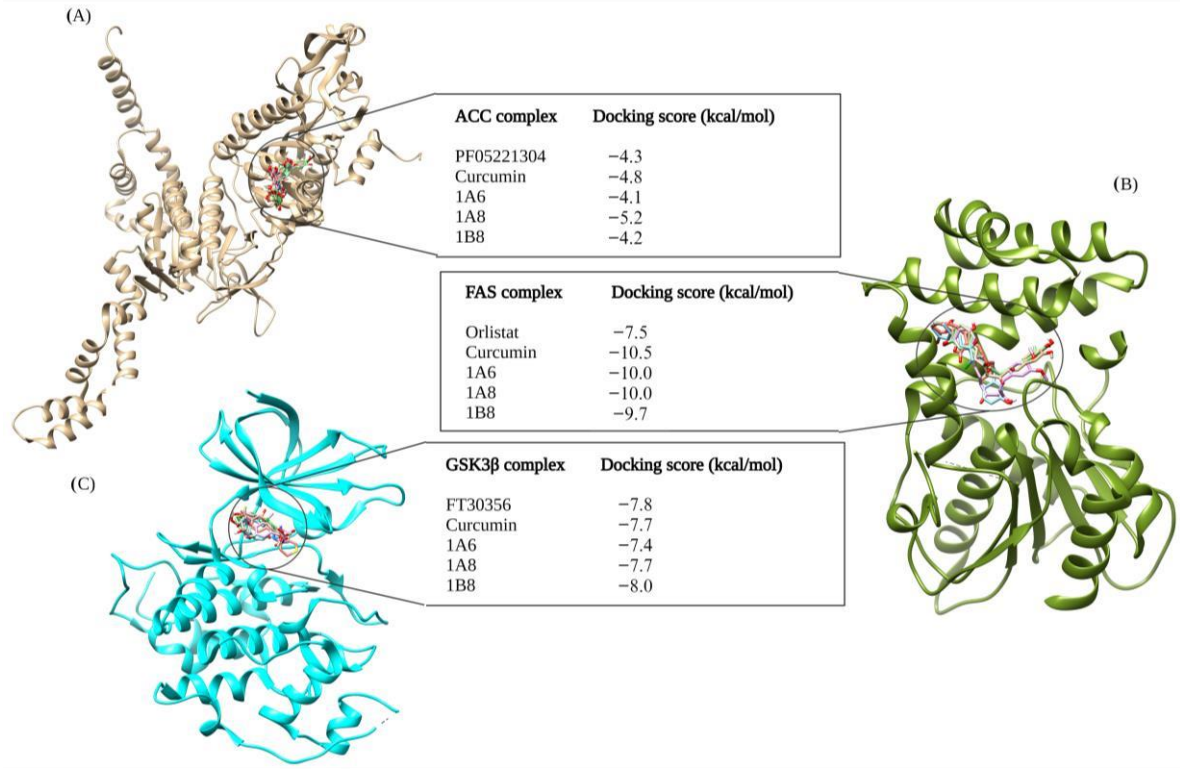


Figure 4.3: *In silico* binding affinity scores and superimposed docked complexes of curcumin and synthetic curcumin derivatives (1A6, 1A8, and 1B8) bound to human target proteins involved in lipid metabolism such as ACC (PDB ID: 3TDC), FAS (PDB ID: 3TJM), and GSK3β (PDB ID: 5F95). All three target proteins were docked with experimentally established inhibiting standards; (A) PF0522104 was docked to ACC with a binding energy of −4.3 kcal/mol, (B) Orlistat was docked to FAS with binding energy of −7.5 kcal/mol, and (C) FT30356 was docked to GSK3β with a binding energy of −7.8 kcal/mol. Abbreviations; ACC—acetyl-CoA carboxylase, FAS—fatty acid synthase, GSK3β—glycogen synthase kinase 3beta. Created with BioRender.com (Accessed on 19 November 2023).

In contrast to other compounds, Orlistat exhibited the weakest binding affinity to the FAS protein, with a docking score of −7.5 kcal/mol (Figure 4.3B). Molecular docking studies revealed that both 1A6 and 1A8 achieved the same docking scores of −10.0 kcal/mol, while 1B8 had a slightly lower binding score of −9.7 kcal/mol to the FAS protein (Figure 4.3B). Curcumin demonstrated the highest stability to the FAS protein, with a docking score of −10.5 kcal/mol (Figure 4.3B). For the GSK3β docking complex, the results showed that FT30356 had a binding score of −7.8 kcal/mol (Figure 4.3C). However, 1B8 surpassed the binding affinity of FT30356, with a docking score of −8.0 kcal/mol. Conversely, 1A6 displayed the weakest binding affinity at −7.4 kcal/mol (Figure 4.3C).

Interestingly, curcumin and 1A8 exhibited the same binding affinities of −7.7 kcal/mol to the GSK3β protein (Figure 4.3C).

Assessment of protein-ligand complex stability and conformational flexibility by MD simulations

Assessing structural stability of PPARγ protein in its interaction with curcumin and synthetic curcumin derivatives using RMSD analysis

Three target proteins, PPARγ, COX2, and FAS, that demonstrated the highest binding affinities in their respective metabolic pathways where further assessed for stabilities using DM simulations and binding free energies. This study evaluated the conformational changes of PPARγ in complex with GW9662, curcumin, 1A6, 1A8, and 1B8. The corresponding RMSD values were observed (Figure 4.4A). The obtained RMSD values shed light on the interactions of PPARγ with different ligands. Briefly, PPARγ without a ligand (APO) showed an RMSD value of 1.8 Å, suggesting that the protein itself was inherently stable during the simulation. This value serves as a baseline for comparing the structural dynamics of PPARγ in complex with different ligands. However, GW9662 exhibited an RMSD value of 2.1 Å, indicating a moderate level of structural variation in the complex. This suggests that the binding of GW9662 to PPARγ may involve some degree of flexibility. On the other hand, curcumin demonstrated an RMSD value of 1.9 Å, indicating a relatively stable binding interaction. This implies a strong and consistent interaction between curcumin and PPARγ. Interestingly, the ligands 1A6, 1A8, and 1B8 displayed RMSD values of 2.0 Å, 1.5 Å, and 2.1 Å, respectively. These values indicate varying degrees of stability in the interactions, with 1A8 showing the most stable binding.

Assessing structural stability of PPARγ protein in its interaction with curcumin and synthetic curcumin derivatives using RMSF analysis

The calculated RMSF values were used to observe the changes in protein structural flexibility as the selected compounds (GW9662, curcumin, 1A6, 1A8, and 1B8) bound to specific regions on the target (Figure 4.4B). Interestingly, all the selected compounds exhibited peak fluctuations in the protein at the residue positions Gly199, Ser200, His201, Met202, Gly203, and Ser204 during the simulation. These positions showed the most significant fluctuation during the binding of the compounds to the protein. Additionally, minor fluctuations were observed at Gly243, Lys244, Lys269, His270, Ile271, Thr272, Leu428, Val450, Gln452, and Tyr477. The RMSF analysis revealed that residues between Gln273 and Glu427 of the complex were the most rigid, with minimal fluctuations observed in this region.

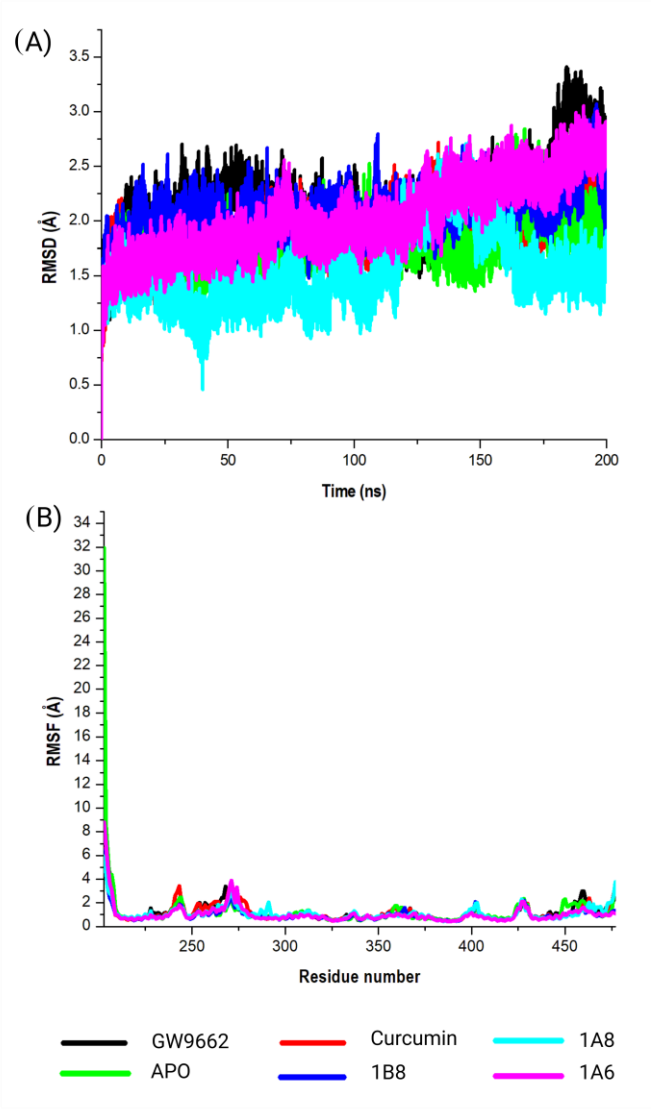


Figure 4.4: Analysis of the MD simulations of PPARγ in complex with GW9662, curcumin, 1A6, 1A8, and 1B8. (A) demonstrates the RMSD values of the MD simulated systems, while (B) illustrates the RMSF values of the MD simulated systems. The native PPARγ is referred to as APO.

Assessing structural stability of COX2 protein in its interaction with curcumin and synthetic curcumin derivatives using RSMD analysis

This study evaluated the conformational changes of COX2 in complex with Naproxen, curcumin, 1A6, 1A8, and 1B8. The corresponding RMSD values were observed (Figure 4.5A). In the absence of a ligand (APO), COX2 exhibited an RMSD value of 1.8 Å. This baseline value provides insight into the inherent stability of the protein during simulations and serves as a reference for assessing ligand-induced structural changes. Meanwhile,

Naproxen exhibited an RMSD value of 2.3 Å, indicating a moderate degree of structural variation during the simulation. This suggests that the binding of Naproxen to COX2 might involve some level of flexibility as shown in Figure 4.5A. Likewise, curcumin displayed an RMSD value of 1.9 Å, suggesting a relatively stable binding interaction. This observation implies a robust and consistent binding between curcumin and COX2. Among the synthetic compounds, 1A6, 1A8, and 1B8, the RMSD values of 1.6 Å, 1.5 Å, and 1.8 Å were respectively observed. These values suggest varying degrees of binding stability, with 1A8 demonstrating the most stable binding interaction among the ligands.

Assessing structural stability of COX2 protein in its interaction with curcumin and synthetic curcumin derivatives using RMSF analysis

The calculated RMSF values were utilized to elucidate alterations in the structural flexibility of the protein upon interaction with the specific compounds (Naproxen, curcumin, 1A6, 1A8, and 1B8) (Figure 4.5B). Intriguingly, all selected compounds displayed prominent peak fluctuations within distinct regions of the protein, particularly at the residue positions Lys79, Leu80, Pro218, Ile279, Glu322, Gln370, Gln543, Val554, and Gln583 throughout the simulation period. These positions experienced the most pronounced variations upon compound binding, indicating their involvement in dynamic interactions. Furthermore, modest fluctuations were discerned in residues spanning between Leu80 and Pro218. A comprehensive RMSF analysis unveiled that residues situated between Gln370 and Gln543 of the complex exhibited elevated rigidity, with minimal fluctuations observed in this specific region.

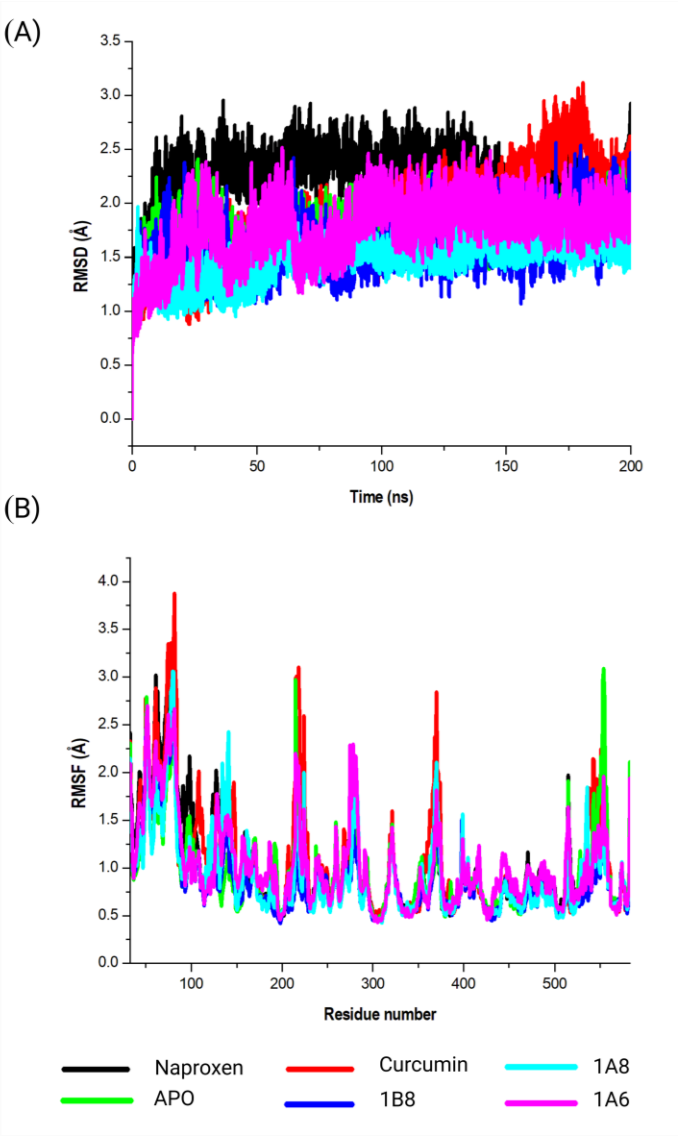


Figure 4.5: Analysis of the MD simulations of COX2 in complex with Naproxen, curcumin, 1A6, 1A8, and 1B8. (A) demonstrates the RMSD values of the MD simulated systems, while (B) illustrates the RMSF values of the MD simulated systems. The native COX2 is referred to as APO.

Assessing structural stability of FAS protein in its interaction with curcumin and synthetic curcumin derivatives using RMSD analysis

This investigation delved into the conformational dynamics of FAS in complex with the ligands Orlistat, curcumin, 1A6, 1A8, and 1B8. The resulting RMSD values were meticulously analyzed as illustrated in Figure 4.6A. Briefly, a significant point of reference was the FAS protein in the absence of a ligand, referred to as “APO”. The APO complex exhibited an RMSD value of 2.0 Å, indicating inherent stability within the protein structure during the simulation. This value serves as a foundational measure for evaluating the dynamic behavior of FAS

in complex with the ligands. Contrasting this baseline, the FAS–Orlistat complex displayed an RMSD value of 2.1 Å, suggesting moderate structural variation within the complex. This hints at a certain level of flexibility in the interaction between Orlistat and FAS. Similarly, the RMSD value for the FAS–curcumin complex was 2.1Å, indicating consistent and stable binding dynamics. Interestingly, the ligands 1A6, 1A8, and 1B8 exhibited RMSD values of 2.1 Å, 2.0 Å, and 2.1 Å, respectively. These values offer insights into varying degrees of stability within these interactions.

Assessing structural stability of FAS protein in its interaction with curcumin and synthetic curcumin derivatives using RSMF analysis

The calculated RMSF values were employed to investigate shifts in the structural flexibility of the protein upon interaction with specific compounds (Orlistat, curcumin, 1A6, 1A8, and 1B8) (Figure 4.6B). Remarkably, all compounds exhibited notable peak fluctuations within distinct protein regions, notably at the residues Asn2218, Val2237, Gln2238, Tyr2462, Asn2463, Lys2354, Leu2355, Thr2356, Pro2357, Gly2358, Cys2359, Gly2470, Lys2471, Val2472, Ser2473, and Val2474 throughout the simulation period. Importantly, the amino acid residues located at 2450 and 2456 of the protein structure were unidentified. This might have resulted from poor construction of the FAS protein crystal structure from X-ray crystallography. These positions demonstrated the most pronounced variations upon compound binding, underscoring their active participation in dynamic interactions. Furthermore, modest fluctuations were observed in residues spanning from Cys2359 to Gly2470. A comprehensive analysis of RMSF unveiled that residues located between Gln2238 and Tyr2462 of the complex exhibited heightened rigidity, with minimal fluctuations within this specific region.

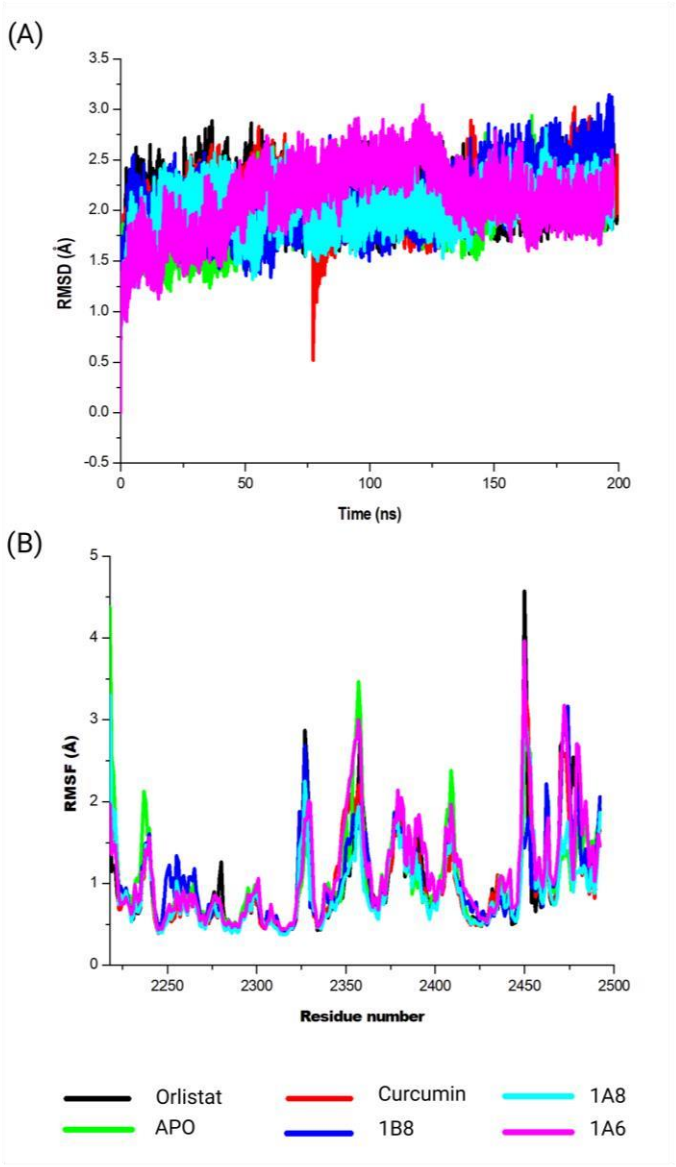


Figure 4.6: Analysis of the MD simulations of FAS in complex with Orlistat, curcumin, 1A6, 1A8, and 1B8. (A) demonstrates the RMSD values of the MD simulated systems, while (B) illustrates the RMSF values of the MD simulated systems. The native FAS is referred to as APO.

Calculation of the binding free energy using the MM/GBSA approach

The binding free energies of the respective reference controls, curcumin, and the synthetic curcumin derivatives were calculated using the MM/GBSA method to measure the interaction strengths (Table 4.4). As indicated in Table 4.4, the highest binding energy was observed when curcumin interacted with PPARγ (−60.2 ± 0.4 kcal/mol) compared to other compounds for this protein. When assessing binding free energies in the COX2 systems, higher binding energy (−64.9 ± 0.2 kcal/mol) was obtained by 1A8. Interestingly, Orlistat (37.9 ± 0.3 kcal/mol) and curcumin (−37.7 ± 0.3 kcal/mol) showed similar binding free energies to FAS, with minor differences.

Table 4.4: The analysis of the MM/BGSA-based binding free energy contributed by residues of the active site of protein–ligand complex.

ystems		Energy Components (kcal/mol)				
		ΔE_{vdw}	ΔE_{ele}	ΔG_{gas}	ΔG_{solv}	ΔG_{bind}
PPARγ	**GW9662**	−14.8 ± 0.4	−0.9 ± 1.6	48.0 ± 1.5	−59.0 ± 1.4	−11.0 ± 0.4
	Curcumin	−60.9 ± 0.3	−42.1 ± 0.6	−103.0 ± 0.6	42.8 ± 0.3	−60.2 ± 0.4
	1A6	−60.9 ± 0.2	−13.3 ± 0.3	−74.2 ± 0.3	23.9 ± 0.2	−50.3 ± 0.3
	1A8	−43.1 ± 0.3	−29.4 ± 0.4	−72.5 ± 0.3	30.0 ± 0.2	−42.5 ± 0.3
	1B8	−55.9 ± 0.3	−17.3 ± 0.4	−73.9 ± 0.5	26.8 ± 0.4	−46.5 ± 0.3
COX2	**Naproxen**	−37.1 ± 0.2	−24.3 ± 0.6	−61.3 ± 0.7	26.7 ± 0.5	−34.6 ± 0.2
	Curcumin	−48.8 ± 0.2	−24.1 ± 0.5	−72.9 ± 0.5	31.0 ± 0.4	−41.9 ± 0.3
	1A6	−57.9 ± 0.2	−15.7 ± 0.3	−73.6 ± 0.4	24.8 ± 0.2	−48.9 ± 0.3
	1A8	−18.4 ± 0.2	−216.6 ± 0.7	−142.0 ± 0.6	77.1 ± 0.5	−64.9 ± 0.2
	1B8	−55.5 ± 0.1	−20.1 ± 0.3	−75.5 ± 0.5	31.2 ± 0.3	−44.3 ± 0.3
FAS	**Orlistat**	−39.0 ± 0.2	−18.1 ± 0.5	−57.2 ± 0.5	19.3 ± 0.4	−37.9 ± 0.3
	Curcumin	−44.2 ± 0.3	−20.5 ± 0.6	−64.7 ± 0.6	27.0 ± 0.5	−37.7 ± 0.3
	1A6	−40.5 ± 0.6	−10.2 ± 0.4	−50.7 ± 0.7	20.4 ± 0.3	−30.3 ± 0.6
	1A8	−35.7 ± 0.2	−25.6 ± 0.6	−61.3 ± 0.6	29.8 ± 0.5	−31.5 ± 0.3
	1B8	−42.6 ± 0.3	−11.8 ± 0.3	−54.4 ± 0.5	21.4 ± 0.3	−33.0 ± 0.4

ΔEvdw—van der Waals forces; ΔEele—electrostatic interactions; ΔGbind—binding free energy; ΔGgas—gas phase interaction; ΔGsol—solvation energy.

Analyzing molecular interactions in MD simulation systems using LigPlot

Based on the binding free energy calculations, an analysis of the ligand interaction plot (Table 4.5) was conducted to validate the intermolecular interactions responsible for the system stabilities of compounds within the binding site of human proteins involved in adipogenesis (PPARγ), inflammation (COX2), and lipid metabolism (FAS) at the end of the MD simulations. According to the interaction plot, the molecular interactions of the compounds within the binding site of PPARγ exhibit conserved interactions with PPARγ residue such as Ser88 (Table 4.5).

Notably, GW9662 displayed one hydrogen bond interaction with Cys84 (3.22 Å) within the binding site. However, the stability of GW9662 within the binding site was primarily maintained by eight hydrophobic interactions. Like GW9662, LigPlot analysis revealed that the hydroxyl groups of curcumin established one hydrogen bond with Glu94 (2.57 Å). Additionally, seventeen amino acid residues participated in hydrophobic interactions with curcumin, thereby enhancing the stability of the system (Table 4.5). It is worth mentioning that 1A6 and 1B8 did not engage in hydrogen bond interactions, but their stability relied on sixteen and fifteen hydrophobic interactions within the binding site, respectively. Interestingly, the hydroxyl groups of 1A8 formed three hydrogen bond interactions with Glu94 (2.57 Å), Ser141 (3.08 Å), and Ser88 (2.83 Å) in the binding site. Furthermore, twelve hydrophobic interactions with binding site residues contributed to the system stability of 1A8 (Table 4.5).

The interaction plot within the binding site of the COX2 protein provided insights into the interactions of compounds, with residues Ser321, Ser498, Arg89, and Tyr323 forming significant conserved interactions with all compounds (Table 4.5). These interactions suggest that the compounds interacted with COX2 in a manner similar to Naproxen. It is interesting to note that all compounds formed hydrogen interactions with an Arg89 residue. Apart from two hydrogen bond interactions formed between the hydroxyl groups of Naproxen and the COX2 residue Arg89 (2.94 Å and 2.98 Å), its interactions were supported by ten hydrophobic interactions within the binding site. As previously mentioned, the hydroxyl group of curcumin engaged in hydrogen bond interactions with the COX2 residue Arg89 (3.00 Å), while relying on thirteen hydrophobic interactions to maintain stability (Table 4.5). Like curcumin, the hydroxyl group of 1A6 formed hydrogen bond interactions with the COX2 residue Arg89 (3.18 Å), while relying on seventeen hydrophobic interactions to maintain stability (Table 4.5). Exclusively, the hydroxyl groups of 1A8 formed three hydrogen interactions with the Arg89 (3.05 Å), Ser498 (2.80 Å), and Tyr353 (2.88 Å) binding site residues of COX2. In addition, its molecular interactions were further stabilized with nine hydrophobic interactions (Table 4.5). Like curcumin and 1A6, 1B8 formed a hydrogen bond interaction with Arg89 (2.970 Å). Additionally, twelve binding site residues contributed to the interaction stability of 1B8 through hydrophobic interactions (Table 4.5).

The compound interaction analysis revealed that the compounds did not form conserved interactions with the binding site residues of FAS. Interestingly, the analysis showed that Orlistat formed two hydrogen bond interactions with Arg211 (20.71 and 3.33 Å) in the binding site. However, the bonding stability of Orlistat in the FAS binding site was supported by hydrophobic interactions with six residues (Table 4.5). Another significant

observation from the interaction analysis was the formation of two hydrogen bonds by curcumin with the Tyr130 (2.71 Å) and Glu214 (2.59 Å) residues of the binding site. In addition, the interactions of curcumin were stabilized by ten hydrophobic interactions with the binding site residues. It is interesting to note that 1A6 and 1B8 did not participate in hydrogen bonding with residues of the binding site of FAS protein. However, the stability of the interactions of 1A6 and 1B8 with the FAS protein was sustained by hydrophobic interactions with five and ten residues, respectively. Like curcumin, the hydroxyl groups of 1A8 formed hydrogen interactions with two binding site residues of FAS protein such as Tyr90 (2.86 Å) and Asp121 (2.58 Å). In addition, this stability was further maintained by hydrophobic interactions with ten binding site residues.

Table 4.5: The LigPlot analysis for the molecular interactions of curcumin, 1A6, 1A8, 1B8, and their corresponding reference standards bound to PPARγ, COX2, and FAS.

Compound Name	Hydrophobic Interactions	Hydrogen Bond (Length-Å)
	Adipogenesis (PPARγ)	
GW9662	Ile80, Leu129, Leu132, Ile140, Arg87, Ala91, Ser88,	Cys84 (3.22) Ile125
Curcumin	His248, Tyr126, Leu252, Tyr272, Leu264, Ser88, Cys84, Leu132, Leu27, Arg87, Phe25, Met128, Ile125, Leu129, His122, and Gln85	Glu94 (2.57) Ala91,
1A6	Ile140, Phe63, Met163, Arg87, Tyr126, Cys84, Ser88, Leu268, Phe81, Tyr272, Phe162, His248, Leu252, Met147, and Leu132	No hydrogen bonds Leu251,
1A8	Phe25, Leu139, Arg87, Ile140, Cys84, Val138, Leu129, Met163, Ile125, Leu132, Met128, and Ala91	Glu94 (2.57), Ser141 (3.08), and Ser88 (2.83)
1B8	Tyr126, Ile126, His122, Ser88, Leu264, Leu268, Met262, Phe159, His248, Leu252, Phe81, Tyr272, Leu129, and Met163	No hydrogen bonds Cys84,
	Inflammation (COX2)	
Naproxen	Ser321, Val185, Ala495, Val317, Leu320, Phe486, Ser498, Val491, Tyr323, and Pro54	Arg89 (2.94 and 2.98)
Curcumin	Ile81, Leu61, Trp68, Phe325, Tyr84, Tyr323, Ser498, Ala495, Leu352, Tyr353, Met490, Gly494, and Ser321	Arg89 (3.00)
1A6	Trp68, Ile81, Val85, Tyr84, Leu61, Val57, Tyr323, Ser321, Leu320, Met490, Val491, Phe349, Phe486, Ser498, Trp355, Gly494, and Leu499	Arg89 (3.18)
1A8	Lys51, Phe325, Leu61, Tyr323, Trp355, Ala495, Leu320, Ser321, and Val85	Arg89 (3.05), Ser498 (2.80), and Tyr353 (2.88)
1B8	Tyr84, Val85, Leu61, Tyr323, Ser321, Leu499, Tyr316, Gly494, Phe349, Ser498, Leu320, Phe486, Met490, and Val317	Arg89 (2.970
	Lipid metabolism (FAS)	

Orlistat	Ala146, Glu149, Ala150, Leu210, Tyr134, and Arg211 (20.71 and 3.33) Phe153	
Curcumin	His163, Gln156, Phe153, Leu210, Ala146, Arg135, Thr131, Tyr134, Glu149, and Ala150	Tyr130 (2.71) and Glu214 (2.59)
1A6	Phe153, Tyr130, Ser133, Tyr237, and Tyr126	No hydrogen bonds
1A8	Tyr134, Thr131, Leu210, Ile33, Tyr126, Tyr237, His256, Ser91, Tyr130, and Phe153	Tyr90 (2.86) and Asp121 (2.58)
1B8	Thr131, Lys209, Leu210, Ser91, Tyr92, Tyr130, Ala233, Gly234, Tyr126, and Gly122	No hydrogen bonds

Discussion

Natural compounds continue to play a crucial role in drug discovery due to their vast chemical diversity and potential therapeutic value. Additionally, natural products such as plant extracts have been a significant source of bioactive compounds throughout history [23,24]. Many drugs currently on the market have their roots in natural products, including antibiotics, anticancer agents, and immunosuppressants. Their biological activity makes them valuable starting points for the development of new drugs [26–29]. Curcumin, a bioactive compound derived from the rhizome of *Curcuma longa*, has reportedly shown great potential as an anti-obesity therapeutic [30–32] due to its ability to modulate various cellular pathways involved in obesity including adipogenesis [12–14], lipid metabolism [10,11], and inflammation [15,16]. In this study, the pharmacological profiles of curcumin and its synthetic derivatives (1A6, 1A8, and 1B8) were explored to unveil insights into their potential anti-obesity activity using molecular recognition techniques.

Firstly, the characterization of curcumin and the synthetic curcumin derivatives was carried out to evaluate the pharmacokinetic, physicochemical, and toxicity properties using online predictive databases. We centered our pharmacokinetic analysis on the LRo5, which serves as a widely recognized standard for evaluating the druglikeness of chemical compounds [33]. This framework, established by Owens and Lipinski in 2003 [34] and further discussed by Pollastri et al. [35], is fundamental in characterizing potential drug candidates and has become a cornerstone in the field of drug discovery [34,35]. Our findings revealed that curcumin and its synthetic derivatives align with the LRo5 criteria, indicating their potential as drug-like substances without any violations. Lipophilicity, as an important physicochemical property of drugs and bioactive compounds, measures the affinity of a compound for lipid environments, which can affect its ability to permeate biological membranes and reach target sites. A higher lipophilicity value suggests a greater affinity for lipid-rich environments [36]. Curcumin had a lipophilicity value of 3.2, which clearly indicates that curcumin falls within the moderately lipophilic range

[37,38]. Interestingly, this reporting is in line with the experimental data previously reported by Clariano et al. [39] and Shereen et al. [40], who evaluated the mechanistic delivery of curcumin in humans and estimated the lipophilicity of curcumin to be in a similar range (~LogP 3.6). The synthetic derivatives 1A6 and 1B8 demonstrated a higher lipophilicity than curcumin, potentially indicating improved membrane permeability which is advantageous for drug development to enhance bioavailability. In contrast, 1A8, notably with the lowest lipophilicity, might face challenges crossing membrane barriers effectively.

Moreover, these compounds are synthetic in nature and exhibit a favorable toxicity profile. It is worth noting that while curcumin along with 1A6 and 1B8 displayed activity towards toxicity endpoints such as hepatotoxicity and immunotoxicity at lethal dosages, their overall toxicity properties were promising. This suggests that further refinement of these compounds may mitigate these specific endpoint effects. In fact, the approach of compound refinement, aimed at reducing toxicity while enhancing effectiveness, is common in several studies [24,41,42]. The synthetic derivative 1A8 was predicted to be the safest since it did not exhibit any toxicity towards the endpoints evaluated. The observed variation in the toxicity and pharmacokinetics outcomes among the compounds could be attributed to structural modifications such as the methoxy, chloro, and phenolic functional groups on the curcumin scaffold, which explains the importance of understanding how a compound's structure influences its biological effects [43].

Examining the metabolism and elimination patterns in the liver is a customary practice in the field of drug discovery and development. This method is crucial for anticipating the amount of a drug that effectively reaches its biological targets following oral administration, commonly referred to as the liver first-pass effect [44]. In our study, we evaluated the potential of curcumin and its synthetic derivatives to be substrates of the enzymes involved in the liver first-pass effect. The findings revealed the activity of these compounds to be common against the CYP3A4 and CYP2C9 enzymes. Of note, these enzymes are part of the cytochrome P450 family and play a crucial role in the biotransformation of various substances, including drugs in the liver [45]. Consequently, our findings suggest that curcumin and its synthetic derivatives may undergo metabolism in the liver, potentially influencing their pharmacokinetics and interaction with other drugs. These findings, especially for curcumin, greatly correlate with those previously articulated in the literature [46] and therefore open avenues for further structural modifications to steer these compounds away from becoming substrates for these biotransformation enzymes. For instance, the modification of curcumin structure with hydroxylation, methoxylation, cyclization,

fluorination, or alkylation can be implemented to enhance its properties for improved stability, solubility, and biological activity.

In general, the enhanced permeability of orally administered drugs in the intestines tends to correlate with improved pharmacokinetic properties [47]. Our study illustrated that curcumin and its synthetic derivatives exhibit high absorption in the intestines, demonstrating their potential to pass into the circulatory system. The literature also indicates that curcumin metabolites such as dihydrocurcumin and tetrahydrocurcumin are traced in the intestines [48]. However, our *in silico* prediction for the intestinal absorption of curcumin does not correlate with previously reported *in vitro* and *in vivo* findings [49]. This may be attributed to the intestinal efflux of the P-gp enzyme on curcumin [49]. The P-gp is a vital membrane protein in the liver, intestines, and other tissues that expels substances from cells [50]. Our study predicted that curcumin and its synthetic derivatives are not substrates for the
P-gp enzyme, indicating that this enzyme does not play a role in expelling these compounds from cells.
Unfortunately, these predictive findings, mainly on curcumin, are opposed by experimental data in the literature [49]. In fact, a recent *in silico* study suggested that synthetic curcumin derivatives interact with the P-gp enzyme as antagonist [51].

The selection of protein targets in this study was vital for investigating the mechanism of action of curcumin and its synthetic derivatives and predicting their potential as anti-obesity therapeutic agents. The systematic approach used predicted targets that are shared by all compounds and are relevant to the metabolic pathways involved in obesity including adipogenesis, lipid metabolism, and inflammation. Based on molecular docking results (binding interaction and docking score), three target proteins, PPARγ, COX2, and FAS, were best docked to curcumin and the synthetic derivatives among the nine target proteins that were selected and evaluated for molecular docking. Moreover, the results showed that the binding interactions and docking affinity between curcumin and the synthetic derivatives were similar for PPARγ, COX2, and FAS. This similarity in binding modes indicates that these derivatives share a common mechanism of action with curcumin, possibly due to structural similarity. Additionally, these compounds exhibited comparable binding affinity to PPARγ, COX2, and FAS when compared to the respective reference ligands (GW9962, Orlistat, and Naproxen).

In the PPARγ complex, curcumin and its synthetic derivatives maintained favorable binding to the target protein. In contrast, GW9662, which served as a reference control, exhibited the lowest binding affinity to PPARγ when compared to curcumin and its synthetic derivatives. This suggests that curcumin and its synthetic derivatives may be potential ligands for PPARγ. PPARγ is a nuclear receptor transcription factor that plays a key role in adipogenesis [52] and is a major therapeutic target for various diseases including obesity, dyslipidemia, type 2 diabetes mellitus, neurodegenerative disorders, and cancers [53]. In experimental studies, curcumin and synthetic analogs of curcumin were demonstrated to induce PPARγ expression in glial and carcinoma cells, thereby providing neuroprotective and anti-cancer effects [54,55]. This further suggests that other than being potential ligands, curcumin and its derivatives may regulate the expression of PPARγ. In the COX2 complex, 1B8 demonstrated a high docking score compared to Naproxen, while curcumin indicated a similar binding affinity to Naproxen. However, 1A6 and 1A8 demonstrated the lowest docking scores. This result suggests that curcumin and its derivative 1B8 may have a higher binding affinity for COX2 than Naproxen. Compared to our study, Sohilait et al. [56] showed that analogs of curcumin strongly bind with COX2. Although 1B8 had the most favorable affinity towards COX2 compared to curcumin and other synthetic derivatives, these findings suggest that 1B8 can be a potential ligand for COX2 regulation.

Orlistat, used as the reference control, exhibited the weakest binding affinity for the FAS protein when compared to curcumin and its derivatives. FAS is an enzyme involved in the synthesis of fatty acids by catalyzing the synthesis of long-chain fatty acids from acetyl-CoA and malonyl-CoA [57]. However, Orlistat, an anti-obesity agent that inhibits gastric and pancreatic lipases, has been experimentally shown to inhibit FAS expression [58]. This implies that Orlistat is particularly effective in binding to FAS, making it a potent inhibitor of this enzyme as recently demonstrated [59]. An *in vivo* study by Maithilikarpagaselvi et al.[60] demonstrated that curcumin facilitates its anti-obesity effects by suppressing fat accumulation through the inhibition of FAS enzymes. Overall, the difference in binding affinity between curcumin and its derivatives was significantly minimal, which could be due to the similarity in the structural scaffold. This structural similarity likely results in comparable binding interactions with the target protein. The observation of similar binding affinities among curcumin and its derivatives can have important implications for drug development. It suggests that while structural modifications might lead to improvements in other aspects (e.g., pharmacokinetics, toxicity, or selectivity), they may not have a pronounced effect on the binding affinity.

To elucidate on the stability of these interactions, molecular dynamics simulations were conducted for both unbound and bound forms of PPARγ, COX2, and FAS. The results revealed that all simulated systems remained stable throughout the 200 nanoseconds of the simulation. Stability was confirmed by minimal atomic deviations, which were within the generally accepted threshold range of 1 to 3 angstroms for good stability [61]. This stability implies that the interactions between the compounds and their respective protein targets were robust and maintained throughout the simulation, providing confidence in the reliability of the binding interactions. In the specific case of PPARγ, the analysis indicated that curcumin, synthetic curcumin derivatives, and GW9662 induced structural flexibility in similar regions of the target protein. This flexibility was characterized by increased fluctuations in these regions when compared to the unbound state of the target. Such fluctuations suggest that the binding of these compounds caused PPARγ to adopt a more flexible conformation, which may have functional implications related to its mode of action. Generally, conformational dynamics of PPARγ inhibitors can be influenced by factors such as ligand structure, binding site interactions, and solvent environment [62,63]. Different conformations of inhibitors can have varying degrees of affinity and specificity towards the PPARγ protein [64].

In the COX2 and FAS systems, curcumin and the synthetic curcumin derivatives showed similar conformational dynamics on each of the targets, which was characterized by increased structural flexibility and a less compact structure in contrast to the unbound targets. The findings could therefore suggest the protein is undergoing more dynamic conformational changes, allowing it to explore a wider range of structural configurations [65,66]. Similarly, FAS and COX2 inhibitors exhibited varying conformational changes to their respective targets depending on the structures of their respective inhibitors [67,68]. Overall, curcumin and the synthetic curcumin derivatives had a similar impact on the conformational dynamics of the target proteins, which is attributed to the similarity in their structures.

In addition, we assessed the amino acids within the binding site responsible for stabilizing molecular interactions following molecular dynamics simulations. This analysis is crucial in drug discovery to tailor molecules that selectively interact with the target protein [69]. Our results revealed that compounds interacting with the binding site of PPARγ consistently engage in specific interactions with residues like Ser88, affirming their association with the localized region of the PPARγ binding site. Notably, the binding of curcumin was sustained through hydrophilic interactions with seventeen amino acid residues and one hydrogen interaction in the binding site, potentially contributing to the observed high binding free energies. The interaction between curcumin and PPARγ

has been well-documented in various studies [70–72]. Furthermore, synthetic derivatives of curcumin exhibited stronger binding free energies compared to the reference compound (GW9662), supported by their hydrophilic and hydrogen interactions and amino acid residues within the binding site. This is speculated to result from the structural similarity shared by curcumin and its derivatives. One study suggested that curcumin analogs interact with PPARγ to suppress adipogenesis more effectively than curcumin [73]. This implies that derivatives of curcumin may outperform curcumin in targeting the PPARγ isoform regulating adipogenesis, while activating the PPARγ isoform associated with inflammation and lipid metabolism suppression. The observed variations underscore the complexity of the molecular interactions and highlight the potential therapeutic implications of curcumin derivatives in modulating PPARγ isoforms.

In this study, we demonstrated consistent interaction of the ligand compounds with amino acid residues like Ser321, Ser498, Arg89, and Tyr323, forming conserved interactions within the binding site of COX2. Remarkably, the synthetic derivative 1A8 exhibited the highest binding free energy, greater than the reference compound (Naproxen). This strong interaction was substantiated by nine hydrophilic and three hydrogen interactions with amino acid residues in the COX2 binding site. The tendency of curcumin analogs to strongly interact with the COX2 binding site has been previously reported [56], while curcumin derivatives have also been reported to selectively interact with COX2 [74]. This specificity may account for the superior interaction demonstrated by 1A8 compared to 1A6 and 1B8. Despite 1A8 outperforming other compounds, it is essential to recognize that curcumin exhibited strong interactions with COX2, surpassing the control inhibitor (Naproxen). Compared to this study, an *in vivo* study demonstrated that curcumin inhibits the expression of COX2 [75,76].

While common interactions were observed for PPARγ and COX2, the ligand compounds did not engage with shared amino acid residues in the binding site of FAS. However, curcumin demonstrated two hydrogen interactions with Tyr130 (2.71 Å) and Glu214 (2.59 Å) residues within the binding site residue of FAS. Additionally, the interaction of curcumin within the FAS binding site was stabilized by ten hydrophilic interactions. This interaction was validated by high binding free energies, comparable to the reference compound (Orlistat). Interestingly, an *in vitro* study on the breast cancer cell line SKBR3 also demonstrated that curcumin decreases the activity and expression of the FAS enzyme [77]. It is crucial to highlight that curcumin displayed substantial interactions with both PPARγ and FAS, possibly due to the involvement of these proteins in lipid metabolism. Curcumin derivatives have been shown to decrease FAS expression, thus suppressing lipid

accumulation in HepG2 cells [78]. This indicates that curcumin and its synthetic derivatives potentially target FAS and regulate its expression.

While our study presents promising findings in the comprehensive analysis of curcumin and its synthetic derivatives, several limitations should be acknowledged. The reliance on computational analyses, without direct *in vitro* and *in vivo* validation, leaves a gap in understanding the clinical implications of our results. Furthermore, the scope of toxicity assessment is primarily focused on acute effects, necessitating extended studies to capture potential long-term impacts and interactions with other physiological systems. In addition, caution is warranted in generalizing the findings, as the study centers on specific derivatives (1A6, 1A8, and 1B8), while variability among curcumin derivatives may exist. Despite overall promising results, specific endpoint effects observed at lethal dosages highlight the need for refinement strategies to enhance the safety profile of the compounds. Additionally, the focus of the study on a select few anti-obesity target proteins may limit the generalizability of the results, and further exploration of interactions with a broader range of relevant proteins is recommended. Lastly, while the study identifies potential interactions with key liver enzymes, a more detailed exploration of the metabolic pathways undergone by these compounds is necessary. This in-depth investigation combines computational methodologies with molecular recognition techniques to unravel the potential anti-obesity activity of curcumin and its synthetic derivatives. The findings provide a foundation for further experimental validation, emphasizing the need for a holistic understanding of the pharmacological profiles of these compounds for effective drug development. The structural insights and mechanistic understanding garnered from this study pave the way for future investigations bringing research close to harnessing the therapeutic potential of curcumin and its derivatives in the fight against obesity.

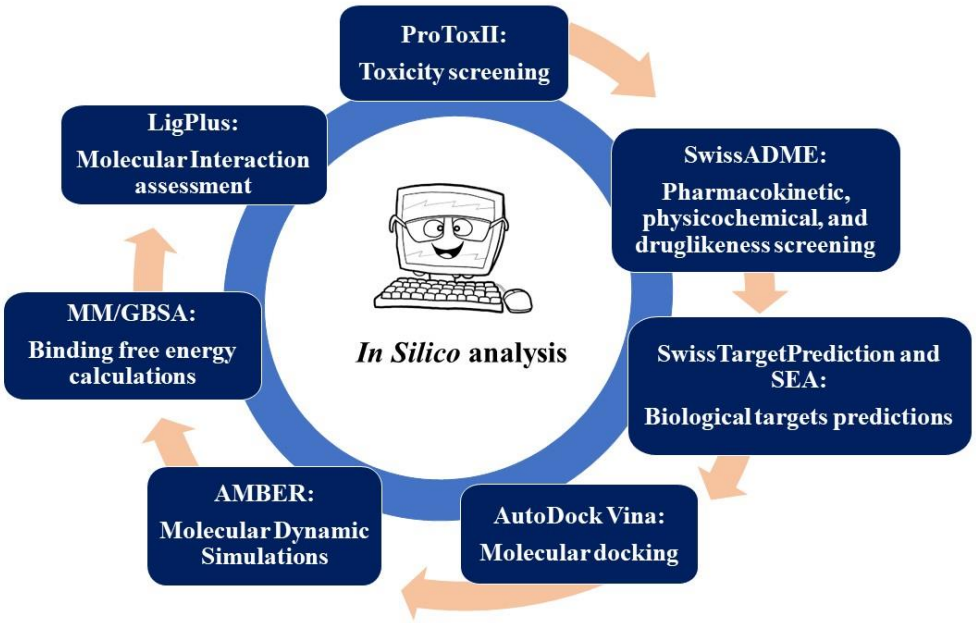


Figure 4.7: The schematic diagram of the study design.

Prediction of toxicological properties of curcumin and synthetic curcumin derivatives

ProTox II is a free webserver that is used to computationally predict the toxicity of compounds in a biological system [79]. The canonical simplified molecular-input line-entry system (SMILES) of curcumin and three synthetic curcumin derivatives (1A6, 1A8, and 1B8) were submitted to the ProTox II webserver to define their toxicological endpoints. These include hepatotoxicity, carcinogenicity, immunotoxicity, and cytotoxicity. ProTox II was also used to predict the median lethal doses (LD_{50}) values using the globally harmonized system of classification of labelling of chemicals (GMS) [79,80]. Furthermore, the predicted toxicity classifications were also assessed. These include extremely toxic (low LD_{50}), highly toxic (moderate LD_{50}), moderately toxic (intermediate LD_{50}), slightly toxic (high LD_{50}), and practically non-toxic (very high LD_{50}) [81].

Predicting the pharmacokinetic, physicochemical, and druglikeness properties of curcumin and synthetic curcumin derivatives

SwissADME [82], which is a free webserver used to predict the pharmacokinetics, druglikeness, and medicinal chemistry properties of a compound, was used to determine the general chemical parameters of curcumin and the three synthetic curcumin derivatives (1A6, 1A8, and 1B8). The physicochemical properties such as lipophilicity (iLOGP) and water solubility (ESOL) were defined, while the gastrointestinal (GI) absorption, which is a

pharmacokinetic parameter, was also predicted. The effect of curcumin, 1A6, 1A8, and 1B8 on the liver drug efflux pump (otherwise known as P-glycoprotein (P-gp) substrate) and the inhibition of cytochrome P450 enzymes (CYP3A4, CYP1A2, CYP2D6, and CYP2C9), which are involved in liver metabolism was assessed [83]. Drug parameters such as druglikeness using Lipinski's rules (LRo5) [84] and synthetic score were also defined.

Identification of the potential biological targets of curcumin and synthetic curcumin derivatives

To determine the potential biological targets of curcumin, 1A6, 1A8, and 1B8, the canonical SMILES of these compounds were submitted to SwissTarget Prediction [85] and SEA (similarity ensemble approach) [86], which are free webservers that identify possible target proteins based on the published experimental literature of the compound or related compounds. In addition, the online databases PubMed and Google Scholar were used to search for studies reporting on the proteins that are targeted by curcumin and regulate adipogenesis, lipid metabolism, and inflammation in adipose tissue. In this regard, three common potential biological targets of these compounds or those that are at least targeted by curcumin in each pathway were selected and used for downstream experiments. The selected target proteins were then used for molecular docking studies to assess the interaction and binding affinities of the compounds (curcumin, 1A6, 1A8, and 1B8) with these target proteins.

Molecular docking of curcumin and synthetic curcumin derivatives to the target

Generation of the three–dimensional structure and energy minimization of the compounds

The two-dimensional structures of curcumin and the three synthetic curcumin derivatives were drawn, whereafter their three-dimensional structures were generated and energy minimized using the ACD/ChemSketch freeware [87]. Experimentally established ligands (PF05221304, Rosiglitazone, Raloxifene, and LY2228820) or Food and Drug Administration (FDA)-approved drugs (BBI608, GW9662, Orlistat, Naproxen, and FT30356) of corresponding target proteins were used as references to confirm the docking poses of the compounds. All generated three-dimensional structures were saved in .mol^2 format. Thereafter, the three-dimensional structures were submitted to Avogadro version 2.0 software for optimization [88]. The Avogadro software is used to optimize the three-dimensional structures of compounds by adding partial charges using Ghemical and Merck molecular force fields 94 (MMFF94s) and then afterwards minimizing energy to yield a more optimal geometric structure of compounds. All optimized compounds were saved in .mol^2 format in preparation for molecular docking.

Protein preparation

The X-ray crystal structures of the target proteins (Table 4.6) were identified online using the RSCB Protein Data Bank (PDB) [89] and downloaded in pdb format. The UCSF Chimera Software package, version 1.17.3 was used to optimize the protein structures for molecular docking by removing water molecules and all other non-standard residues [90]. Thereafter, the optimized protein structures were saved in PBD format in preparation for molecular docking.

Table 4.6: The predicted target proteins of curcumin and the three synthetic curcumin derivatives. Identified from the RSCB Protein Data Bank [89].

Protein	PDB ID	Metabolic Pathway
Proliferator-activated receptor-gamma (PPARγ)	7WGO	
Mitogen-activated protein kinase 14 (MAPK14)	5XYX	Adipogenesis
Signal transducer and activator of transcription 3 (STAT3)	6NUQ	
Acetyl-CoA carboxylase (ACC)	3TDC	
Fatty acid synthase (FAS)	2VZ8	Lipid metabolism
Glycogen synthase kinase-3 beta (GSK3β)	5F95	
Cyclooxygenase 2 (COX2)	5F1A	
Interleukin 6 (IL-6)	1ALU	Inflammation
Adiponectin	6U66	

Identification of the binding sites of the predicted protein targets

Crystal structures of target proteins retrieved from the PDB with unknown ligand-binding sites were submitted to the Computed Atlas of Surface Topography of proteins (CASTp) free webserver, using their PDB ID (5F1A, 1ALU, and 6U66), for the prediction of binding sites. CASTp is an online protein analytic tool that assesses the surface topography of a protein. The CASTp tool also identifies and highlights pockets and cavities in the threedimensional crystal structure of a protein [91]. Pockets predicted to have a high surface area and volume were considered as potential interactive sites responsible for the binding of ligands.

Molecular docking studies

The purpose of molecular docking is to assess the binding affinity of two molecules using various scoring algorithms [92]. The Autodock Vina Plugin found on UCSF Chimera was used to dock the generated three dimensional structures to the target proteins, thus defining the best ligand–protein binding conformation as the output. For each target protein, molecular docking simulations were carried out with the docking grid box

containing different co-ordinates as shown in Table 4.7. After molecular docking, the docked complexes were arranged in consistent order, while reference compounds were outlined first, and the root mean square from the original docking mode of each compound was determined. Superimposition was carried out to confirm that compounds were docked within the identified conserved regions.

Table 4.7: Grid box co-ordinates of molecular docking for the predicted protein targets.

Target Protein	Centre (X, Y, Z)	Dimensions of Grid Box (X, Y, Z)
PPARγ	−15.2125, 9.29439, 11.01	15.7975, 13.9009, 17.6109
MAPK14	10.5915, 27.7279, 3.79848	18.5886, 14.9989, 15.8401
STAT3	5.5637, 37.1142, 12.1653	10.9664, 13.6214, 19.9643
ACC	32.2003, 61.7848, 40.5045	13.7853, 12.3731, 13.918
FASN	0.967647, 66.8543, 47.8479	19.5167, 19.0018, 20.6675
GSK3β	76.6598, −0.578815, 13.9848	17.0805, 18.7096, 17.3094
COX2	−35.499, −48.6516, −23.2359	20.5025, 29.0627, 22.0537
IL-6	25.5171, −14.866, 15.8218	13.9402, 12.7375, 13.6888
Adiponectin	9.88392, 17.1713, −37.7544	14.1579, 12.833, 12.5061

Molecular dynamic simulations of curcumin and synthetic curcumin derivatives

The SANDER engine provided as part of the AMBER package was used for molecular dynamic (MD) simulations, and the AMBER force field, FF14SB [93], was utilized to describe the systems. To determine atomic partial charges for the ligand, we utilized ANTECHAMBER along with the restrained electrostatic potential (RESP) and general amber force field (GAFF) procedures. Hydrogen atoms were added to the systems using the Leap module of AMBER 14. Neutralization was attained by adding 6 Na^+ on the PPARγ and FAS protein structures, and 1 Na^+ on the COX2 protein structure. The amino acids were renumbered based on the dimeric form of the protein, resulting in residues numbered from 1 to 276 for PPARγ, 1 to 551 for COX2, and 1 to 275 for FAS. To create the simulation systems, the systems were placed within an orthorhombic box filled with TIP3P water molecules. The positioning ensured that all atoms were within 10 Å of any box edge.

An initial minimization was performed with a restraint potential of 500 kcal/mol applied to both substances of interest (solutes). The minimization consisted of 1000 steps using the steepest descent method followed by 1000 steps of conjugate gradients. An additional full minimization of 1000 steps were carried out using the conjugate gradient algorithm without any restraints. The systems were gradually heated from 0 K to 310.5 K (physiological temperature) during a 0.05 ns MD simulation. The number of atoms and volume of the systems were kept fixed.

The solutes within the systems were subjected to a potential harmonic restraint of 10 kcal/mol and a collision frequency of 0.001 ns. Following the heating phase, an equilibration step of approximately 0.5 ns was performed for each system. The temperature was maintained at 310.5 K during this equilibration process. The systems were simulated under an isobaric–isothermal ensemble (NPT), with several features kept constant, including the number of atoms and pressure. The pressure of the system was maintained at 1 bar using the Berendsen barostat.

The MD simulations were conducted for 200 ns through AMBER 18 using the GPU version. In each simulation, the SHAKE algorithm was employed to constrain the bonds involving hydrogen atoms. The time step for the simulations was set to 2 fs, and an SPFP precision model was used. The simulations followed the isobaric–isothermal ensemble (NPT) conditions, with randomized seeding, a constant pressure of 1 bar maintained by the Berendsen barostat, a pressure-coupling constant of 0.002 ns, a physiological temperature, and a Langevin thermostat with a collision frequency of 0.001 ns.

Post-molecular dynamic simulations analysis

After saving the coordinates of all eighteen systems, trajectory analysis was performed at every 100 ns interval using PTRAJ. The analysis included calculating the root mean square deviation (RMSD) and root mean square fluctuation (RMSF). These analyses were conducted using the CPPTRAJ module. For molecular interaction analysis, Molegro Molecular Viewer version 2.2 [94] and LigPlot version 2.2.8 [95] software were utilized to define ligand binding interactions and intermolecular interactions within the binding site of the protein at the end of the simulation period (200 ns).

Binding free energy calculations

To evaluate and compare the binding affinity of the systems, the binding free energy was determined using the molecular mechanics/generalized born surface area method (MM/GBSA) [96]. The calculation of the binding free energy involved averaging 200 snapshots extracted from the 200 ns trajectory. The binding free energy (ΔG) obtained through this method [97] for each molecular species (complex, ligand, and receptor) can be described as follows:

1. ΔGbind = Gcomplex − Greceptor – Gligend;
2. ΔGbind = Egas + Gsol -ST;
3. Egas = Eint + Evdw + Eele;

4. Gsol = GGB + GSA;
5. GSA = ΔSASA.

The term “Egas” represents the energy in the gas phase, which includes the internal energy “Eint”, the Coulomb energy “Eele”, and the Van der Waals energy “Evdw”. The Egas value was directly calculated using the FF14SB force field terms. The solvation free energy, “Gsol”, was estimated by considering the energy contributions from both polar states, “GGB”, and non-polar states, “G”. The non-polar solvation energy, “GSA”, was determined based on the solvent accessible surface area (SASA) using a water probe radius of 1.4 Å. On the other hand, the polar solvation contribution, “GGB”, was estimated by solving the generalized born (GB) equation. The terms “S” and “T” represent the total entropy of the solute and the temperature, respectively.

Data analysis

OriginPro version 9.1 data analysis software [98] was used to generate plots for all raw data. Discovery Studio Visualizer version 21.1.0.20298 [99] and LigPlot^{+} version 2.2 [100] software were used for visualization.

Conclusions

In conclusion, our comprehensive analysis comparing curcumin with its synthetic derivatives reveals promising findings across pharmacokinetic, toxicity, and physicochemical parameters. The derivatives, namely 1A6, 1A8, and 1B8, align with druglikeness criteria, showcasing potential as drug candidates. Physicochemical properties, particularly lipophilicity, indicate variations that could impact membrane permeability and bioavailability, with 1A8 potentially offering improved membrane penetration. Toxicity profiles highlight overall promise, with 1A8 demonstrating the safest profile. However, refinement strategies for all compounds are recommended to mitigate specific endpoint effects observed at lethal dosages. Metabolism analyses suggest potential interactions with key liver enzymes, emphasizing the importance of structural modifications to optimize pharmacokinetics and minimize potential drug interactions. Molecular docking and molecular dynamics simulations underscore the similarities in binding affinities and interactions among curcumin and its derivatives with pivotal anti-obesity target proteins—PPARγ, COX2, and FAS. Stability throughout the simulations and identified amino acid interactions within binding sites support the robustness of these interactions.

Collectively, the *in silico* exploration of the pharmacokinetic and pharmacodynamic profiles of curcumin and its synthetic derivatives reveals insightful mechanisms, suggesting their potential as anti-obesity agents by targeting

key metabolic pathways. Although our computational results suggest a similarity in interactive activity between curcumin and its synthetic derivatives, it is crucial to conduct additional experimental validation to enhance our understanding of their regulatory capabilities. *In vitro* experiments, including gene and protein expression assays, should be undertaken on the identified biological targets to explore the mechanisms of action associated with these compounds and validate the findings of this study. The structural insights and mechanistic understanding derived from this study provide valuable guidance for future research and optimization efforts aimed at harnessing the therapeutic capabilities of these compounds.

Author Contributions: M.T.M. conceived and designed computational experiments, performed computational experiments, analyzed and interpreted the data, and wrote, edited, and approved the final manuscript. P.R. conceived and designed computational experiments and wrote, edited, and approved the final manuscript. E.Y.S. designed computational experiments, analyzed and interpreted the data, and wrote, edited, and approved the final manuscript. B.U.J., C.P., S.J.J.T., and S.E.M.-M. edited and approved the final manuscript. All authors have read and agreed to the published version of the manuscript.

Funding: This research was funded by the South African Medical Research Council (SAMRC) biomedical and research innovation platform (BRIP) and the NRF Thuthuka Programme (Grant Number: 129508) awarded to Babalwa Jack.

Institutional Review Board Statement: Not applicable
Informed Consent Statement: Not applicable

Data Availability Statement: All additional data including raw data will be provided upon request after this paper is published.

Acknowledgments: Marakiya T. Moetlediwa is funded by the National Research Foundation (NRF) of South Africa and North-West University (NWU) master's funding. The authors would like to acknowledge the National Integrated Cyberinfrastructure System's Centre for High Performance Computing (NICIS-CHPC) for the computing resources required for this study.

Conflicts of Interest: The authors declare no conflicts of interest.

References

[1] Di Cesare, M.; Bentham, J.; Stevens, G.A.; Zhou, B.; Danaei, G.; Lu, Y.; Bixby, H.; Cowan, M.J.; Riley, L.M.; Hajifathalian, K.; et al. Trends in adult body-mass index in 200 countries from 1975 to 2014: A pooled analysis of 1698 population-based measurement studies with 19.2 million participants. *Lancet* 2016, *387*, 1377–1396. https://doi.org/10.1016/S0140-6736 (16)30054-X

[2]. Wu H.; Ballantyne, C.M. Metabolic Inflammation and Insulin Resistance in Obesity. *Circ. Res.* 2020, *126*, 1549–1564. https://doi.org/10.1161/CIRCRESAHA.119.315896.

[3] Yazıcı D.; Sezer, H. Insulin resistance, obesity and lipotoxicity. *Adv. Exp. Med. Biol.* 2017, *960*, 277– 304.

[4] Feingold, K.R. Obesity and Dyslipidemia. *Endotext* 2020. Available online: http://www.ncbi.nlm.nih.gov/pubmed/26247088 (accessed on 10 June 2021).

[5] Al-Sulaiti H.; Diboun, I.; Agha, M.V.; Mohamed, F.F.S.S.; Atkin, S.; Dömling, A.S.; Elrayess, M.A.; Mazloum, N.A. Metabolic signature of obesity-associated insulin resistance and type 2 diabetes. *J. Transl. Med.* 2019, *17*, 348. https://doi.org/10.1186/s12967-019-2096-8.

[6] Powell-Wiley, T.M.; Poirier, P.; Burke, L.E.; Després, J.P.; Gordon-Larsen, P.; Lavie, C.J.; Lear, S.A.; Ndumele, C.E.; Neeland, I.J.; Sanders, P.; et al. Obesity and Cardiovascular Disease A Scientific Statement From the American Heart Association. *Circulation* 2021, *143*, E984–E1010. https://doi.org/10.1161/CIR.0000000000000973.

[7] Davoodi SH, , S.H.; Malek-Shahabi, T.; Malekshahi-Moghadam, A.; Shahbazi, R.; Esmaeili, S. Obesity as an important risk factor for certain types of cancer. *Iran. J. Cancer Prev.* 2013, *6*, 186–194.

[8] Tapsell LC, L.C.; Hemphill, I.; Cobiac, L.; Patch, C.S.; Sullivan, D.R.; Fenech, M.; Roodenrys, S.; Keogh, J.B.; Clifton, P.M.; Williams, P.G.; et al. Health benefits of herbs and spices: The past, the present, the future. *Med. J. Aust.* 2006, *185*, S1–S24. https://doi.org/10.5694/j.13265377.2006.tb00548.x

[9] Liu RH. R.H. Health-promoting components of fruits and vegetables in the diet. *Adv. Nutr.* 2013, *4*, 384S–392S. https://doi.org/10.3945/an.112.003517.

[10] Xie, X.; Kong, P.-R.; Wu, J.; Li, Y.; Li, Y. Curcumin attenuates lipolysis stimulated by tumor necrosis factor-α or isoproterenol in 3T3-L1 adipocytes. *Phytomedicine* 2012, *20*, 3–8. https://doi.org/10.1016/j.phymed.2012.09.003.

[11] Kobori, M.; Takahashi, Y.; Takeda, H.; Takahashi, M.; Izumi, Y.; Akimoto, Y.; Sakurai, M.; Oike, H.; Nakagawa, T.; Itoh, M.; et al. Dietary Intake of Curcumin Improves eIF2 Signaling and Reduces Lipid Levels in the White Adipose Tissue of Obese Mice. *Sci. Rep.* 2018, *8*, 9081. https://doi.org/10.1038/s41598-018-27105-w.

[12] Ejaz, A.; Wu, D.; Kwan, P.; Meydani, M. Curcumin inhibits adipogenesis in 3T3-L1 adipocytes and angiogenesis and obesity in C57/BL mice. *J. Nutr.* 2009, *139*, 919–925. https://doi.org/10.3945/jn.108.100966.

[13] Tian , L.; Song, Z.; Shao, W.; Du, W.W.; Zhao, L.R.; Zeng, K.; Yang, B.B.; Jin, T. Curcumin represses mouse 3T3-L1 cell adipogenic differentiation via inhibiting miR-17-5p and stimulating the Wnt signalling pathway effector Tcf7l2. *Cell Death Dis.* 2017, *8*, e2559. https://doi.org/10.1038/cddis.2016.455.

[14] Wu, L.Y.; Chen, C.W.; Chen, L.K.; Chou, H.Y.; Chang, C.L.; Juan, C.C. Curcumin attenuates adipogenesis by inducing preadipocyte apoptosis and inhibiting adipocyte differentiation. *Nutrients* 2019, *11*, 2307. https://doi.org/10.3390/nu11102307.

[15] Islam T.; Koboziev, I.; Albracht-Schulte, K.; Mistretta, B.; Scoggin, S.; Yosofvand, M.; Moussa, H.; Zabet-Moghaddam, M.; Ramalingam, L.; Gunaratne, P.H.; et al. Curcumin Reduces Adipose Tissue Inflammation and Alters Gut Microbiota in Diet-Induced Obese Male Mice. *Mol. Nutr. Food Res.* 2021, *65*, e2100274. https://doi.org/10.1002/mnfr.202100274.

[16] Mokgalaboni, K.; Ntamo, Y.; Ziqubu, K.; Nyambuya, T.M.; Nkambule, B.B.; Mazibuko-Mbeje, S.E.; Gabuza, K.B.; Chellan, N.; Tiano, L.; Dludla, P.V. Curcumin supplementation improves biomarkers of oxidative stress and inflammation in conditions of obesity, type 2 diabetes and NAFLD: Updating the status of clinical evidence. *Food Funct.* 2021, *12*, 12235–12249. https://doi.org/10.1039/D1FO02696H.

[17] Anand, P.; Kunnumakkara, A.B.; Newman, R.A.; Aggarwal, B.B. Bioavailability of curcumin: Problems and promises. *Mol. Pharm.* 2007, *4*, 807–818. https://doi.org/10.1021/mp700113r.

[18] Moetlediwa, M.T.; Ramashia, R.; Pheiffer, C.; Titinchi, S.J.J.; Mazibuko-Mbeje, S.E.; Jack, B.U. Therapeutic Effects of Curcumin Derivatives against Obesity and Associated Metabolic Complications: A Review of *In vitro* and *In vivo* Studies. *Int. J. Mol. Sci.* 2023, *24*, 14366. https://doi.org/10.3390/ijms241814366.

[19] Badano, A. *In silico* imaging clinical trials: Cheaper, faster, better, safer, and more scalable. *Trials* 2021, *22*, 64. https://doi.org/10.1186/s13063-020-05002-w.

[20] Ooko E, E.; Alsalim, T.; Saeed, B.; Saeed, M.E.M.; Kadioglu, O.; Abbo, H.S.; Titinchi, S.J.J.; Efferth, T. Modulation of P-glycoprotein activity by novel synthetic curcumin derivatives in sensitive and multidrug-resistant T-cell acute lymphoblastic leukemia cell lines. *Toxicol. Appl. Pharmacol.* 2016, *305*, 216–233. https://doi.org/10.1016/J.TAAP.2016.06.002.

[21] Tian, S.; Wang, J.; Li, Y.; Li, D.; Xu, L.; Hou, T. The application of *in silico* drug-likeness predictions in pharmaceutical research. *Adv. Drug Deliv. Rev.* 2015, *86*, 2–10. https://doi.org/10.1016/j.addr.2015.01.009.

[22] Xiong G, G.; Wu, Z.; Yi, J.; Fu, L.; Yang, Z.; Hsieh, C.; Yin, M.; Zeng, X.; Wu, C.; Lu, A.; et al. ADMETlab 2.0: An integrated online platform for accurate and comprehensive predictions of ADMET properties. *Nucleic Acids Res.* 2021, *49*, W5–W14. https://doi.org/10.1093/nar/gkab25.

[23] Di, L.; Kerns, E.H. *Drug-like Properties*; Elsevier: Amsterdam, The Netherlands, 2016. https://doi.org/10.1016/C2013-0-18378-X.

[24] Fang, J.; Liu, C.; Wang, Q.; Lin, P.; Cheng, F. *In silico* polypharmacology of natural products. *Brief. Bioinform.* 2017, *19*, 1153–1171. https://doi.org/10.1093/bib/bbx045.

[25] Newman, D.J.; Cragg, G.M. Natural Products as Sources of New Drugs over the Nearly Four Decades from 01/1981 to 09/2019. *J. Nat. Prod.* 2020, *83*, 770–803. https://doi.org/10.1021/acs.jnatprod.9b01285.

[26] Newman, D.; Cragg, G. Natural Products in Medicinal Chemistry. *Bioorgan. Med. Chem.* 2009, *17*, 2120. https://doi.org/10.1016/j.bmc.2009.03.010.

[27] Von Nussbaum, F.; Brands, M.; Hinzen, B.; Weigand, S.; Häbich, D. Antibacterial natural products in medicinal chemistry—Exodus or revival? *Angew. Chem. Int. Ed.* 2006, *45*, 5072–5129.

https://doi.org/10.1002/anie.200600350.

[28] Atanasov, , A.G.; Zotchev, S.B.; Dirsch, V.M.; Orhan, I.E.; Banach, M.; Rollinger, J.M.; Barreca, D.; Weckwerth, W.; Bauer, R.; Bayer, E.A.; et al. Natural products in drug discovery: Advances and opportunities. *Nat. Rev. Drug Discov.* 2021, *20*, 200–216. https://doi.org/10.1038/s41573-020-00114-z.

[29] Kong, L. Current Study of Natural Products for Medicinal Chemistry. *Curr. Med. Chem.* 2021, *28*, 5189–5190. https://doi.org/10.2174/0929867328252108161147 55.

[30] Alappat, L.; Awad, A.B. Curcumin and obesity: Evidence and mechanisms. *Nutr. Rev.* 2010, *68*, 729– 738. https://doi.org/10.1111/j.1753-4887.2010.00341.x.

[31] Bradford, P.G. Curcumin and obesity. *BioFactors* 2013, *39*, 78–87. https://doi.org/10.1002/biof.1074.

[32] Zhang, L, Zheng J, Ma M, Zhao Y, Song J, Chen X, et al. Drug-guided screening for pancreatic lipase inhibitors in functional foods. Food Funct. 2021 May;12(10):4644–53.

[33] Doak, , B.C.; Kihlberg, J. Drug discovery beyond the rule of 5—Opportunities and challenges. *Expert Opin. Drug Discov.* 2017, *12*, 115–119. https://doi.org/10.1080/17460441.2017.1264385.

[34] Owens, J.; Lipinski, C.A. Chris Lipinski discusses life and chemistry after the Rule of Five. *Drug Discov. Today* 2003, *8*, 12–16. https://doi.org/10.1016/S1359-6446(02)02556-4.

[35] Pollastri, M.P. Overview on the rule of five. *Curr. Protoc. Pharmacol.* 2010, *49*, 9.12.1–9.12.8. https://doi.org/10.1002/0471141755.ph0912s49.

[36] Vidović, D.; Milošević, N.; Pavlović, N.; Todorović, N.; Panić, J.Č.; Ćurčić, J.; Banjac, N.; Trišović, N.; Božić, B.; Lalić-Popović, M. *In silico–in vitro* estimation of lipophilicity and permeability association for succinimide derivatives using chromatographic anisotropic systems and parallel artificial membrane permeability assay. *Biomed. Chromatogr.* 2022, *36*, e5413. https://doi.org/10.1002/bmc.5413.

[37] Schott, H. Hydrophilic-Lipophilic Balance, Solubility Parameter, and Oil-Water Partition Coefficient as Universal Parameters of Nonionic Surfactants. *J. Pharm. Sci.* 1995, *84*, 1215–1222. https://doi.org/10.1002/jps.2600841014.

[38] Yamashita, Y.; Sakamoto, K. Hydrophilic–Lipophilic Balance (HLB): Classical Indexation and Novel Indexation of Surfactant. In *Encyclopedia of Biocolloid and Biointerface Science 2V Set*; Wiley: Hoboken, NJ, USA, 2016; pp. 570–574.

[39] Clariano, M.; Marques, V.; Vaz, J.; Awam, S.; Afonso, M.B.; Jesus Perry, M.; Rodrigues, C.M.P. Monocarbonyl Analogs of Curcumin with Potential to Treat Colorectal Cancer. *Chem. Biodivers.* 2023, *20*, e202300222. https://doi.org/10.1002/cbdv.202300222.

[40] Yousef, S.A.; Mohammed, Y.H.; Namjoshi, S.; Grice, J.E.; Benson, H.A.E.; Sakran, W.; Roberts, M.S. Mechanistic evaluation of enhanced curcumin delivery through human skin *in vitro* from optimised nanoemulsion formulations fabricated with different penetration enhancers. *Pharmaceutics* 2019, *11*, 639. https://doi.org/10.3390/pharmaceutics11120639.

[41] E. G. Lewars, Computational Chemistry. Cham: Springer International Publishing, 2016. doi: 10.1007/978-3-319-30916-3.

[42] Salum, L.B.; Andricopulo, A.D. Fragment-based QSAR strategies in drug design. *Expert Opin. Drug Discov.* 2010, *5*, 405–412. https://doi.org/10.1517/17460441003782277.

[43] Indira Priyadarsini, K. Chemical and Structural Features Influencing the Biological Activity of Curcumin. *Curr. Pharm. Des.* 2013, *19*, 2093–2100. https://doi.org/10.2174/138161213805289228.

[44] Herman, T.F.; Santos, C. *First Pass Effect*; 2023. Available online: http://www.ncbi.nlm.nih.gov/pubmed/6362950 (accessed on 20 November 2023).

[45] Almazroo, O.A.; Miah, M.K.; Venkataramanan, R. Drug Metabolism in the Liver. *Clin. Liver Dis.* 2017, *21*, 1–20. https://doi.org/10.1016/j.cld.2016.08.001.

[46] Yang, T.; Chen, Y.; Xu, J.; Li, J.; Liu, H.; Liu, N. Bioinformatics screening the novel and promising targets of curcumin in hepatocellular carcinoma chemotherapy and prognosis. *BMC Complement. Med. Ther.* 2022, *22*, 21. https://doi.org/10.1186/s12906-021-03487-9.

[47] Domínguez-Avila, , J.A.; Wall-Medrano, A.; Velderrain-Rodríguez, G.R.; Chen, C.-Y.O.; SalazarLópez, N.J.; Robles-Sánchez, M.; González-Aguilar, G.A. Gastrointestinal interactions, absorption, splanchnic metabolism and pharmacokinetics of orally ingested phenolic compounds. *Food Funct.* 2017, *8*, 15–38. https://doi.org/10.1039/C6FO01475E.

[48] Hassaninasab, A.; Hashimoto, Y.; Tomita-Yokotani, K.; Kobayashi, M. Discovery of the curcumin metabolic pathway involving a unique enzyme in an intestinal microorganism. *Proc. Natl. Acad. Sci. USA* 2011, *108*, 6615–6620. https://doi.org/10.1073/PNAS.1016217108.

[49] Xue, M.; Cheng, Y.; Xu, L.; Zhang, L. Study of the Intestinal Absorption Characteristics of Curcumin *In vivo* and *In vitro*. *J. Appl. Pharm.* 2017, *9*, 1000246. https://doi.org/10.21065/1920-4159.1000246.

[50] Ahmed Juvale, I.I.; Abdul Hamid, A.A.; Abd Halim, K.B.; Che Has, A.T. P-glycoprotein: New insights into structure, physiological function, regulation and alterations in disease. *Heliyon* 2022, *8*, e09777. https://doi.org/10.1016/j.heliyon.2022.e09777.

[51] Sagnou, M.; Novikov, F.N.; Ivanova, E.S.; Alexiou, P.; Stroylov, V.S.; Titov, I.Y.; Tatarskiy, V.V.; Vagida, M.S.; Pelecanou, M.; Shtil, A.A.; et al. Novel curcumin derivatives as P-glycoprotein inhibitors: Molecular modeling, synthesis and sensitization of multidrug resistant cells to doxorubicin. *Eur. J. Med. Chem.* 2020, *198*, 112331. https://doi.org/10.1016/j.ejmech.2020.112331.

[52] Kim, B.-R.; Lee, G.Y.; Yu, H.; Maeng, H.J.; Oh, T.J.; Kim, K.M.; Moon, J.H.; Lim, S.; Jang, H.C.; Choi, S.H. Suppression of Nrf2 attenuates adipogenesis and decreases FGF21 expression through PPAR gamma in 3T3-L1 cells. *Biochem. Biophys. Res. Commun.* 2018, *497*, 1149–1153. https://doi.org/10.1016/j.bbrc.2017.01.107.

[53] Wang, Q.; Imam, M.U.; Yida, Z.; Wang, F. Peroxisome Proliferator-Activated Receptor Gamma (PPARγ) as a Target for Concurrent Management of Diabetes and Obesity-Related Cancer. *Curr. Pharm. Des.* 2017, *23*, 3677–3688. https://doi.org/10.2174/1381612823666170704125104.

[54] Bernardo, A.; Plumitallo, C.; De Nuccio, C.; Visentin, S.; Minghetti, L. Curcumin promotes oligodendrocyte differentiation and their protection against TNFα through the activation of the nuclear receptor PPAR-γ. *Sci. Rep.* 2021, *11*, 4952. https://doi.org/10.1038/s41598-021-83938-y.

[55] Mohankumar, K.; Francis, A.P.; Pajaniradje, S.; Rajagopalan, R. Synthetic curcumin analog: Inhibiting the invasion, angiogenesis, and metastasis in human laryngeal carcinoma cells via NF-kB pathway. *Mol. Biol. Rep.* 2021, *48*, 6065–6074. https://doi.org/10.1007/s11033-021-06610-8.

[56] Sohilait, M.R.; Pranowo, H.D.; Haryadi, W. Molecular docking analysis of curcumin analogues with COX2. *Bioinformation* 2017, *13*, 356–359. https://doi.org/10.6026/97320630013356.

[57] Ioannou, M.S.; Jackson, J.; Sheu, S.-H.; Chang, C.-L.; Weigel, A.V.; Liu, H.; Pasolli, H.A.; Xu, C.S.; Pang, S.; Matthies, D.; et al. Neuron-Astrocyte Metabolic Coupling Protects against Activity-Induced Fatty Acid Toxicity. *Cell* 2019, *177*, 1522–1535.e14. https://doi.org/10.1016/j.cell.2019.04.001.

[58] Browne, C.D.; Hindmarsh, E.J.; Smith, J.W. Inhibition of endothelial cell proliferation and angiogenesis by orlistat, a fatty acid synthase inhibitor. *FASEB J.* 2006, *20*, 2027–2035. https://doi.org/10.1096/fj.055404com.

[59] Othman, Z.A.; Zakaria, Z.; Suleiman, J.B.; Ghazali, W.S.W.; Mohamed, M. Anti-Atherogenic Effects of Orlistat on Obesity-Induced Vascular Oxidative Stress Rat Model. *Antioxidants* 2021, *10*, 251. https://doi.org/10.3390/antiox10020251.

[60] Maithilikarpagaselvi, N.; Sridhar, M.G.; Swaminathan, R.P.; Sripradha, R.; Badhe, B. Curcumin inhibits hyperlipidemia and hepatic fat accumulation in high-fructose-fed male Wistar rats. *Pharm. Biol.* 2016, *54*, 2857–2863. https://doi.org/10.1080/13880209.2016.1187179.

[61] Ramírez, D.; Caballero, J. Is It Reliable to Take the Molecular Docking Top Scoring Position as the Best Solution without Considering Available Structural Data? *Molecules* 2018, *23*, 1038. https://doi.org/10.3390/molecules23051038.

[62] Schaefer, K.L.; Takahashi, H.; Morales, V.M.; Harris, G.; Barton, S.; Osawa, E.; Nakajima, A.; Saubermann, L.J. PPARγ inhibitors reduce tubulin protein levels by a PPARγ, PPARδ and proteasomeindependent mechanism, resulting in cell cycle arrest, apoptosis and reduced metastasis of colorectal carcinoma cells. *Int. J. Cancer* 2007, *120*, 702–713. https://doi.org/10.1002/ijc.22361.

[63] Schaefer, K.L. PPARγ inhibitors as novel tubulin-targeting agents. *PPAR Res.* 2008, *2008*, 785405. https://doi.org/10.1155/2008/785405.

[65] Teilum, K.; Olsen, J.G.; Kragelund, B.B. Protein stability, flexibility and function. *Biochim. Biophys. Acta Proteins Proteom.* 2011, *1814*, 969–976. https://doi.org/10.1016/j.bbapap.2010.11.005.

[66] Karshikoff, A.; Nilsson, L.; Ladenstein, R. Rigidity versus flexibility: The dilemma of understanding protein thermal stability. *FEBS J.* 2015, *282*, 3899–3917. https://doi.org/10.1111/febs.13343.

[67] Polo-Cuadrado, E.; Acosta-Quiroga, K.; Rojas-Peña, C.; Rodriguez-Nuñez, Y.A.; Duarte, Y.; Brito, I.; Cisterna, J.; Gutiérrez, M. Molecular modeling and structural analysis of some tetrahydroindazole and cyclopentanepyrazole derivatives as COX2 inhibitors. *Arab. J. Chem.* 2022, *15*, 103540. https://doi.org/10.1016/j.arabjc.2021.103540.

[68] Singh, S.; Karthikeyan, C.; Moorthy, N.S.H.N. Classification analysis of fatty acid synthase inhibitors using multialgorithms on topological descriptors and structural fingerprints. *Chem. Biol. Drug Des.* 2023, *101*, 395–407. https://doi.org/10.1111/cbdd.14138.

[69] Patil, R.; Das, S.; Stanley, A.; Yadav, L.; Sudhakar, A.; Varma, A.K. Optimized Hydrophobic Interactions and Hydrogen Bonding at the Target-Ligand Interface Leads the Pathways of DrugDesigning. *PLoS ONE* 2010, *5*, e12029. https://doi.org/10.1371/journal.pone.0012029.

[70] Lin, J.; Chen, A. Activation of peroxisome proliferator-activated receptor-γ by curcumin blocks the signaling pathways for PDGF and EGF in hepatic stellate cells. *Lab. Investig.* 2008, *88*, 529–540. https://doi.org/10.1038/labinvest.2008.20.

[71] Liu Z.-J.; Liu, W.; Liu, L.; Xiao, C.; Wang, Y.; Jiao, J.-S. Curcumin Protects Neuron against Cerebral Ischemia-Induced Inflammation through Improving PPAR-Gamma Function. *Evid. Based Complement. Altern. Med.* 2013, *2013*, 470975. https://doi.org/10.1155/2013/470975.

[72] Mazidi, M.; Karimi, E.; Meydani, M.; Ghayour-Mobarhan, M.; Ferns, G.A.; Laboratory, V.B.; Mayer, J. Potential effects of curcumin on peroxisome proliferator-activated receptor-γ *in vitro* and *in vivo*. *World J. Methodol.* 2016, *6*, 112. https://doi.org/10.5662/wjm.v6.i1.112.

[73] Alalaiwe, A.; Fang, J.-Y.J.Y.; Lee, H.-J.H.J.; Chiu, C.H.C.-H.; Hsu, C.Y.C.-Y. The demethoxy derivatives of curcumin exhibit greater differentiation suppression in 3T3-L1 adipocytes than curcumin: A mechanistic study of adipogenesis and molecular docking. *Biomolecules* 2021, *11*, 1025. https://doi.org/10.3390/biom11071025.

[74] Mohan, M.; Hussain, M.A.; Khan, F.A.; Anindya, R. Symmetrical and un-symmetrical curcumin analogues as selective COX-1 and COX2 inhibitor. *Eur. J. Pharm. Sci.* 2021, *160*, 105743. https://doi.org/10.1016/j.ejps.2021.105743.

[75] Choi, G.-Y.; Kim, H.-B.; Hwang, E.-S.; Lee, S.; Kim, M.-J.; Choi, J.-Y.; Lee, S.-O.; Kim, S.-S.; Park, J.-H. Curcumin Alters Neural Plasticity and Viability of Intact Hippocampal Circuits and Attenuates Behavioral Despair and COX2 Expression in Chronically Stressed Rats. *Mediat. Inflamm.* 2017, *2017*, 6280925. https://doi.org/10.1155/2017/6280925.

[76] Yuan, J.; Liu, R.; Ma, Y.; Zhang, Z.; Xie, Z. Curcumin Attenuates Airway Inflammation and Airway Remolding by Inhibiting NF-κB Signaling and COX2 in Cigarette Smoke-Induced COPD Mice. *Inflammation* 2018, *41*, 1804–1814. https://doi.org/10.1007/s10753-018-0823-6.

[77] Younesian, O.; Kazerouni, F.; Dehghan-Nayeri, N.; Omrani, D.; Rahimipour, A.; Shanaki, M.; Rezapour Kalkhoran, M.; Cheshmi, F. Effect of Curcumin on Fatty Acid Synthase Expression and Enzyme Activity in Breast Cancer Cell Line SKBR3. *Int. J. Cancer Manag.* 2017, *10*, e8173. https://doi.org/10.5812/ijcm.8173.

[78] Chen, J.-W.W.; Kong, Z.-L.L.; Tsai, M.-L.L.; Lo, C.-Y.Y.; Ho, C.-T.T.; Lai, C.-S.S. Tetrahydrocurcumin ameliorates free fatty acid-induced hepatic steatosis and improves insulin resistance in HepG2 cells. *J. Food Drug Anal.* 2018, *26*, 1075–1085. https://doi.org/10.1016/j.jfda.2018.01.005.

[79] Banerjee, P.; Eckert, A.O.; Schrey, A.K.; Preissner, R. ProTox-II: A webserver for the prediction of toxicity of chemicals. *Nucleic Acids Res.* 2018, *46*, W257–W263. https://doi.org/10.1093/nar/gky318.

[80] TA, G.C.; Mokhtar, M.B.; Peterson, P.J.; Yahaya, N. Bin A Comparison of Mandatory and Voluntary Approaches to the Implementation of Globally Harmonized System of Classification and Labelling of Chemicals (GHS) in the Management of Hazardous Chemicals. *Ind. Health* 2011, *49*, 765–773. https://doi.org/10.2486/indhealth.MS1258.

[81] Raina, A.; Chandra, M.; Dogra, T.; Raj, J.; Pahuja, M. Determination of median lethal dose of combination of endosulfan and cypermethrin in wistar rat. *Toxicol. Int.* 2013, *20*, 1. https://doi.org/10.4103/0971-6580.111531.

[82] Daina, A.; Michielin, O.; Zoete, V. SwissADME: A free web tool to evaluate pharmacokinetics, druglikeness and medicinal chemistry friendliness of small molecules. *Sci. Rep.* 2017, *7*, 42717. https://doi.org/10.1038/srep42717.

[83] Iversen, D.B.; Andersen, N.E.; Dalgård Dunvald, A.; Pottegård, A.; Stage, T.B. Drug metabolism and drug transport of the 100 most prescribed oral drugs. *Basic Clin. Pharmacol. Toxicol.* 2022, *131*, 311– 324. https://doi.org/10.1111/bcpt.13780.

[84] Lipinski, C.A.; Lombardo, F.; Dominy, B.W.; Feeney, P.J. Experimental and computational approaches to estimate solubility and permeability in drug discovery and development settings. *Adv. Drug Deliv. Rev.* 2012, *64*, 4–17. https://doi.org/10.1016/j.addr.2012.09.019.

[85] Daina, , A.; Michielin, O.; Zoete, V. SwissTargetPrediction: Updated data and new features for efficient prediction of protein targets of small molecules. *Nucleic Acids Res.* 2019, *47*, W357–W3664. https://doi.org/10.1093/nar/gkz382.

[86] Keiser, M.J.; Roth, B.L.; Armbruster, B.N.; Ernsberger, P.; Irwin, J.J.; Shoichet, B.K. Relating protein pharmacology by ligand chemistry. *Nat. Biotechnol.* 2007, *25*, 197–206. https://doi.org/10.1038/nbt1284.

[87] Hunter, A.D. ACD/ChemSketch 1.0 (freeware); ACD/ChemSketch 2.0 and its Tautomers, Dictionary, and 3D Plug-ins; ACD/HNMR 2.0; ACD/CNMR 2.0. *J. Chem. Educ.* 1997, *74*, 905. https://doi.org/10.1021/ed074p905.

[88] Hanwell, M.D.; Curtis, D.E.; Lonie, D.C.; Vandermeerschd, T.; Zurek, E.; Hutchison, G.R. Avogadro: An advanced semantic chemical editor, visualization, and analysis platform. *J. Cheminform.* 2012, *4*, 17. https://doi.org/10.1186/1758-2946-4-17/FIGURES/14.

[89] Burley, S.K.; Bhikadiya, C.; Bi, C.; Bittrich, S.; Chao, H.; Chen, L.; Craig, P.A.; Crichlow, G.V.; Dalenberg, K.; Duarte, J.M.; et al. RCSB Protein Data bank: Tools for visualizing and understanding biological macromolecules in 3D. *Protein Sci.* 2022, *31*, e4482. https://doi.org/10.1002/pro.4482.

[90] Yang, , Z.; Lasker, K.; Schneidman-Duhovny, D.; Webb, B.; Huang, C.C.; Pettersen, E.F.; Goddard, T.D.; Meng, E.C.; Sali, A.; Ferrin, T.E. UCSF Chimera, MODELLER, and IMP: An integrated modeling system. *J. Struct. Biol.* 2012, *179*, 269–278. https://doi.org/10.1016/j.jsb.2011.09.006.

[91] Binkowski, T.A.; Naghibzadeh, S.; Liang, J. CASTp : Computed Atlas of Surface Topography of proteins. *Nucleic Acids Res.* 2003, *31*, 3352–3355. https://doi.org/10.1093/nar/gkg512.

[92] Verdonk, M.L.; Cole, J.C.; Hartshorn, M.J.; Murray, C.W.; Taylor, R.D. Improved protein-ligand docking using GOLD. *Proteins* 2003, *52*, 609–623. https://doi.org/10.1002/prot.10465.

[93] Nair, P.C.; Miners, J.O. Molecular dynamics simulations: From structure function relationships to drug discovery. *Silico Pharmacol.* 2014, *2*, 4. https://doi.org/10.1186/s40203-014-0004-8.

[94] Bitencourt-Ferreira, G.; de Azevedo, W.F. Molegro Virtual Docker for Docking. *Methods Mol. Biol.* 2019, *2053*, 149–167. https://doi.org/10.1007/978-1-4939-9752-7_10.

[95] Laskowski, R.A.; Swindells, M.B. LigPlot+: Multiple ligand-protein interaction diagrams for drug discovery. *J. Chem. Inf. Model.* 2011, *51*, 2778–2786. https://doi.org/10.1021/ci200227u.

[96] Ylilauri, M.; Pentikäinen, O.T. MMGBSA as a tool to understand the binding affinities of filaminpeptide interactions. *J. Chem. Inf. Model.* 2013, *53*, 2626–2633. https://doi.org/10.1021/ci4002475.

[97] Wang, L. *Molecular Dynamics—Studies of Synthetic and Biological Macromolecules*; Wang, L., Ed.; InTech: Rijeka, Croatia, 2012. https://doi.org/10.5772/2652.

[98] Seifert, E. OriginPro 9.1: Scientific Data Analysis and Graphing Software—Software Review. *J. Chem. Inf. Model.* 2014, *54*, 1552. https://doi.org/10.1021/CI500161D.

[99] Systèmes, D. BIOVIA Discovery Studio Dassault. In *Dassault Systèmes BIOVIA, Discovery Studio Visualizer, 21.1.0.20298*; 2021. Available online: https://discover.3ds.com/discovery-studio-visualizerdownload (accessed on 7 July 2023).

[100] Wallace, A.C.; Laskowski, R.A.; Thornton, J.M. Ligplot: A program to generate schematic diagrams of protein-ligand interactions. *Protein Eng. Des. Sel.* 1995, *8*, 127–134. https://doi.org/10.1093/protein/8.2.127.

Disclaimer/Publisher's Note: The statements, opinions and data contained in all publications are solely those of the individual author(s) and contributor(s) and not of MDPI and/or the editor(s). MDPI and/or the editor(s) disclaim responsibility for any injury to people or property resulting from any ideas, methods, instructions or products referred to in the content.

CHAPTER 5

Chapter outline:

This chapter describes *in vitro* bioactivity testing of curcumin and the three synthetic curcumin derivatives (1A6, 1A8, and 1B8) in 3T3-L1 adipocytes. This chapter is based on the last two objectives of this research study.

Introduction

Over the past decades, the prevalence of obesity has rapidly increased, presenting a significant global health concern [1]. Obesity has profound implications for morbidity and premature mortality rates worldwide and is associated with the increased risk of developing chronic diseases such as T2D, CVDs, and various cancers [1]. Central to the pathogenesis of obesity is abnormal adipose tissue function which is characterized by dysregulated lipid metabolism and chronic low-grade inflammation, processes that contribute to the development of metabolic complications such as insulin resistance [2]. Hence, targeting adipose tissue through various therapeutic strategies can present a potential for combating obesity and its associated metabolic complications. Current obesity intervention strategies include lifestyle modifications (reduced caloric consumption and increased physical activity), pharmaceutical drugs, and bariatric surgery [3,4]. Despite the significant progress in understanding obesity and developing treatment strategies, there are limitations associated with the current approaches to managing obesity. These include long-term success, treatment adherence, accessibility, and adverse effects [5,6]. As a result, there is an urgent need for innovative, safe, and effective therapeutic alternatives to combat obesity and its related metabolic disorders. A promising avenue of research involves exploring natural compounds such as curcumin as potential anti-obesity agents.

Curcumin, a bioactive polyphenolic compound derived from the rhizome of turmeric (*Curcuma longa*), has garnered scientific interest for its diverse pharmacological properties [7]. Numerous pre-clinical and clinical studies have highlighted the anti-obesity potential of curcumin, particularly with adipose tissue as a potential therapeutic target [8]. Specifically, studies have demonstrated the ability of curcumin to ameliorate inflammation, modulate lipid metabolism, and improve insulin sensitivity in adipose tissue [9–12]. Despite its widely recognized anti-obesity potential, the clinical application of curcumin as an anti-obesity drug is impeded by challenges such as low solubility in aqueous solvents, instability in aqueous conditions, poor bioavailability, and limited absorption and cellular uptake [13]. To overcome these limitations and enhance its biological efficacy, structural modifications of curcumin through the synthesis of curcumin-based derivatives present a potential solution. In this study, we aimed to evaluate the effects of curcumin and the three synthetic curcumin derivatives (1A6, 1A8, and 1B8) on ameliorating dysregulated lipid metabolism and chronic low-grade inflammation in adipocytes. This was done by assessing the effects of curcumin, 1A6, 1A8, and 1B8 on cell viability, lipolysis, lipid accumulation, and adipocytokine secretion in 3T3-L1 adipocytes treated with a combination of tumor necrosis factor alpha

(TNFα), lipopolysaccharide (LPS) and palmitic acid (PA). Moreover, the effects of curcumin, 1A6, 1A8, and 1B8 on the expression of genes involved in lipid metabolism and inflammation were assessed in this study.

Materials and methods

Cell culture and differentiation

Mouse 3T3–L1 embryonic fibroblasts (preadipocytes) were obtained from the American Type Culture Collection and were cultured in growth media containing Dulbecco's Modified Eagle Medium (DMEM) supplemented with 10% fetal bovine serum (FBS) in T75 flasks at 37°C in humidified air with 5% CO_2, and the cells were then subsequently sub-cultured with medium refreshed every 2 days. For assay purposes, 3T3–L1 preadipocytes were seeded in 96- (4×10^3 cells/well), 24- (2×10^4 cells/well), and 6- (6.0×10^4 cells/well) multi-well plates and cultured in growth medium until they reached 100% confluence. Fully confluent 3T3–L1 preadipocytes were then differentiated into matured 3T3–L1 adipocytes as previously described [14–17]. Briefly, on day 0, cells were incubated in adipocyte differentiation medium (ADM) containing DMEM media supplemented with 10% FBS, 0.5 mM 3-isobutyl-1-methylxanthine (IBMX), 1 μg/mL insulin, and 1 μM dexamethasone for 72 hours. After 72 hours (day 3), ADM was substituted with adipocyte maintenance medium (AMM) consisting of DMEM, 10% FBS, and 1 μg/mL insulin, and the cells were incubated for 48 hours. After 48 hours (day 5), AMM was replaced with growth media, and the cells were cultured for 3 days until fully differentiated 3T3–L1 adipocytes were obtained on day 8 (observed using the Olympus inverted light microscope).

Treatment

The ameliorative effect of curcumin and the three synthetic curcumin derivatives (1A6, 1A8, and 1B8) on lipid metabolism and inflammation was evaluated in 3T3–L1 adipocytes treated with a combination of TNFα, LPS, and PA. Briefly, mature 3T3–L1 adipocytes (on day 8) were washed with DPBS, and treated with TNFα (10 ng/mL), LPS (100 ng/mL), and PA (0.75 mM) combination for 24 hours as previously described [14] to induce an *in vitro* adipocyte model of dysregulated lipid metabolism and inflammation. Treatments were prepared fresh in treatment medium (phenol red-free DMEM containing 25 mM glucose, 3.7 g/L sodium bicarbonate, and 2% fatty acid-free bovine serum albumin). Cells were then treated for another 24 hours with curcumin, 1A6, 1A8, and

1B8 at 1.25, 2.5, 5, 10, 20, and 40 μM (for cell viability and lipolysis assays) or optimal doses of 10 and 20 μM (for lipid accumulation, adipokine secretion assays, and gene expression analysis) in the presence or absence of

TNFα (10 ng/mL), LPS (100 ng/mL), and PA (0.75 mM) combination. The cells were also treated with the positive controls, CL-316,243 (10 μM) and metformin (1 μM). In addition, the untreated group (treatment media only) and the model group (TNFα, LPS, and PA in treatment media) were used as controls.

Metabolic activity

The effects of curcumin, 1A6, 1A8, and 1B8 on the cell's metabolic activity were assessed by quantifying the intracellular adenosine triphosphate (ATP) content using the ViaLight™ plus cell proliferation and cytotoxicity bioassay kit as per the manufacturer's instructions with minor modifications. Following treatments, cells were rinsed with DPBS (pre-warmed), and the 96-well plate was allowed to cool at room temperature. Subsequently, cells were incubated at room temperature for at least 10 minutes with an ATP cell lysis reagent diluted with DPBS (2-fold dilution). The cell lysate was then thoroughly mixed by shaking the plate at 60 rpm for 5 minutes at room temperature and then 100 μL of the cell lysate was transferred to a 96-well luminescence compatible plate (whitewalled and clear bottom). One hundred microliters volume of the ATP standards (10, 8, 6, 4, 2, 0 μM concentrations) prepared in DPBS were also transferred to the 96-well luminescence plate in duplicate. A reconstituted ATP monitoring reagent plus (100 μL) was added to the cell lysate and standards, and the plate was incubated for 2 minutes at room temperature (protected from light). Luminescence was measured on a SpectraMax® i3x Multi-Mode Microplate reader using the SoftMax Pro 7 Software (Molecular Devices, San Jose, California, United States). Intracellular ATP content was derived from the standard curve and the results were expressed as a percentage relative to the untreated control cells set to 100%.

Lipolysis

The effects of curcumin and the three synthetic curcumin derivatives (1A6, 1A8, and 1B8) on lipolysis were assessed by quantifying glycerol secretion in the cell culture supernatant using the Glycerol assay kit, based on the manufacturer's instructions [14]. In brief, the glycerol standard curve was prepared with 0 mM, 0.3 mM, 0.6 mM, and 1.0 mM concentrations. Thereafter, 10 μL of the standards and the undiluted samples were incubated with 100 μL of the reaction master mix for 20 minutes at room temperature. This facilitates a coupled enzyme reaction involving glycerol kinase and glycerol phosphate oxidase that leads to the formation of a calorimetric product proportional to the quantity of glycerol present in the sample. Thereafter, absorbance was measured at a wavelength of 570 nm using the SpectraMax® i3x Multi-Mode Microplate reader and SoftMax Pro 7 Software

(Molecular Devices). Glycerol concentrations (expressed as mM) in the samples were calculated from the standard curve.

Lipid accumulation

The effects of curcumin, 1A6, 1A8, and 1B8 on intracellular lipid accumulation were evaluated using the Oil Red O (ORO) staining as previously reported [14–17]. After treatment, cells were washed with 500 µL of PBS and then fixed using 200 µL of 10 % (v/v) neutral buffered formalin for 15 – 30 minutes at room temperature. The neutral buffer was removed, and cells were washed with 500 µL of PBS. This was followed by staining the cells by adding 200 µL of 0.7% (v/v) ORO working solution for 30 minutes at room temperature. The ORO working solution was prepared by diluting 1% (w/v) of ORO stock solution (prepared in 100% 2-propanol) with distilled water. After staining, cells were washed three times with 400 µL of distilled water, to remove any unbound ORO dye. The Nikon Eclipse Ti inverted microscope and NIS-Elements imaging software (Nikon, Japan) were used for capturing images of ORO-stained cells (minimum of 5 fields per well) using a 20× objective. Thereafter, lipid accumulation was quantified by eluting the ORO dye retained by the cells using 200 µL of 100% 2-propanol and measuring optical density (OD) at 510 nm using the SpectraMax® i3x Multi-Mode Microplate reader and SoftMax Pro 7 Software (Molecular Devices). Lipid content was normalized to cell density (Figure S2), which was quantified using the crystal violet (CV) staining (measured at OD_{570} nm) as previously described [14–17]. Briefly, the wells of the ORO-stained cells were washed with 500 µL of 70% ethanol. Subsequently, the wells were washed and dried, followed by the addition of 400 µL of CV working solution to each well. They were then incubated for 5 minutes at room temperature. The CV was aspirated, and the wells were washed three times with PBS. The CV stain was extracted using 70% ethanol, and 100 µL of CV stain was transferred to a microassay plate. Finally, the OD of the CV stain was read at 570 nm using the SpectraMax® i3x Multi-Mode Microplate reader and SoftMax Pro 7 Software (Molecular Devices). Lipid accumulation was then presented as a percentage relative to the untreated control cells set to 100%.

Messenger RNA (mRNA) gene expression

The effects of curcumin and the three synthetic curcumin derivatives (1A6, 1A8, and 1B8) on the mRNA expression of genes involved in lipid metabolism and inflammation were assessed by quantitative reverse transcription-polymerase chain reaction (qRT-PCR). After treatment, total RNA was extracted from 3T3–L1 adipocytes using the Qiazol lysis reagent and purified using the RNeasy Mini kit, according to the manufacturer's

recommendations (Qiagen). RNA concentration and purity were assessed using the NanoDrop One/One^{C} microvolume UV-Vis Spectrophotometer (ThermoFisher Scientific, Waltham, Massachusetts, United States), by measuring absorbance at a wavelength of 260 nm (A260) and 280 nm (A280). The High-Capacity Reverse Transcription kit (Applied Biosystems) was used to generate complementary DNA (cDNA) from 1 µg of RNA, following the manufacturer's instructions. Thereafter, the Taqman® gene expression assays (Table 5.1) and the TaqMan™ fast advanced master mix were used to amplify the synthesized cDNA and measure the transcription of genes (Table 5.1) using the QuantStudio™ 7 Flex Real-Time PCR System (Applied Biosystems). The relative standard curve quantification method was then used to calculate the transcription levels of genes and the relative expression levels were normalized to the average of two house-keeping genes, beta 2 microglobulin (*B2m*) and ribosomal protein L13a (*Rpl13a*) (Table S1).

Table 5.1: Taqman gene probes used in this study.

Taqman gene expression assays	**Assay ID**	**Role**
Peroxisome proliferator-activated receptor gamma (*Pparγ*)	Mm00440940_m1	Lipid metabolism
Acetyl-CoA carboxylase alpha (*Acaca*)	Mm01304258_m1	Lipid metabolism
Fatty acid synthase (*Fasn*)	Mm00662319_m1	Lipid metabolism
Glycogen synthase kinase 3-beta (*Gsk3β*)	Mm00444911_m1	Lipid metabolism
Sterol regulatory element-binding transcription factor 1 (*Srebf1*)	Mm00550338_m1	Lipid metabolism
Patatin-like phospholipase domain-containing protein 2 (*Pnpla3/Atgl*)	Mm00503040_m1	Lipid metabolism
Lipase (*Lipe/Hsl*)	Mm00495359_m1	Lipid metabolism
Lipoprotein lipase (*Lpl*)	Mm00434764_m1	Lipid metabolism
Mitogen-activated protein kinase 14 (*Mapk14*)	Mm01301009_m1	Inflammation
Signal transducer and activator of transcription 3 (*Stat3*)	Mm01219775_m1	Inflammation
Cyclooxygenase 2 *(Ptgs2/Cox2)*	Mm00478374_m1	Inflammation
Adiponectin (*AdipoQ*)	Mm04933656_m1	Inflammation
Interleukin 6 (*Il-6*)	Mm00446190_m1	Inflammation
Chemokine (C-C motif) ligand 2 (*Ccl2/Mcp1*)	Mm00441242_m1	Inflammation
Beta 2 microglobulin (*B2m*)	Mm00437760_m1	Housekeeping
Ribosomal protein L13a (*Rpl13a*)	Mm05910660_g1	Housekeeping

Adipokine secretion

The effects of curcumin, 1A6, 1A8, and 1B8 on adipokine secretion were assessed by quantifying interleukin 6 (IL-6) and Adiponectin (ADIPOQ) secreted levels in the cell culture supernatant using the DuoSet® ELISA kits (R&D Systems), as per manufacturer's instructions [14]. Briefly, the 96-well ELISA plates were coated with 100 µL of rat anti-mouse IL-6 and ADIPOQ capture antibodies overnight at room temperature. The following day, the capture antibodies were removed, and the wells were thoroughly rinsed thrice with a wash buffer, followed by

blocking the wells with the reagent diluent at room temperature for a minimum of 1 hour. Subsequently, 100 µL of the standards and cell culture supernatants (undiluted samples for IL-6 and 1:200 diluted samples for ADIPOQ) in duplicate were allowed to bind to the ELISA-coated plates for 2 hours at room temperature. Thereafter, 100 µL of biotinylated goat anti-mouse IL-6 and ADIPOQ detection antibodies were added to their respective plates, and the plates were incubated at room temperature for 2 hours. One hundred microliters of streptavidin horseradish peroxidase (HRP) working dilutions (1:40 dilution for IL-6 and 1:200 dilution for ADIPOQ) were then added to their respective plates and incubated for 20 minutes at room temperature (away from light). This was followed by incubating the plates for another 20 minutes at room temperature (protected from) with 100 µL of the substrate solution. The ELISA reaction was stopped by adding 50 µL of the stop solution, absorbance was measured at 450 nm and 540 nm on a SpectraMax® i3x Multi-Mode Microplate reader using the SoftMax Pro 7 Software (Molecular Devices). The absorbance readings at 540 nm were subtracted from the absorbance readings at 450 nm to correct for optical imperfections in the plate. Thereafter, the standard curve was constructed and used to calculate the secreted levels of IL-6 and ADIPOQ in pg/mL concentration.

Data and statistical analysis

Data presented in this study were captured and analyzed using Microsoft® Excel® for Microsoft 365 (Microsoft Corporation, Redmond, Washington, United States). The results are presented as the mean ± standard error of the mean (SEM) of three independent experiments, each conducted in triplicate or more. Statistical analysis was performed using GraphPad Prism software (Graph Pad Software Inc. V7.03, San Diego, California, United States). For normally distributed data (determined by the Shapiro-Wilk test), statistical significance between groups was determined using the one-way analysis of variance (ANOVA) followed by Dunnett's multiple comparisons posttest. In cases where data was not normally distributed (determined by the Shapiro-Wilk test), the Kruskal-Wallis test was used, followed by Dunn's multiple comparisons post-hoc test. A p-value of < 0.05 was considered statistically significant.

Results

The effects of curcumin and the three synthetic curcumin derivatives on metabolic activity

The dose-dependent (1.25, 2.5, 5, 10, 20, and 40 µM) effects of curcumin and the three synthetic curcumin derivatives (1A6, 1A8, and 1B8) on the cell's metabolic activity were assessed by quantifying intracellular ATP

content in 3T3–L1 adipocytes with the combination of TNFα (10 ng/mL), LPS (100 ng/mL), and PA (0.75 mM). Compared to the untreated control cells (100 ± 5.80%), the ATP content was reduced by 53% (46.98 ± 4.43%, p < 0.0001) in cells treated with the combination of TNFα, LPS, and PA (model control) (Figure 5.1A-C). The ATP content was further reduced by 21.2% (30.54 ± 2.16%, p<0.05), 42.8% (18.81 ± 0.62%, p<0.01), and 44.5% (18.00 ± 3.48%, p<0.01) in cells treated with curcumin, 1A6, and 1A8 at 40 µM when compared to the model control (Figure 5.1A-C). Meanwhile, treatment with curcumin, 1A6, and 1A8 at 1.25, 2.5, 5, 10, and 20 µM had no effects on the ATP content when compared to the model control. Interestingly, treatment with 1B8 at all tested concentrations had no significant effect on the ATP content when compared to the model control (Figure 5.1C). Similarly, treatment with metformin (1 µM) and CL-316,243 (10 µM) had no effects compared to the model control (Figure 5.1A-C).

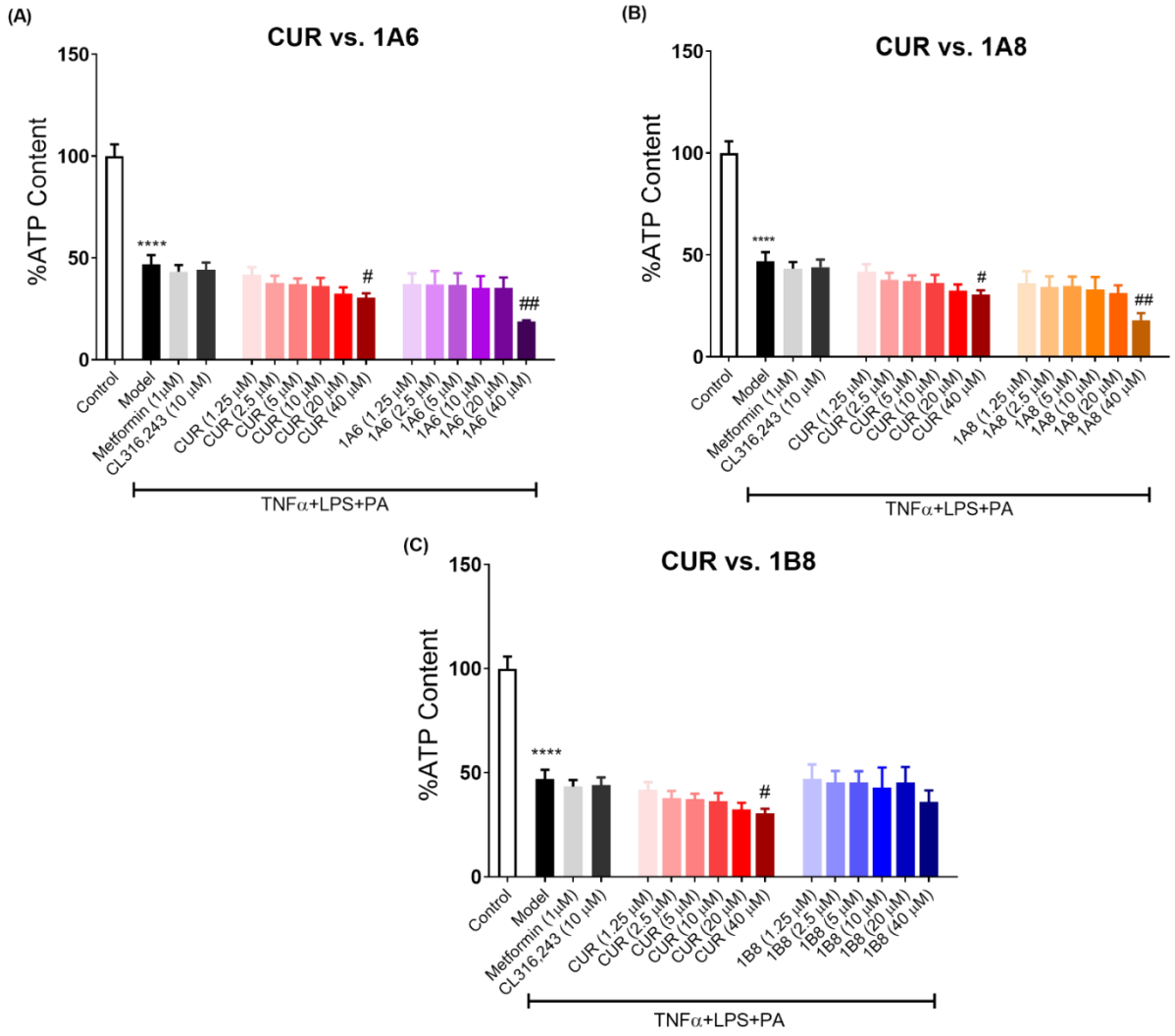


Figure 5.1: The effects of curcumin and the three curcumin derivatives (1A6, 1A8, and 1B8) on the metabolic activity of 3T3–L1 adipocytes co-treated with TNFα, LPS, and PA combination. Differentiated 3T3–L1

adipocytes were induced with TNFα (10 ng/mL), LPS (100 ng/mL), and PA (10 mM) combination (model) or left untreated (control) for 24 hours. Thereafter, the cells were treated with curcumin (CUR), 1A6 (A), 1A8 (B), and 1B8 (C) at 1.25, 2.5, 5, 10, 20, and 40 μM, metformin (1 μM), and CL-316,243 (10 μM) in the presence of TNFα, LPS, and PA combination for 24 hours. Metabolic activity was assessed by measuring ATP content using a commercial assay kit. The results are expressed as a percentage relative to the untreated control cells (set at 100%) and are shown as mean ± standard error of the mean (SEM) for three independent experiments. Statistical significance is depicted as ****p<0.0001 vs. the untreated control cells; $^{\#}p$<0.05 and $^{\#\#}p$<0.01 vs. the model control.

The effects of curcumin, 1A6, 1A8, and 1B8 on lipolysis

The dose-dependent (1.25, 2.5, 5, 10, 20, and 40 μM) effects of curcumin and the three synthetic curcumin derivatives (1A6, 1A8, and 1B8) on lipolysis were assessed by quantifying glycerol secretion in 3T3–L1 adipocytes induced with the combination of TNFα (10 ng/mL), LPS (100 ng/mL), and PA (0.75 mM). The results showed that glycerol secretion was significantly increased by 898.46% (0.519 ± 0.028 mM, p<0.0001) in cells treated with the combination of TNFα, LPS, and PA (model control) compared to the untreated control cells (0.05 ± 0.003 mM) (Figure 5.2A-C). Meanwhile, treatment with metformin (1 μM) and CL-316,243 (10 μM) did not affect glycerol release in comparison to the model control (Figure 5.2A-C). Curcumin exhibited a significant reduction in glycerol secretion at 5 μM (21.7%, 0.406 ± 0.025 mM, p<0.05), 10 μM (21.58%, 0.407 ± 0.027 mM, p<0.05), and 20 μM (29.54%, 0.3654 ± 0.024, p<0.01) compared to the model control (Figure 5.2A-C). Treatment with 1A6 reduced glycerol secretion by 29.73% (0.364 ± 0.033 mM, p<0.01), 24.80% (0.390 ± 0.034 mM, p<0.05), 29.95% (0.363 ± 0.037 mM, p<0.01), and 25.65% (0.386 ± 0.034 mM, p<0.05) at 2.5, 5, 10, and 20 μM when compared to the model control (Figure 5.2A). In addition, 1A8 reduced glycerol secretion by 28.87% (0.369 ± 0.021 mM, p<0.05) and 31.66% (0.354 ± 0.026 mM, p<0.05) at 2.5 and 10 μM compared to the model control (Figure 5.2B). In contrast, treatment with 1B8 had no significant effect on glycerol secretion at all tested concentrations when compared to the model control (Figure 5.2B).

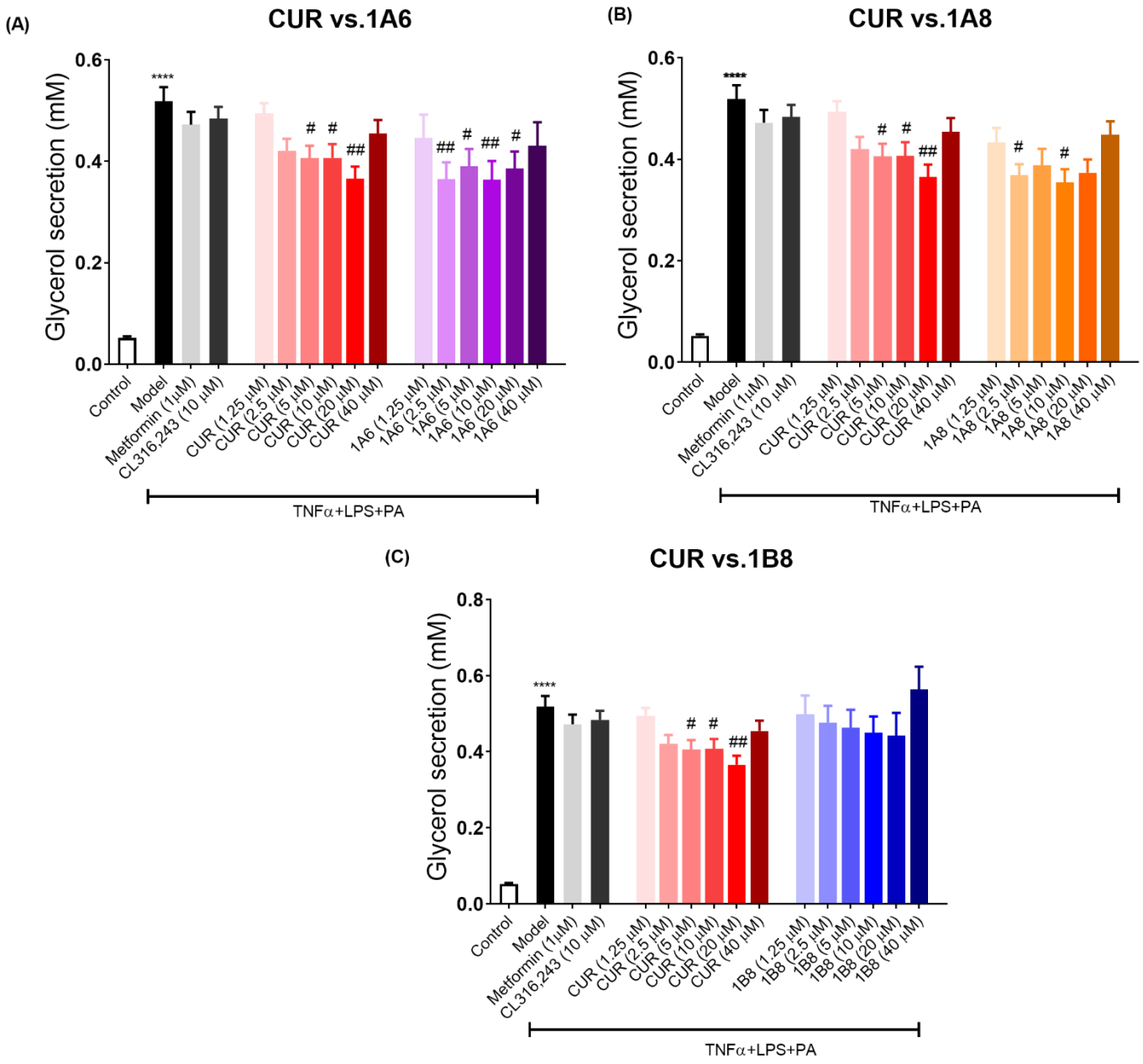


Figure 5.2: The effects of curcumin and the three curcumin derivatives (1A6, 1A8, and 1B8) on lipolysis in 3T3–L1 adipocytes induced with TNFα, LPS, and PA combination. Differentiated 3T3–L1 adipocytes were treated with TNFα (10 ng/mL), LPS (100 ng/mL), and PA (10 mM) combination (model) or left untreated (control) for 24 hours. Thereafter, the cells were treated with curcumin (CUR), 1A6 (A), 1A8 (B), and 1B8 (C) at 1.25, 2.5, 5, 10, 20, and 40 μM, metformin (1 μM), and CL-316,243 (10 μM) in the presence of TNFα, LPS, and PA combination for 24 hours. Lipolysis was assessed by quantifying glycerol secretion using a commercial assay kit. The results are expressed as mM concentration and are shown as mean ± standard error of the mean (SEM) for three independent experiments. Statistical significance is depicted as ****$p<0.0001$ vs. the untreated control cells; $^{\#}p<0.05$ and $^{\#\#}p<0.01$ vs. the model control.

The effects of curcumin and the three synthetic curcumin derivatives on lipid accumulation

The two optimal doses of curcumin, 1A6, 1A8, and 1B8 (10 and 20 μM) selected based on the ATP content and glycerol release data were evaluated for their effects on lipid accumulation in 3T3–L1 adipocytes co-treated with TNFα (10 ng/mL), LPS (100 ng/mL), and PA (0.75 mM) combination using the ORO staining. Compared to the untreated control cells (100 ± 8.151%), lipid accumulation was significantly reduced by 28.41% (71.59 ± 2.881%, $p<0.05$) in cells treated with the combination of TNFα, LPS, and PA (model control) (Figure 5.3A, B). In contrast, treatment with metformin (1 μM) and CL-316,243 (10 μM) increased lipid accumulation by 40.3% (100.5 ± 5.954%, $p<0.05$) and 46.67% (105 ± 4.329%, $p<0.01$), respectively when compared to the model control (Figure 5.3A, B). Similarly, treatment with curcumin at 10 and 20 μM resulted in a significant increase in lipid accumulation by 51.56% (108.5 ± 5.058%, $p<0.0001$) and 40.66% (100.7 ± 6.673%, $p<0.01$), respectively compared to the model control (Figure 5.3A, B). The two chloro curcumin derivatives, 1A6 and 1A8 also increased lipid accumulation at both concentrations (10 and 20 μM), but this was not significant compared to the model control (Figure 5.3A, B). In addition, 1B8 significantly increased lipid content at 10 and 20 μM by 66.76% (119.4 ± 8.091%, $p<0.01$) and 66.76% (119.4 ± 10.22%, $p<0.001$), respectively compared to the model control (Figure 5.3A, B).

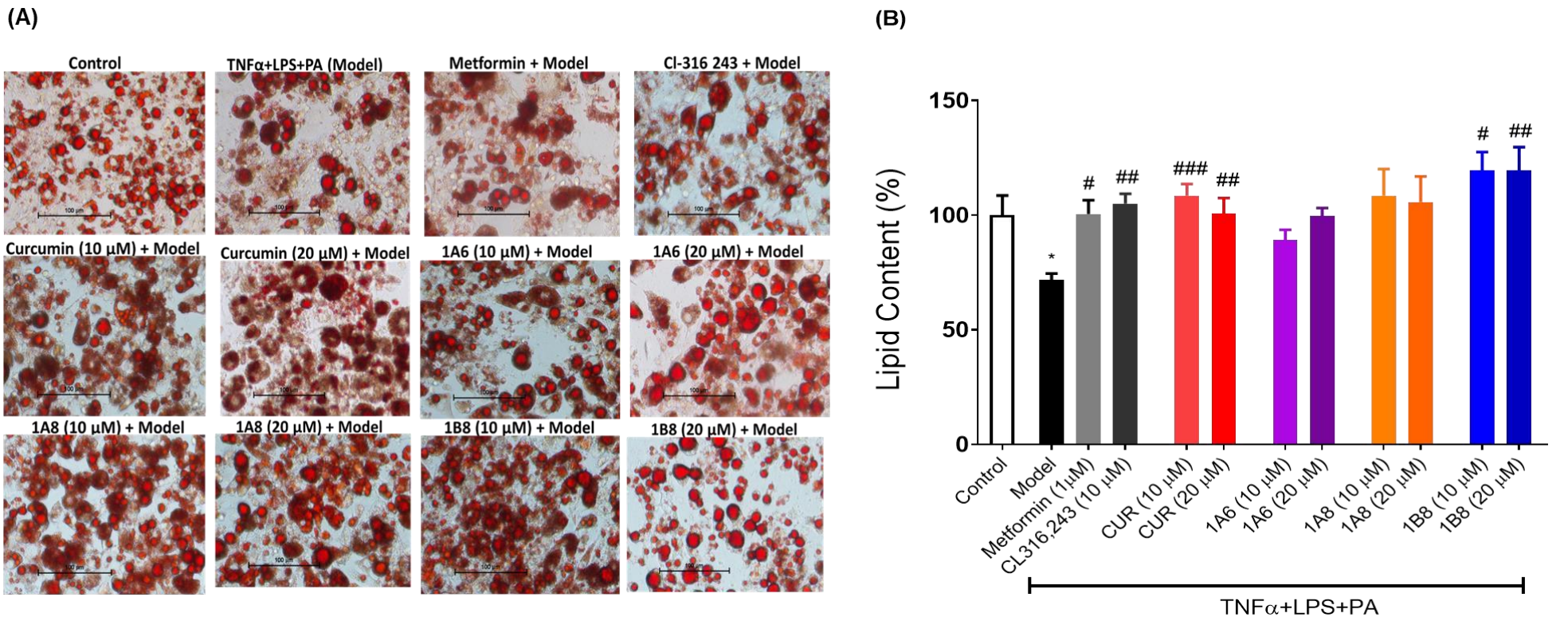


Figure 5.3: The effects of curcumin and the three curcumin derivatives (1A6, 1A8, and 1B8) on lipid accumulation in 3T3–L1 adipocytes induced with TNFα, LPS, and PA combination. Differentiated 3T3–L1 adipocytes were treated with TNFα (10 ng/mL), LPS (100 ng/mL), and PA (10 mM) combination (model) or left untreated (control) for 24 hours. Thereafter, the cells were treated with curcumin (CUR), 1A6, 1A8, and 1B8 at 10 and 20 µM, metformin (1 µM), and CL-316,243 (10 µM) in the presence of TNFα, LPS, and PA combination for 24 hours. Intracellular lipid content was quantified using (A) Oil Red O staining and (B) imaging. The results are expressed as a percentage relative to the untreated control cells (set at 100%) and are shown as mean ± standard error of the mean (SEM) for three independent experiments. Oil Red O-stained images

were captured using the Nikon Eclipse Ti inverted microscope and NIS Elements imaging software at 20× magnification. Statistical significance is depicted as *$p<0.05$ vs. the untreated control cells; $^{\#}p<0.05$, $^{\#\#}p<0.01$, and $^{\#\#\#}p<0.01$ vs. model control.

The effects of curcumin, 1A6, 1A8, and 1B8 on mRNA gene expression levels

The effect of curcumin and the three curcumin derivatives (1A6, 1A8, and 1B8) on the mRNA expression of genes involved in lipid metabolism and inflammation was investigated in 3T3–L1 adipocytes induced with TNFα, LPS, and PA using quantitative reverse transcription-polymerase chain reaction (qRT-PCR) (PCR amplification efficiencies, Table S1). Compared to the untreated control, the mRNA expression of hormone-sensitive lipase (*Lipe* or *Hsl*) was decreased 3.9-fold ($p<0.01$) in cells treated with the combination of TNFα, LPS, and PA (model control), while no effect was observed in the mRNA expression levels of *Lipe* in cells treated with metformin (1 μM), CL-316,243 (10 μM), as well as curcumin, 1A6, 1A8, and 1B8 at 10 and 20 μM compared to the model control (Figure 5.4A). Although not statistically significant, treatment with the combination of TNFα, LPS, and PA (model control) reduced patatin-like phospholipase domain containing 2 (*Pnpla3* or *Atgl*) mRNA expression levels 2.1-fold ($p=0.170$) compared to untreated control cells (Figure 5.4B). In addition, *Pnpla3* mRNA expression was increased 1.9-fold ($p=0.297$), 1.6-fold ($p=0.760$), 0.9-fold ($p=0.409$), and 2.0-fold ($p<0.05$) in cells treated with 20 μM curcumin, 1A6, 1A8, and 1B8, respectively when compared to the model control (Figure 5.4B).

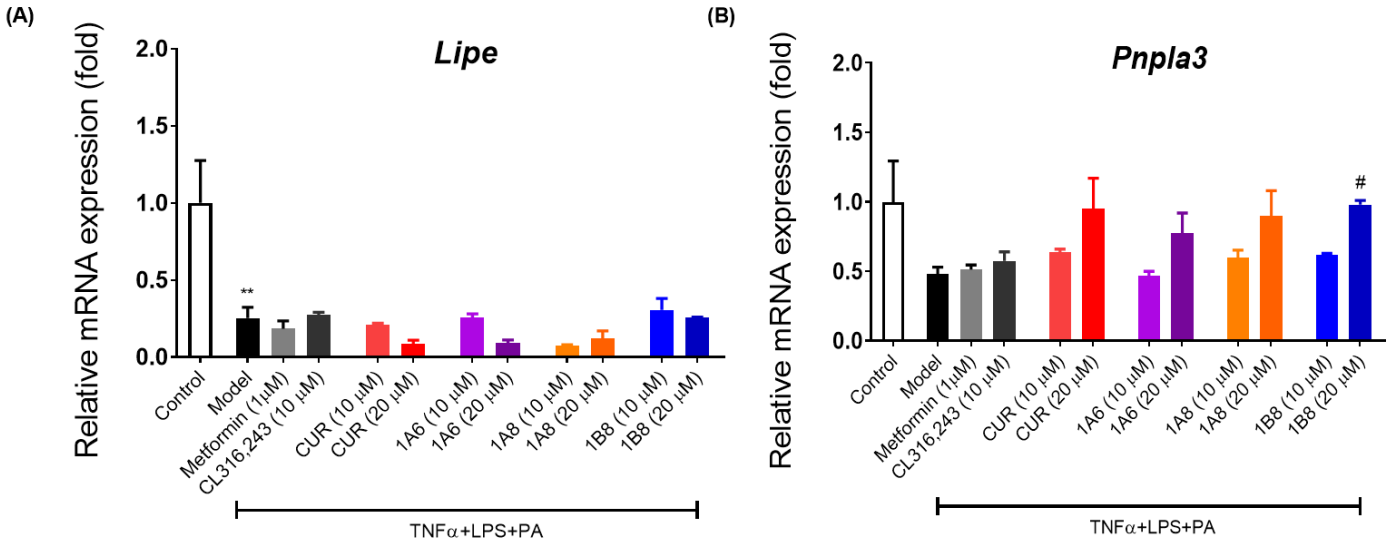


Figure 5.4: The effects of curcumin and the three curcumin derivatives (1A6, 1A8, and 1B8) on the mRNA expression of *Lipe* (A) and *Pnpla3* (B) in 3T3–L1 adipocytes induced with TNFα, LPS, and PA combination. Differentiated 3T3–L1 adipocytes were treated with TNFα (10 ng/mL), LPS (100 ng/mL), and PA (10 mM) combination (model) or left untreated (control) for 24 hours. Thereafter, the cells were treated with curcumin (CUR), 1A6, 1A8, and 1B8 at 10 and 20 μM, metformin (1 μM), and CL-316,243 (10 μM) in the presence of TNFα, LPS, and PA combination for 24 hours. Gene expression was quantified using qRT-PCR and the expression

was normalized to the average of *Rpl13a* and *B2m* and represented as fold changes. Statistical significance is depicted as $^{**}p<0.01$ vs. the untreated control cells; $^{\#}p<0.05$ vs. the model control.

Additionally, qRT-PCR was used to quantify the mRNA expression of genes involved in lipid metabolism. Compared to the untreated control, the relative mRNA expression of peroxisome proliferator-activated receptor gamma (*Pparγ*) was reduced 4-fold ($p<0.0001$) and the relative mRNA expression of sterol regulatory element binding transcription factor 1 (*Srebf1*) was reduced 2.0-fold ($p<0.01$) in the model control (Figure 5.5A, B). Treatment with metformin (1 μM), CL-316,243 (10 μM), as well as curcumin, 1A6, 1A8, and 1B8 at 10 and 20 μM did not affect *Pparγ* and *Srebf1* expression when compared to the model control (Figure 5.5A, B). Compared to the untreated control, the relative mRNA expression of acetyl-coA carboxylase alpha (*Acaca*) was reduced 1.4fold ($p=0.163$) in the model control, while the relative mRNA expression of fatty acid synthase (*Fasn*) was reduced 4.1-fold ($p<0.001$) in the model control (Figure 5.5C, D). The mRNA expression of *Acaca* was further reduced 2.3-fold ($p<0.05$) in cells treated with 20 μM 1A6, meanwhile, the expression of *Fasn* was further reduced in cells treated with 10 μM curcumin (2.4-fold, $p<0.05$), 10 μM 1A6 (3.0-fold, $p<0.05$), 20 μM 1A6 (3.0-fold, $p<0.05$), 10 μM 1A8 (3.0-fold, $p<0.05$), and 20 μM 1A8 (3.2-fold, $p<0.05$) when compared to the model control (Figure 5.5C, D). Treatment with metformin (1 μM), CL-316,243 (10 μM), and 1B8 (10 and 20 μM) did not affect *Pparγ* and *Srebf1* expression when compared to the model control (Figure 5.5C, D). Furthermore, the relative mRNA expression of lipoprotein lipase (*Lpl*) was decreased 2.7-fold ($p<0.0001$) in the model control, while glycogen synthase kinase 3-beta (*Gsk3β*) mRNA was reduced 4.0-fold ($p<0.01$) in the model control (Figure 5.5E, F). Treatment with metformin (1 μM), CL-316,243 (10 μM), as well as curcumin, 1A6, 1A8, and 1B8 at 10 and 20 μM did not affect the relative mRNA expression levels of *Lpl* and *Gsk3β* when compared to the model control (Figure 5.5E, F).

The results also showed that treatment with the combination of TNFα, LPS, and PA (model control) reduced adiponectin (*AdipoQ*) mRNA expression by 6.9-fold ($p<0.0001$) compared to the untreated control, while the mRNA expression of interleukin 6 (*Il-6*) was increased 5.3-fold ($p < 0.05$) in the model control when compared to the untreated control (Figure 5.6A, B). The relative mRNA expression level of *AdipoQ* and *Il-6* was not affected by treatment with metformin (1 μM), CL-316,243 (10 μM), as well as curcumin, 1A6, 1A8, and 1B8 at 10 and 20 μM when compared to the model control, although treatment with CL-316,243 (10 μM) further increased *Il-6* mRNA expression (1.9-fold, $p<0.05$) when compared to the model control (Figure 5.6A, B). In addition, the mRNA expression of monocyte chemoattractant protein 1 (*Mcp1* or *Ccl2*) was increased 7.0-fold ($p<0.01$) in the

model control when compared to the untreated control, and treatment with curcumin and 1A8 at 10 μM further increased *Mcp1* expression by 1.8-fold (p<0.01) and 1.7-fold (p<0.05) when compared to the model control (Figure 5.6C). As illustrated in Figure 5.6D, co-treatment with TNFα, LPS, and PA combination (model control) resulted in a significant increase (23.2-fold, p<0.01) in the mRNA expression of cyclooxygenase 2 (*Cox2* or *Ptgs2*) when compared to the untreated control. In contrast, the mRNA expression of *Cox2* was reduced in cells treated with 10 μM curcumin (5.0-fold, p<0.05), 20 μM curcumin (4.6-fold, p<0.05), 10 μM 1A6 (4.6-fold, p<0.05), 20 μM 1A6 (2.5-fold, p<0.01), 20 μM 1A8 (6.2-fold, p<0.05), 10 μM 1B8 (5.0-fold, p<0.05), and 20 μM 1B8 (2.8-fold, p<0.01) compared to the control model (Figure 5.6D). Compared to the untreated control, there was no significant effect observed on the mRNA expression of mitogen-activated protein kinase 14 (*Mapk14*) and signal transducer and activator of transcription 3 (*Stat3*) when cells were exposed to model control (Figure 5.6E, F). Additionally, treatment with metformin (1 μM) and CL-316,243 (10 μM), as well as curcumin, 1A6, 1A8, and 1B8 did not affect the mRNA expression of *Mapk14* and *Stat3* when compared to the model control (Figure 5.6E, F).

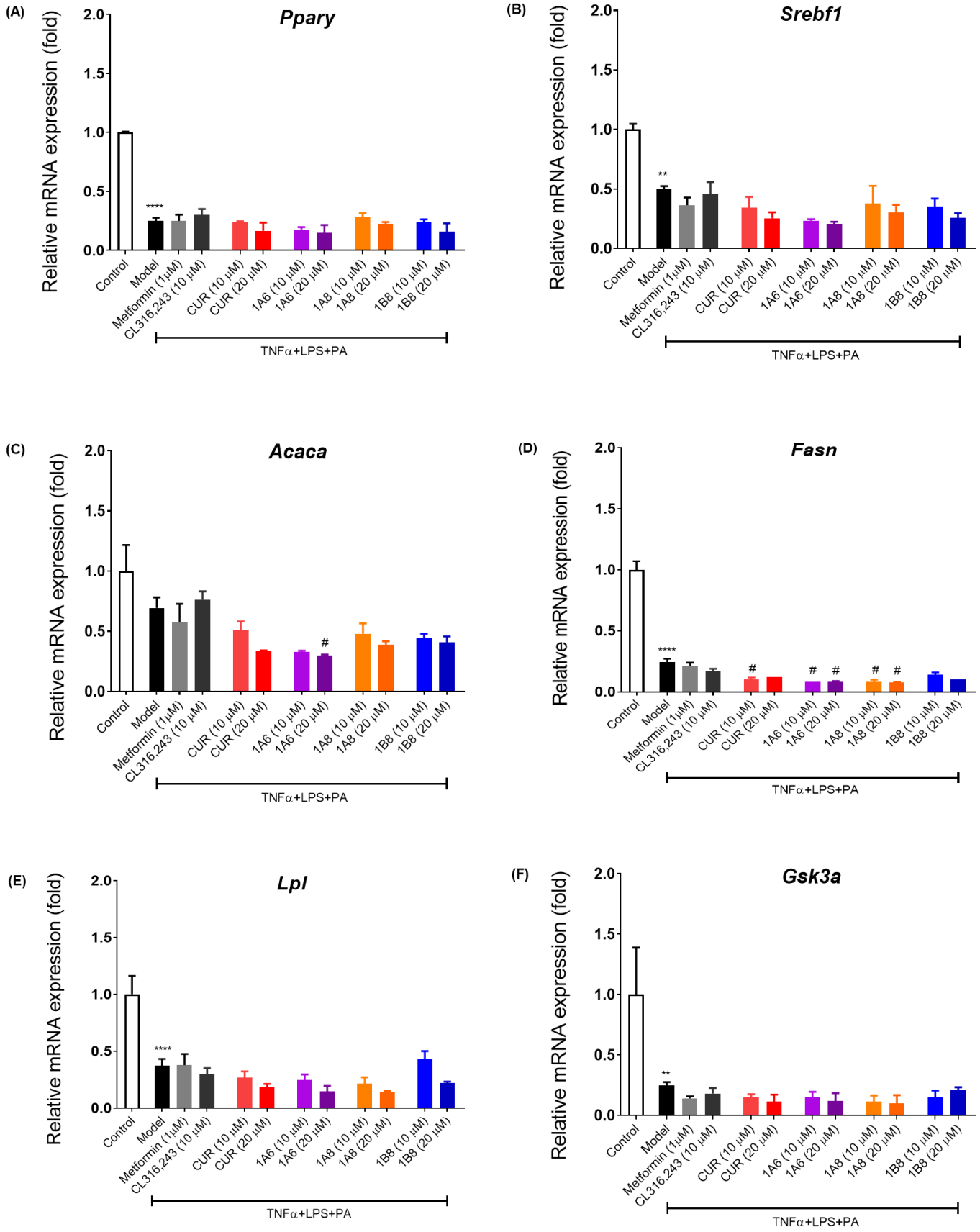


Figure 5.5: The effects of curcumin and the three curcumin derivatives (1A6, 1A8, and 1B8) on the mRNA expression of *Pparγ* (A), *Srebf1* (B), *Acaca* (C), *Fasn* (D), *Lpl* (E), and *Gsk3a* (F) in 3T3–L1 adipocytes induced

with TNFα, LPS, and PA combination. Differentiated 3T3–L1 adipocytes were treated with TNFα (10 ng/mL), LPS (100 ng/mL), and PA (10 mM) combination (model) or left untreated (control) for 24 hours. Thereafter, the cells were treated with curcumin (CUR), 1A6, 1A8, and 1B8 at 10 and 20 μM, metformin (1 μM), and CL-316,243 (10 μM) in the presence of TNFα, LPS, and PA combination for 24 hours. Gene expression was quantified using qRT-PCR and the expression was normalized to the average of *Rpl13a* and *B2m* and represented as fold changes. Statistical significance is depicted as $^{**}p<0.01$ and $^{****}p<0.0001$ vs. the untreated control cells; $^{\#}p<0.05$ vs. the model control.

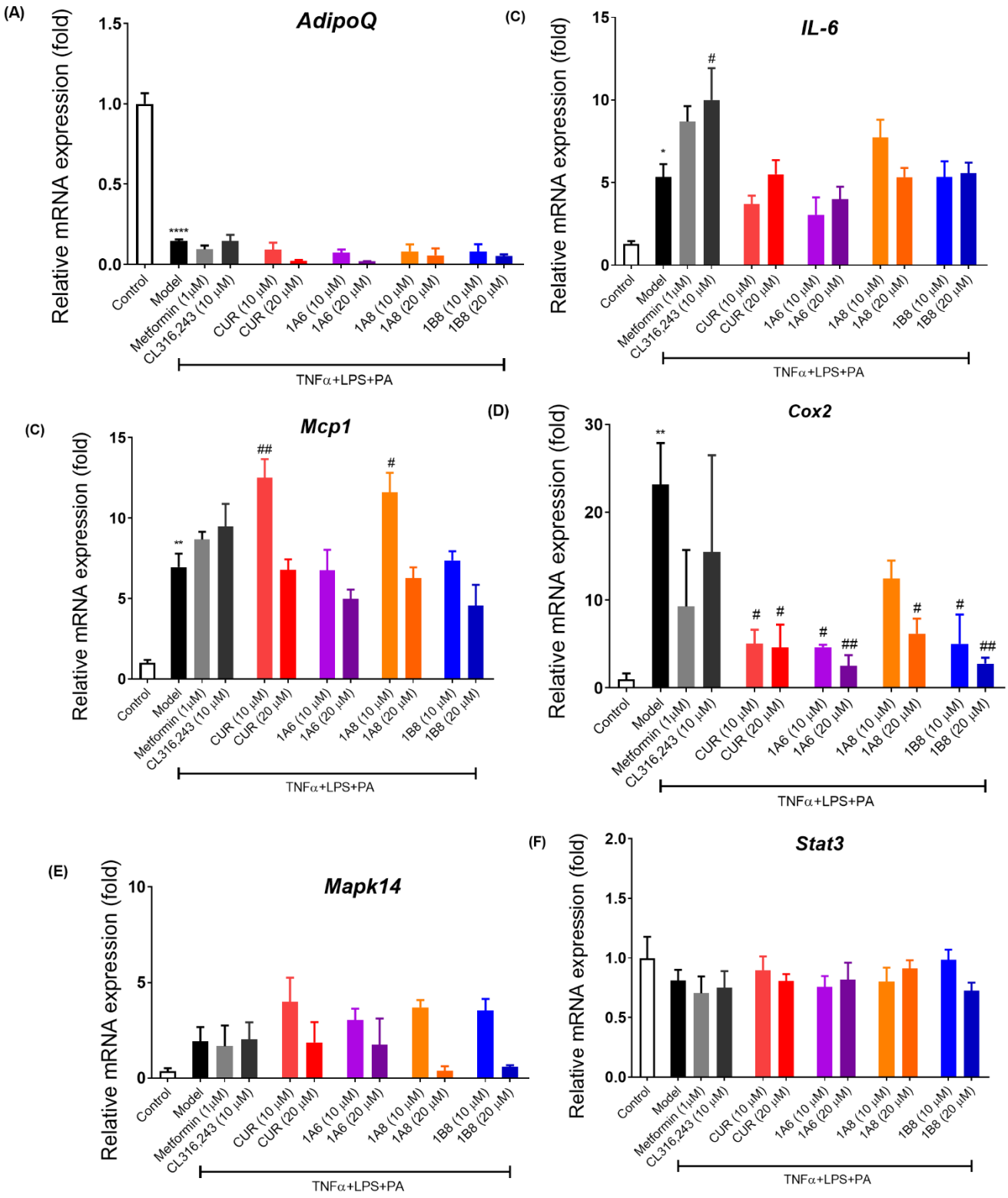


Figure 5.6: The effects of curcumin and the three curcumin derivatives (1A6, 1A8, and 1B8) on the mRNA expression of *AdipoQ* (A), *Il-6* (B), *Mcp1* (C), *Cox2* (D), *Mapk14* (E), and *Stat3* (F) in 3T3–L1 adipocytes induced with TNFα, LPS, and PA combination. Differentiated 3T3–L1 adipocytes were treated with TNFα (10 ng/mL), LPS (100 ng/mL), and PA (10 mM) combination (model) or left untreated (control) for 24 hours. Thereafter, the

cells were treated with curcumin (CUR), 1A6, 1A8, and 1B8 at 10 and 20 µM, metformin (1 µM), and CL-316,243 (10 µM) in the presence of TNFα, LPS, and PA combination for 24 hours. Gene expression was quantified using qRT-PCR and the expression was normalized to the average of *Rpl13a* and *B2m* and represented as fold changes. Statistical significance is depicted as *p<0.05, **p<0.01, and ****p<0.0001 vs. the untreated control cells; $^{\#}p$<0.05 and $^{\#\#}p$<0.01 vs. the model control.

The effects of curcumin and the three synthetic curcumin derivatives (1A6, 1A8, and 1B8) on ADIPOQ and IL-6 secreted levels

The effect of curcumin and the three curcumin derivatives (1A6, 1A8, and 1B8) on ADIPOQ and IL-6 secretion was evaluated in 3T3–L1 adipocytes induced with TNFα, LPS, and PA combination using ELISA assays. In comparison to the untreated control (137538 ± 8803 pg/mL), treatment with TNFα, LPS, and PA combination (model control) significantly decreased ADIPOQ secretion by 72.9% (37289 ± 5754 pg/mL, p<0.0001) (Figure 5.7A). However, treatment with metformin (1 µM) and CL-316,243 (10 µM), as well as curcumin, 1A6, 1A8, and 1B8 at 10 and 20 µM did not affect ADIPOQ secretion compared to the model control (Figure 5.7A). IL-6 secretion levels were increased by 509.8% (2227 ± 155.3 pg/mL, p<0.0001) in cells treated with TNFα, LPS, and PA combination (model control) when compared to the untreated control (Figure 5.7B). Meanwhile, IL-6 secretion levels were reduced by 40% (1448 ± 187.9 pg/mL, p<0.01), 51.46% (1081 ± 157.3 pg/mL, p<0.0001), 33.86% (1473 ± 79.79 pg/mL, p=0.138), 50.20% (1109 ± 152.9 pg/mL, p<0.05), 50.56% (1101 ± 303.8 pg/mL, p<0.001), 22.86% (1718 ± 280.4 pg/mL, p=0.004), and 63.60% (810.6 ± 274.7 pg/mL p<0.001) in cells treated with 10 µM curcumin, 20 µM curcumin, 10 µM 1A6, 20 µM 1A6, 20 µM 1A8, 10 µM 1B8, and 20 µM 1B8, respectively when compared to the model control (Figure 5.7B).

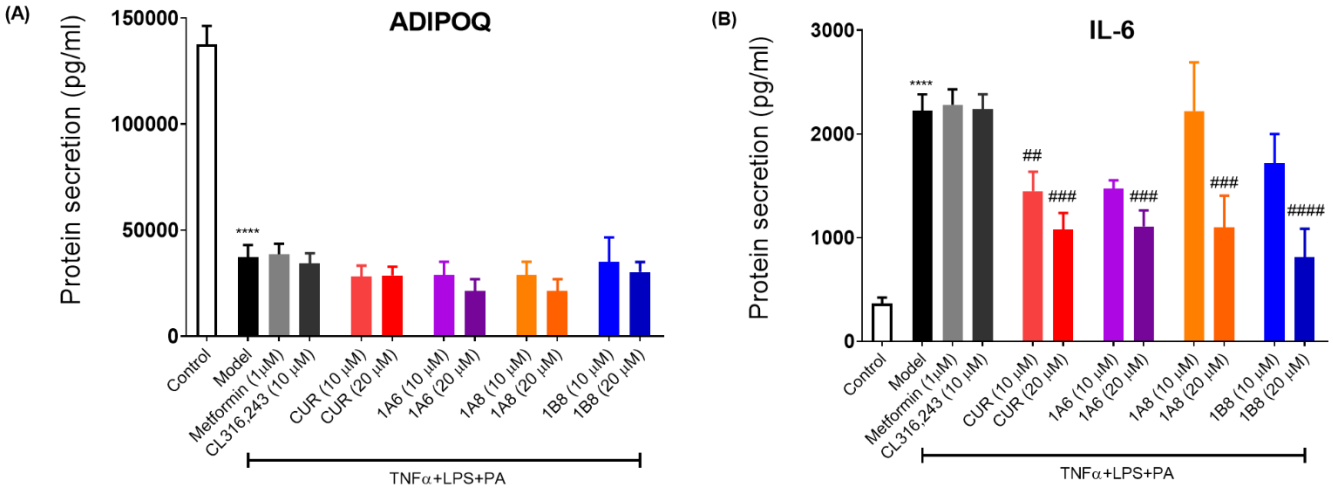


Figure 5.7: The effects of curcumin and the three curcumin derivatives (1A6, 1A8, and 1B8) on ADIPOQ (A) and IL-6 (B) secretion in 3T3–L1 adipocytes induced with TNFα, LPS, and PA combination. Differentiated 3T3– L1 adipocytes were treated with TNFα (10 ng/mL), LPS (100 ng/mL), and PA (10 mM) combination (model) or left untreated (control) for 24 hours. Thereafter, the cells were treated with curcumin (CUR), 1A6, 1A8, and 1B8 at 10 and 20 μM, metformin (1 μM), and CL-316,243 (10 μM) in the presence of TNFα, LPS, and PA combination for 24 hours. The secreted levels of ADIPOQ and IL-6 were quantified in the cell culture medium using commercial ELISA kits. The results are expressed as a pg/mL concentration and are shown as mean ± standard error of the mean (SEM) for three independent experiments. Statistical significance is depicted as ****$p<0.0001$ vs. the untreated control cells; $^{\#}p<0.05$, $^{\#\#}p<0.01$, $^{\#\#\#}p<0.001$, and $^{\#\#\#\#}p<0.0001$ vs. the model control.

Discussion

Obesity is a serious global health concern due to its association with chronic diseases including T2D, CVDs, and several types of cancers [1]. Furthermore, adipose tissue dysfunction, which is characterized by excessive lipid accumulation, dysregulated lipid metabolism, and chronic low-grade inflammation, contributes to the development of obesity-associated metabolic conditions. This makes adipose tissue an attractive therapeutic target for obesity and its associated complications [18–20]. This study aimed to investigate the effect of curcumin and the three synthetic curcumin derivatives (1A6, 1A8, and 1B8) on dysregulated lipid metabolism and inflammation in 3T3–L1 adipocytes. Treatment with the combination of TNFα, LPS, and PA was used in this study to induce an *in vitro* adipocyte cell model of dysregulated lipid metabolism and increased inflammation as previously reported
[14].

First, we evaluated the dose-dependent effects (1.25, 2.5, 5, 10, 20, and 40 μM) of curcumin, 1A6, 1A8, and 1B8 on metabolic activity and lipolysis in 3T3–L1 adipocytes induced with TNFα, LPS, and PA by quantifying the intracellular ATP content and glycerol secretion levels. Our results showed that treatment with TNFα, LPS, and PA reduced metabolic activity by decreasing ATP content by 53% in 3T3–L1 adipocytes. These cells were chronically exposed to TNFα, LPS, and PA treatment for 48 hours, resulting in the drastic reduction of ATP content. Similarly, results from the previously published work showed that treatment with TNFα individually or the combination of TNFα, LPS, and PA for 24 hours reduced ATP content in 3T3–L1 adipocytes [14]. The ATP assay is indicative of cell viability, and our results suggest that treatment with TNFα, LPS, and PA reduced cell

viability by 53% in these cells. Thus, further studies evaluating the effects of chronic treatment with TNFα, LPS, and PA combination on cytotoxicity are warranted. This will confirm whether the significant reduction in the ATP is due to the chronic exposure and cytotoxic effects of TNFα, LPS, and PA treatment.

Treatment with curcumin, 1A6, 1A8, and 1B8 significantly reduced ATP content at the highest concentration (40 μM), while lower concentrations (1.25, 2.5, 5, 10, and 20 μM) had no effect. This suggests that high concentrations of these compounds may be cytotoxic, however, this remains to be further evaluated. Similarly, other studies have also demonstrated that curcumin, at concentrations of 5 – 20 μM, does not affect metabolic activity in various 3T3–L1 adipocyte models [21–23]. In particular, curcumin and its derivatives, demethoxycurcumin and bisdemethoxycurcumin, at lower concentrations (0 –20 μM) had no effects on cell viability in differentiating 3T3–L1 adipocytes, while the highest concentration (40 μM) reduced cell viability, determined by the mitochondrial dehydrogenase activity (MTT) assay [23]. This suggests that the cytotoxic effects of curcumin and its derivatives may be concentration dependent.

Healthy adipocytes facilitate lipolysis, which refers to the breakdown of triglycerides into glycerol and free fatty acids (FFAs). These FFAs are taken up by surrounding adipocytes and re-esterified into triglycerides, leading to lipid accumulation within the cells [26]. However, adipocytes with disrupted lipid metabolism undergo excessive lipolysis [24], resulting in increased circulation of FFAs, peripheral lipotoxicity and insulin resistance [25]. In this study, treatment with the combination of TNFα, LPS, and PA increased glycerol secretion compared to the untreated control. These findings suggest that exposure to the combination of TNFα, LPS, and PA induces lipolysis in 3T3–L1 adipocytes. These results are consistent with our previous findings [14], and suggest that exposure to TNFα in combination with LPS and PA induces dysregulated lipid metabolism by increasing lipolysis. Our results showed that treatment with curcumin (5 – 20 μM), 1A6 (2.5 – 20 μM), and 1A8 (2.5 and 10 μM) reduced glycerol secretion levels in adipocytes subjected to TNFα, LPS, and PA combination treatment. While the anti-lipolytic effects of 1A6 and 1A8 are demonstrated for the first in this study, several other studies have reported that curcumin suppresses lipolysis in adipose tissue from obese mice [27] and 3T3-L1 adipocytes stimulated with TNFα or isoproterenol [22]. The chloro curcumin derivatives (1A6 and 1A8) showed effects in reducing glycerol secretion, however, the asymmetric curcumin derivative (1B8) had no effect. We speculate that this is due to the structural similarities of curcumin, 1A6, and 1A8 (i.e. the symmetrical aryl side chains of these compounds). However, further investigation on the structure–to–activity relationship of curcumin and the three synthetic curcumin derivatives (1A6, 1A8, and 1B8) is imperative to confirm their effects on glycerol secretion.

Contrary to the glycerol secretion data, our results showed that treatment with the TNFα, LPS, and PA combination decreased the mRNA expression of *Lipe* (Hsl) and *Pnpla3* (ATGL), key genes that facilitate the hydrolysis of diglycerides and triglycerides, respectively, during lipolysis [28]. Similar to our results, Jack et al. [14] reported that treating 3T3–L1 adipocytes with TNFα, LPS, and PA combination significantly reduced the mRNA expression of *Lipe.* These observed effects could be related to posttranscriptional modifications, hence changes in the expression levels of Lipe and Pnpla3 could be occurring at the protein level. Treatment with curcumin, 1A6, and 1A8 did not affect *Lipe* and *Pnpla3* mRNA expression, while 1B8 at 20 μM increased *Pnpla2* expression. Although this is the first study reporting increased *Pnpla3* mRNA expression in response to treatment with 1B8, curcumin was shown to improve glycolipid metabolism in adipose tissue of obese mice by increasing *Lipe* and *Pnpla3* expression [29]. Similarly, in this study, the increased *Pnpla3* mRNA expression by 1B8 could indicate improved lipid metabolism. Surprisingly, treatment with CL-316,243, used as a positive control in this study, did not affect glycerol secretion and the mRNA expression of *Lipe*, and *Pnpla3*. In contrast, glycerol secretion was significantly increased in PA-induced insulin-resistant 3T3–L1 adipocytes treated with CL-316,243 [30]. CL-316,243 is a highly potent selective β3-adrenoceptor agonist known to stimulate lipolysis in 3T3–L1 adipocytes [31] and modulate metabolic activities in adipocytes [32].

The main function of adipocytes is to store lipids in the form of triglycerides [26], but in dysfunctional adipocytes lipid storage capacity is reduced due to adipocyte hypertrophy, impaired adipogenesis, and increased lipolysis [33]. We demonstrate that exposing differentiated 3T3–L1 adipocytes to the combination of TNFα, LPS, and PA reduced lipid accumulation, suggesting that treatment with TNFα, LPS, and PA combination disrupts the lipid storage capacity of 3T3–L1 adipocytes by inducing excessive lipolysis. A study by Jack et al. [14] similarly demonstrated that the combination of TNFα, LPS, and PA decreased lipid content in 3T3–L1 adipocytes. Our results showed that curcumin and 1B8 (10 and 20 μM) significantly increased lipid accumulation in 3T3–L1 adipocytes induced with TNFα, LPS, and PA combination treatment, while 1A6 and 1A8 had no effect. Once again, the differences observed for the curcumin derivatives (1B8 vs. 1A6 and 1A8) could be related to their structural characteristics. Contrary to our data, studies have shown that curcumin reduces lipid accumulation in hydrogen peroxide (H_2O_2)-induced 3T3–L1 adipocytes [10], differentiating 3T3–L1 pre-adipocytes [23,34], and in *Caenorhabditis elegans* [35]. Meanwhile, the role of 1B8 in increasing lipid accumulation in TNFα, LPS, and

PA-induced 3T3–L1 adipocytes is a novel finding. We speculate that curcumin and 1B8 improve lipid metabolism in dysfunctional adipocytes by increasing lipid accumulation.

Both 1A6 and 1A8 (chloro curcumin derivatives) reduced lipolysis, while 1B8 (asymmetric curcumin derivative) increased lipid accumulation in these cells, suggesting that these compounds improve lipid metabolism via different mechanisms based on their structural characteristics. Curcumin improved lipid metabolism by decreasing lipolysis and increasing lipid accumulation. In addition, treatment with metformin and CL–316,243 increased lipid accumulation.

The decrease in lipid accumulation in response to treatment with the combination TNFα, LPS, and PA was accompanied by the reduced expression of the transcription factors, *Pparγ* and *Srebf1*, and their downstream target genes including*, Fasn, Acaca*, *Lpl*, and *Gsk3β* in 3T3–L1 adipocytes. These genes regulate lipid metabolism by increasing adipogenesis, fatty acid transport and fatty acid synthesis [40–44]. Therefore, this suggest that TNFα, LPS, and PA combination treatment reduces lipid accumulation via the downregulation of *Pparγ*, *Srebf1*, *Fasn, Acaca*, *Lpl*, and *Gsk3β* as previously reported [14]. Treatment with curcumin, the three synthetic curcumin derivatives (1A6, 1A8, and 1B8), metformin and CL–316,243 had no effects on *Pparγ*, *Srebf1*, *Lpl*, and *Gsk3β* expression. In contrast, curcumin was shown to increase *Pparγ* mRNA expression in 3T3–L1 adipocytes induced with H_2O_2 [10] and phosphorylated GSK3β protein levels in adipose tissue of obese mice [45]. Interestingly, the mRNA expression of *Acaca* was significantly reduced in 3T3–L1 adipocytes treated with 1A6 (20 μM). In addition, treatment with curcumin (10 μM), 1A6 (10 and 20 μM), and 1A8 (10 and 20 μM) significantly reduced *Acaca* mRNA expression. Although the reduced expression of *Acaca* and *Fasn* is associated with decreased lipid accumulation [46,47], the effects of curcumin, 1A6, and 1A8 on regulating ACACA and FASN expression remains to be further investigated in our experimental model, especially since the data for lipid accumulation and gene expression analysis are not consistent.

Adipocyte dysfunction is associated with chronic low-grade inflammation, characterized by reduced secretion of anti-inflammatory adipokines and an increase in pro-inflammatory adipokines [48,49]. Consistent with previously published data [14], exposure to TNFα, LPS, and PA combination significantly reduced ADIPOQ mRNA expression and its secreted levels in culture supernatants of 3T3–L1 adipocytes. ADIPOQ is an anti-inflammatory adipokine primarily secreted by adipocytes and is inversely correlated with obesity and related metabolic disorders

such as T2D and CVDs [50–53]. Treatment with curcumin and its synthetic derivatives (1A6, 1A8, and 1B8) did not affect the mRNA expression and secretion levels of ADIPOQ in our experimental model. Our results align with those reported by Ohara et al. [54], wherein curcumin exhibited no effect on ADIPOQ secretion in 3T3–L1 adipocytes subjected to LPS, TNFα, and IFNγ treatment. However, another study showed that treatment with curcumin increased ADIPOQ secretion in 3T3–L1 adipocytes induced with H_2O_2 [10].

Treatment with TNFα, LPS, and PA combination significantly increased IL-6 mRNA expression and its secreted levels in culture supernatants of 3T3–L1 adipocytes, as previously reported [14]. IL-6 is a multifunctional cytokine that plays a central role in regulating the immune response and inflammation [55]. Increased IL-6 levels are implicated in the pathogenesis of obesity, insulin resistance, and T2D [56,57]. Interestingly, treatment with curcumin (10 and 20 μM), 1A6 (10 and 20 μM), 1A8 (20 μM), and 1B8 (10 and 20 μM) reduced IL-6 secretion in 3T3–L1 adipocytes induced with TNFα, LPS, and PA combination. These results suggest that curcumin and its synthetic derivatives mitigate TNFα, LPS, and PA-induced inflammation in 3T3–L1 adipocytes by reducing IL6 secretion. Our results are consistent with literature demonstrating that curcuminoids reduce the secretion of IL6 in H_2O_2-induced, LPS-induced, and TNFα-induced 3T3–L1 adipocytes [10,58]. Treatment with curcumin, 1A6, 1A8, and 1B8 did not affect the mRNA expression of *Il-6* in our experimental model, suggesting that these compounds do not affect the transcriptional activity of the IL-6 gene but do regulate post-transcriptional events to reduce secreted IL-6 levels. CL–316,243 was shown to further increase *Il-6* expression in our experimental model. Similarly, IL-6 expression levels were increased in epididymal and inguinal white adipose tissue of mice subjected to acute treatment with CL–316,243 [59].

As expected, treatment with TNFα, LPS, and PA combination increased Mcp1 and Cox2 mRNA expression. MCP1 is a chemokine involved in the recruitment and activation of macrophages in dysfunctional adipose tissue and contributes to inflammation [60]. Unexpectedly, this study revealed that curcumin and 1A8 (10 μM) significantly increased the mRNA expression of Mcp1. Other studies have shown that curcumin inhibits MCP1 secretion in 3T3–L1 adipocytes and THP-1 macrophages [61,62], hence further studies evaluating the effects of curcumin and its derivatives on MCP1 protein expression are warranted. COX2 plays a key role in inflammatory response and is responsible for catalyzing the conversion of arachidonic acid into prostaglandins, which are lipid

mediators involved in inflammation [63,64]. In this study, we demonstrated a significant decrease in the mRNA expression of Cox2 in adipocytes treated with curcumin (10 and 20 μM), 1A6 (10 and 20 μM), 1A8 (20 μM), and 1B8 (10 and 20 μM). While we demonstrate novel findings for COX2 inhibitory effects of the three synthesis curcumin derivatives (1A6, 1A8, and 1B8), several studies have shown that curcumin reduces COX2 expression [65–68]. More specifically, the mRNA expression of IL-6 and COX2 was reduced in TNFα-induced 3T3–L1 adipocytes treated with curcumin [58].

Conclusion

In conclusion, this study shows that TNFα, LPS, and PA combination treatment modulates lipid metabolism and inflammation by increasing lipolysis and pro-inflammatory responses while decreasing lipid accumulation and anti-inflammatory responses in 3T3–L1 adipocytes. Results from this study further demonstrate that curcumin and its three synthetic derivatives (1A6, 1A8, and 1B8) ameliorate dysregulated lipid metabolism in 3T3–L1 adipocytes by reducing lipolysis and increasing lipid accumulation. Curcumin, 1A6, 1A8, and 1B8 attenuate inflammation by reducing pro-inflammatory markers in 3T3–L1 adipocytes. These results thus support the use of curcumin and its three synthetic derivatives (1A6, 1A8, and 1B8) as therapeutic agents to reduce inflammation and dysregulated lipid metabolism in adipocytes.

Reference

[1] A. Hruby and F. B. Hu, "The Epidemiology of Obesity: A Big Picture," Pharmacoeconomics, vol. 33, no. 7, pp. 673–689, 2015, doi: 10.1007/s40273-014-0243-x.

[2] R. Adabimohazab, A. Garfinkel, E. C. Milam, O. Frosch, A. Mangone, and A. Convit, "Does Inflammation Mediate the Association Between Obesity and Insulin Resistance?," Inflammation, vol. 39, no. 3, pp. 994–1003, Jun. 2016, doi: 10.1007/s10753-016-0329-z.

[3] Y. T. Lagerros and S. Rössner, "Obesity management: What brings success?" Therap. Adv. Gastroenterol., vol. 6, no. 1, pp. 77–88, 2013, doi: 10.1177/1756283X12459413.

[4] R. F. Kushner, "Weight Loss Strategies for Treatment of Obesity: Lifestyle Management and Pharmacotherapy," Progress in Cardiovascular Diseases, vol. 61, no. 2. W.B. Saunders, pp. 246–252, Jul. 01, 2018. doi: 10.1016/j.pcad.2018.06.001.

[5] Y. J. Tak and S. Y. Lee, "Long-Term Efficacy and Safety of Anti-Obesity Treatment: Where Do We Stand?," Current Obesity Reports, vol. 10, no. 1. Springer, pp. 14–30, Mar. 06, 2021. doi: 10.1007/s13679-020-00422-w.

[6] R. Lim, A. Beekley, D. C. Johnson, and K. A. Davis, "Early and late complications of bariatric operation," Trauma Surg. Acute Care Open, vol. 3, no. 1, p. e000219, Oct. 2018, doi: 10.1136/tsaco2018-000219.

[7] S. M. Barbalho et al., "The Effects of Curcumin on Diabetes Mellitus : A Systematic Review," Front. Endocrinol. (Lausanne), vol. 12, no. May, p. 443, May 2021, doi: 10.3389/fendo.2021.669448.

[8] K. Kasprzak-Drozd, T. Oniszczuk, M. Gancarz, A. Kondracka, R. Rusinek, and A. Oniszczuk, "Curcumin and Weight Loss: Does It Work?," Int. J. Mol. Sci., vol. 23, no. 2, p. 639, Jan. 2022, doi: 10.3390/ijms23020639.

[9] Z. Song et al., "Dietary Curcumin Intervention Targets Mouse White Adipose Tissue Inflammation and Brown Adipose Tissue UCP1 Expression," Obesity, vol. 26, no. 3, pp. 547–558, Mar. 2018, doi: 10.1002/oby.22110.

[10] A. Septembre-Malaterre, F. Le Sage, S. Hatia, A. Catan, L. Janci, and M.-P. Gonthier, "Curcuma longa polyphenols improve insulin-mediated lipid accumulation and attenuate proinflammatory response of 3T3-L1 adipose cells during oxidative stress through regulation of key adipokines and antioxidant enzymes.," Biofactors, vol. 42, no. 4, pp. 418–430, Jul. 2016, doi: 10.1002/biof.1288.

[11] M. Kobori et al., "Dietary Intake of Curcumin Improves eIF2 Signaling and Reduces Lipid Levels in the White Adipose Tissue of Obese Mice.," Sci. Rep., vol. 8, no. 1, p. 9081, Jun. 2018, doi: 10.1038/s41598-018-27105-w.

[12] A. Priyanka, G. L. Shyni, N. Anupama, P. S. Raj, S. S. Anusree, and K. G. Raghu, "Development of insulin resistance through sprouting of inflammatory markers during hypoxia in 3T3-L1 adipocytes and amelioration with curcumin," Eur. J. Pharmacol., vol. 812, pp. 73–81, Oct. 2017, doi: 10.1016/J.EJPHAR.2017.07.005.

[13] N. Ghalandarlaki, A. M. Alizadeh, and S. Ashkani-esfahani, "Nanotechnology-Applied Curcumin for Different Diseases Therapy," vol. 2014, 2014, doi: 10.1155/2014/394264.

[14] B. U. Jack, M. Mamushi, A. Viraragavan, S. Dias, and C. Pheiffer, “Comparing the effects of tumor necrosis factor alpha, lipopolysaccharide and palmitic acid on lipid metabolism and inflammation in murine 3T3-L1 adipocytes,” Life Sci., vol. 297, no. May 2021, p. 120422, May 2022, doi: 10.1016/j.lfs.2022.120422.

[15] P. V. Dludla et al., “A dose-dependent effect of dimethyl sulfoxide on lipid content, cell viability and oxidative stress in 3T3-L1 adipocytes,” Toxicol. Reports, vol. 5, no. March, pp. 1014–1020, 2018, doi: 10.1016/j.toxrep.2018.10.002.

[16] B. U. Jack et al., “A polyphenol-enriched fraction of Cyclopia intermedia decreases lipid content in 3T3-L1 adipocytes and reduces body weight gain of obese db/db mice,” South African J. Bot., vol. 110, pp. 216–229, May 2017, doi: 10.1016/j.sajb.2016.08.007.

[17] B. U. Jack et al., “Polyphenol-Enriched Fractions of Cyclopia intermedia Selectively Affect Lipogenesis and Lipolysis in 3T3-L1 Adipocytes,” Planta Med., vol. 84, no. 2, pp. 100–110, 2018, doi: 10.1055/s-0043-119463.

[18] S. S. Ranaweera et al., “Anti-obesity effect of sulforaphane in broccoli leaf extract on 3T3-L1 adipocytes and ob/ob mice,” J. Nutr. Biochem, vol. 100, p. 108885, Feb. 2022, doi: 10.1016/j.jnutbio.2021.108885.

[19] M. Blüher, “Adipose tissue dysfunction in obesity,” Experimental and Clinical Endocrinology and Diabetes, vol. 117, no. 6. © J. A. Barth Verlag in Georg Thieme Verlag KG Stuttgart · New York, pp. 241–250, Jun. 2009. doi: 10.1055/s-0029-1192044.

[20] G. S. Hotamisligil, N. S. Shargill, and B. M. Spiegelman, “Adipose expression of tumor necrosis factor-alpha: direct role in obesity-linked insulin resistance,” Science, vol. 259, no. 5091, pp. 87–91, 1993, doi: 10.1126/SCIENCE.7678183.

[21] A. Priyanka, S. S. Anusree, V. M. Nisha, and K. G. Raghu, “Curcumin improves hypoxia induced dysfunctions in 3T3-L1 adipocytes by protecting mitochondria and down regulating inflammation.,” Biofactors, vol. 40, no. 5, pp. 513–523, 2014, doi: 10.1002/biof.1175.

[22] X. Xie, P.-R. Kong, J. Wu, Y. Li, and Y. Li, “Curcumin attenuates lipolysis stimulated by tumor necrosis factor-α or isoproterenol in 3T3-L1 adipocytes,” Phytomedicine, vol. 20, no. 1, pp. 3–8, Dec. 2012, doi: 10.1016/j.phymed.2012.09.003.

[23] A. Alalaiwe, J.-Y. J. Y. Fang, H.-J. H. J. Lee, C. H. C.-H. Chiu, and C. Y. C.-Y. Hsu, “The demethoxy mechanistic study of adipogenesis and molecular docking,” Biomolecules, vol. 11, no. 7, pp. 1–18, Jul. 2021, doi: 10.3390/biom11071025.

[24] G. F. Grabner, H. Xie, M. Schweiger, and R. Zechner, “Lipolysis: cellular mechanisms for lipid mobilization from fat stores,” Nat. Metab., vol. 3, pp. 1445–1465, 2021, doi: 10.1038/s42255-02100493-6.

[25] M. Lafontan, “Adipose tissue and adipocyte dysregulation,” Diabetes Metab., vol. 40, no. 1, pp. 16–28, Feb. 2014, doi: 10.1016/j.diabet.2013.08.002.

[26] L. Segalla, S. Chirumbolo, and A. Sbarbati, “Dermal white adipose tissue: Much more than a metabolic, lipid-storage organ?,” Tissue Cell, vol. 71, p. 101583, Aug. 2021, doi: 10.1016/j.tice.2021.101583.

[27] L. Wang, B. Zhang, F. Huang, B. Liu, and Y. Xie, “Curcumin inhibits lipolysis via suppression of ER

stress in adipose tissue and prevents hepatic insulin resistance," J. Lipid Res., vol. 57, no. 7, pp. 1243– 1255, Jul. 2016, doi: 10.1194/JLR.M067397.

[28] G. Frühbeck, L. Méndez-Giménez, J.-A. Fernández-Formoso, S. Fernández, and A. Rodríguez, "Regulation of adipocyte lipolysis," Nutr. Res. Rev., vol. 27, no. 1, pp. 63–93, Jun. 2014, doi: 10.1017/S095442241400002X.

[29] Y. Pan et al., "Curcumin improves glycolipid metabolism through regulating peroxisome proliferator activated receptor γ signalling pathway in high-fat diet-induced obese mice and 3T3-L1 adipocytes," R. Soc. Open Sci., vol. 4, no. 11, p. 170917, Nov. 2017, doi: 10.1098/rsos.170917.

[30] S. E. Mazibuko-Mbeje et al., "Isoorientin ameliorates lipid accumulation by regulating fat browning in palmitate-exposed 3T3-L1 adipocytes," Metab. Open, vol. 6, p. 100037, Jun. 2020, doi: 10.1016/j.metop.2020.100037.

[31] L.-N. Ding et al., "The β3 Adrenergic Receptor Agonist CL316243 Ameliorates the Metabolic Abnormalities of High-Fat Diet-Fed Rats by Activating AMPK/PGC-1α Signaling in Skeletal Muscle," Diabetes, Metab. Syndr. Obes. Targets Ther, vol. Volume 14, pp. 1233–1241, Mar. 2021, doi: 10.2147/DMSO.S297351.

[32] S. Zhang et al., "Acute activation of adipocyte lipolysis reveals dynamic lipid remodeling of the hepatic lipidome," J. Lipid Res., p. 100434, Aug. 2023, doi: 10.1016/j.jlr.2023.100434.

[33] J. Xiao et al., "Obesity promotes lipid accumulation in lymph node metastasis of gastric cancer: a retrospective case–control study," Lipids Health Dis., vol. 21, no. 1, p. 123, Nov. 2022, doi: 10.1186/s12944-022-01734-7.

[34] J. Zhao, X.-B. B. Sun, F. Ye, and W.-X. X. Tian, "Suppression of fatty acid synthase, differentiation and lipid accumulation in adipocytes by curcumin," Mol. Cell. Biochem, vol. 351, no. 1–2, pp. 19–28, May 2011, doi: 10.1007/s11010-010-0707-z.

[35] Y. Yue, G. Hao, J. Cho, and Y. Park, "Curcumin reduced fat accumulation in Caenorhabditis elegans," Curr. Res. food Sci., vol. 4, pp. 551–556, Jan. 2021, doi: 10.1016/j.crfs.2021.08.005.

[36] Y. Wang et al., "Metformin Improves Mitochondrial Respiratory Activity through Activation of AMPK," Cell Rep., vol. 29, no. 6, pp. 1511-1523.e5, Nov. 2019, doi: 10.1016/j.celrep.2019.09.070.

[37] S. Luo, C. M. Schooling, I. C. K. Wong, and S. L. Au Yeung, "Evaluating the impact of AMPK activation, a target of metformin, on risk of cardiovascular diseases and cancer in the UK Biobank: a Mendelian randomisation study," Diabetologia, vol. 63, no. 11, pp. 2349–2358, Nov. 2020, doi: 10.1007/s00125-020-05243-z.

[38] L. Yang et al., "Metformin Inhibits Lipid Droplets Fusion and Growth via Reduction in Cidec and Its Regulatory Factors in Rat Adipose-Derived Stem Cells," Int. J. Mol. Sci., vol. 23, no. 11, p. 5986, May 2022, doi: 10.3390/ijms23115986.

[39] S.-J. Chuang et al., "AMPK activation by SC4 inhibits noradrenaline-induced lipolysis and insulin-stimulated lipogenesis in white adipose tissue," Biochem. J., vol. 478, no. 21, pp. 3869–3889, Nov. 2021, doi: 10.1042/BCJ20210411.

[40] A. Bhattarai, E. M. Likos, C. M. Weyman, and G. C. Shukla, "Regulation of cholesterol biosynthesis

and lipid metabolism: A microRNA management perspective," Steroids, vol. 173, p. 108878, Sep. 2021, doi: 10.1016/j.steroids.2021.108878.

[41] E. D. Dixon, A. D. Nardo, T. Claudel, and M. Trauner, "The Role of Lipid Sensing Nuclear Receptors (PPARs and LXR) and Metabolic Lipases in Obesity, Diabetes and NAFLD," Genes (Basel), vol. 12, no. 5, p. 645, Apr. 2021, doi: 10.3390/genes12050645.

[42] A. Kumari, K. K. Kristensen, M. Ploug, and A.-M. L. Winther, "The Importance of Lipoprotein Lipase Regulation in Atherosclerosis," Biomedicines, vol. 9, no. 7, p. 782, Jul. 2021, doi: 10.3390/biomedicines9070782.

[43] Y.-M. Kim, I. Song, Y.-H. Seo, and G. Yoon, "Glycogen Synthase Kinase 3 Inactivation Induces Cell Senescence through Sterol Regulatory Element Binding Protein 1-Mediated Lipogenesis in Chang Cells," Endocrinol. Metab, vol. 28, no. 4, p. 297, 2013, doi: 10.3803/EnM.2013.28.4.297.

[44] Y. Peng, H. Li, K. Shen, W. Pan, J. Zhang, and D. Zhou, "Nano-selenium alleviating the lipid metabolism disorder of LMH cells induced by potassium dichromate via down-regulating ACACA and FASN," Environ. Sci. Pollut. Res., vol. 28, no. 48, pp. 69426–69435, Dec. 2021, doi: 10.1007/s11356021-14775-9.

[45] L. Ding et al., "Curcumin rescues high fat diet-induced obesity and insulin sensitivity in mice through regulating SREBP pathway," Toxicol. Appl. Pharmacol., vol. 304, pp. 99–109, Aug. 2016, doi: 10.1016/j.taap.2016.05.011.

[46] J. Dong, M. Li, R. Peng, Y. Zhang, Z. Qiao, and N. Sun, "ACACA reduces lipid accumulation through dual regulation of lipid metabolism and mitochondrial function via AMPK- PPARα- CPT1A axis," J. Transl. Med., vol. 22, no. 1, p. 196, Feb. 2024, doi: 10.1186/s12967-024-04942-0.

[47] S. Guo, K. Yan, X. Fang, Y. Ni, W. Ma, and R. Zhao, "α-Lipoic Acid Alleviates Hepatic Lipid Deposition by Inhibiting FASN Expression via miR-3548 in Rats," Nutrients, vol. 13, no. 7, p. 2331, Jul. 2021, doi: 10.3390/nu13072331.

[48] K. Makki, P. Froguel, and I. Wolowczuk, "Adipose Tissue in Obesity-Related Inflammation and Insulin Resistance: Cells, Cytokines, and Chemokines," vol. 2013, p. 12, 2013, doi: 10.1155/2013/139239.

[49] X. Unamuno, J. Gómez-Ambrosi, A. Rodríguez, S. Becerril, G. Frühbeck, and V. Catalán, "Adipokine dysregulation and adipose tissue inflammation in human obesity," Eur. J. Clin. Invest, vol. 48, no. 9, p. e12997, Sep. 2018, doi: 10.1111/eci.12997.

[50] C. Pheiffer, S. Dias, B. Jack, N. Malaza, and S. Adam, "Adiponectin as a Potential Biomarker for Pregnancy Disorders," Int. J. Mol. Sci., vol. 22, no. 3, p. 1326, Jan. 2021, doi: 10.3390/ijms22031326.

[51] O. F. Khabour, M. A. Alomari, and A. A. Abu Obaid, "The Relationship of adiponectin level and ADIPOQ gene variants with BMI among young adult women,"Dermatoendocrinol. vol. 10, no. 1, p. e1477902, Jan. 2018, doi: 10.1080/19381980.2018.1477902.

[52] M.-C. Chen, C.-J. Lee, C.-F. Yang, Y.-C. Chen, J.-H. Wang, and B.-G. Hsu, "Low serum adiponectin level is associated with metabolic syndrome and is an independent marker of peripheral arterial stiffness in hypertensive patients," Diabetol. Metab. Syndr, vol. 9, no. 1, p. 49, Dec. 2017, doi: 10.1186/s13098-017-0247-8.

[53] W. Liu et al., “Serum leptin, resistin, and adiponectin levels in obese and non-obese patients with newly diagnosed type 2 diabetes mellitus,” Medicine (Baltimore), vol. 99, no. 6, p. e19052, Feb. 2020, doi: 10.1097/MD.0000000000019052.

[54] K. Ohara, A. Uchida, R. Nagasaka, H. Ushio, and T. Ohshima, “The effects of hydroxycinnamic acid derivatives on adiponectin secretion,” Phytomedicine, vol. 16, no. 2–3, pp. 130–137, Mar. 2009, doi: 10.1016/j.phymed.2008.09.012.

[55] T. Kishimoto, “Interleukin-6: Discovery of a pleiotropic cytokine,” Arthritis Res. Ther., vol. 8, no. SUPPL. 2, Jul. 2006, doi: 10.1186/ar1916.

[56] K. Rehman, M. S. H. Akash, A. Liaqat, S. Kamal, M. I. Qadir, and A. Rasul, “Role of Interleukin-6 in Development of Insulin Resistance and Type 2 Diabetes Mellitus,” Crit. Rev. Eukaryot. Gene Expr., vol. 27, no. 3, pp. 229–236, 2017, doi: 10.1615/CritRevEukaryotGeneExpr.2017019712.

[57] K. Eder, N. Baffy, A. Falus, and A. K. Fulop, “The major inflammatory mediator interleukin-6 and obesity,” Inflamm. Res., vol. 58, no. 11, pp. 727–736, Nov. 2009, doi: 10.1007/s00011-009-0060-4.

[58] A. M. Gonzales and R. A. Orlando, “Curcumin and resveratrol inhibit nuclear factor-kappaB-mediated cytokine expression in adipocytes,” Nutr. Metab. (Lond), vol. 5, no. 1, p. 17, Dec. 2008, doi: 10.1186/1743-7075-5-17.

[59] S. L. Buzelle, R. E. K. Macpherson, W. T. Peppler, L. Castellani, and D. C. Wright, “The contribution of IL-6 to beta 3 adrenergic receptor mediated adipose tissue remodeling,” vol. 3, pp. 1–13, 2015, doi: 10.14814/phy2.12312.

[60] H. Kanda et al., “MCP-1 contributes to macrophage infiltration into adipose tissue, insulin resistance, and hepatic steatosis in obesity,” vol. 116, no. 6, 2006, doi: 10.1172/JCI26498DS1.

[61] H.-M. Woo, J.-H. Kang, T. Kawada, H. Yoo, M.-K. Sung, and R. Yu, “Active spice-derived components can inhibit inflammatory responses of adipose tissue in obesity by suppressing inflammatory actions of macrophages and release of monocyte chemoattractant protein-1 from adipocytes.,” Life Sci., vol. 80, no. 10, pp. 926–931, Feb. 2007, doi: 10.1016/j.lfs.2006.11.030.

[62] Y. Zhong, C. Liu, J. Feng, J. Li, and Z. Fan, “Curcumin affects ox-LDL-induced IL-6, TNF-α, MCP-1 secretion and cholesterol efflux in THP-1 cells by suppressing the TLR4/NF-κB/miR33a signaling pathway,” Exp. Ther. Med., Jun. 2020, doi: 10.3892/etm.2020.8915.

[63] G. S. Hotamisligil, “Inflammation and metabolic disorders,” Nature, vol. 444, no. 7121, pp. 860–867, Dec. 2006, doi: 10.1038/nature05485.

[64] L. S. Simon, “Role and regulation of cyclooxygenase-2 during inflammation,” Am. J. Med., vol. 106, no. 5, pp. 37S-42S, May 1999, doi: 10.1016/S0002-9343(99)00115-1.

[65] “Curcumin and Rutin Down-regulate Cyclooxygenase-2 and Reduce Tumor-associated Inflammation in HPV16-Transgenic Mice,” Anticancer Res., vol. 38, no. 3, Mar. 2018, doi: 10.21873/anticanres.12371.

[66] T. Vasanthkumar, M. Hanumanthappa, and R. Lakshminarayana, “Curcumin and capsaicin modulates LPS induced expression of COX-2, IL-6 and TGF-β in human peripheral blood mononuclear cells,” Cytotechnology, vol. 71, no. 5, pp. 963–976, Oct. 2019, doi: 10.1007/s10616-019-00338-x.

[67] M. Z. Gutierrez et al., “Co-nanoencapsulated meloxicam and curcumin improves cognitive impairment induced by amyloid-beta through modulation of cyclooxygenase-2 in mice,” Neural Regen. Res., vol. 16, no. 4, p. 783, 2021, doi: 10.4103/1673-5374.295339.

[68] J. Yuan, R. Liu, Y. Ma, Z. Zhang, and Z. Xie, “Curcumin Attenuates Airway Inflammation and Airway Remolding by Inhibiting NF-κB Signaling and COX-2 in Cigarette Smoke-Induced COPD Mice,” Inflammation, vol. 41, no. 5, pp. 1804–1814, Oct. 2018, doi: 10.1007/s10753-018-0823-6.

CHAPTER 6

Chapter outline:

This chapter provides the summary and conclusion of this research study and highlights the strengths and limitations of this study. Furthermore, future work is also proposed.

Summary

The obesity epidemic has persisted for decades, is escalating globally, and affecting both developed and developing countries [1]. Various treatment approaches, including lifestyle modifications, pharmacotherapy, and bariatric surgery, have been utilized to combat the prevalence of obesity [2–4]. However, their effectiveness is constrained by associated side effects and lack of adherence. In response to these challenges, natural compounds like curcumin, a polyphenol derived from the rhizome of turmeric, have garnered scientific attention for their potential metabolic benefits in treating obesity [5]. However, the clinical applicability of curcumin is hindered by its poor pharmacokinetic profile, prompting the exploration of synthetic curcumin derivatives to enhance its biological while also improving its pharmacokinetic profile [6][7].

Previously, drug-sensitive acute lymphoblastic CCRF-CEM leukemia cells and their multidrug-resistant P-gpoverexpressing subline cells, CEM/ADR5000 were used to test 19 novel synthetic curcumin derivatives for anticancer properties [8]. Results from this study showed that the 19 synthetic curcumin derivatives exerted strong cytotoxic effects and P-glycoprotein (P-gp) inhibitory activity compared to curcumin [8]. In particular, the two chlorocurcumin derivatives (1A6 and 1A8) and the asymmetric curcumin derivative (1B8) displayed potent efficacy amongst the 19 derivatives [8]. Several signaling pathways involved in lipid metabolism and inflammation are common between cancer and obesity [9–11], therefore, this study provided us with the rationale to further explore the efficacy of these three synthetic curcumin derivatives against obesity. As such, this study aimed to evaluate the effects of curcumin and the three synthetic curcumin derivatives (1A6, 1A8, and 1B8) on adipocyte dysfunction and adipogenesis using *in silico* and *in vitro* experimental approaches. For each of the study's objectives, the summary is provided below, while detailed findings are described in their respective chapters.

In this study, the three curcumin derivatives, including two chloro curcumin derivatives (1A6 and 1A8) and the asymmetric curcumin derivative (1B8), were synthesized and characterized using previously reported protocols (objective 1) [8]. The two chloro curcumin derivatives were structurally modified in the active methylene with a chlorine substitution and in the aryl side chains with symmetrical aldehydes. Meanwhile, the asymmetric curcumin derivative (1B8) was structurally modified in the aryl side chains by substituting with two asymmetric aldehydes. The three curcumin derivatives were successfully synthesized with the highest purity (>99%), while lower yields of 31% (1A6), 25% (1A8), and 17% (1B8) were obtained. The synthesized curcumin derivatives had high melting points at 168 °C – 170 °C (1A6), 218 °C – 220 °C (1A8), and 139 °C – 140 °C (1B8), confirming their thermal stability.

Furthermore, characterization using mass spectrometry, FT-IR, and ^{1}H–NMR spectroscopy validated molecular mass, functional groups, and chemical structure formula of the three synthesized curcumin derivatives.

In silico computation was used to predict the toxicity, pharmacokinetic profiles, biological targets, and the molecular interactions of curcumin and the three synthetic curcumin derivatives (1A6, 1A8, and 1B8) with predicted biological targets (objective 2). In this study, curcumin and its synthetic derivatives possessed drug-like attributes as seen by their compliance with the LRo5. The safety of curcumin was affirmed through predictive toxicity screening, and its synthetic derivatives exhibited a secure profile based on LD_{50} values. Specifically, the synthetic curcumin derivative, 1A8, displayed inactivity across all selected toxicity endpoints. For lipophilicity, 1A8 exhibited the lowest value, implying that this compound has potential challenges with membrane permeability. Curcumin and its three synthetic derivatives were active for CYP3A4 and CYP2C9 drug metabolizing enzymes, suggesting that their interactions might influence pharmacokinetic profiles. Molecular docking and molecular dynamic simulation studies showed that curcumin and the three synthetic curcumin derivatives have similar binding affinities and molecular interactions for the predicted biological targets, including PPARγ, COX2, and FAS.

This study also aimed to assess the effects of curcumin and its three synthetic derivatives (1A6, 1A8, and 1B8) on lipid metabolism and inflammation in 3T3–L1 adipocytes (objectives 3 and 4). The validity of the experimental model was confirmed as the induction treatment (TNFα, LPS, and PA combination treatment) successfully induced metabolic dysfunction characterized by reduced metabolic activity, increased lipolysis, decreased lipid accumulation, reduced anti-inflammatory, and increased pro-inflammatory markers. Results revealed that curcumin and the two chloro curcumin derivatives (1A6 and 1A8) reduced the metabolic activity of 3T3–L1 adipocytes only at the highest concentration (40 μM), while lower concentrations (1.25 – 20 μM) did not affect metabolic activity. Similarly, treatment with curcumin (5 – 20 μM), 1A6 (2.5 – 20 μM), and 1A8 (2.5 and 10 μM) attenuated lipolysis induced by TNFα, LPS, and PA combination treatment via reducing glycerol secretion levels. The asymmetric curcumin derivative (1B8) did not affect metabolic activity and lipolysis in 3T3–L1 adipocytes. Curcumin and 1B8 (10 – 20 μM) increased lipid accumulation in 3T3–L1 adipocytes co-treated with TNFα, LPS, and PA combination, while the chloro curcumin derivatives (1A6 and 1A8) had no effect. Furthermore, the results showed that the mRNA expression of *Pnpla3* was increased by treatment with 1B8 (20 μM), while *Acaca* mRNA expression was reduced by 1A6 (20 μM), and *Fasn* mRNA expression was decreased by curcumin (10 μM), 1A6 (10 and 20 μM), and 1A8 (10 and 20 μM). In the context of inflammation, curcumin (10 and 20 μM), 1A6 (10 and 20 μM), 1A8 (20 μM), and 1B8 (10 and

20 μM) reduced *Cox2* mRNA expression levels, while treatment with curcumin (10 and 20 μM), 1A6 (10 and 20 μM), 1A8 (20 μM), and 1B8 (10 and 20 μM) also decreased IL-6 secretion levels. Curcumin and the three synthetic curcumin derivatives (1A6, 1A8, and 1B8) did not affect ADIPOQ expression and secretion levels.

Strength and limitations

This study has several strengths. The efficacy of curcumin and three curcumin derivatives, that were synthesized using organic chemistry, were evaluated using *in silico* prediction and *in vitro* experimental approaches. The use of organic chemistry to structurally modify bioactive compounds provides the ability to improve biological properties [12]. The use of *in silico* computational prediction provides a high-throughput screening method that is relatively quicker, easier, and more cost effective compared to laboratory experiments. An established *in vitro* model of dysregulated lipid metabolism and inflammation was used in this study to mimic the pathophysiology of adipocyte dysfunction, thus providing relevance to obesity. The biological activity of curcumin and the three synthetic curcumin derivatives were assessed *in vitro* using a dose-dependent response. In addition to bioactivity assays, gene expression analysis and ELISAs were used to elucidate the molecular mechanisms of curcumin and the three synthetic derivatives in our experimental model.

However, the study is not without its limitations. Although the three synthetic curcumin derivatives were synthesized with the highest purity, their yields were relatively low. The reliability of *in silico* data often requires experimental validations, hence both *in silico* computation and *in vitro* experimental approaches were conducted in this study. Further experimental work to investigate the bioavailability of synthetic curcumin derivatives is warranted. Due to time constraints and limited resources, the effects of curcumin and the three synthetic derivatives on adipogenesis could not be assessed. The mRNA expression data did show an effect in response to curcumin, 1A6, 1A8, and 1B8 treatment for several of the genes evaluated (*Pparγ*, *Srebf1*, *Lpl*, *Gsk3β, ADIPOQ, IL-6, Mapk14,* and *Stat3*), and western blot analysis to validate the expression of these genes at the protein level was not conducted. Due to limited time and resources, the time-dependent effect of curcumin and the three synthetic derivatives could not be evaluated in our *in vitro* experimental model.

Conclusion

In this study, three synthetic curcumin derivatives, including the two chloro curcumin derivatives (1A6 and 1A8) and the asymmetric curcumin derivative (1B8) were successfully synthesized and characterized as previously reported. *In silico* prediction studies showed that curcumin and the three synthetic derivatives have similar pharmacokinetic profiles and exhibit similar molecular interactions with selected biological targets. *In vitro* studies showed that curcumin and the three synthetic derivatives improved lipid metabolism and attenuated inflammation in dysfunctional adipocytes. The results from this study also demonstrate that curcumin and the three synthetic derivatives have similar biological effects on lipid metabolism and inflammation in adipocytes. This study suggests that curcumin and the three synthetic curcumin derivatives (1A6, 1A8, and 1B8) ameliorate adipocyte dysfunction by modulating lipid metabolism and inflammation and regulate adipogenesis by targeting key adipogenic and lipid metabolism proteins, thus exerting potential anti-obesity effects.

Future work

Further experimental work is warranted to validate the *in silico* prediction, specifically, experimental assays such as drug affinity responsive target stability (DARTS) assays and cellular thermal shift assays (CETSA) will be conducted to validate the binding conformation and molecular interactions of curcumin, 1A6, 1A8, and 1B8 with the selected biological targets. *In vitro* experiments to evaluate the effects of curcumin and the three synthetic curcumin derivatives on adipogenesis will be conducted by treating 3T3-L1 preadipocytes during differentiation with various doses of curcumin, 1A6, 1A8, and 1B8. Future studies will also conduct western blot analysis to validate mRNA expression data at the protein level. The pharmacokinetic properties of the three synthetic curcumin derivatives will be assessed and compared to curcumin. Furthermore, the pharmacokinetic profile of curcumin and its synthetic derivatives will be assessed using Caco cells and animal experimental models.

References

[1] N. D. Ford, S. A. Patel, and K. M. V. Narayan, “Obesity in Low- and Middle-Income Countries: Burden, Drivers, and Emerging Challenges,” Annu. Rev. Public Health, vol. 38, pp. 145–164, 2017, doi: 10.1146/annurev-publhealth-031816-044604.

[2] Y. T. Lagerros and S. Rössner, “Obesity management: What brings success?,” Therap. Adv. Gastroenterol., vol. 6, no. 1, pp. 77–88, 2013, doi: 10.1177/1756283X12459413.

[3] D. K. Patel and F. C. Stanford, “Safety and tolerability of new-generation anti-obesity medications: a narrative review,” Postgrad. Med., vol. 130, no. 2, pp. 173–182, Mar. 2018, doi: 10.1080/00325481.2018.1435129.

[4] R. Kassir et al., “Complications of bariatric surgery: Presentation and emergency management,” Int. J. Surg., vol. 27, pp. 77–81, Mar. 2016, doi: 10.1016/J.IJSU.2016.01.067.

[5] V. Soleimani, A. Sahebkar, and H. Hosseinzadeh, “Turmeric (Curcuma longa) and its major constituent (curcumin) as nontoxic and safe substances: Review,” Phyther. Res., vol. 32, no. 6, pp. 985–995, Jun. 2018, doi: 10.1002/ptr.6054.

[6] M. Zintle, V. Khwaza, and A. A. Blessing, “Curcumin and Its Derivative agents in Prostate, Colon and Breast Cancers,” 2019.

[7] S. Oliveira, T. Monteiro-Alfredo, S. Silva, and P. Matafome, “Curcumin derivatives for Type 2 Diabetes management and prevention of complications,” Arch. Pharm. Res., vol. 43, no. 6, pp. 567–581, Jun. 2020, doi: 10.1007/s12272-020-01240-3.

[8] E. Ooko et al., “Modulation of P-glycoprotein activity by novel synthetic curcumin derivatives in sensitive and multidrug-resistant T-cell acute lymphoblastic leukemia cell lines,” Toxicol. Appl. Pharmacol., vol. 305, pp. 216–233, Aug. 2016, doi: 10.1016/j.taap.2016.06.002.

[9] R. Kolb, F. S. Sutterwala, and W. Zhang, “Obesity and cancer: inflammation bridges the two,” Curr. Opin. Pharmacol., vol. 29, pp. 77–89, Aug. 2016, doi: 10.1016/j.coph.2016.07.005.

[10] N. M. Iyengar, A. Gucalp, A. J. Dannenberg, and C. A. Hudis, “Obesity and Cancer Mechanisms: Tumor Microenvironment and Inflammation,” J. Clin. Oncol, vol. 34, no. 35, pp. 4270–4276, Dec. 2016, doi: 10.1200/JCO.2016.67.4283.

[11] K. I. Avgerinos, N. Spyrou, C. S. Mantzoros, and M. Dalamaga, “Obesity and cancer risk: Emerging biological mechanisms and perspectives,” Metabolism, vol. 92, pp. 121–135, Mar. 2019, doi: 10.1016/j.metabol.2018.11.001.

[12] Y. Ding and X. Xue, “Medicinal Chemistry Strategies for the Modification of Bioactive Natural Products,” Molecules, vol. 29, no. 3, p. 689, Feb. 2024, doi: 10.3390/molecules29030689.

Appendix A and Supplementary Information

Ethics approval for this study

Private Bag X1290, Potchefstroom
South Africa 2520

Tel: 086 016 9698
Web: http://www.nwu.ac.za/

North-West University Animal Care, Health and Safety Research Ethics Committee (NWU-AnimCareREC)

Tel: 018 299-1208
Email: Ethics-AnimCare@nwu.ac.za (for animal studies)

8 December 2023

ETHICS APPROVAL LETTER OF STUDY

Based on approval by the North-West University Animal Care, Health and Safety Research Ethics Committee (NWU-AnimCareREC) on 8/12/2023, the NWU-AnimCareREC hereby approves your study as indicated below. This implies that the NWU-AnimCareREC grants its permission that, provided the general conditions specified below are met and pending any other authorisation that may be necessary, the study may be initiated, using the ethics number below.

Study title: Evaluating the efficacy of novel curcumin derivatives on adipocyte dysfunction and adipocyte differentiation
Principal Investigator/Study Supervisor/Researcher: Prof S Mazibuko-Mbeje
Student: MT Moetlediwa - 30099358

Ethics number: N W U - 0 0 7 5 4 - 2 3 - A 5
Institution Study Number Year Status
Status: S = Submission; R = Re-Submission; P = Provisional Authorisation; A = Authorisation

Application Type: Single study
Commencement date: 08/12/2023
Expiry date: 28/02/2025
Risk: Category 0

Approval of the study is provided for a year, after which continuation of the study is dependent on receipt and review of an annual monitoring report and the concomitant issuing of a letter of continuation. A monitoring report is required at the end of February annually until completion of the study.

General conditions:

While this ethics approval is subject to all declarations, undertakings and agreements incorporated and signed in the application form, the following general terms and conditions will apply:

- *The principal investigator/study supervisor/researcher must report in the prescribed format to the NWU-AnimCareREC:*
  - *Annually on the monitoring of the study, whereby a letter of continuation will be provided annually, and upon completion of the study; and*
  - *without any delay in case of any adverse event or incident (or any matter that interrupts sound ethical principles) during the course of the study.*
- *The approval applies strictly to the proposal as stipulated in the application form. Should any amendments to the proposal be deemed necessary during the course of the study, the principal investigator/study supervisor/researcher must apply for approval of these amendments at the NWU-AnimCareREC, prior to implementation. Should there be any deviations from the study proposal without the necessary approval of such amendments, the ethics approval is immediately and automatically forfeited.*
- *Annually a number of studies may be randomly selected for active monitoring.*

9.1.5.4.2 Ethics Approval Letter of Study 1

- *The date of approval indicates the first date that the study may be started.*
- *In the interest of ethical responsibility, the NWU-AnimCareREC reserves the right to:*
  - *request access to any information or data at any time during the course or after completion of the study;*
  - *to ask further questions, seek additional information, require further modification or monitor the conduct of your research or the informed consent process;*
  - *withdraw or postpone approval if:*
    - *any unethical principles or practices of the study are revealed or suspected;*
    - *it becomes apparent that any relevant information was withheld from the NWU-AnimCareREC or that information has been false or misrepresented;*
    - *submission of the annual monitoring report, the required amendments, or reporting of adverse events or incidents was not done in a timely manner and accurately; and/or*
    - *new institutional rules, national legislation or international conventions deem it necessary.*
- *NWU-AnimCareREC can be contacted for further information via Ethics-AnimCare@nwu.ac.za or 018 299 1208*

NWU-AnimCareREC would like to remain at your service and wishes you well with your study. Please do not hesitate to contact the NWU-AnimCareREC for any further enquiries or requests for assistance.

Yours sincerely,

C Weldon

Vice-Chairperson: NWU-AnimCareREC

Current details: C:\Users\22654704\OneDrive - North-West University\NWU-AnimCareREC\9.1.5.1_NWU-AnimCareREC Ethics\NWU-00754-23-S5 (Mazibuko-Mbeje - Moetlediwa)\9.1.5.1.1_FV\9.1.5.4_Approval

File Reference: 9.1.5.4

List of reagents and chemicals used in this study.

Name	Supplier
Dulbecco`s modified Eagle`s medium (DMEM)	Gibco, Thermo Fisher Scientific, Waltham, United States
Dulbecco`s phosphate buffered saline (DPBS)	Lonza, Walkersville, United States
0.1% Trypsin blue solution	Invitrogen
Newborn calf serum	Gibco (Invitrogen)
Fetal bovine serum (FBS)	Gibco (Invitrogen)
Dexamethasone	Sigma
Methylisobutylxanthine (IBMX)	Sigma
Insulin (human)	Sigma
IL–6 DuoSet ELISA kit	R&D systems, biotechne
Adiponectin DuoSet ELISA kit	R&D systems, biotechne
N,N-diaminobenzaldehyde	Merck Darmstadt, Germany
3-hydroxybenzaldehyde	Merck Darmstadt, Germany
4-formylacetanalide	Merck Darmstadt, Germany
3,4-dimethoxy benzaldehyde	Merck Darmstadt, Germany
3,4,5-trimethoxybenzaldehyde	Merck Darmstadt, Germany
Vanillin	Merck Darmstadt, Germany
α-methyl cinnamaldehyde	Merck Darmstadt, Germany
3-chloroacetylacetone	Merck Darmstadt, Germany
Trimethylborate	Merck Darmstadt, Germany
Acetylacetone	RDH,
Cinnamaldehyde	RDH
4-methylbenzaldehyde	Aldrich Taufkirchen, Germany
4-methoxybenzaldehyde	Aldrich Taufkirchen, Germany
4-propylbenzaldehyde	Aldrich Taufkirchen, Germany
4-propyloxybenzaldehyde	Aldrich Taufkirchen, Germany
4-octylbenzaldehyde	Aldrich Taufkirchen, Germany
4-octyloxybenzaldehyde	Aldrich Taufkirchen, Germany
4-hexylbenzaldehyde	Aldrich Taufkirchen, Germany
4-pentylbenzaldehyde	Aldrich Taufkirchen, Germany
4-heptyloxy benzaldehyde	Aldrich Taufkirchen, Germany
4-ethoxy benzaldehyde	Aldrich Taufkirchen, Germany
Peprinal	Aldrich Taufkirchen, Germany
Boric oxide	HiMedia
3-indolcarboxaldehyde	HiMedia
ViaLight^{TM} plus kit	LONZA, USA
Glycerol assay kit	Sigma-Aldrich, USA
Oil Red O (ORO)	Sigma
Isopropanol	Sigma
Molecular graded water	Sigma
Crystal Violet	Sigma
TagMan Fast Advanced Master Mix	Thermofisher
High capacity cDNA kit	Applied Biosystem
Mouse 3T3–L1 preadipocytes	ATCC, Manassas, Virginia, United States
Dulbecco’s Phosphate Buffered Saline	Walkersville, Maryland, United States

Cell culture water	Walkersville, Maryland, United States
ViaLight™ plus cell proliferation and cytotoxicity bioassay kit	Walkersville, Maryland, United States
Bovine Serum Albumin Fraction V fatty acid free (FAFBSA)	Roche (Mannheim, Germany)
Curcumin, LPS, TNFα, PA, CL-316,243, metformin hydrochloride, and isopropanol	Sigma-Aldrich (St. Louis, Missouri, United States)
ELISA, IL-6, and AdipoQ	R&D Systems (Minneapolis, Minnesota, United States)
QIAzol Reagent and RNeasy Mini kit	Qiagen (Hilden, Germany)
High-Capacity Reverse Transcription kit, TaqMan™ fast advanced master mix, and Taqman® gene expression assays	Applied Biosystems (Foster City, California, United States)

List of equipment and materials used in this study

Name	Supplier
Biosafety cabinets, class 2	United Scientific
Invert light microscope	Olympus (Wirsam)
PipeeteBoy/ pipette aid	whitehead Scientific
Aspirator	Sigma
Flame Boy (FireBoy Eco)	Lebotec
CO_2	Airproducts
CO_2 incubator	RS BioTech, Nuve
Inverted Light Microscope	Olympus (Wirsam)
Benchtop centrifuge	Unicen (United Scientific)
Pipette	Sigma and Eppendorf
96 well CellBind plate	Corning
24 well Cellbind plate	Corning
6 well Cellbind plate	Corning
10 ml serological pipette	Corning
25 ml serological pipette	Corning
50 ml serological pipette	Corning
Cell Counting chamber	Invetrogen
BioTek ELX 800 plate reader	BioTek

Effects of DMSO on cell viability

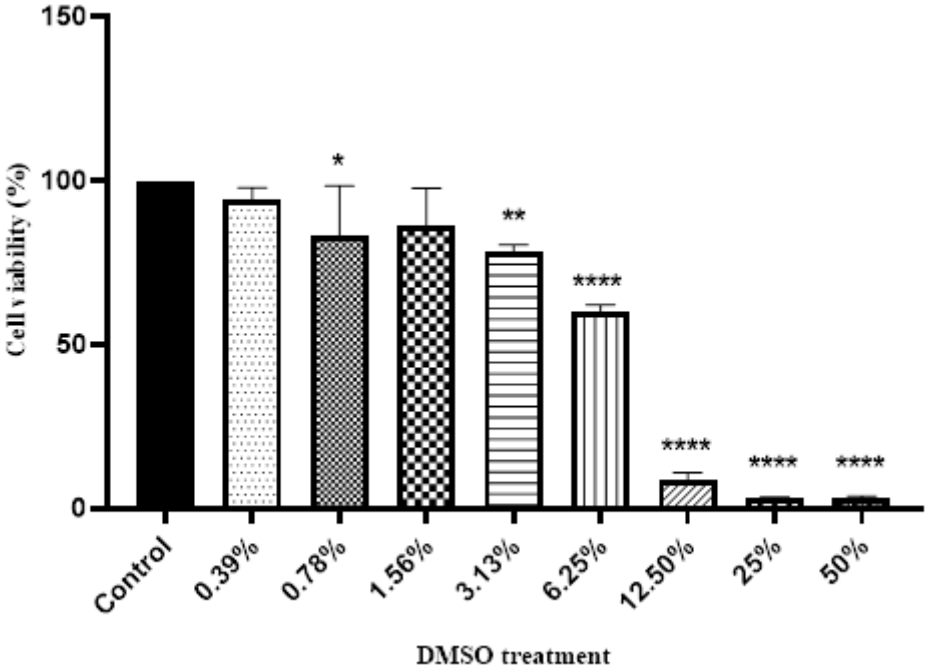


Figure S1: Effect of DMSO on viability of 3T3-L1 mature adipocytes. **Cell density (Crystal violet)**

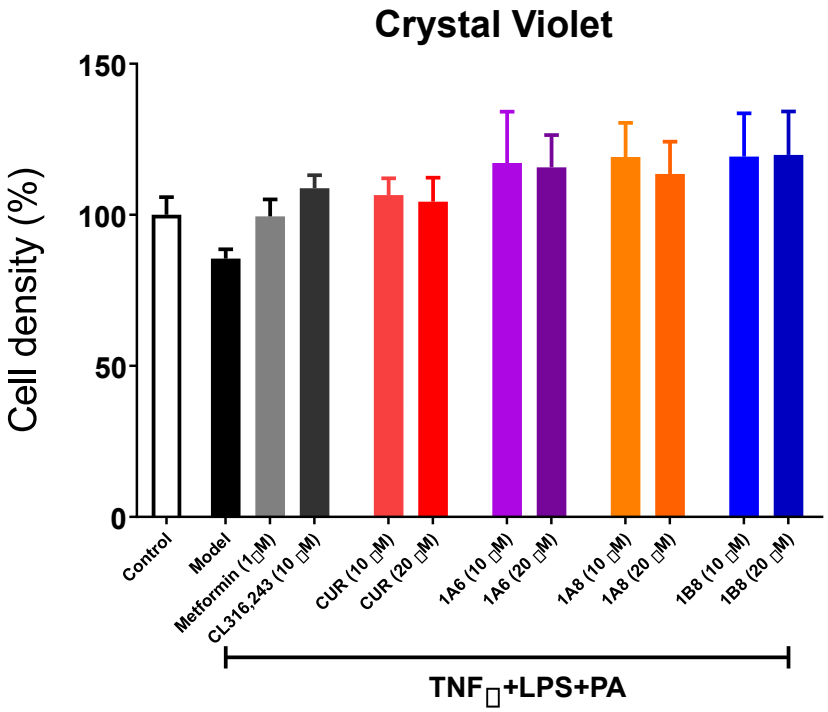


Figure S2: Effects of treatment with curcumin, 1A6, 1A8, and 1B8 on Crystal Violet on the cell density in 3T3-L1 mature adipocytes.

PCR Standard curve and optimization Table

S1: PCR standard curve.

Target	Slope	Y-intercept	R^2	%Efficiency	Error
Acaca	-3.424	30.387	0.989	95.925	0.130
AdipoQ	-3.451	26.879	0.999	94.897	0.028
B2m	-3.258	22.475	0.998	102.721	0.049
Cox2	-3.570	31.684	0.998	90.602	0.053
Fasn	-3.359	29.501	0.996	98.468	0.072
Gsk3b	-3.303	28.725	0.998	100.783	0.053
Il–6	-3.265	28.647	0.998	102.441	0.046
Lipe	-3.434	28.042	0.997	95.542	0.066
Lpl	-3.484	25.067	0.996	93.672	0.067
Mapk14	-3.251	28.942	0.988	103.048	0.119
Mcp1	-3.388	26.21	0.999	97.319	0.025
Pnpl1	-3.395	28.869	0.998	97.023	0.054
Pparg	-3.390	29.778	0.999	97.224	0.042
Rpl13a	-3.132	29.12	0.991	108.561	0.097
Srebf1	-3.004	30.93	0.992	115.207	0.087
Stat3	-3.409	28.773	0.999	96.486	0.042